Toxicity of thallium to the water flea (*Daphnia magna*) and rainbow trout (*Oncorhynchus mykiss*)

by

Andrew Hengyin Nagel

A thesis submitted in partial fulfillment of the requirements for the degree of

Doctor of Philosophy

in

Conservation Biology

Department of Renewable Resources

University of Alberta

Abstract

Thallium (Tl) is a trace metal that can be found at elevated concentrations in waters associated with the mining and refinement of coal and base metals. Although the effects of Tl on aquatic biota are poorly studied, the Canadian Council of Ministers of the Environment (CCME) have established a guideline value of 0.8 µg L^{-1} total Tl in fresh water. However, this value is based primarily on effects of Tl to an aquatic plant, and little is known regarding how protective this guideline is to freshwater animals. The goal of this thesis was to use two regulatory model freshwater species, the water flea *Daphnia magna* and the rainbow trout (*Oncorhynchus mykiss*) to expand mechanistic understanding of waterborne Tl toxicity and determine whether the current guideline value is likely to be protective of aquatic animals. An acute exposure of *Daphnia* to Tl established a median lethal Tl concentration of 1860 µg L^{-1}, and the use of asymmetrical flow field-flow fractionation suggests that most Tl in natural waters is in the ion form (Tl^{+}), even in the presence of binding ligands such as dissolved organic matter. Over a 21-d chronic exposure, complete mortality of *D. magna* occurred between Tl concentrations of 702 and 1112 µg L^{-1}, with median effect concentrations of 1.6 µg Tl L^{-1} for growth and 11.1 µg Tl L^{-1} for reproduction (all concentrations as dissolved Tl). A study examining effects of Tl on daphnid behaviour showed that the presence of Tl significantly affected phototaxis, an effect that was mediated by sensory impairment, indicating that neurotoxicity may be a conserved mode of Tl toxicity between mammals and aquatic biota. The interaction between Tl and potassium (K^{+}), known to be a key mediator of toxicity in mammals, was shown to also persist in *D. magna*. Elevated water K^{+} protected against Tl toxicity, the presence of Tl impaired K^{+} uptake, and pharmaceutical agents thought to block K^{+} channels modified the effects of Tl on whole-body K^{+} concentration. The acute (96-h) and sub-chronic (28-d) exposure of rainbow trout to waterborne

Tl resulted in the significant accumulation of Tl in all measured tissues (plasma, gill, muscle, otolith). However, in all soft tissues accumulation decreased with increased exposure time, indicating the presence of mechanisms that act to reduce Tl body burden. Thallium acutely stimulated renal proton ATPase activity, but sub-chronically inhibited branchial sodium/potassium ATPase activity, indicating the potential for ionoregulatory disruption in rainbow trout. Conversely, despite evidence of such a mechanism of Tl toxicity in mammals, there were no significant effects of waterborne Tl exposure on any measured oxidative stress endpoint in rainbow trout. These data indicate that CCME water quality guidelines for Tl in freshwater environments are likely to be protective against Tl toxicity in freshwater animals. However, this thesis does indicate that there may be some risk from human consumption of fish sourced from waters that have highly elevated Tl concentrations.

Preface

This is an original work by Andrew Nagel. The research projects, of which this thesis is a part, received research ethics approval (AUP2712) from the University of Alberta Biosciences Animal Care and Use Committee. The research conducted for this thesis forms part of a collaboration, led by Dr. Chris Glover at Athabasca University, with Dr. William Shotyk as the lead collaborator from the Department of Renewable Resources at the University of Alberta, and the supervisor of the thesis. Further support was provided by Dr. Chad Cuss at the School of Science and the Environment at Memorial University, Grenfell Campus, with expertise in environmental chemistry, and Dr. Greg Goss from the Department of Biological Sciences at University of Alberta with the provision of research space and laboratory materials.

Chapter 2 of this thesis has been published, in a modified form, as A.H. Nagel, C.W. Cuss, G.G. Goss, W. Shotyk, and C.N. Glover, "The effects of major ions and dissolved organic matter on complexation and toxicity of dissolved thallium to *Daphnia magna"*, in *Environmental Toxicology and Chemistry,* vol. 38: 2472-2479. I was responsible for study design, data collection and analysis, and drafting of the manuscript. Cuss, Goss, and Shotyk contributed to manuscript edits. Glover was the supervisory author, and was involved with study design and manuscript development.

Chapter 3 of this thesis has been published, in a modified form, as A.H. Nagel, C.W. Cuss, G.G. Goss, W. Shotyk, and C.N. Glover, "Chronic toxicity of waterborne thallium to *Daphnia magna"*, in *Environmental Pollution*, vol. 268B: 115776. I was responsible for study design, data

collection and analysis, and drafting of the manuscript. Cuss, Goss, and Shotyk contributed to manuscript edits. Glover was the supervisory author, and was involved with study design and manuscript development.

Chapter 4 of this thesis is currently in press, in a modified form, as A.H. Nagel, A.S.R. Robinson, G.G. Goss, and C.N. Glover, "Effect of thallium on phototactic behaviour in *Daphnia magna*," in *Environmental Science and Pollution Research*. I supervised Robinson's undergraduate thesis, and we were jointly responsible for study design, data collection and analysis as well as the drafting of the manuscript. Goss contributed to manuscript edits. Glover was the supervisory author, and was involved with study design and manuscript development.

Chapters 5-8 of this thesis are currently unpublished. I was responsible for study design, data collection and analysis as well as the drafting of the chapters. Glover assisted with study design and chapter editing.

Acknowledgements

I would like to gratefully acknowledge the technical expertise of I. Grant-Weaver for help with ICPMS analysis. The analytical chemistry work in this thesis was performed in the "SWAMP" in the Department of Renewable Resources at the University of Alberta. The infrastructure of this facility was funded by: Alberta Advanced Education, the Canada Foundation for Innovation, the Government of Alberta, and the Faculty of Agriculture, Life, and Environmental Sciences at the University of Alberta. I am grateful to a stipend supplied through funds provided by the Campus Alberta Innovation Program Research Chair to Chris Glover.

I would like to thank my supervisors Dr. Chris Glover and Dr. William Shotyk for their support not only regarding research and academic opportunities but in being nurturing and understanding particularly when personal issues had arisen. Additionally, I would like to thank Dr. Chris Glover for giving me a chance at pursing my dream to obtain a Ph.D. Special thanks goes to Dr. Chad Cuss who had allowed me to become a part of the Miwasin project and further develop my research skill set. I would like to further extend thanks to the many friends I have made through this program who had welcomed me to the city of Edmonton and made a foreign country feel like home, in addition to my friends and family in the United States, and loving wife Miranda Wanninger for the support they have provided through the entirety of this program. Lastly, I would like to thank my friend and mentor Dr. David Thompson from the department of Biology at Northern Kentucky University. Without the opportunities he had provided me with during my undergraduate research career to the present, this thesis would have never existed.

Table of contents

List of tables

Tables:

List of figures

Figures:

List of abbreviations

A: Amiodarone

AChE: Acetylcholinesterase

ADI: Acceptable daily intake

ADP: Adenosine diphosphate

AF4: Asymmetrical flow field-flow fractionation

Ag: Silver

ANOVA: Analysis of variance

ATP: Adenosine triphosphate

AU: Absorbance units

BAF: Bioaccumulation factor

BCF: Bioconcentration factor

BK: Big (large conductance) potassium channel

BLM: Biotic ligand model

Ca^{+}: Calcium

CAT: Catalase

CBR: Critical body residue

CCME: Canadian Council of Ministries of the Environment

Cd: Cadmium

Ch: Chlorpropamide

CI: Confidence intervals

Cl: Clozapine

Cl^-: Chloride

CPS: Counts per second

Cu: Copper

DMSO: Dimethylsulfoxide

DNPH: 2,4-dinitrophenylhydrazine

DOC: Dissolved organic carbon

DOM: Dissolved organic matter

dw: dry weight

EC_x: Effect concentration where x percent of the exposed population experiences the effect

EGTA: Egtazic acid

FAAS: Flame atomic absorption spectrometry

Fe: Iron

GFAAS: Graphite furnace atomic absorption spectrometry

GPx: Glutathione peroxidase

GR: Glutathione reductase

GSH: Glutathione reduced glutathione

GSSG: Oxidized glutathione

H2: Histamine receptor 2

H_2O_2: Hydrogen peroxide

HCN: Hyperpolarization-activated cyclic nucleotide-gated sodium potassium channel

Hg: Mercury

HNO_3: Nitric acid

HPLC: High-performance liquid chromatography

ICPMS: Inductively coupled plasma mass spectrometry

IC_x: Inhibiting concentration where x percent of the exposed population experiences inhibition

I_p: Phototaxis Index

ISO: International Organization for Standardization

K^+: Potassium

K_{ir}: Inwardly rectifying potassium channel

K_m: Michaelis-Menten affinity constant

K_v: Voltage-gated potassium channel

LC_x: Lethal concentration where x percent of the exposed population experiences mortality

LDH: Lactate dehydrogenase

LEAFS: Laser-excited atomic fluorescence spectrometry

LOD: Limit of detection

LOEC: Lowest observed effect concentration

Log K: Stability or binding constant

LOQ: Limit of quantification

MCL: Maximum contaminant level

MCLG: Maximum contaminant level goal

MES-1: Multi element standard-1

MT: Metallothionein

Na^+: Sodium

NADH: Nicotinamide adenine dinucleotide

NADPH: Nicotinamide adenine dinucleotide phosphate

NEM: N-ethylmaleimide

Ni: Nickel

NIST: National Institute of Standards and Technology

NKA: Sodium/potassium ATPase

NKCC: Na^{+}-K^{+}-$2Cl^{-}$ cotransporter

NOEC: No observed effect concentration

NOM: Natural organic matter

$O_2^{\cdot-}$: Superoxide

OECD: Organisation for Economic Cooperation and Development

$OH^{\cdot}$: Hydroxyl radical

Pb: Lead

PEP: Phosphoenolpyruvate

PK: Pyruvate kinase

ROS: Reactive oxygen species

RT-qPCR: Real time quantitative polymerase chain reaction

SE: Standard error

SEID: Sucrose/ethylenediaminetetraacetic acid/imidazole/deoxycholate buffer

SIET: Scanning ion-selective electrode technique

SHM: Stockholm humic model

SOD: Superoxide dismutase

SRM: Standard reference material

TCA: Trichloroacetic acid

Tl: Thallium

Tl^{+}: Thallium ion

Tl(I): Monovalent thallium

Tl(III): Trivalent thallium

TRAP: Toxicity Relationship Analysis Program

TRA: Tissue Residue Approach

USEPA: United States Environmental Protection Agency

UV: Ultraviolet

WHAM: Windermere Humic Aqueous Model

YCT: Yeast, cerophyll, trout chow feed for daphnids

Zn: Zinc

Equations:

1. General Introduction

1.1. Introduction

1.1.1. *Introduction to thallium and historical overview*

The post-transition metal thallium (Tl), atomic number 81, was discovered in 1861 by Sir William Crookes, a British chemist, while he was examining seleniferous residues from a sulfuric acid factory (Weeks 1932). Upon spectroscopic examination of these residues, which were believed to contain tellurium, Crookes described a previously unidentified green line in the spectrum. This new element was named Tl after the Latin word *thallus* which means "budding twig" and at the time was commonly used to describe the green tint of young vegetation. Independently, Claude Aguste Lamy, a French chemist, also discovered Tl a year later. Work by Lamy ultimately resulted in the purification and isolation of the metal (Lamy 1862; Weeks 1932).

Thallium is of great interest to the fields of chemistry and toxicology, a consequence of its chemical and physical properties, which are summarized in Table 1.1. These properties contribute to both the industrial uses of Tl (see Section 1.2), and its toxicity (see Section 1.8). Thallium is considered a trace element, and in seawater is the 81st most abundant element, similar in abundance to lead (Pb), and one to two orders of magnitude less abundant than trace metals such as copper (Cu), zinc (Zn), silver (Ag), and cadmium (Cd) (Ronov and Yaroshevsky 1969). However, Tl is considered an element of concern, as it may be enriched in aquatic environments due to anthropogenic processes (Sections 1.2-1.4). Thallium has a unique place in human toxicology due to its use as a poisoning agent, and in mammalian systems Tl is suggested to be more toxic than other well-known human toxicants such as mercury (Hg), Cd and Pb (see Section 1.8; Peter and Viraraghavan 2005). However, much less is known regarding the

sensitivity of aquatic biota to Tl. Indeed, despite environmental concerns regarding Tl contamination associated with some industrial practices, and the potential for Tl toxicity, the toxicological impacts of this metal on aquatic biota are only poorly characterized.

Table 1.1. Physical and chemical properties of thallium.

Category	Property	Value
Physical properties	Atomic number	81
	Molar mass	204.38 g mol^{-1}
	Ground state electronic configuration	[Xe] $4f^{14}5d^{10}6s^{2}6p^{1}$
	Melting point	577 K
	Boiling point	1746 K
	Density	11.85 g cc^{-1}
	Effective ionic radius	150 pm
Redox potential	$Tl^{+} + e^{-} \rightarrow Tl(s)$	-0.336 V
	$Tl^{3+} + 3e^{-} \rightarrow Tl(s)$	0.741 V
	$Tl^{3+} + 2e^{-} \rightarrow Tl^{+}$	1.28 V
Oxidative states	Tl(I)	Tl^{+}
	Tl(III)	Tl^{3+}

Adapted from Nriagu 1998.

1.1.2. *Uses of thallium*

Thallium was initially used in the 1930's as a treatment for diseases including syphilis, ringworm, tuberculosis, and gonorrhea (Gleich 1931; Nriagu 1998; Genchi et al. 2021). However, the therapeutic use of Tl was associated with mortality. For example, the application of Tl as a ringworm treatment in American children resulted in 447 cases of Tl poisoning with 6 deaths (Munch 1934). As a consequence, the medical use of Tl was stopped. However, because

of its toxic properties, Tl was subsequently utilized as a pest control agent (Munch and Silver 1931). Rodenticides containing Tl salts were highly effective, but in 1965 the United States Environmental Protection Agency (USEPA) prohibited the use of Tl as a pesticide following several reports of human Tl poisoning (Thompson 1981; Peter and Viraraghavan 2005). Among these was a case where Tl entered the human food chain via contaminated barley, resulting in 7 deaths (Munch et al. 1932). Following further research, several commercial applications for Tl compounds were developed, which are still in use today. These include the use of Tl sulfide in photocells, Tl bromide in infrared detectors, and Tl oxide in fiber glass (ATSDR, 1992; Peter and Viraraghavan, 2005). Additionally, Tl nitrate is a component of some fireworks, emitting a green flame when burned (Peter and Viraraghavan, 2005). Other applications of Tl include Tl chloride in suntan lamps and Tl acetate in ozone measurement.

1.1.3. *Sources of thallium*

The concentration of Tl in the Earth's crust is 0.8 $\mu g\ g^{-1}$ (Sahl et al. 1978), where it is principally associated with base metal ores containing Zn, Pb, Cu and iron (Fe). Concentrations of Tl within sulfide ores, the minerals galena and pyrite, and coal, range from 0.5 to 45 $\mu g\ g^{-1}$ (Zitko 1975; Smith and Carson 1977). Since Tl is lithophilic it is also commonly found in association with silicate minerals such as potassium feldspars, in which Tl concentrations range from 0.5 to 600 $\mu g\ g^{-1}$ (Sahl et al. 1978).

Thallium is commercially-sourced as a by-product of the mining and smelting of base metals. Recovery of Tl occurs through electrolysis, precipitation and reduction during the smelting process. These efforts result in average annual Tl yields of 9 tonnes globally (USGS 2018). In particular, Tl is recovered in large quantities during the smelting of Zn ores that contain greater than 2 μg Tl g^{-1}. However, Tl recovery also occurs when smelting Pb, Cu, and Fe ores

(Nriagu 1998). Worldwide, reserves of Tl are estimated at 17,000 tonnes, which are mostly located in Canada, Europe and the United States (USGS 2018).

1.1.4. *Thallium in aquatic environments*

The current commercial uses of Tl pose little threat to life. However, as a result of anthropogenic processes, Tl can enter aquatic environments, through sources such as the atmospheric deposition of Tl volatilized during the burning of coal, and the leaching of Tl-rich mine tailings (Nriagu 1998). These can contribute to environmental Tl concentrations that are of regulatory concern.

Environmental measures of aquatic trace elements are reported as either total or dissolved. 'Total' is the concentration determined without filtration. Alternatively, 'dissolved' is the concentration following filtration through a 0.45 micron filter. As it relates to Tl in natural waters, differences in concentrations between total and dissolved can be as much as 23-fold (Ghotbizadeh et al. 2022). This is particularly true in waters where Tl(III) dominates, as this oxidative state of Tl is reactive and will react with particulate matter, excluding it from the dissolved fraction. Conversely, Tl(I) is relatively inert and will partition mostly into the dissolved fraction (Belzile and Chen 2017). In this thesis, focused on Tl(I) in artificial laboratory waters, total Tl will be practically equivalent to dissolved Tl (see Chapter 2).

In surface waters free of Tl enrichment, such as the Athabasca River in Alberta, Canada, dissolved Tl concentrations average 3 ng L^{-1} (Shotyk et al. 2019). However, concentrations of Tl in surface waters can reach levels several orders of magnitude above natural background (Table 1.2; Karbowska 2016), while concentrations in wastewaters can be as high as 15000 µg L^{-1} total Tl (Williams-Beam and Twidwell 2003). The areas where the greatest Tl enrichment occur are generally linked with the refinement of Zn ores and steel manufacture, while total Tl

concentrations in mining effluents regularly exceed 80 µg L^{-1}. In Canadian surface waters Tl concentrations are generally low. However, historically there has been concern regarding Tl in waters of the Great Lakes, which are a predicted sink for Tl deposition (Lin and Nriagu 1999). In fact, concentrations of Tl in Great Lakes fish have been found to approach levels that may result in risk for human consumption (Lin et al. 2001). Thallium is also found in sediments, with concentrations averaging 0.6 µg Tl g^{-1} (Belzile and Chen 2017). However, near mining sites, sediment concentrations can reach 20000 µg Tl g^{-1} (Bačeva et al. 2014).

Table 1.2. Global concentrations of thallium in water and wastewater.

Region	Sampling site	Concentration range ($\mu g\ L^{-1}$)	Reference
Canada	Coal mining, wastewater	0.89-2.66[d]	Cheam 2001
	Coal mining, effluent water	0.13[d]	
	Lake Erie, Central Basin, pore water	0.07-0.11[d]	
	Lake Ontario, Kingston Basin, pore water	0.05-0.21[d]	
	New Brunswick, surface water	0.05-4.39[d]	
	Alberta, surface water	0.003[d]-0.26[t]	
			Shotyk et al. 2019
China	Zn factory, wastewater	19.5-3000[t]	Liu et al. 2019
	Pb-Zn smelter, wastewater	370-470[t]	
	Polymetallic mine deposit, surface water	2[t]	
	Steel factory, wastewater	3-2500[t]	
	Sulfuric acid factory, wastewater	15.4-400[t]	Liu et al. 2010
	Sulfuric acid factory, effluent water	9.3-21.6[t]	Chen and Zhou 2000
	Yunfu pyrite mine, mine water	101-194[t]	Liu et al. 2016
	Lanmuchang Hg-Tl mine, mine water	27[t]	Xiao et al. 2012
	Lanhua As-Tl mine, mine water	17[t]	Zhang et al. 1998
	Lanhua As-Tl mine, surface river water	3[t]	
	Cu mine, mine water	1520[t]	Zhang 2017
	Hengshi and Wengjiang River, surface water	0.11[t]	Chan et al. 2021
	Cement industries, wastewater	20[d]	Schoer 1984
	Zinc mine, effluent water	1520[t]	Xu et al. 2019
France	Pb-Zn mine, surface water	1.16-5.44[d]	Casiot et al. 2009

Table 1.2. cont.

Region	Sampling site	Concentration range ($\mu g\ L^{-1}$)	Reference
Germany	River Rhine, multiple industrial sources	102[t]	Cleven and Fokkert 1994
	Al-plant, wastewater	86[t]	Deb et al. 1998
	Kankali tank, surface water	166[t]	
	Cement plant, surface water	7.3[d]	Mathys 1981
Italy	Baccatoio Stream, surface water	0.53-19.8[d]	D'Orazio et al. 2020
	Pollone mine, surface water	170[d]	Perotti et al. 2017
Poland	Boleslaw-Bukowno, mining area (Upper Silesia)	50[d]	Ospina-Alvarez et al. 2015
Sweden	Surface water	0.05-0.21[d]	Karlsson 2006a
	Kvarntorp, leachates	0.74[d]	
Switzerland	Wastewater	672-2400[t]	IPCS 1996
	Surface water	80[t]	
	Seepage water, waste rock dump	250[d]	Pleßow and Heinrichs 2000
United Kingdom	Seaton River, surface water	0.03[d]	Tatsi and Turner 2014
	East Looe River, surface water	0.02[d]	
	Fowey River, surface water	0.02[d]	
	Portreath effluent, surface water	0.54[d]	
	Red effluent, surface water	0.14[d]	
	Hayle effluent, surface water	0.28[d]	
	Carnon effluent, surface water	0.86[d]	
	Wheal Jane mine, surface water	0.372- 1.383[d]	Law and Turner 2011
USA	Oil drilling	12.9-672[t]	Korkisch and Steffan 1979
	Lead smelter, effluent water	15000[t]	Williams-Beam and Twidwell 2003

[t]: Total concentration [d]: Dissolved concentration

1.1.5. *Thallium speciation and bioavailability*

The speciation of Tl in water, as a function of oxidation-reduction potential and pH, is demonstrated by the Pourbaix diagram depicted in Figure 1.1. The dashed lines in this figure represent the redox conditions that normally exist within natural waters. Therefore, based on this model, at pH values between 5 and 8 (the pH range most common in freshwater ecosystems; Morgan et al. 2001), the dominant species of Tl is the unbound monovalent ion (Tl^{+}). Some studies have, however, suggested that Tl can form stable complexes with sulfur-containing ligands (Sillen et al. 1964; Baes and Mesmer 1976). For example, based on stability constants, the major aqueous complexes of Tl(I) would include $TlSO_4^{-}$, $Tl(SO_3)_4^{5-}$, and $Tl(S_2O_3)_4^{5-}$ (log K: 1, 34, 41). However, modelling predicts the contribution of these species to be low, making up only 0.4% of total Tl in river water (Kaplan and Mattigod 1998). In general, Tl speciation appears to be relatively unaffected by naturally-occurring dissolved ligands, such as dissolved organic carbon (DOC) (Martin et al. 2020). Indeed, modeling of Tl species suggests that a Tl-fulvic acid complex would make up only 15% of Tl species in a standard river water, with 83% existing as Tl^{+} (Kaplan and Mattigod 1998).

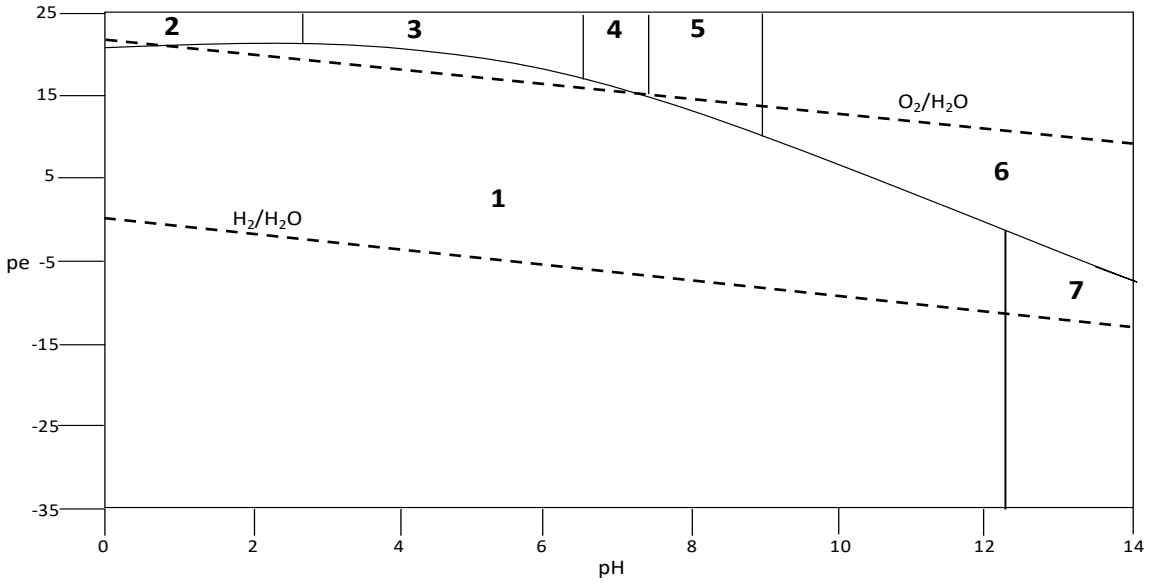

Figure 1.1. Pourbaix diagram (pe-pH) for Tl species in freshwater assuming that dissolved Tl concentration is fixed at 30 μM at 25°C. Adapted from Lin and Nriagu (1998). The different Tl species are represented by numbers: 1, Tl^{+}; 2, Tl^{3+}; 3, $Tl(OH)_2^{2+}$; 4, $Tl(OH)_2^{+}$; 5, $Tl(OH)_3^{0}$; 6, $Tl(OH)_4^{-}$; 7, $Tl(OH)^{0}$.

The dominance of the monovalent Tl species is of great importance when assessing aquatic toxicity. In general, the major uptake species of waterborne trace metals are free ions (Bury et al. 2003). For essential metals such as Cu and Zn, specific transporters may exist that achieve uptake, but for non-essential metals bioavailability is largely governed through their mimicry of major ions such as sodium (Na^{+}) and calcium (Ca^{2+}). Thus, the persistence of Tl in natural waters as a free ion, is likely to mean that waterborne Tl has a high bioavailability.

While the dominant species of Tl in freshwater ecosystems is the monovalent ion, Tl can also exist in a trivalent oxidative state (Tl(III)). Notably, the Tl(III) ion is more reactive than the Tl(I) ion and can form stable complexes with environmental ligands (Wade and Banister 1973). In freshwater, the dominant Tl(III) forms are the hydroxyl species, which include aqueous

$Tl(OH)^{2+}$ at pH up to 6.3, $Tl(OH)_2^+$ from pH 6.3-7.4, and insoluble $Tl(OH)_3$ at pH 7.4-8.8 (Nriagu 1998). In oxidizing and alkaline sediments, Tl(I) is readily converted to Tl(III) (Migaszewski and Galuszka 2021). Additionally, monovalent Tl can be oxidized by planktonic bacteria (Twining et al. 2003), and through photooxidation. The latter occurs in the presence of aqueous cations such as Fe(III), resulting in the formation of inert $Tl(OH)_3$ (Cotton and Wilkinson 1988). Unlike Tl(I), Tl(III) forms stable complexes with DOC (Kaplan and Mattigod 1998). The higher reactivity of Tl(III) means that under conditions where this oxidative state prevails, Tl is effectively unavailable for uptake from the water. However, in most surface fresh waters, redox conditions favour the Tl(I) oxidative state (Figure 1.1; Kaplan and Mattigod 1998). In this thesis, the notation "Tl" will therefore be synonymous with "Tl^+" in most circumstances. Since aquatic ecosystems are dominated by the bioavailable Tl^+ species, one consideration when assessing bioavailability and the potential for Tl uptake is the interaction of Tl with potassium (K^+). Chemically the two ions share similarities in size (K^+: 137 pm, Tl^+: 150 pm), charge (+1), and charge density (K^+: 9, Tl^+: 11) (Shannon 1976). As a consequence, geochemically Tl has been found to displace K^+ from organic ligands (Sager 1992). Similarly, in mammalian and insect systems, Tl^+ is well described as a K^+ mimic (Britten and Blank 1968; Rabon and Sachs 1981; Belowitz and O'Donnell 2013), and this mimicry of K^+ by Tl^+ can result in competition between the two cations (Belowitz and O'Donnell 2013). The uptake of Tl from aquatic environments is also believed to involve pathways of K^+. Evidence for Tl/K^+ interactions in aquatic biota includes studies showing that Tl toxicity can be affected by water K^+ concentrations (Hassler et al. 2007; Rickwood et al. 2015; Tatsi et al. 2015). For example, research using the algae *Chlorella* showed that a 250-fold excess of K^+ over Tl ameliorated the inhibition of algal growth by Tl (Hassler et al. 2007). Indeed, work by Hassler et al. (2007) has

suggested that the ratio of Tl to K^+ could be used as a predictor of toxicity. However, the relationship between K^+ and Tl in terms of uptake and toxic effect requires further investigation.

1.1.6. *Measurement of Tl in freshwater samples*

Thallium in freshwater can be measured using several different approaches (Karbowska 2016; Table 1.3). Single element techniques such as flame atomic absorption spectrometry (FAAS) and graphite furnace atomic absorption spectrometry (GFAAS) take advantage of the fact that different elements absorb light at different wavelengths (Van Loon 2012). After a sample is atomized the magnitude and specific wavelength of absorption are measured, and concentration can be determined by reference to standard solutions. Other techniques such as laser-excited atomic fluorescence spectrometry (LEAFS) use a light source to excite the analyte atoms, quantifying elements based on the resulting fluorescence (Cheam et al. 1996). Differential pulse anodic stripping voltammetry (DPASV) utilizes a 4-step process that includes cleaning, electroplating, deposition and stripping, and which subsequently quantifies specific ionic species based on the measurement of electrical current (Barón-Jaimez et al. 2013). However, mass spectrometry-based techniques are considered the "gold standard" in trace metal analysis (Wilschefski and Baxter 2019). In particular, inductively coupled plasma mass spectrometry (ICPMS) is widely used due to the high sensitivity, precision and selectivity of the technique (Gaillardet et al. 2003; Wilschefski and Baxter 2019). This technique also has the very practical advantage of having a broader measurable concentration range than approaches such as GFAAS, a factor that makes sample preparation easier (Garbarino 1999). The effectiveness of the ICPMS for analytical analysis is further shown by its ability to measure concentrations of several elements simultaneously, reducing overall runtime. The key advantage of ICPMS over other techniques, however, is its low level of detection (LOD) for most elements, with the capacity to

quantify metals at ultratrace levels (0.1 ng L^{-1}) (Nriagu et al. 1993). Briefly, ICPMS measures ions from a liquid sample that is nebulized into an aerosol before being transported into the plasma torch (Wilschefski and Baxter 2019). The plasma torch, which is fueled by argon gas, then ionizes the sample. The resulting ions are then separated on the basis of mass-to-charge ratios by a quadrupole mass analyzer using alternating electrical fields, before being quantified by a detector (Wilschefski and Baxter 2019).

Inductively coupled plasma mass spectrometry can be coupled with other techniques to provide additional information such as trace metal speciation. One advancement is the coupling of ICPMS to asymmetrical flow field-flow fractionation (AF4). The AF4 technique allows for the non-destructive diffusion-based separation of particles, and has the ability to characterize colloids, proteins and polymers from 1- 1000 nm in size (Wahlund and Giddings 1987). Since the development of this technique, AF4 has been used for determining the different size fractions of trace metals in freshwater samples (Cuss et al. 2017). The greatest value of this approach is in the differentiation of the various trace metal species that exist in the "dissolved" fraction. As noted above, dissolved metal is considered to be the fraction that passes through a 0.45 μm filter, and is frequently used as a proxy for the bioavailable fraction of waterborne metals (USEPA 1992). However, this fraction includes free metal ions as well as metals complexed to small ligands and present in colloids, the latter of which are likely to have limited bioavailability (Cuss et al. 2020). The AF4 technique allows a more refined assessment of trace metal in the dissolved fraction and thus a more accurate assessment of bioavailability. Briefly, AF4-ICPMS works by the injection of a sample onto a semi-permeable membrane. The membrane then undergoes a focusing step, in which the sample is focused into a thin band. Thereafter, an eluent solution with selectable pH is passed over the membrane and the molecules on the membrane are sent to the

detector with their arrival time based upon their relative size (i.e., low molecular weight particles and ions reach the detector before larger complexes). Detected trace elements can subsequently be resolved into 4 separate size fractions: (1) void peak which contains ionic species and organic-associated material with low molar mass; (2) organic matter-associated elements larger than 300 Da in size; (3) inorganic colloids; and (4) inorganic material greater than 20.7 kDa in size, such as oxyhydroxide complexes (Cuss et al. 2017). Through the use of deconvolution and statistical analysis based on the data outputs from both AF4 and ICPMS, fractograms are generated that provide visualizations of potential metal species associated with the different size fractions. By identifying the size fractions a trace metal exists in, in the dissolved fraction, a better understanding of bioavailability of trace metals is generated. This technique has been applied in the Athabasca River and its tributaries, and has shown that bioaccessibility of trace elements decreased with distance downstream in the Athabasca River system (Cuss et al. 2018).

Table 1.3. Methods for measuring Tl in water.

Method	LOD ($ng\ L^{-1}$)	Reference
Inductively Coupled Plasma Mass Spectrometry (ICPMS)	0.1	Chapter 2
Laser Excited Atomic Fluorescence Spectrometry (LEAFS)	0.1	Cheam et al. 1996
Differential Pulse Anodic Stripping Voltammetry (DPASV)	2	Lukaszewski et al. 1996
Graphite Furnace Atomic Absorption Spectrometry (GFAAS)	0.1	USEPA 1983
Inductively Coupled Plasma Optical Emission Spectrometry (ICP-OES)	40000	USEPA 1983
Flame Atomic Absorption Spectrometry (FAAS)	100000	USEPA 1983

LOD: Limit of detection

1.1.7. *Thallium bioaccumulation*

Given that most Tl is present in the environment in a bioavailable form, then Tl accumulation in aquatic biota would be expected. Supporting this, field studies have shown that in fish Tl accumulates in several tissues including gill, muscle, intestine, kidney and otolith (LIS 1980, as cited in Couture et al. 2011; Shotyk et al. 2019; Mijošek et al. 2020; Chan et al. 2021). Based on ratios of tissue to dissolved environmental Tl concentration (i.e., bioaccumulation or bioconcentration factors (BAF/BCF); see Chapter 6), Tl does not generally appear to bioaccumulate to levels that are considered by regulators to be of concern (i.e., BAF/BCF: >5000; Environment Canada 2000a). There are some exceptions, however. For example, BAF values for field-collected lake trout from Lake Michigan (BAF 10071, whole body; Lin et al. 2001), and ayu from the Wengjiang River (BAF 8750, muscle; Chan et al. 2021), exceed the threshold of regulatory concern. As the accumulation of trace metals is frequently linked to their toxic impact (Souid et al. 2013; Moyson et al. 2016), and is an important component of aquatic risk assessments for trace metals (DeForest et al. 2007), more studies of Tl bioaccumulation are required. A detailed exploration of Tl bioaccumulation in aquatic organisms can be found in Chapter 6.

As mentioned above, the bioaccumulation of Tl is believed to be linked to K^+ (Cvjetko et al. 2010). For example, in phytoplankton reduced Tl accumulation can be observed in the presence of elevated K^+ (Twiss et al. 2004). Other evidence across a range of organisms and study systems provides mechanistic support for this observation, by indicating that Tl^+ uptake occurs via K^+ transporters (Britten and Blank 1968; Belowitz and O'Donnell 2013). Indeed, some studies have shown that Tl^+ has a greater affinity for uptake through K^+ transporters than K^+ itself (Britten and Blank 1968), and that Tl substitution can occur without affecting physiological function (Britten and Blank 1968; Galván-Arzate and Santamaria 1998; Carmosino

et al. 2013). However, at high concentrations Tl can inhibit K^+ transporter function (Cavieres and Ellory 1974; Sherstobitov et al. 2010).

Following uptake, Tl is handled much like a K^+ ion (Leonard and Gerber 1997). As a result, Tl tends to accumulate in K^+-rich tissues such as muscle and kidney, before being excreted through the feces and urine (ATSDR 1992). At an intracellular level, Tl has been found to sequester in the mitochondria (Herman and Bensch 1967; Fukumoto et al. 1997). As mitochondria rely on K^+ transport for processes such as adenosine triphosphate (ATP) production (Laskowski et al. 2016), mitochondria may be an important loci of Tl toxicity (Fukumoto et al. 1997). Interactions between Tl^+ and K^+ are the result of similarities in charge (+1) and in effective ionic radii (Tl^+: 150 pm; K^+: 137 pm) (Shannon 1976).

1.1.8. *Thallium toxicity*

Thallium poisoning has been well characterized in humans, with calculated lethal doses of Tl ranging from 10 to 15 mg kg^{-1} (Moeschlin 1980). However, the diagnosis of Tl poisoning can be difficult, as Tl toxicity is complex and symptoms can initially be generic in nature (Cvjetko et al. 2010). Following acute exposure to Tl, gastrointestinal symptoms are first to develop, while prolonged exposure can result in paresthesia, severe pain and neurological effects (Kou et al. 2005). Neurological symptoms include sensory effects such as hypoesthesia, and locomotor effects such as hyporeflexia and deterioration of muscle strength (Kou et al. 2005). Interestingly, gastrointestinal symptoms such as vomiting, nausea and diarrhoea become mild or non-existent as exposure to Tl lengthens (Zhang et al. 1998). One treatment that has been found effective in ameliorating toxic effects of Tl following poisoning, is the administration of Prussian blue ($Fe_4[Fe(CN)_6]_3$). Prussian blue adsorbs Tl^+, reduces its bioavailability, and facilitates excretion of Tl from the body (Rauws and Canton 1976).

As noted above, Tl is a neurotoxicant in humans. For example, respiratory depression, muscle weakness, blurred vision and nerve paralysis are all neurological symptoms characteristic of human Tl poisoning (Desenclos et al. 1992), and can persist for extended periods following exposure (Lu et al. 2007). Effects of Tl as a neurotoxicant have also been seen in mammalian model organisms. For instance, in rats Tl exposure can induce brain lesions (Barroso-Moguel et al. 1994), neuromuscular paralysis (Wiegand et al. 1984), and altered brain neurochemistry (Hasan et al. 1978). At a whole animal level these effects can manifest as changes in locomotor activity (Osorio-Rico et al. 2015).

Most of the existing knowledge of Tl toxicity in aquatic organisms focuses on mortality following acute, sub-chronic, and chronic laboratory exposures (Table 1.4). The acute median lethal concentration (LC_{50}) of Tl to aquatic invertebrate species ranges from 0.66 to 2.01 mg Tl L^{-1}. Interestingly, the concentrations that elicit lethal effects in invertebrate species are similar to those reported in fish (0.86 - 4.27 mg Tl L^{-1}; LeBlanc and Dean 1984; Pickard et al. 2001; Tatsi et al. 2015), suggesting a similar sensitivity to acute Tl toxicity across phyla. Studies assessing the chronic toxicity of Tl to aquatic organisms are limited. However, a chronic (28-d) LC_{50} value for *Daphnia magna* of 0.39 mg L^{-1} has been determined (Kimball 1978). Additionally, in an embryo-larval bioassay, the 28-d LC_{50} value for rainbow trout was calculated at 0.17 mg Tl L^{-1} (Birge 1978).

Effects of Tl on growth and reproduction have also been measured in aquatic biota. In the cladoceran crustacean *Ceriodaphnia dubia*, the first quartile effect concentration (EC_{25}) at which growth and reproduction were significantly impacted by waterborne Tl was 0.17 and 0.10 mg Tl L^{-1}, respectively (Pickard et al. 2001; Rickwood et al. 2015). However, the EC_{25} has been observed to decrease (i.e., Tl becomes more toxic) when organisms were exposed in K^+-depleted

media (Rickwood et al. 2015). In fish, Tatsi and colleagues (2015) observed that fathead minnow larvae experienced abnormal growth following a 96-h exposure to 0.8 mg Tl L^{-1}. An effect on growth has also been observed in female fathead minnow larvae following a 7-d exposure to 0.8 µg Tl L^{-1} (LeBlanc and Dean 1984). Other whole animal effects of Tl on fish include decreases in oxygen consumption and increased ammonia nitrogen excretion following exposure to 0.1 µg Tl L^{-1} (Ma et al. 2019; Li et al. 2020), and a decreased heart rate after a 96-h exposure to 0.8 mg Tl L^{-1} (LeBlanc and Dean 1984). Additionally, Tl causes structural changes in the gill of adult zebrafish following a 96-d exposure to 0.5 µg Tl L^{-1} (Wang et al. 2021).

Although Tl is a neurotoxicant in mammals, there is limited evidence for such effects in aquatic animals. One recent study did, however, show that medaka (*Oryzias latipes*) exposed to soils with elevated Tl exhibit altered swimming behaviour (Hsu et al. 2022). Specifically, Tl at 15 mg kg^{-1} increased maximum swimming velocity. This finding is similar to outcomes from a study where fish exposed to 42 µg Tl L^{-1} exhibited hyperexcitability (Farag et al. 2021). Although data are scarce regarding the neurological effects of Tl on aquatic biota, research to date, coupled with evidence for such effects in mammalians systems (see above), indicates that this could be an important mechanism by which Tl affects aquatic animal health.

In studies performed thus far, two main cellular/biochemical mechanisms of Tl toxicity can be recognized. The first is interference with K^+ homeostasis. As noted above, Tl gains access to cells through K^+ transporters, but there is also evidence that Tl can interfere with K^+ handling. For example, exposure of human blood cells to Tl causes an inhibition of sodium/potassium ATPase (NKA) activity (Cavieres and Ellory 1974; Skulskii et al. 1975; Sherstobitov et al. 2010). This enzyme plays a critical role in the maintenance of cellular electrochemical gradients, which are responsible for cellular ion transport and organismal salt and water balance (Moller et

al. 1996). Effects of Tl on NKA activity have also been observed following whole animal exposure to Tl. In Hou et al. (2017), NKA activity significantly increased when zebrafish were exposed to concentrations as low as 0.02 µg Tl L^{-1} for 96-d. Notably, the effects of Tl on K^+-dependent ionoregulatory enzymes are not restricted to NKA. For example, at exposure concentrations above 613 mg L^{-1}, Tl inhibited (K,H)-ATPase activity in hog gastric mucosal epithelia (Rabon and Sachs 1981). Since Tl exposure appears to affect K^+ handling, altered ion homeostasis might ultimately be the cause of Tl mortality in aquatic biota, at least by analogy with other ion-disrupting metal ion toxicants (Grosell et al. 2002).

The second key mechanism of Tl toxicity is the induction of oxidative stress (Appenroth and Winnefeld 1999; Kiliç and Kutlu 2010; Kiliç and Kiliç 2017). The generation of reactive oxygen species (ROS) is a normal consequence of oxidative metabolism, but if present in excess, ROS can cause oxidative damage (Pizzino et al. 2017). In most cells, under normal conditions, antioxidants act to scavenge excess ROS, preventing damage from occurring. In rats, Tl exposure results in changes in antioxidant enzyme activity (Appenroth and Winnefeld 1998; Kiliç and Kutlu 2010), and in concentrations of non-enzymatic antioxidants such as glutathione (GSH) (Villaverde et al. 2004). For example, in livers of rats injected with 32 mg kg^{-1} Tl, activity of the enzyme antioxidants superoxide dismutase (SOD) and glutathione peroxidase (GPx) was significantly inhibited, and the content of GSH was decreased (Kiliç and Kutlu 2010). Notably, these changes in protective mechanisms were such that Tl exposure resulted in lipid peroxidation, a form of ROS-mediated oxidative damage. Effects of Tl on antioxidant capacity have also been observed in aquatic organisms. One study by Kiliç and Kiliç (2017) showed that following a 7-d exposure of the aquatic oligochaete *Tubifex* to 1 µg Tl L^{-1}, catalase (CAT) and GPx activity increased, as did GSH content. As the length of exposure increased to 15-d, CAT

activity remained elevated, but decreases in glutathione S-transferase and GPx activity and GSH content were observed. Similarly, decreases in antioxidant enzyme activity of CAT and SOD were seen in Nile tilapia (*Oreochromis niloticus*) exposed to 42 µg Tl L^{-1} for 60 days (Farag et al. 2021). These studies suggest that oxidative stress is a conserved mechanism of Tl toxicity, although further work is required to extend these findings to other species and exposure scenarios.

Table 1.4. Acute and chronic lethal and effect concentrations of Tl to algae, aquatic invertebrates, and fish.

Exposure Type	Group	Common name	Latin name	Endpoint	Exposure length (h)	Medium	Tl Concentration (mg L^{-1})	Reference
Acute	Algae	Microalga	*Raphidocelis subcapitata*	EC_{50} (Growth)	72	OECD 201	0.087	Tatsi et al. 2015
				EC_{50} (Reprod.)			0.033	
				EC_{25} (Growth)			0.04	
				EC_{25} (Reprod.)			0.017	
				IC_{25} (Growth)		Not specified	0.09	Pickard et al. 2001
			Chlorella sp.	EC_{25} (Growth)		M4 without K	0.005	Rickwood et al. 2015
				EC_{50} (Growth)		Fraquil	0.16	Hassler et al. 2007
						Fraquil without K	0.002	
	Invert.	Amphipod	*Gammarus* sp.	LC_{100}		Not specified	4	Nehring 1962
		Crustacean	*Ceriodaphnia dubia*	LC_{50}	48	EPA "moderately" hard water	0.66	Lin et al. 2005
			Daphnia magna				1.66	
						Not specified	2.01	Pickard et al. 2001
						OECD 202	1.86[d]	Chapter 2
					1	OECD 202	571[d]	Chapter 5
				EC_{25} (Immobil.)	48	OECD 202	0.75	Tatsi et al. 2015
						Tap water	0.35	

Table 1.4. cont.

Exposure Type	Group	Common name	Latin name	Endpoint	Exposure length (h)	Medium	Tl Concentration (mg L^{-1})	Reference
Acute	Invert.	Crustacean	*Daphnia magna*	EC_{50} (Immobil.)	48	OECD 202	1.18[t]	Tatsi et al. 2015
						Tap water	0.51[t]	
			Daphnia pulex	EC_{25} (Immobil.)		OECD 202	0.725[t]	
						Tap water	0.58[t]	
				EC_{50} (Immobil.)		OECD 202	0.98[t]	
						Tap water	0.74[t]	
	Fish	Zebrafish	*Danio rerio*	LC_{50}	96	Tap water	0.87[t]	
		Bluegill sunfish	*Lepomis macrochirus*			Well water	132	Dawson et al. 1977
		Rainbow trout	*Oncorhynchus mykiss*			Not specified	4.27[n]	Pickard et al. 2001
				LC_{100}	72		10-15[t]	Nehring 1962
		European Perch	*Perca fluviatilis*				60[t]	
		Common roach	*Rutilus rutilus*				40-60[t]	
		Fathead minnow	*Pimephales promelas*	LC_{50}	96	Well water	0.86[ns]	LeBlanc and Dean 1984
				IC_{25} (Weight)	168	Tap water	0.201[d]	Rickwood et al. 2015

Table 1.4. cont.

Exposure Type	Group	Common name	Latin name	Endpoint	Exposure length (h)	Medium	Tl Concentration (mg L^{-1})	Reference
Chronic	Invert.	Amphipod	*Hyalella azteca*	LC_{25}	672	Tap water	0.01^{ns}	Borgmann et al. 1998
						Artificial medium without K	0.002^{ns}	
				EC_{25} (Growth)	1008		0.007^{ns}	
						Tap water	0.002^{ns}	
		Crustacean	*Daphnia* sp.	LC_{100}	168	Not specified	2-4[t]	Nehring 1962
			Ceriodaphnia dubia	LC_{50}			0.37^{n}	Pickard et al. 2001
				EC_{25} (Reprod.)			0.1^{n}	
		Crustacean		EC_{25} (Growth)		M4 without K	0.035^{d}	Rickwood et al. 2015
						M4	0.16^{d}	
			Daphnia magna	LC_{50}	672	Not specified	0.39^{ns}	Kimball 1978
				EC_{50} (Reprod.)	504	OECD 202	0.01^{d}	Chapter 3
				EC_{50} (Growth)			0.002^{d}	

Table 1.4. cont.

Exposure Type	Group	Common name	Latin name	Endpoint	Exposure length (h)	Medium	Tl Concentration (mg L^{-1})	Reference
Chronic	Fish	Fathead minnow	*Pimephales promelas*	LC_{50}	168	Tap water	$> 0.5^{d}$	Rickwood et al. 2015
					720	Well water	0.35^{ns}	LeBlanc and Dean 1984
		Zebrafish	*Danio rerio*		144	Tap water	0.29^{t}	Tatsi et al. 2015
							0.16^{t}	
		Rainbow trout	*Oncorhynchus mykiss*		672	Not specified	0.17^{ns}	Birge 1978

[t]: Total concentration
[d]: Dissolved concentration
[n]: Nominal concentration
[ns]: Total or dissolved not specified
LC_{25}: Concentration where 25% of the exposed population would experience mortality.
LC_{100}: Concentration where 100% of the exposed population would experience mortality.
IC_{25}: Concentration where 25% of the exposed population would experience inhibited function.
EC_{25}: Concentration where 25% of the exposed population would experience an effect.
Invert: Invertebrate
Reprod: Reproduction
Immobil: Immobilization

1.1.9. *Thallium regulations and water quality guidelines*

Based on the knowledge that Tl is bioavailable and can cause toxicity to aquatic organisms and humans, some regulatory bodies have developed guidelines for the protection of human health and aquatic ecosystems (Table 1.5). For example, there are USEPA guideline values that consider the exposure of human populations to Tl through drinking water and diet (0.24 µg Tl L^{-1}), and through diet alone (0.47 µg Tl L^{-1}) (USEPA 2002a). Additionally, drinking water standards have been developed. These include a maximum contaminant level (MCL) of 2 µg Tl L^{-1}, with a maximum contaminant level goal (MCLG) of 0.5 µg L^{-1} (USEPA 2009a). Thallium is also included on the USEPA's priority pollutant list (USEPA 2014), which are chemical pollutants of specific interest, and which are subject to regulatory control.

In Canada, the Canadian Council of Ministries of the Environment (CCME) have set a guideline value for the protection of aquatic life against Tl toxicity (0.8 µg L^{-1}: CCME 1999). In the development of this guideline, acute LC_{50} values of Tl toxicity to an aquatic invertebrate *Daphnia magna* (0.68 mg Tl L^{-1}), and fathead minnows (0.86 mg Tl L^{-1}) were considered (Kimball 1978; LeBlanc and Dean 1984). Additionally, chronic lowest observed effect concentration (LOEC) values for growth of fathead minnow embryos (0.08 mg Tl L^{-1}) and reproduction of *Daphnia magna* (0.39 mg Tl L^{-1}) were evaluated (Kimball 1978; CCME 1999). Ultimately, however, the water quality guideline for Tl was based upon studies assessing the bioaccumulation and toxicity of Tl in an aquatic plant, common duckweed (*Lemna minor*) (Brown and Rattigan 1979; Kwan and Smith 1988). The guideline for Tl was calculated by multiplying the *L. minor* 14-d EC_{50} value (8 µg L^{-1}) by a safety factor of 0.1. As the route of uptake and mechanisms of toxicity of Tl to plants can differ greatly from those of animals (Karbowska 2016), it is unknown whether this guidance adequately protects aquatic animals

against Tl toxicity. Additionally, since the development of the Tl guideline, the CCME has published a new protocol for the derivation of water quality guidelines (CCME 2007). This protocol is a 7-step process that considers all available toxicity data, as well as toxicity modifying factors, for a chemical substance of interest. As such, more data regarding the toxicity of Tl to aquatic animals will ultimately be of regulatory value.

Given the hypothesized protective effect of K^+ on Tl toxicity (Hassler et al. 2007), guideline values may be improved by considering K^+ concentrations when assessing the risk of aquatic Tl contamination. One approach that may prove useful is the Biotic Ligand Model (BLM), a predictive risk assessment tool for the protection of aquatic ecosystems against trace metal toxicity (Di Toro et al. 2001). In a BLM, toxicity is predicted by incorporating mechanistic understanding of trace metal uptake; the relationship between accumulation and toxicity; and knowledge of the interactions between the trace metal and water chemistry (Di Toro et al. 2001; Niyogi and Wood 2004). For example, Ag^+ is taken up across the gills of aquatic animals through apical Na^+ channels (Bury and Wood 1999). It is known that DOC binds Ag, reducing bioavailability, and consequently Ag toxicity (Glover and Wood 2005a). Similarly, elevated water Na^+ can outcompete Ag^+ for uptake, also reducing toxicity (Bury and Wood 1999). Thus, with the knowledge of how Na^+ and DOC can reduce bioavailability and toxicity, site-specific predictions of toxic impact can be made based on water chemistry parameters and measured Ag concentration. Under the same paradigm, if bioavailability of Tl is effectively reduced by K^+ concentration, and if Tl bioaccumulation relates to Tl toxicity, then measures of water K^+ can be incorporated for a more accurate prediction of the risk associated with a given concentration of waterborne Tl. Indeed, a Tl BLM has been developed by Hassler et al. (2007), in which effect concentrations for Tl inhibition of microalgal growth were shown to be governed by K^+

concentration. This relationship showed that a 40- to 160-fold molar excess of K^+ over Tl was needed to ameliorate Tl toxicity in *Chlorella* sp. However, the applicability of this relationship in terms of its capacity to protect other aquatic organisms from Tl toxicity has not been established.

Table 1.5. Regulatory guidelines for human health and aquatic life.

Agency	Limit value ($\mu g\ L^{-1}$)	Reference
USEPA, human health water quality criteria for consumption of water + organism	0.24[ns]	USEPA 2003
USEPA, human health water quality criteria for consumption of organism only	0.47[ns]	USEPA 2003
USEPA, drinking water, MCLG	0.5[ns]	USEPA 2009
USEPA, drinking water, MCL	2[ns]	USEPA 2009
CCME, freshwater	0.8[t]	CCME 1999
China, water quality	0.1[ns]	CMEP 2002
China, drinking water	0.1[ns]	MHC 2006

MCLG: Maximum contaminant level guideline.
MCL: Maximum contaminant level.
[ns]: Dissolved/total not specified
[t]: Total concentration

1.1.10. *Model organisms*

The studies in this thesis are focussed on two freshwater species, the cladoceran *Daphnia magna* and rainbow trout (*Oncorhynchus mykiss*). *Daphnia magna* are freshwater crustaceans commonly found in lacustrine ecosystems across the Northern hemisphere. They display a number of traits that make them important indicator species, including rapid growth, a short maturation time, high reproductive output, and a general sensitivity to aquatic contaminants (Baudo 1987). Furthermore, daphnids serve as an important model organism in toxicology, and are the subject of standardized toxicity testing methods for the CCME, USEPA and Organisation for Economic Cooperation and Development (OECD)(Biesinger et al. 1987; Environment

Canada 2000b; OECD 2004). These methods exist for the assessment of both acute and chronic endpoints including survival/immobility, growth, and reproduction (Biesinger et al. 1987; OECD 2004). To date, several studies have assessed Tl toxicity to *D. magna* (Pickard et al. 2001; Tatsi et al. 2015), reporting 48-h LC_{50}/EC_{50} values in the range of 1.2 to 4 mg L^{-1}. The variability in these numbers highlights the need for further studies in this species, especially as data derived using daphnids are foundational in many regulatory assessment schemes (CCME 1999; 2007). The other focal species in this thesis is the rainbow trout (*Oncorhynchus mykiss*). This teleost fish is native to Pacific Ocean tributaries and has long been associated with healthy streams in North America (USGS 1998). Historically, salmonid fish are considered among the most sensitive to trace metals, although this is a pattern that does not appear to be true for all metal contaminants (Besser et al. 2020). Importantly, however, rainbow trout have been recognized as a surrogate species for cold-water fish by the USEPA (Dwyer et al. 1995). Additionally, like *D. magna*, standardized protocols have been developed for rainbow trout for measuring toxicity and sub-lethal effects of aquatic contaminants (USEPA 2002b; Lazorchak and Smith 2007). Although data on Tl toxicity to rainbow trout are scarce, acute (96-h) and sub-chronic (28-d) LC_{50} values of 4.3 mg L^{-1} and 0.17 mg L^{-1}, respectively, have been derived (Birge 1978; Pickard et al. 2001). The studies described in this thesis add to the understanding of Tl toxicity to rainbow trout through addressing hypotheses associated with Tl bioaccumulation, and effects on ionoregulation and oxidative stress.

1.2. Research goals and objective

The goal of this thesis is to develop a greater understanding of the effects of dissolved Tl on aquatic organisms as they relate to bioavailability, bioaccumulation, and the underlying mechanisms that cause Tl toxicity. Through the use of molecular, biochemical, physiological,

behavioural, and toxicological assays, and advanced analytical chemistry, this work will: determine the modifying effects of water chemistry (including major ion concentration) on Tl toxicity; delineate patterns of Tl accumulation; and document effects of Tl on the key toxicological model species *Daphnia magna* and rainbow trout (*Oncorhynchus mykiss*). These will be demonstrated over both acute and (sub)chronic exposure periods. All exposures throughout this thesis were conducted at circumneutral pH and reported Tl concentrations are dissolved unless otherwise stated. The overall goal of this research is to provide data that can contribute towards the creation and refinement of global and Canadian water quality guidelines for Tl.

1.3. Thesis outline

1.3.1. *The effects of major ions and dissolved organic matter (DOM) on complexation and toxicity of dissolved thallium to Daphnia magna:*

Changes in water chemistry influence the speciation and bioavailability of metals in aquatic ecosystems. To date, however, little is known regarding the effects of water chemistry on Tl bioavailability, and thus toxicity. In Chapter 2 the effects of changes in water ions and the presence of DOM (a ubiquitous metal-binding ligand in natural waters) on Tl toxicity to *Daphnia magna* is examined. Metal speciation was modeled using visual MINTEQ and measured using AF4 to determine if changes in water chemistry affected Tl speciation. It was hypothesized that Tl toxicity would be influenced by water K^+ concentration as Tl is a known K^+ mimic. Also, the presence of DOM was predicted to reduce Tl toxicity by forming non-exchangeable organic complexes, thus reducing Tl bioavailability.

1.3.2. *Chronic toxicity of waterborne thallium to Daphnia magna:*

Although several studies have considered acute toxicity of Tl to aquatic organisms, there is little literature related to chronic toxicity. Therefore, the effects of chronic Tl exposure to *Daphnia magna* were examined. In particular, survival, reproduction, growth and body burden were assessed. In this study (Chapter 3) it was hypothesized that chronic Tl exposure would result in an increased Tl body burden and decreased survival, growth, and reproduction.

1.3.3. *Effects of thallium exposure on phototactic behaviour in Daphnia magna*:

Thallium is a known neurotoxicant in humans. However, there are few studies that provide experimental support for this being a mechanism of importance in aquatic organisms. In the presented work (Chapter 4), phototactic behaviour in the presence of Tl was assessed in *Daphnia magna*. In addition, biochemical assays were used to determine if observed effects on behaviour were the result of sensory or motor impairment. As acute Tl exposure can cause sensory impairment in mammals, it was hypothesized that Tl would impair phototactic behaviour through a similar mechanism in aquatic organisms.

1.3.4. *Mechanistic examination of thallium and potassium interactions in Daphnia magna:*

The major mechanism of Tl toxicity appears to be related to its ability to mimic K^+, as demonstrated by studies that show a modifying effect of water K^+ on Tl toxicity. To develop a better mechanistic understanding of this relationship, the effects of K^+ on Tl toxicity were examined using K^+ analogues and putative K^+ transport blockers. In this study it was hypothesized that changes in water K^+ concentration would influence Tl toxicity, and that Tl exposure would interfere with K^+ uptake.

1.3.5. *Accumulation of thallium in rainbow trout (Oncorhynchus mykiss) following acute and sub-chronic exposure:*

Thallium is bioavailable and accumulates in aquatic biota. Chapter 6 aimed to measure tissue-specific Tl accumulation in rainbow trout, and determine how it relates to exposure concentration and exposure length. In this study, gill, blood plasma, muscle and otolith tissues were examined for Tl burden. Additionally, K^+ concentration was measured in blood plasma and muscle tissue to delineate any effect of Tl on K^+ homeostasis. It was hypothesized that Tl accumulation following acute and sub-chronic exposure would be observed, and be associated with uptake through the gills, distribution through the body via blood, resulting in further accumulation in tissues such as muscle and otolith.

1.3.6. *Effects of acute and sub-chronic waterborne thallium exposure on ionoregulatory transporters in the gill and kidney of rainbow trout:*

One of the mechanisms by which trace metals induce toxicity is the disruption of ion transport. In freshwater teleosts, branchial and renal transporters are critical for maintaining ionoregulatory homeostasis. Since Tl handling is commonly linked to its ability to mimic K^+, it is possible that Tl exposure can result in changes in ionoregulatory transporter function due to interactions between the two cations. In this study (Chapter 7) it was hypothesized that following acute and sub-chronic exposure to Tl, changes in ionoregulatory transporters would occur in the gill and kidney of rainbow trout.

1.3.7. *Effects of acute and sub-chronic waterborne thallium exposure on antioxidant capacity and protein carbonylation in liver of rainbow trout:*

Oxidative stress is a known mechanism of Tl toxicity. To date, however, effects of Tl on oxidative stress endpoints such as antioxidant capacity and protein damage have not been assessed in freshwater regulatory species such as rainbow trout. For this study (Chapter 8), I

hypothesized that Tl exposure would cause changes in antioxidant capacity, which would also be reflected in altered protein carbonylation, indicative of an effect of Tl on oxidative stress.

2. The effect of major ions and DOM on complexation and toxicity of dissolved thallium to *Daphnia magna*

2.1. Introduction

Thallium is a trace element of significant concern with respect to its potential impact on aquatic biota (Couture et al. 2011). Commonly associated with the mining of base metals and coal, Tl has been observed in mine tailing waters at levels as high as 15 mg L^{-1}, values that are above LC_{50} values for a number of aquatic species (Pickard et al. 2001; Williams-Beam and Twidwell 2003). For example, the acute Tl LC_{50} values for the key freshwater toxicity test species *Daphnia magna* and rainbow trout are reported to be 2.01 and 4.27 mg L^{-1}, respectively (Pickard et al. 2001). While such high concentrations are rare and Tl is present in most aquatic systems at very low concentrations (Couture et al. 2011), a recent study has shown that Tl has a considerable capacity for bioaccumulation. Concentrations of Tl averaged approximately 3 ng L^{-1} in the Athabasca River in Northern Alberta, Canada, but of all trace elements analyzed in fish otoliths collected from these waters, Tl showed the greatest tissue enrichment relative to its concentration in water (6071 fold; Shotyk et al. 2017; 2019). Because of the association between trace metal accumulation and toxicity, these findings raise concerns regarding Tl toxicity, especially in waters where Tl concentrations are elevated.

In order to protect aquatic biota against the harmful effects of elevated Tl, some jurisdictions have developed water quality criteria for this trace element. In Canada, for example, the criterion value for Tl is 0.8 µg L^{-1}. This value was derived by taking the 14-d median effect concentration obtained from studies of Tl toxicity to the aquatic plant duckweed (*Lemna minor*; Brown and Rattigan 1979), and multiplying by a correction factor of 0.1 (CCME 1999). The

resulting criterion is one that is regularly exceeded in Canadian waters as a consequence of enrichment from industry (Cheam 2001).

In recent years there has been a move towards incorporating assessments of bioavailability into water quality criteria for trace elements in natural waters. One such approach is the BLM (Di Toro et al. 2001). This tool uses water chemistry to predict the bioavailable fraction of a metal (more specifically, its free ionic form), as this is a measure that governs the bioaccumulation of the metal at a biologically sensitive site (e.g. the fish gill). Ultimately, the magnitude of bioaccumulation determines effect, allowing site-specific predictions of toxic impact by calculation of bioavailable metal fraction. Biotic ligand models have been developed to predict the toxicity of multiple trace elements in aquatic and terrestrial settings, over both acute and chronic exposure periods. For example, extensive validation of freshwater models for metals such as Cu and nickel (Ni) has led to their inclusion in regulatory frameworks worldwide (Rüdel et al. 2015). Bioavailability of a trace element is usually associated with the dissolved fraction, which is operationally defined as any particle that can pass through a 0.45 μm filter. However, this definition does not account for the presence of metals that are complexed by or bound to particles such as colloids and dissolved organic matter (DOM), which may pass through a 0.45 μm filter, but which may not be bioavailable, and therefore do not contribute towards toxicity (e.g., Buffle and Leppard 1995).

To date there is very little understanding of how water chemistry influences Tl speciation and/or toxicity. Thallium is found in two oxidation states in natural waters: Tl(I) and Tl(III), with the former state predominating (Lin and Nriagu 1998). This is a consequence of the rapid reduction of Tl(III) to Tl(I) in waters with circumneutral pH (Kaplan and Mattigod 1998). In its monovalent form, Tl is considered to cause toxicity through its mimicry of K^+ (Nehring 1962;

Pickard et al. 2001; Tatsi et al. 2015). This effect is mediated principally through similar ionic radii and charge, allowing the hydrated Tl^+ to cross epithelia via K^+ transport pathways, and inhibit processes related to K^+ transport (Nriagu 1998; Couture et al. 2011). Consequently, Tl toxicity should be affected by the concentration of monovalent ions in the water and/or the presence of ligands that complex with Tl, preventing it from accessing transport pathways.

The goal of the present study was to examine the toxicity of Tl to *Daphnia magna* as a function of water chemistry. Specifically, the roles of complexation and competition in mediating the toxic effects of Tl in freshwaters were investigated. This analysis included assessing dissolved Tl speciation using Visual MINTEQ and measuring its complexation with DOM using AF4 coupled to ICPMS. This latter approach fractionates dissolved material in the 1–100 μm range using a diffusion-based non-destructive separation (Cuss et al. 2017). This facilitates the fractionation of trace elements into different forms, and the identification of interactions of dissolved metals with organic and inorganic ligands. *Daphnia magna* were chosen for the present study as they are a commonly employed laboratory toxicity test species that exhibit relatively high sensitivity to trace metals, including Tl (Tatsi et al. 2015). Because of the known interaction between Tl and K^+, it was hypothesized that Tl toxicity to *Daphnia magna* would be reduced in waters with elevated K^+ concentrations. The effects of water pH (through elevated bicarbonate, which may also increase inorganic complexation of Tl), and the role of DOM were also tested. Dissolved organic matter has a well described protective effect against many metal contaminants (e.g., Glover et al. 2005), an effect mediated through complexation of cationic metals by DOM, which reduces the capacity for ion mimicry. To date, however, the effects of DOM on Tl toxicity remain unexplored. Ultimately, developing a mechanistic understanding of relationships between water chemistry, Tl speciation and toxicity may

contribute to site-specific guidelines for this element, through the development of water quality criteria that incorporate bioavailability.

2.2. Methods

2.2.1. *Daphnia magna culture*

A *Daphnia magna* culture was acquired from Aquatic Research Organisms (Hampton, New Hampshire, USA), and maintained in the Department of Biological Sciences at the University of Alberta. *Daphnia* were kept in a reconstituted artificial water as recommended in the Organization for Economic Co-operation and Development guidelines (International Organization for Standardization (ISO) test water 1; OECD 2004). The composition of this water was (in mM): 2.0 $CaCl_2$, 0.5 $MgSO_4 \bullet 7H_2O$, 0.77 $NaHCO_3$, 0.08 KCl; pH 7.5, made up in a high-quality ultrapure water (>18 MΩ·cm at 25°C, ELGA LabWater, High Wycombe, UK). This medium is hereafter referred to as OECD water. The *Daphnia* culture was maintained on a 16:8 hour dark: light cycle, at 22°C, with daily feeding (Roti-Rich Liquid Invertebrate Food).

2.2.2. *Chemicals*

Thallium(I) nitrate (purity 99.999%, trace metals basis) was purchased from Sigma-Aldrich (St. Louis, Missouri, USA), and a stock solution of 50 mg L^{-1} was reconstituted in 1% trace element grade nitric acid (HNO_3), with pH adjusted to 7.5 using 0.1 M sodium hydroxide. Freshly prepared stock solutions were used to dose all exposure solutions. Powdered reverse osmosis DOM samples (Suwannee River natural organic matter (NOM), Suwannee River Fulvic Acid, and Suwannee River Humic Acid) were obtained from the International Humic Substances Society. These sources were reconstituted in ultrapure water.

2.2.3. *Toxicity assays*

To determine the acute LC_{50}, appropriate volumes of the Tl stock solution were added to 50 mL of OECD water in 50-mL acid-washed glass beakers to give nominal test concentrations of 0 (no added Tl), 0.1, 0.25, 0.5, 1, 2, 4, 8 mg L^{-1}. Solutions were made up 24-h prior to test initiation to facilitate speciation equilibration. To initiate the test, 10 *Daphnia magna* neonates (<24-h old) were added to each glass beaker, with each test concentration replicated six times (i.e., n = 6). *Daphnia* were not fed during the test duration to avoid potential confounding effects of food on metal speciation. Tests were conducted at 22°C, under a 16:8 hour dark: light cycle. Water samples were taken at 0-h (immediately after *Daphnia* addition) and at 48-h, either without treatment (total) or after passage through an acid cleaned 0.45 µm filter ("dissolved"; 0.45-µm Millex-HV Syringe Filter; Sigma-Aldrich; Saint Louis, MO, USA) for analysis of Tl concentration (see Section 2.2.5). After 48-h, *Daphnia* mortality (cessation of any movement) was recorded.

2.2.4. *Effect of water chemistry*

Using the LC_{50} value determined from the previous experiment, Tl was added to water of a number of different compositions to a final concentration of 1.86 mg L^{-1} (see Table 2.1). For each of these compositions, a control experiment was conducted in the absence of Tl to ensure that toxicity was not related to the water chemistry. No mortalities were observed in any control experiments, with the exception of $CaCl_2$ (see Section 2.3.3). To minimize the effect of biomass on water chemistry these assays were performed at a low biomass to water ratio, in 250-mL acid-washed glass beakers (n = 6-11), but otherwise followed the protocol described in Section 2.2.3. Samples of total and dissolved water were collected at 0 and 48-h for analysis via AF4-ICPMS.

Table 2.1. Nominal chemistry of experimental waters.

Water Chemistry Manipulation	pH*	$[Na^+]$ mM	$[K^+]$ mM	$[Cl^-]$ mM	$[Mg^{2+}]$ mM	$[SO_4]$ mM	$[CO_3^{2-}]$ mM	$[Ca^{2+}]$ mM	[DOC] mg C L^{-1}
OECD water	7.5	0.77	0.08	4.08	0.5	0.5	0.77	2	0
+ 10 mM $CaCl_2$	8.3	0.77	0.08	14.6	0.5	0.5	0.77	10	0
+ 10 mM NaCl	6.8	10	0.08	14.08	0.5	0.5	0	2	0
+ 10 mM $NaHCO_3$	8.5	10	0.08	4.08	0.5	0.5	10	2	0
+ 10 mM KCl	8.5	0.77	10	14	0.5	0.5	0.77	2	0
+ 10 mg/L Suwannee River Natural Organic Matter	7.5	0.77	0.04	4.08	0.5	0.5	0.77	2	5
+ 10 mg/L Suwannee River Fulvic Acid	7.5	0.77	0.04	4.08	0.5	0.5	0.77	2	5
+ 10 mg/L Suwannee River Humic Acid	7.5	0.77	0.04	4.08	0.5	0.5	0.77	2	5

* pH value measured via calibrated Fisher Scientific Ab15 pH meter.

2.2.5. *Metal speciation and concentration analysis*

Metal concentration and speciation within dissolved water samples were analyzed by AF4-ICPMS. Total metal concentrations were measured via introduction of the sample to an injection valve downstream from the AF4. Full details regarding analysis and procedures are described in Cuss et al. (2017), but are briefly outlined here. Thallium speciation analysis was conducted using an AF4 equipped with a 300 Da membrane to reduce overall loss of small organics and other colloids through the membrane. Samples (300 µL) were initially injected via autosampler, focused for 6 min at a crossflow rate of 2.1 mL min^{-1}, and then eluted. The eluent was composed of $(NH_4)_2CO_3$ buffer, adjusted to pH = 8.3, and specific conductance = 300 µS

cm^{-1}. During analysis, blanks were analyzed after every sample to clean the membrane and monitor carryover, and the channel and ICPMS instrument response/accuracy were respectively recalibrated after every 10 samples using a mixture of bromophenol blue and polystyrene sulfonate size standards (0.67–20.7 kDa), multi-element standard solution, and standard reference materials: Spectrapure Standard Surface Water 2 (SPS SW2) diluted 100 fold, and National Institute of Standards and Technology (NIST) 1640a diluted 10 fold. Samples were acidified online downstream of the AF4 by adding double-distilled HNO_3 to a final concentration of 2% through a micro-mixing tee. The acid solution was spiked with 5 µg L^{-1} of indium and bismuth as internal standards to correct for fluctuations in the sensitivity of ICPMS measurements. The limit of detection for ICPMS analysis was determined to be 0.1 ng L^{-1}, calculated as the mean of three blank injections plus three times the standard deviation of the blank. Analysis of metal concentrations from AF4-ICPMS analysis were performed using Qtegra™ Intelligent Scientific Data Solution™ Software, and speciation was assessed using statistical fractogram deconvolution in Matlab (Cuss and Guéguen 2012; Cuss et al. 2017). Data were normalized by intensity to allow for discrete analysis of peaks and DOM. To determine if the measured speciation agreed with predictions based on thermodynamic equilibrium models, results from the AF4 analyses were compared to data obtained by modelling speciation using Visual MINTEQ (ver. 3.1; Gustafsson 2015). For all speciation calculations, ionic strength was fixed at 0.001 and the Stockholm Humic Model (SHM) was employed to characterize Tl-DOM interactions. To further validate the speciation outcomes derived from Tl analyses, a positive control was employed. Copper is a trace element that is known to readily form strong complexes with DOM and inorganic anions (Craven et al. 2012). Consequently, solutions of Cu (0.17 to

0.62 µg L^{-1}) were subjected to AF4-ICPMS analysis in the same base waters that were used to test Tl toxicity.

2.2.6. *Statistics*

The Toxicity Relationship Analysis Program (TRAP; USEPA) was used to determine LC_{10}, LC_{20}, and LC_{50} values and their 95% confidence intervals (CI). The effects of water chemistry on Tl toxicity were analyzed using a one-way analysis of variance (ANOVA) via Prism Graph Pad, followed by a post hoc Tukey's test, at an alpha level of 0.05. This analysis was performed after ensuring that data conformed to assumptions of parametric analysis using the Shapiro-Wilk test for normality, and the F-test for homogeneity of variance.

2.3. Results and discussion

2.3.1. *Water thallium concentrations*

Measured Tl concentrations in LC_{50} experiments were closely matched to nominal values (Table 2.2). Indeed, all measured values fell comfortably within the 95% CI for a given test concentration. For tests examining the effects of varying water composition, measured Tl concentrations averaged 1.90 ± 0.20 mg L^{-1} across all water treatments, and therefore closely matched nominal values (1.86 mg L^{-1})(data not shown).

Table 2.2. Nominal and measured (mean ± SE) water Tl concentrations in LC_{50} experiments.

Nominal Tl concentration (mg L^{-1})	Dissolved (mg L^{-1})	Total (mg L^{-1})
0	a	a
0.1	0.11 ± 0.001	0.11 ± 0.001
0.25	0.27 ± 0.014	0.27 ± 0.008
0.5	0.57 ± 0.002	0.55 ± 0.002
1	1.10 ± 0.047	1.03 ± 0.003
2	2.28 ± 0.036	2.22 ± 0.042
4	4.35 ± 0.026	4.48 ± 0.102

a = control dissolved Tl was 1.1 ± 0.2 µg L^{-1} and control total Tl was 1.5 ± 1.6 µg L^{-1}

2.3.2. *Acute thallium toxicity*

The calculated 48-h LC_{50} value for Tl was 1.86 (95% CI 1.55–2.17) mg L^{-1} (Figure 2.1). The 48-h LC_{10} and LC_{20} values were calculated as 0.69 (95% CI 0.13–1.25) and 1.08 (95% CI 0.68–1.49) mg L^{-1} (Table 2.3). With the exception of the $CaCl_2$ treatment (see Section 2.3.3 below), no mortalities were recorded in control replicates.

The LC_{50} calculated in the current study suggests that Tl-related mortality of *Daphnia* would occur in highly Tl-contaminated mining effluents, where Tl concentrations are in the mg L^{-1} range (Williams-Beam and Twidwell 2003). However, there is limited risk of *Daphnia* mortality in most global freshwaters, where Tl concentrations are generally in the order of a few ng L^{-1} (Couture et al. 2011). The toxicity data generated here are generally aligned with values reported previously in the literature. For example, Pickard and colleagues (2001) reported an LC_{50} of 2.01 mg L^{-1} for Tl toxicity to *Daphnia magna*, while Lin and colleagues (1995) determined an LC_{50} of 1.66 mg L^{-1}. Both of these values overlap with the 95% CI's obtained in

the present work. However, using the same water composition as in the current study (i.e., OECD water), Tatsi and colleagues (2015) found *D. magna* to be more sensitive to Tl, with an LC_{50} value of 1.18 mg L^{-1}. This latter finding could be a function of experimental design and toxicity calculation. In the previous work the highest test concentration was 1.2 mg L^{-1} (i.e. very close to the LC_{50}), and mortality was less than 60% at this concentration (Tatsi et al. 2015). This results in uncertainty because the survival curve must be extrapolated to complete mortality and contravenes the OECD test guideline recommendation that at least one test concentration should induce total lethality (OECD 2004). Consequently, the experiments of Tatsi and colleagues may overestimate Tl toxicity to *D. magna*.

Table 2.3. Lethal concentrations of thallium to *Daphnia magna*.

Response	LC_x (mg/L)	95% Lower Confidence Level (LCL) (mg L^{-1})	95% Upper Confidence Level (UCL) (mg L^{-1})
LC_{10}	0.69	0.13	1.25
LC_{20}	1.08	0.68	1.49
LC_{50}	1.86	1.55	2.17

Values generated via the USEPA TRAP software
LC_x: Lethal concentration where x percent of the exposed population experiences mortality

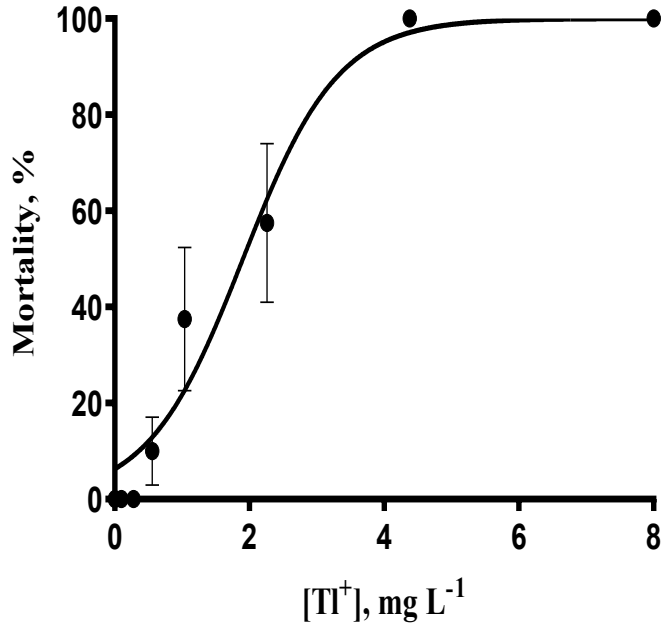

Figure 2.1. Calculated 48-h median lethal toxicity of Tl to *Daphnia magna* in OECD water. Plotted points represent the means (± SE) of 6 replicates.

2.3.3. *Effect of water chemistry on thallium toxicity*

When *D. magna* were exposed to the Tl LC_{50} concentration in waters with variable chemistry, elevated mortality (82 ± 15%) was observed when the base OECD water was supplemented with 10 mM $CaCl_2$ (Figure 2.2). However, it is important to note that this was not an effect of Tl, as the control water (with no Tl added) showed complete (i.e. 100%) mortality (data not shown). Calcium is known to exert considerable influence on *Daphnia* health and survival, although mostly from the perspective of calcium deficiency (e.g. Hamza et al. 1998). While calcium toxicity is not well studied, harmful effects of $CaCl_2$ to daphnids have been reported: a 64-h lethal threshold of 920 mg L^{-1} (8.3 mM) was observed for *D. magna*, and a 48-h LC_{50} of 1663 mg L^{-1} (15.0 mM) has been reported for *Ceriodaphnia dubia* (Anderson 1950; Mount et al. 2016). The specific mechanism of $CaCl_2$ toxicity has not been investigated, but it may be due to interference with Na^+ transport. Sodium uptake across the gill of *D. magna* is

achieved by the electrogenic 2 Na^+/H^+ exchanger, a transporter that may also be used by Ca^{2+} (Glover and Wood 2005b). Consequently, high Ca^{2+} concentrations may outcompete Na^+ for uptake, inhibiting the capacity of daphnids to recover Na^+ lost to the surrounding medium via diffusion. Since previous research has noted that $CaCl_2$ is more toxic to daphnids than $CaSO_4$ and $CaCO_3$, it seems likely that the chloride (Cl^-) component also plays a role (Mount et al. 2016).

No other water chemistry significantly affected the survival of *D. magna* that were exposed to the LC_{50} concentration of Tl (Fig. 2.2). There was, however, a trend ($p = 0.2$) for decreased mortality when the K^+ concentration of exposure water (added as KCl) was elevated. This trend was not observed with NaCl supplementation, suggesting that it was driven by the cation. An effect of K^+ supplementation on Tl toxicity was hypothesized owing to known interactions between the monovalent charged forms of these ions in biology, likely resulting from similar ionic radii (Rossi and Norby 1993). For example, Tl is known to substitute for K^+ in K^+-facilitated transport processes (Tao et al. 2008), and K^+ supplementation also ameliorates Tl toxicity to the alga *Chlorella* (Hassler et al. 2007). The lack of significant impact of KCl on Tl toxicity in the current work may be a consequence of experimental design.

Thallium has an affinity for K^+ transporters that is 2- to 10-fold greater than K^+ itself (Brismar 1998). Consequently, significantly higher concentrations of K^+ are required to outcompete Tl for binding sites, reduce Tl uptake, and thus ameliorate toxicity. For example, Hassler and colleagues (2007) noted that a K^+ excess of 40- to 160-fold was required to offset the toxic effects of Tl in *Chlorella*. At the test concentration of 1.86 mg Tl L^{-1} (9 µM) that was used in the current work, KCl supplementation produced a K^+ concentration of 134 µM, representing only a 15-fold excess, one that may have been insufficient to outcompete Tl for

binding sites. However, a previous study did see a significant decrease in the LC_{50} of Tl in *D. magna* in a tap water (0.51 mg L^{-1}) relative to a reconstituted water (1.18 mg L^{-1}) (Tatsi et al. 2015). At the LC_{50} value for the tap water, the K^+:Tl ratio was 15, compared to 31 for the reconstituted water. This pattern also suggests a role of K^+ in the amelioration of Tl toxicity, supporting the hypothesis that the K^+:Tl ratio was insufficient to observe a significant effect in the current work.

The lack of a significant impact of DOM on Tl toxicity is another key finding (Figure 2.2). Dissolved organic matter is a ubiquitous and heterogeneous component of all natural waters, with important roles in metal toxicity amelioration. Cationic metals form stable complexes with negatively charged functional groups in DOM, decreasing metal bioavailability and thus toxicity (e.g., Glover et al. 2005). There are two major extractable components of DOM: fulvic acids and humic acids. Fulvic acids and humic acids have distinct structures and functional groups, and differ in molecular weight and solubility. Consequently, some authors have noted differences in metal binding and toxicity for these different extracts (Doig and Liber 2007; He et al. 2017). In the current work the effects of commercially-available DOM extracts were assessed to determine if these would ameliorate Tl toxicity to *Daphnia*. The lack of apparent amelioration suggests a low binding affinity of Tl for the functional groups that were present in the different DOM extracts that were tested. For example, reported values for the mean binding constants (log K) for Tl to hydroxyl and carboxyl sites on fulvic acid are 3.32 and 4.83, respectively (Kaplan and Mattigod 1998). On the other hand, Cu has a strong affinity for DOM, with log K values near 9 for some binding sites (Playle 1998). The concentrations of DOM used in the current study (5 mg C L^{-1}) are characteristic of typical DOM concentrations in northern lakes and streams (Thurman 1985). These results thus suggest that DOM does not play

a significant role in ameliorating Tl toxicity in natural waters. This experimental was verified using analytical speciation analysis and biogeochemical speciation modelling, as discussed below.

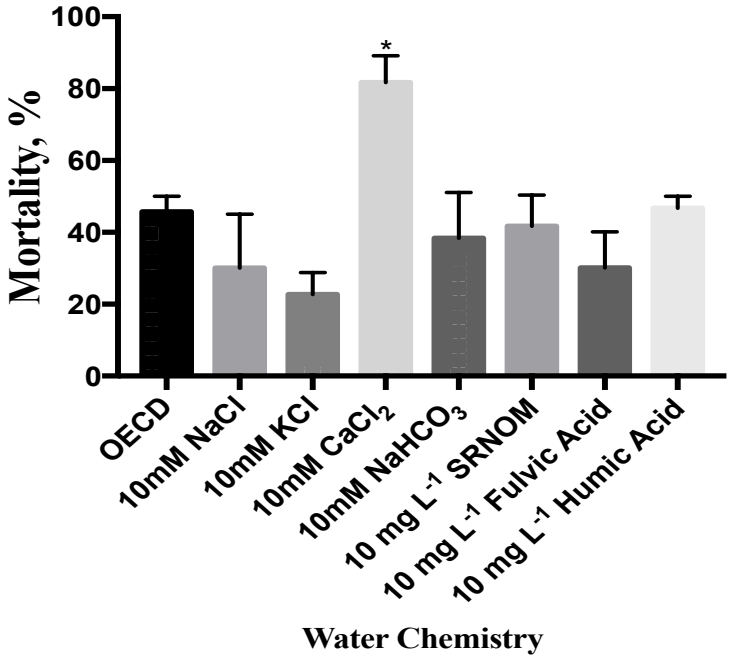

Figure 2.2. Effect of water chemistry on mortality of *Daphnia magna* after 48-h at a Tl concentration of 1.86 mg L^{-1}. Full water chemistry details are provided in Table 2.1. Plotted points represent the mean (± SE) of 6-11 replicates. Asterisk indicates significant difference relative to the control (OECD water), as determined by one-way ANOVA, with post hoc Tukey's test, at $\alpha = 0.05$.

2.3.4. *Thallium speciation*

Geochemical speciation modelling (Figure 2.3) predicted that Tl was mainly present in its ionic form in the waters used for the LC_{50} experiments, and that speciation was largely unaffected by changes in water chemistry. Indeed, in all conditions geochemical speciation modelling predicted that more than 94% of Tl was present as a monovalent ion (Tl^+), with small amounts of TlCl, and $TlSO_4^-$. No significant concentrations of Tl-DOM complexes were

predicted, and the presence or absence of DOM in the model had no impact upon Tl speciation. This speciation differs significantly from more labile metals such as Cu. The modelling of Cu speciation in our waters suggested that, in contrast to Tl, Cu speciation was predicted to be significantly influenced by both inorganic and organic ligands (Table 2.4).

Additional modelling was performed (not shown) to determine whether more extreme water chemistry scenarios, and/or lower, more environmentally-realistic, Tl concentrations, affected Tl speciation. A pH range of 4 to 11 was examined and no differences in Tl speciation was observed irrespective of model Tl concentration.

In the current study, speciation modelling was performed via Visual MINTEQ, using the SHM approach to model Tl-DOM interactions. The SHM framework is similar to the humic ion-binding model incorporated into Windermere Humic Aqueous Model (WHAM) VII, but WHAM VII has not been parameterized for Tl, likely because of the relative paucity of data regarding Tl-DOM interactions. Reflecting their general similar approaches to speciation modelling (Tipping et al. 2011; Gustafsson 2015), studies have shown that predicted outcomes modeled via Visual MINTEQ and WHAM VII are largely in agreement (e.g., Leguay et al. 2016). Furthermore, given that DOM does not appear to be a high affinity ligand for Tl, and that Visual MINTEQ model outcomes matched the measured speciation via AF4, then the choice of speciation model was unlikely to have markedly influenced predictions of Tl speciation in the experimental waters.

The fractionation of Tl and Cu into mainly ionic and DOM-associated species via AF4-ICPMS confirmed the results of speciation modelling (Figures 2.4A, 2.4B). Using Tl at the LC_{50} concentration in OECD water, it was apparent that the void peak for Tl occurs early, and there are no other peaks. Metals in their ionic form that are retained by electrostatic repulsion from the

membrane are not focused by the flow field, and so will move through the channel more rapidly than other, larger species. The fractionation profile therefore indicates that Tl is present mainly in its ionic form. In the absence of DOM, the profile of Cu was similar to that of Tl (Figure 2.4A). Copper was used as a positive control for AF4 analyses since there is a better understanding of its speciation in freshwaters, and it is known to complex strongly with DOM (Playle 1998). Figure 2.4B shows the predicted speciation of Tl and Cu in the presence of Suwannee River fulvic acid. In agreement with its known ability to bind DOM, the Cu peak occurs later than the Tl peak, and at the same time as the DOM, indicative of a complex between the metal and the organic ligand. The earlier elution of Tl in the void peak was consistent with the pattern observed for Tl in the absence of DOM, and shows that Tl is in its ionic form and did not associate with the retained DOM. These data suggest that Tl does not have a strong affinity for DOM under the test conditions, supporting the lack of apparent protection against Tl toxicity seen in Figure 2.2.

The outcomes of the AF4-ICPMS speciation analysis may be influenced by the relative concentration of free ions in the solution. For example, at high Tl concentrations such as the 1.86 mg L^{-1} Tl that was used in Fig. 2.4, the binding of Tl to DOM could be obscured by the tail of the peak from the larger proportion of free, ionic Tl. To assess this, AF4-ICPMS analysis was conducted using much lower concentrations of Tl and Cu (0.2 μg L^{-1}), accompanied by DOM. Even at these low concentrations, there was no apparent association between Tl and DOM (Figure 2.5). This is in direct contrast to the pattern observed for Cu, which tracks closely with DOM, indicative of Cu-DOM complexes.

A key component of Tl speciation not considered in the current study is its oxidation state. In waters of circumneutral pH (6-8), Tl is capable of existing in either a monovalent or trivalent state (Nriagu 1998). However, while Tl(I) is inert and exists mainly in an ionic form,

Tl(III) is readily reduced to Tl(I) or it will precipitate as $Tl(OH)_3$. In its trivalent state, Tl will also have distinct affinities for potential natural binding ligands, so that Tl speciation and toxicity is likely dependent on oxidation state (Nriagu 1998). Supporting this, some studies have shown Tl(III) to be more toxic than Tl(I) (Rickwood et al. 2015; Molina et al. 2017). However, the lack of any measured Tl species aside from the free ion in the current experiments suggests that Tl was mainly present as Tl(I). Indeed, the apparent lack of association between DOM and Tl characterized by AF4-ICPMS reflects the behaviour of this oxidation state. Nevertheless, in acidic waters subjected to photooxidation, Tl(III) could be present in significant quantities (Campanella et al. 2018).

Table 2.4. Predicted speciation (percentage of total) of copper in experimental waters.

	OECD	10 mM $NaHCO_3$	10 mM $CaCl_2$	10 mM NaCl	10 mM KCl	10 mg/L SRNOM
Cu^{+2}	13.90	0.10	2.65	78.90	1.46	0
$CuOH^{+}$	12.58	0.94	15.15	14.24	13.19	0
$Cu(OH)_2$ (aq)	0.71	0.53	5.39	0.16	7.44	0
$CuCl^{+}$	0.10	0	0.07	1.90	0.04	0
$CuCO_3$ (aq)	71.09	69.78	75.22	0	75.27	0
$CuHCO_3^{+}$	0.53	0.05	0.09	0	0.06	0
$Cu(CO_3)_2^{-2}$	0.22	28.58	1.29	0	2.36	0
$Cu(OH)_3^{-}$	0	0	0.04	0	0.10	0
$CuNO_3^{+}$	0	0	0	0.03	0	0
$CuSO_4$(aq)	0.86	0	0.09	4.76	0.09	0
FA2-Cu(6) (aq)	0	0	0	0	0	98.85
FA1-Cu(6) (aq)	0	0	0	0	0	1.15

[a] Speciation modeled via Visual MINTEQ. Full water chemistry details are provided in Table 2.1; [aq]: aqueous; OECD: Organisation for Economic Co-operation and Development; SRNOM: Suwannee River natural organic matter; FA: fulvic acid

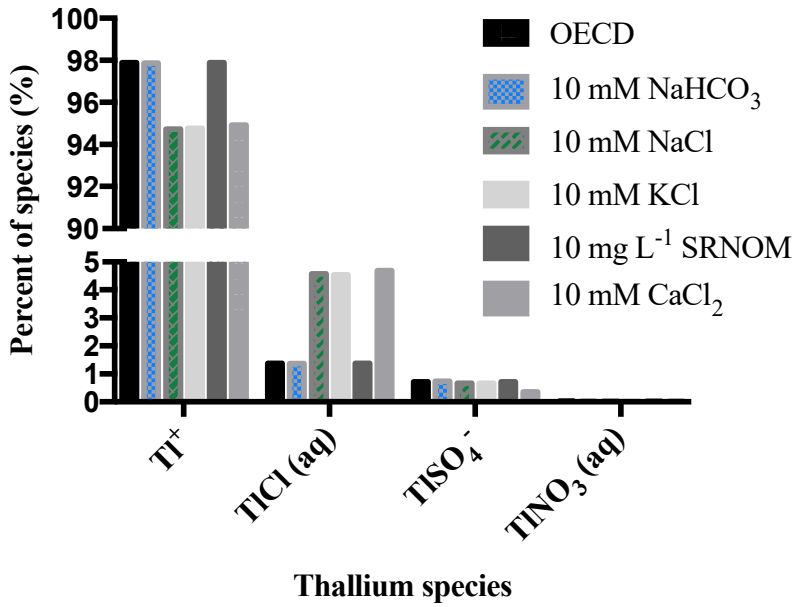

Figure 2.3. Speciation of Tl in different water chemistries as predicted by Visual MINTEQ (Gustafsson 2015). Full water chemistry details are provided in Table 2.1.

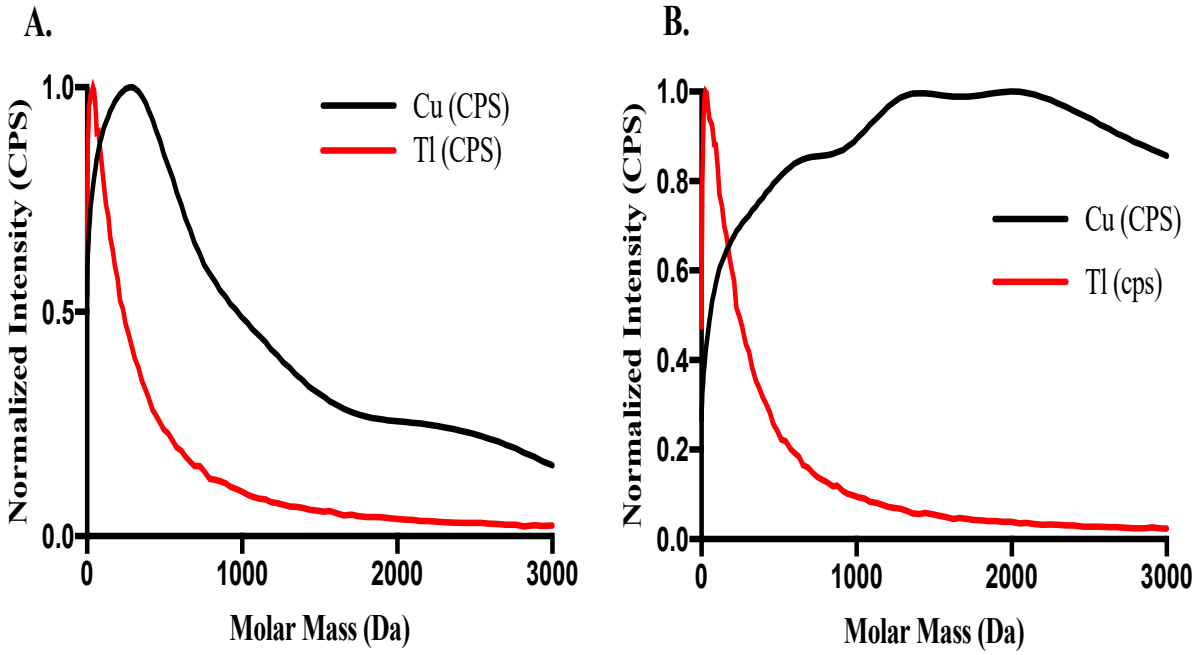

Figure 2.4. Thallium (Tl; 1.86 mg L^{-1}) and copper (Cu; 0.62 µg L^{-1}) speciation in OECD water (A) and OECD water supplemented with 10 mg/L Suwannee River fulvic acid (B), as determined by AF4. Counts per second (CPS) for samples normalized by intensities.

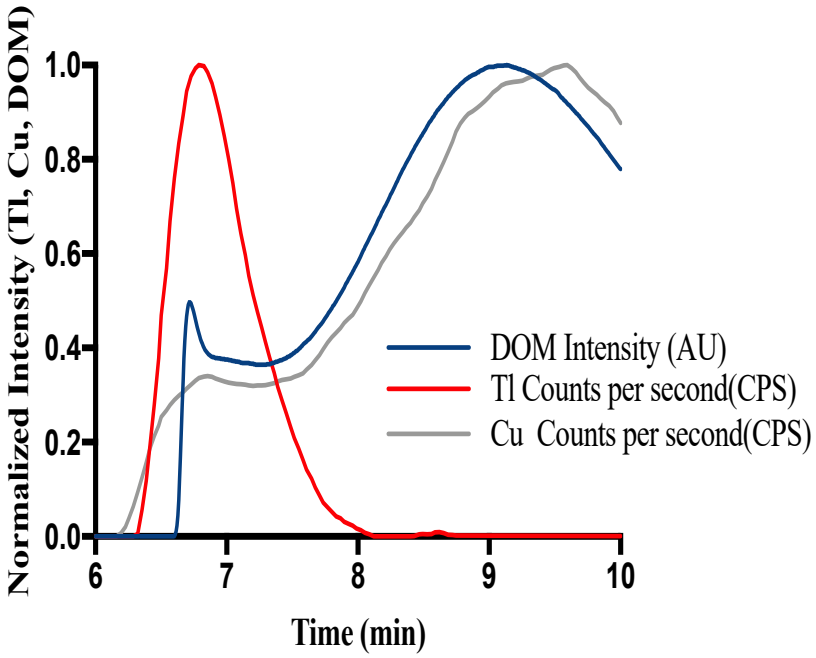

Figure 2.5. Fractionation of Tl (0.2 µg L^{-1}) and Cu (0.2 µg L^{-1}) in the presence of DOM (10 mg C L^{-1}). Overlay of peak intensity over time (min), where absorbance (AU) and counts per second (CPS) have been normalized to intensity.

2.4. Conclusion

This study systematically assessed the effect of water chemistry on Tl toxicity to *Daphnia magna*. While the toxicity of most metals can be ameliorated by organic and inorganic complexation, the data presented here show that Tl was relatively inert, and largely unaffected by changes in the organic and inorganic components of natural waters. Using an advanced speciation analysis technique (AF4-ICPMS), the speciation of Tl in synthetic waters that was predicted by geochemical modelling was experimentally confirmed, validating the utility of this technique for studies in aquatic toxicology. Importantly, these results suggest that risk assessments of Tl toxicity in most natural waters will not need to account for the speciation of dissolved Tl, owing to the lack of apparent complexation with organic and inorganic ligands.

This lack of complexation was present even at low Tl concentrations (e.g. 0.2 µg L^{-1}; Fig. 2.5), suggesting that the outcomes of the current study will also be relevant in chronic exposure scenarios in which effects of Tl are manifested at much lower exposure concentrations than those used here (Couture et al. 2011). Consequently, water quality criteria for dissolved Tl will likely not be significantly improved by incorporating speciation models such as the BLM, at least in neutral waters where Tl(I) dominates.

3. Chronic toxicity of waterborne thallium to *Daphnia magna*

3.1. Introduction

Little is known regarding the toxic impacts of the trace metal Tl in natural waters. In part this is because Tl is not a prominent contaminant of aquatic systems, with background levels of Tl ranging between 1 and 10 ng L^{-1} in surface waters (e.g., Shotyk et al. 2019). However, environmental enrichment of Tl may occur, particularly associated with base metal mining and smelting, the burning of coal, and cement production. Such processes can result in total Tl effluent concentrations as high as 15 mg L^{-1} (Nriagu 1998; Williams-Beam and Twidwell 2003). Consequently, even though Tl is not a trace metal of high concern, the presence of Tl point sources has resulted in the development of regulatory guidance. Most notably, CCME has established a water quality guideline, which sets the maximum limit for total Tl concentration in surface waters at 0.8 µg L^{-1} (CCME 2007). This value does not discriminate between the two oxidation states of Tl in natural waters: Tl(I) and Tl(III). Although Tl(III) is considered more toxic (Lan and Lin 2005), it rapidly precipitates, adsorbs to surfaces or is oxidized to Tl(I) (Karlsson et al. 2006b). Thus, in natural oxic waters Tl(I) tends to dominate the dissolved, bioavailable fraction (Casiot et al. 2011), and is likely to be of greater ecotoxicological relevance.

Highlighting the general lack of knowledge regarding aquatic Tl toxicity, the CCME guideline value is based on the responses of the aquatic plant *Lemna minor* (Brown and Rattigan 1979; Kwan and Smith 1988). These studies noted an LOEC for the effect of Tl on *L. minor* frond area of 8.4 µg L^{-1} (Kwan and Smith 1988), and a 14-d median effect concentration (EC_{50}) for whole-plant damage of 8 µg L^{-1} (Brown and Rattigan 1979). The 0.8 µg L^{-1} guideline value was ultimately reached by the application of a safety factor (multiplication by 0.1; CCME 2007).

To date, however, there is limited understanding of how this guideline value relates to the impacts of waterborne Tl on other aquatic biota. Such knowledge is critical because even though the criterion value of 0.8 µg L^{-1} is orders of magnitude above background concentrations, it is a value that is regularly exceeded in Canadian waters as a result of enrichment from industry (Cheam 2001; CCME 2007).

Relative to *L. minor*, aquatic animals appear considerably more tolerant to Tl, at least in studies conducted over acute time-frames. Acute median lethal concentrations have been derived for regulatory model species such as rainbow trout (96-h LC_{50} = 4.27 mg L^{-1}; Pickard et al. 2001), and the freshwater invertebrate *Daphnia magna* (48-h LC_{50} = 1.66 - 1.86 mg L^{-1}; Lin et al. 2005; Chapter 2). Mechanistically, acute Tl toxicity is associated with interference of K^+ homeostasis, a requirement for proper functioning of the neural and cardiovascular systems (Baylor 1942; Pichon et al. 1987). This interaction between Tl and K^+ appears to be conserved across studied phyla (e.g., Kwan and Smith 1991; Hassler et al. 2007; Rickwood et al. 2015).

Despite studies of acute toxicity, there is very little information regarding the chronic toxicity of Tl. Chronic data are preferable for the development of water quality guidelines, in part because such data better reflect environmental exposure scenarios (CCME 1991). Studies in fish indicate LOEC values for Tl in the 40 to 80 µg L^{-1} range (Kimball 1978; Le Blanc and Dean 1984). In the freshwater invertebrate *Hyalella azteca*, chronic effects of Tl on survival (4-week LC_{25}: 48 nmol L^{-1} = 9.8 µg L^{-1}), growth (6-week EC_{25}: 35 nmol L^{-1} = 7.2 µg L^{-1}) and reproduction (10-week EC_{25}: 10 nmol L^{-1} = 2.0 µg L^{-1}) have been assessed, where these values represent geometric means calculated across several water chemistry compositions (Borgmann et al. 1998). A 7-d LC_{50} of 370 µg L^{-1} and a 7-d reproductive EC_{25} of 97 µg L^{-1} have been reported for the daphnid *Ceriodaphnia dubia* exposed to waterborne Tl (Pickard et al. 2001), while a 28-d

LC_{50} of 393 μg L^{-1} has been measured for *D. magna* (Kimball 1978). As might be expected, these long-term studies show effects at Tl concentrations lower than those seen for short-term exposures, emphasising the need for further investigations of chronic Tl toxicity to aquatic biota. In particular, there is a requirement for studies that utilize measured Tl exposure concentrations to calculate threshold values, and which employ sufficiently high numbers of replicate tests. These are factors that currently limit the usefulness of existing literature.

One important target species for chronic Tl toxicity research is *Daphnia magna*. Commonly employed in the development of regulatory guidelines (Lewis and Horning 1987; OECD 2004; CCME 2007), these small-bodied freshwater crustaceans display rapid growth, a short maturation time, high reproductive output, and are generally sensitive to aquatic contaminants (Baudo 1987; OECD 2012). These properties make them particularly amenable to the laboratory testing of aquatic toxicity. Furthermore, using survival as an endpoint, studies to date show that *D. magna* is relatively sensitive to Tl over short-term exposure durations (Nehring 1962; Lin et al. 2005; Tatsi et al. 2015; Chapter 2), suggesting that advanced knowledge of its chronic sensitivity to Tl will be of value for the development and refinement of water quality criteria.

The goal of the present study was to examine the effects of a 21-d exposure of dissolved Tl(I) to *Daphnia magna*, using traditional endpoints such as survival, growth and reproduction. Whole-body K^+ concentration and Tl body burden were also analyzed to develop a greater understanding of the relationship between exposure and effect, on the basis of these endpoints being two key indicators of organismal impacts (Hassler et al. 2007; Turner and Furniss 2012). Furthermore, these relationships have been critical for the development of predictive tools that facilitate assessment of toxicological impact on the basis of site-specific water chemistry (e.g.,

BLM; Di Toro et al. 2001). Ultimately, this study aimed to provide data that could be used by regulatory agencies for the protection of freshwater systems against Tl toxicity.

3.2. Materials and methods

3.2.1. *Daphnia magna*

Daphnia magna were acquired from Aquatic Research Organisms (Hampton, NH, USA), and maintained in the Department of Biological Sciences at the University of Alberta. *Daphnia* were reared in ISO test water 1 (OECD 2004) (in mM): 2.0 $CaCl_2$, 0.5 $MgSO_4 \cdot 7H_2O$, 0.77 $NaHCO_3$, 0.08 KCl, pH 7.5. In this chapter this water is referred to as ISO water, but it is identical to what is referred to as OECD water in other chapters of this thesis. The culture was maintained on a 16:8 h dark: light cycle at 22 °C, with daily feeding of YCT (a yeast, cereal leaf, trout chow mix), algae (*Raphidocelis subcapitata*) and Roti-Rich Liquid Invertebrate Food.

3.2.2. *Chronic toxicity assay*

Individual *Daphnia* neonates (< 24-h) were placed into 40 mL of test solution in a 50-mL acid-washed glass beaker. Test solutions consisted of ISO water to which Tl was added from a freshly-prepared thallium(I) nitrate (purity 99.999%, trace metal basis; Sigma-Aldrich, St Louis, MO) stock solution. Stock solutions consisted of this Tl salt reconstituted in 1% trace element-grade HNO_3, with pH adjusted to 7.5 using 0.1 M sodium hydroxide. Exposure concentrations were based upon CCME water quality guidelines: 0.8 µg L^{-1} (the guideline value), 8 µg L^{-1} (10 x the guideline value) or 80 µg L^{-1} (100 x the guideline value). In addition, we also examined values derived from acute toxicity studies (Chapter 2): 410 µg L^{-1} (the 48-h LC_5), 689 µg L^{-1} (the 48-h LC_{10}), and 1080 µg L^{-1} (the 48-h LC_{20}). Each concentration was replicated 10 times. Exposure waters were prepared 24-h in advance of daphnid introduction to allow for equilibration of the metal (Glover et al. 2005).

During exposures, daphnids were fed YCT and algae daily, with a water change every 72-h. Ranges for exposure water pH, dissolved oxygen and temperature were 7.5-7.9, 91-99%, and 21-22°C, respectively. A 10-mL water sample was taken before and after each water change, filtered through a 0.45 µm syringe filter, acidified with 3 drops of 70% trace HNO_3, and stored refrigerated for later analysis of waterborne Tl concentration (see below). During the course of the 21-d exposure, survival and reproduction were monitored daily. At the conclusion of the exposure, adult daphnids were carefully removed from their treatments, placed on tissue paper to gently blot dry, and then weighed on a microbalance (Orion Cahn C-35; Thermo Electron Corporation, Waltham, Massachusetts, USA), for a measure of final wet weight body mass (a surrogate of growth).

3.2.3. *Burden analysis and gut clearance*

Following final wet weight body mass measurement from the chronic toxicity assay, daphnids were collected and stored for whole-animal elemental analysis. For analysis of whole-body Tl burden and whole-body K^+ status, individual daphnids were placed in a 1.5-mL tube, and dried to constant mass in a clean air cabinet, before a final measurement of dry mass. Five dried daphnids were then pooled into a 15-mL tube and digested using 3 mL of double-distilled trace metal grade HNO_3. These digests were then diluted 1:10 in ultrapure water (18.2 MΩ cm) and analyzed as detailed below.

The exception to this protocol was a separate depuration study to examine whether daphnid Tl burden could be explained by its uptake via the diet (i.e. Tl adsorption to feed components and subsequent ingestion). In this study daphnids were individually exposed to 80 µg L^{-1} Tl for 21-d, as described above. Following exposure, individual daphnids were held in clean (i.e. no added Tl) ISO water for 8-h, while a further group were held separately in ISO

water to which food (YCT and algae) was added in order to facilitate gut clearance (Gillis et al. 2005). After 8-h, daphnids were processed for Tl body burden as described above, and both of these groups were compared to a concurrently-run control exposed to 80 μg L^{-1} Tl, but without any depuration period.

3.2.4. *Metal and ion concentration analysis*

Dissolved Tl concentrations and daphnid Tl burden were analyzed using ICPMS. Quality assurance for this analysis included the use of Multi Element Standard-1 (MES-1), and the surface water standard reference materials SPS-SW2 (diluted 10- and 500-fold) and NIST 1640a (diluted 10- and 100-fold). The calculated LOD and LOQ for Tl were 0.11 and 0.76 ng L^{-1}, respectively. Blank values were determined using the average of three 2% HNO_3 replicates. An internal standard (a 10% HNO_3 solution spiked with 5 μg L^{-1} indium and bismuth) was used to account for any drift in ICPMS sensitivity.

Whole-body K^+ concentration was assessed using FAAS. Measured absorbances were quantified against a freshly-made standard curve constructed from a KCl salt solution diluted in ultrapure water (18.2 MΩ cm). Each standard and all samples had 1 g L^{-1} $CsNO_3$ added to suppress ionization of K^+ in the analyte.

3.2.5. *Calculations and statistics*

No observable effect concentrations (NOEC) and LOEC values were defined as the measured Tl concentrations at which no effect, and the first observed significant effect, in relation to the control group was observed, respectively. Median effective concentrations for mass and reproduction, were calculated using Prism Graph Pad. Briefly, concentrations of Tl were converted to log values, while measured responses were converted to percentages, where the value of the largest effect was fixed at 0% and the control value fixed at 100%. The EC_{50}

values were then determined via application of a sigmoidal model according to the following equation:

Equation 3.1:

$$y = \frac{100}{1+10^{((\text{LogEC}_{50}-x)*\text{Hill Slope})}}$$

Prior to statistical analysis, Grubbs test was employed for detection and subsequent removal of outliers. This reduced n values from 10 to 8 in some analyses. All data were then analyzed using one-way ANOVA via Prism Graph Pad, followed by a post hoc Tukey's test, at an alpha level of 0.05. Assumptions of parametric analysis were confirmed by the Shapiro-Wilk test for normality, and the Brown Forsythe test for homogeneity of variance. Pearson correlation analysis was employed to determine the relationships between measured endpoints and whole-body Tl burden. Unless otherwise stated, all reported values represent the mean ± standard deviation.

3.3. Results

3.3.1. *Tl exposure concentrations*

Measured dissolved Tl exposure concentrations were close to nominal levels (Table 3.1). Background concentrations of Tl in ISO water were 0.003 ± 0.002 μg L^{-1}. Analysis revealed that there was no significant difference in exposure Tl concentrations over the course of 72-h. From this point forth, measured values will be referred to in this chapter.

Table 3.1. Nominal and measured dissolved exposure Tl concentrations.

Nominal Concentration ($\mu g\ L^{-1}$)	Measured Concentration ($\mu g\ L^{-1}$)
0	0.003 ± 0.002
0.8	0.89 ± 0.50
8	8.79 ± 0.75
80	83.1 ± 10.4
410	424 ± 140
689	702 ± 242
1080	1112 ± 377

Measured values represent the mean (± standard deviation) of 6 replicate water samples.

3.3.2. *Survival*

Complete mortality was observed at Tl concentrations greater than 424 $\mu g\ L^{-1}$, with Tl concentrations equal to this or lower displaying 100% survival (data not shown). Because of the lack of any exposure concentrations exhibiting partial mortality, and a lack of variance between replicates in each exposure group, LC_{50}, NOEC and LOEC values for survival were not able to be calculated. However, the LC_{50} value would lie between 424 and 702 $\mu g\ L^{-1}$, the highest concentration with no mortality and the lowest concentration with complete mortality.

3.3.3. *Thallium body burden*

As waterborne Tl exposure concentration increased, so too did daphnid Tl body burden (Figure 3.1a). Indeed, daphnids exposed to the highest Tl concentration at which survival occurred, and at which burden could therefore be measured (424 $\mu g\ L^{-1}$), displayed whole-animal Tl concentrations that were 710-fold greater than controls not exposed to Tl. However, only at this highest concentration was Tl body burden significantly different from the control value. Plotting body burden as a function of Tl exposure concentration yielded a relationship that was a better fit to a hyperbolic function ($r^2 = 0.74$), than to a linear function ($r^2 = 0.68$; data not shown).

The depuration study indicated that there was no significant difference in Tl body burden between daphnids that were gut cleared for 8-h and those that were held in clean water without

gut clearance for 8-h (Figure 3.1b). Both these groups exhibited Tl burdens that were only 20% of those in daphnids sampled directly after the 21-d exposure.

Correlation analyses (data not shown) demonstrated that whole-body Tl burden was significantly correlated to reproduction (total neonate production over 21-d; r = -0.71; P-value: 0.003). Conversely, there was no significant relationship between daphnid Tl burden and final body mass (r = -0.39; P-value: 0.15).

Although altered body K^+ status is an indication of acute Tl toxicity, in the current study there were no significant differences in daphnid whole-body K^+ in response to waterborne Tl (Figure 3.2). Indeed, even though the effect was not significant, at a Tl concentration of 8.8 µg L^{-1}, whole-body K^+ was 2.3-fold greater than that observed in the control daphnids.

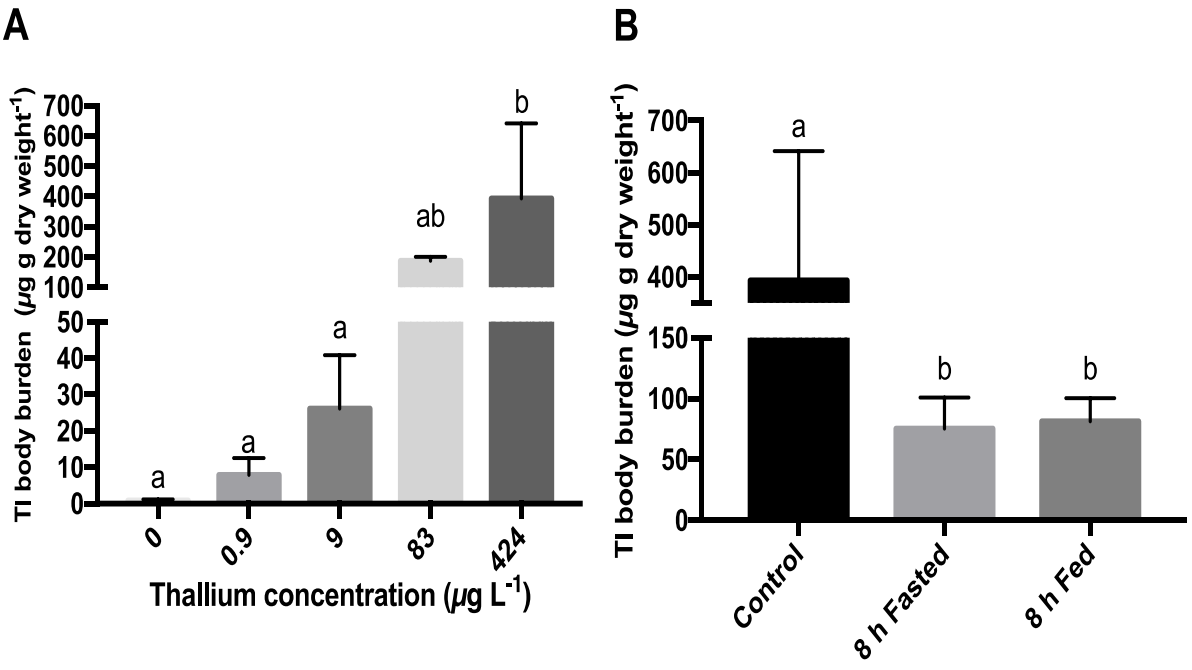

Figure 3.1. Concentration-dependence of daphnid Tl body burden (µg g dry weight^{-1}) following a 21-d exposure to Tl (A), and after a subsequent 8-h period (B), where burdens were measured immediately after exposure to 80 µg L^{-1} Tl (control; black bar), and after 8-h in Tl-free water (light grey bar), and after 8-h in Tl-free water with access to Tl-free food (dark grey bar). Plotted

points represent means (± standard deviation) of 3 replicates. Bars sharing letters are not statistically significantly different.

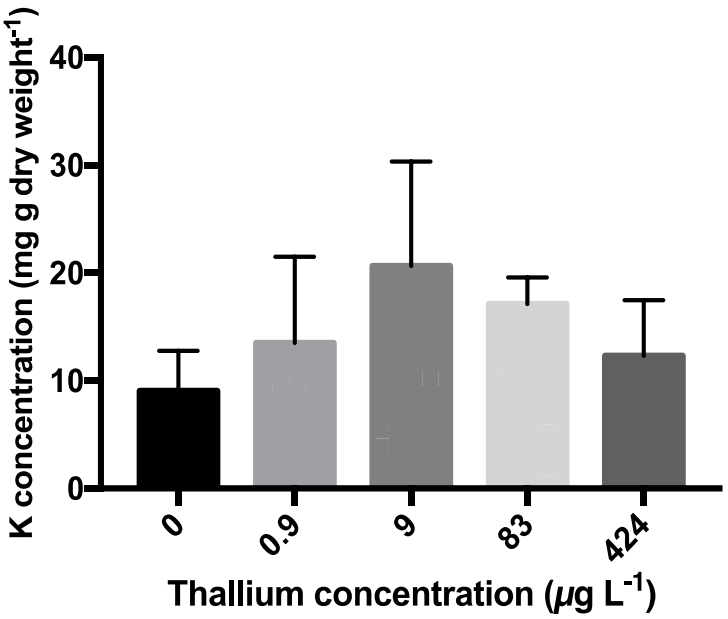

Figure 3.2. Whole-animal potassium concentration (mg g dry weight^{-1}) in *Daphnia magna* following a 21-d exposure to waterborne Tl concentrations. Plotted points represent means (± standard deviation) of 8-10 replicates.

3.3.4. *Final body mass*

Significant differences in the final body mass of *Daphnia* were observed after a 21-d exposure to waterborne Tl (Figure 3.3). At Tl concentrations of 8.8 µg L^{-1} and above (i.e., 83, 424 µg L^{-1}), daphnid final body mass was significantly reduced relative to the Tl-free control (P-value$_{Tukeys}$: < 0.05). No significant differences in final body mass were observed between the 8.8, 83, and 424 µg L^{-1} treatment groups. These data were used to calculate an EC_{50} for the effect of waterborne Tl of growth (1.6 (95% CI 1.0 – 3.1) µg L^{-1}; Table 3.2). Values for the NOEC and LOEC were determined to be 0.9 and 8.8 µg L^{-1}, respectively (Table 3.2).

Table 3.2. Calculated toxicity endpoint values.

Metric	Endpoint	Tl concentration (µg L^{-1})
EC_{50}	Reproduction	11.1 (5.5 - 21.8)
	Growth	1.6 (1.0 - 3.1)
LOEC	Reproduction	8.8 - 424
	Growth	8.8
NOEC	Reproduction	0.9 - 83
	Growth	0.9

EC_{50}: calculated value (95% confidence interval).

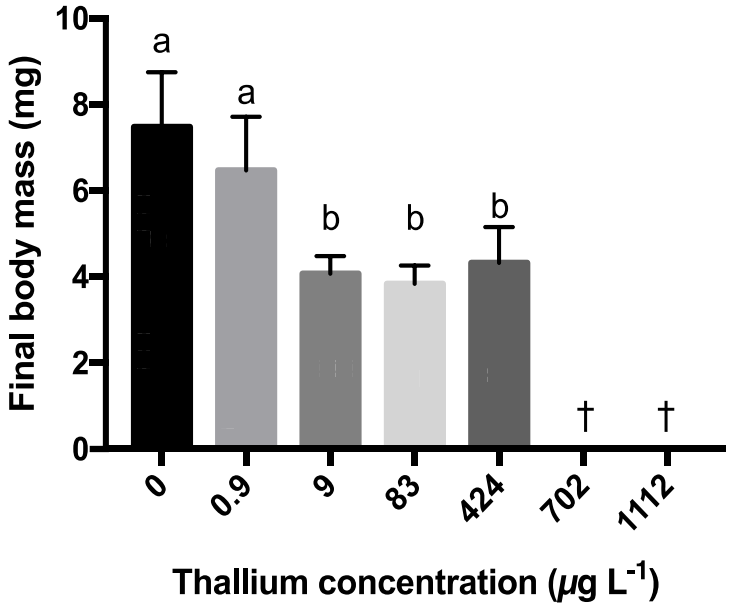

Figure 3.3. Final body mass (wet weight) following 21-d waterborne Tl exposure to *Daphnia magna*. Plotted points represent means (± standard deviation) of 8-10 replicates. Bars sharing letters are not statistically significantly different. † = groups where mortality occurred.

3.3.5. *Reproduction*

Control animals produced more than 60 neonates over the course of the 21-d exposure, meeting the criterion for a valid chronic toxicity test (OECD 2012). The mean total number of daphnid neonates produced by a single adult over 21-d was significantly affected at waterborne Tl concentrations as low as 8.8 µg L^{-1} (Figure 3.4a). No significance differences were observed

between Tl exposure concentrations of 8.8 µg L^{-1} and 83 µg L^{-1}, but at 424 µg L^{-1} a further significant fall in neonate production was noted. At concentrations greater than 424 µg L^{-1} no reproduction was noted as all animals died prior to their first brood.

The time that daphnids took to produce their first brood was significantly different from the control at waterborne Tl concentrations of 8.8 µg L^{-1} and greater (Figure 3.4b). At 8.8 µg Tl L^{-1} the first brood took 13% longer to produce than for daphnids exposed to the Tl-free control. The number of neonates produced in the first brood was not significantly different between all treatment groups that produced neonates (Figure 3.4c). However, the number of neonates produced in the final brood of the 21-d exposure was significantly reduced in the 8.8 and 83 µg L^{-1} treatment groups compared to control groups (Figure 3.4d). Significant differences in the total number of neonate-producing broods were observed, starting at a Tl exposure concentration of 8.8 µg L^{-1} (Figure 3.4e). Although the number of broods produced by daphnids in the 0.9 µg L^{-1} exposure group trended towards a decline relative to the control, this narrowly missed statistical significance ($P\text{-value}_{Tukeys}$: 0.110). The calculated EC_{50} for reproduction, based on total neonate production, was 11.1 (95% CI 5.5 – 21.8) µg L^{-1} (Figure 3.4f). Overall, NOEC values for reproductive parameters ranged from 0.9 (total neonates, time to first brood, number of broods) to 83 (number of first brood neonates) µg L^{-1}; while LOEC values ranged from 8.8 (total neonates, time to first brood, number of broods) to 424 (number of first brood neonates) µg L^{-1} (Table 3.2).

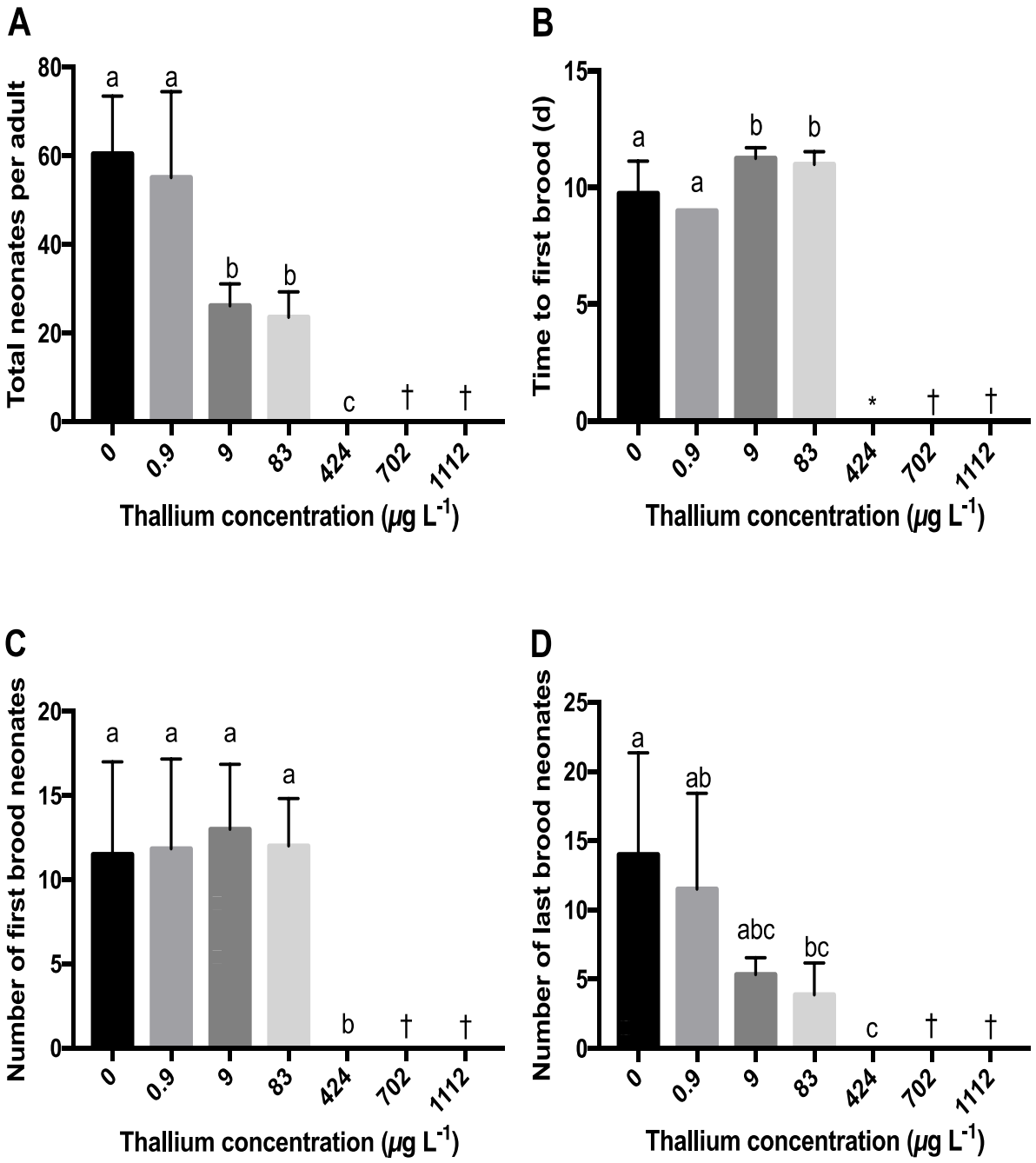
A
Total neonates per adult
80
60
40
20
0
a
a
b
b
c
†
†
0
0.9
9
83
424
702
1112
Thallium concentration (μg L-1)
B
Time to first brood (d)
15
10
5
0
a
a
b
b
*
†
†
0
0.9
9
83
424
702
1112
Thallium concentration (μg L-1)
C
Number of first brood neonates
20
15
10
5
0
a
a
a
a
b
†
†
0
0.9
9
83
424
702
1112
Thallium concentration (μg L-1)
D
Number of last brood neonates
25
20
15
10
5
0
a
ab
abc
bc
c
†
†
0
0.9
9
83
424
702
1112
Thallium concentration (μg L-1)

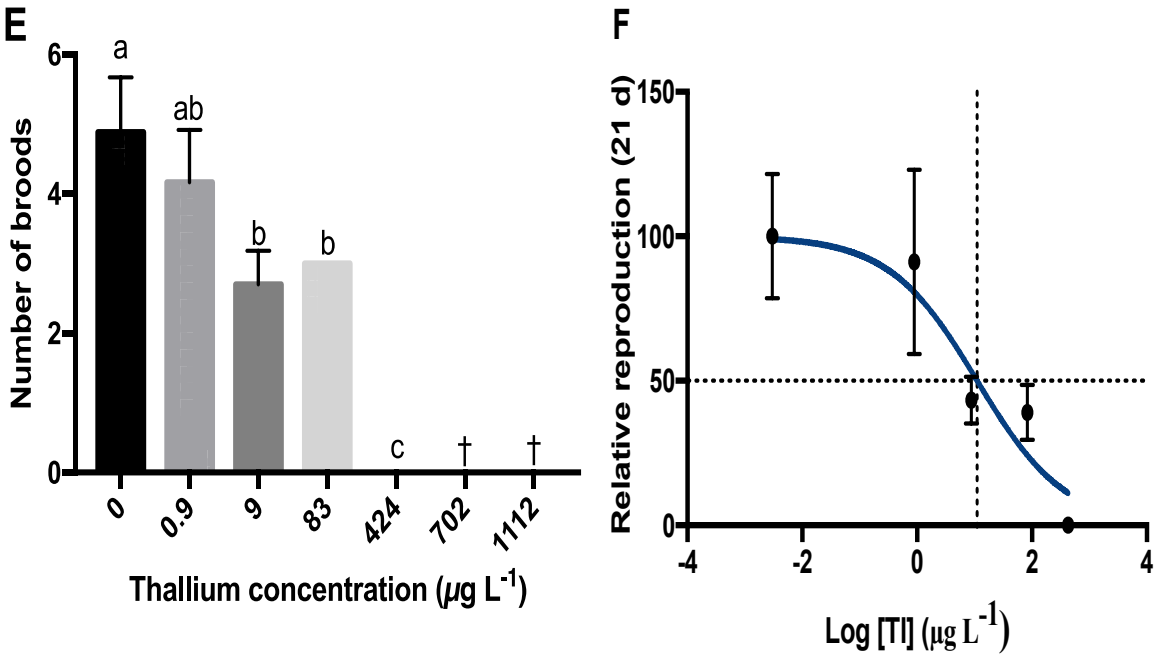

Figure 3.4. Effect of a 21-d waterborne Tl exposure on total neonates per adult (A); days to first reproductive event (i.e., brood; B); number of neonate daphnids produced at the first (C) and last (D) brood; total number of broods (E); in *Daphnia magna*. Panel F represents relative daphnid reproduction, as defined in Section 3.2.5, where the dotted line represents the median effective concentration of Tl. Plotted points represent means (± standard deviation) of 8-10 replicates. Bars sharing letters are not statistically significantly different. † = groups where mortality occurred and which therefore did not reproduce.

3.4. Discussion

3.4.1. *Survival*

In the current study a 21-d chronic LC_{50} for the toxicity of waterborne Tl to *Daphnia magna* was unable to be determined. However, total survival was observed at 424 µg $L^{-1,}$ and total mortality seen at 702 µg L^{-1}, so the median lethal concentration would lie between these two concentrations. Although differences in factors such as exposure water chemistry, test

species, the use of nominal versus measured Tl concentration, and exposure durations complicate comparisons between studies, our derived value range is similar to previous reports of chronic Tl toxicity to daphnid crustaceans. For example, Kimball (1978) recorded a 28-d LC_{50} value of 393 µg L^{-1} in *D. magna*, while Pickard et al. (2001) determined a 7-d LC_{50} of 370 µg L^{-1} in *Ceriodaphnia dubia*. In another crustacean species commonly employed in toxicity assays, the amphipod *Hyalella azteca*, Borgmann and colleagues (1998) measured water chemistry-dependent 28-d Tl LC_{25} values ranging from 2.5 to 19 µg L^{-1}, emphasising the high tolerance of *D. magna* to waterborne Tl relative to other freshwater invertebrates, at least with respect to survival as an endpoint. Furthermore, *D. magna* is also more tolerant to Tl over long-term exposure periods than tested fish species. Early life-stages of fathead minnows (*Pimephales promelas*) showed complete mortality over 30-d at a Tl concentration of 350 µg L^{-1} (LeBlanc and Dean 1984), while the rainbow trout 28-d LC_{50} was 170 µg L^{-1} (Birge 1978).

This pattern of comparatively high survival tolerance of *D. magna* to long-term Tl exposure is quite distinct from that observed for acute Tl toxicity. In short-term exposures LC_{50} values for *D. magna* (e.g., 48-h: 1.86 mg L^{-1}; Chapter 2) are bracketed by acute toxicity values for *Hyalella azteca* (7-d LC_{50}, 11 to 123 µg L^{-1} depending on water chemistry; Borgmann et al. 1998), and those for some fish species such as rainbow trout (*Oncorhynchus mykiss,* 96-h $LC_{50,}$ 4.27 mg L^{-1}; Pickard et al. 2001), and bluegill sunfish (*Lepomis macrochirus*: 96-h $LC_{50,}$ 132 mg L^{-1}; Dawson et al. 1977). On an acute basis Tl is thought to cause toxicity through a specific effect on K^+ homeostasis. For example, studies in algae and *Hyalella* that lowered water K^+ concentration, showed enhanced Tl toxicity (Borgmann et al. 1998; Hassler et al. 2007). In daphnids a similar effect of exposure K^+ concentration on Tl toxicity has been noted (Tatsi et al. 2015). The exact mechanism by which this effect is exerted is unknown, but there is evidence for

Tl competition with epithelial K^+ transporters in different phyla (Henning and Forth 1982; Belowitz and O'Donnell 2013). However, in the current work there was no effect of a 21-d Tl exposure on whole-body K^+ concentration (Fig. 3.2). This suggests that daphnids are capable of enacting mechanisms over long-term exposure periods that compensate for the acute effects of Tl on K^+ balance. One possibility is that the presence of food in the exposures acts as a source of K^+, with upregulation of gastrointestinal K^+ transport compensating for waterborne Tl inhibition of K^+ transport at the gill. Similar effects have been observed in fish, where waterborne Cd exposure leads to an increase in gastrointestinal Ca^{2+} uptake (Franklin et al. 2005). Irrespective of the processes involved, it is likely that the mechanism of waterborne Tl toxicity differs between short- and long-term exposures. This could be problematic for the calibration of regulatory tools. For example, the BLM is a regulatory approach that relates water chemistry to short-term body burden, which in turn is related to toxic impact (Di Toro et al. 2001). As such, if acclimation occurs and the acute mechanism of toxicity differs from chronic toxicity, then the predictive capacity of the BLM will be compromised (Niyogi and Wood 2004).

3.4.2. *Thallium body burden*

Thallium body burden increased in a dose-dependent manner in the current study (Fig. 3.1A). In laboratory studies, bioaccumulation of Tl has been linked to toxic effects (Borgmann et al. 1998; Turner and Furniss 2012), suggesting that Tl bioaccumulation may be the most robust measure of toxicological impact (Borgmann et al. 1998). However, while the current study found that the relationship between whole-animal body burden and reproduction was significant ($r = -0.71$ $p = 0.003$), the relationship between body burden and the most sensitive toxicological endpoint, final body mass, was not significant ($r = -0.39$, $p = 0.146$). The utility of Tl bioaccumulation as a predictor of toxicity for *D. magna* therefore requires further investigation.

One complicating factor in long-term exposures is the presence of food in the exposure medium. Because of the capacity for waterborne metals to bind to chemical moieties in food, it is possible that a component of accumulation could be ascribed to dietary exposure. In general, metals absorbed via the gut will contribute towards accumulation, but are considered to be less bioreactive (DeForest and Meyer 2015). Therefore, if a significant amount of Tl was being absorbed via the daphnid gut, this could distort the relationship between accumulation and effect. In the current work, there was no difference in the whole-body Tl burdens between gut cleared animals (kept in Tl-free media for 8-h in the presence of food), and animals that were not gut cleared (kept in Tl-free media without food for 8-h; Fig. 3.1B). This indicates that the Tl burdens measured were not compromised by the presence of unabsorbed Tl in the gut, and suggests that the exposure of daphnids to the metal was almost exclusively via the water. This is indirectly supported by previous studies showing that waterborne Tl is relatively inert and does not display a high affinity for potential binding ligands (Chapter 2).

The other key finding of the gut clearance study was that 80% of the whole-body Tl burden accumulated over the 21-d exposure was depurated in 8-h (Fig. 3.1B). Previous research examining metal depuration in daphnids has shown that the rates and magnitudes of loss vary as a function of the specific metal of interest (Yu and Wang 2002). For example, approximately 65% of Ag body burden was depurated in 8-h, following a 24-h accumulation (Glover and Wood 2005a). After a 7-d waterborne accumulation phase, whole-daphnid body burdens of manganese (Mn), cobalt (Co), and caesium (Cs) fell by ~25, 35, and 50% in the first 8-h of depuration, respectively (Adam et al. 2001). Data from Yu and Wang (2002) for selenium (Se), Zn, Cd and chromium (Cr) demonstrated 8-h depuration rates ranging between ~10 and 45% of a whole-body burden accumulated over an 8-d waterborne exposure. On the basis of these data,

accumulated Tl in daphnids is labile relative to other trace metals. This is reinforced by a study in the alga *Chlorella*, which noted rapid cellular turnover of Tl, driven by high cellular efflux rates (Hassler et al. 2007). This may be a consequence of a generally low binding affinity of Tl for possible cellular ligands, and suggests a handling strategy based around rapid elimination of the metal, as opposed to sequestration in a detoxified form (Glover and Wood 2005a). Furthermore, the relationship between Tl exposure concentration and body burden was better described by a hyperbolic function, than a linear function (Section 3.3.3), indicating that body burden did saturate with increasing Tl concentrations. This also supports the concept that there are mechanisms for regulating Tl body burden, with efficient excretory pathways one possible means of achieving this.

3.4.3. *Final body mass and reproduction*

A key finding of the current study was the sensitivity of daphnid growth (measured as final body mass) to waterborne Tl exposure, with an EC_{50} of 1.6 μg L^{-1} being determined (Table 3.2). Although this value is twice the CCME regulatory limit (0.8 μg L^{-1}), it is in the range of environmental concentrations associated with some industrial effluents (e.g., mine and power plant discharges in Eastern Canada exhibit mean Tl concentrations of 1.4 μg L^{-1}; Cheam 2001). Growth is a factor of considerable ecological consequence in *Daphnia*, with body size affecting feeding and swimming behaviours (McMahon 1965; Dodson and Ramcharan 1991), bacterial infection rates (Garbutt and Little 2017), and sensitivity to toxicants (Vesela and Vijverberg 2007). This suggests that the presence of Tl in some industrial effluents could have an important ecological impact on daphnid populations.

Our finding that waterborne Tl affects the growth of a freshwater crustacean supports the research of Borgmann and colleagues (1998) on the amphipod *Hyalella*, which noted an effect of

waterborne Tl on animal growth (6-week EC_{50} of 7.2 µg L^{-1}). This effect concentration represented a value equal to 73% of the 4-week LC_{50} for this species (9.8 µg L^{-1}), albeit measured over a longer exposure duration. In contrast, the 21-d EC_{50} determined here for *D. magna* represents a concentration that is only a small fraction of the Tl concentration that causes mortality (424-702 µg L^{-1}). This suggests that growth is a particularly sensitive endpoint for Tl-exposed daphnids, and stands in contrast to the relative magnitude of effect concentrations for reproduction. For example, in *Hyalella* the 10-week EC_{50} for the effect of Tl on reproduction was just 29% of that for growth, indicating a higher toxicity (Borgmann et al. 1998). In the current study, the EC_{50} for reproduction (11.1 µg L^{-1}) was an order of magnitude greater (i.e. less toxic) than the EC_{50} for growth. These data indicate fundamental differences in the toxic responses of waterborne Tl between *Daphnia* and *Hyalella*.

The EC_{50} for the effect of Tl on total neonate production over 21-d was 11.1 µg L^{-1}, with a LOEC value of 8.8 µg L^{-1} for most reproductive endpoints examined (Table 3.2). Consequently, under our exposure conditions *D. magna* were more sensitive to reproductive effects of Tl than has been noted in a previous study (LOEC = 181 µg L^{-1}; Kimball 1978). They are also more sensitive to Tl than the smaller daphnid species *C. dubia,* which exhibits mean 7-d reproduction EC_{25} values ranging between 97 and 160 µg L^{-1} (Pickard et al. 2001; Rickwood et al. 2015). The best-known modifying factor for waterborne Tl toxicity is waterborne K^+ (Borgmann et al. 1998; Hassler et al. 2007). Unfortunately, previous studies have not always been explicit regarding exposure water chemistry, preventing analysis of whether dissolved K^+ is likely to be a factor contributing towards the noted differences in toxicological impact. However, given the lack of effect of Tl on whole-animal K^+ concentration (Fig. 3.2), it is unlikely that

water K^+ level played a significant role. It is clear that a more detailed mechanistic analysis of how Tl mediates chronic toxicity in *D. magna* is warranted.

Effects on daphnid growth and reproduction are frequently reported following trace metal exposure (e.g. Biesinger and Christensen 1972; Sadeq and Beckerman 2019). Changes in these metrics are likely linked to altered energy metabolism. Under toxicant exposure, maintenance costs (e.g., upregulation of detoxification pathways, greater demand for cellular and tissue repair) may increase, while there are often direct effects of toxicants on energy acquisition (e.g., impairment of nutrient/oxygen uptake; assimilation efficiency; Beyers et al. 1999; Baillieul et al. 2005). Together, or independently, these effects will reduce the energy available to a toxicant-exposed animal, and will force a compromise between maintenance of homeostatic pathways for survival, growth and reproduction. Consequently, the observed effects on growth and reproduction in the current study likely reflect changes in the overall energy budget. Further research examining metabolic rate (Knops et al. 2001), and/or changes in cellular energy substrates (De Coen and Janssen 2003), would be required to confirm this hypothesis.

3.5. Conclusion

Over a 21-d exposure period, Tl induced changes in reproduction and growth of *D. magna* at concentrations characteristic of some industrial wastewaters (Cheam 2001). However, no statistically significant effects were reported at exposure concentrations close to the current regulatory threshold (0.8 $\mu g\ L^{-1}$: CCME 2007), indicating that under controlled laboratory conditions in the present study *D. magna* is significantly less sensitive to Tl toxicity than the organism on which the current regulations are based (*L. minor*). Intriguingly, the current work highlighted distinct responses to waterborne Tl exposure to those determined in previous studies in freshwater crustaceans. For example, there were notable differences in the relative sensitivity

of growth and reproduction, and a lack of evidence for an effect on whole-animal K^+ status. This suggests that differences in toxic mechanisms likely exist between studied freshwater crustacean species, and also between short- and long-term exposures. This has important implications for the development of water quality criteria using predictive modelling approaches such as the BLM, where it is assumed that mechanism of toxicity is conserved across time and species (Niyogi and Wood 2004).

4. Effect of thallium on phototactic behaviour in *Daphnia magna*

4.1. Introduction

The freshwater invertebrate, *Daphnia magna*, is a key species for assessing the effects of toxicants on aquatic ecosystems from the perspective of both their ecological and regulatory importance. Daphnids occupy a critical niche in freshwater food chains, feeding on phytoplankton and acting as a food source for higher trophic levels (e.g., Miner et al. 2012). Furthermore, because of their relative ease of culture and general sensitivity to toxicants (Baudo 1987), daphnids are regulatory species recommended by multiple organizations, including the USEPA, CCME) and OECD (CCME 2007; OECD 2004; USEPA 2002). In addition, *D. magna* is considered a sensitive bioindicator of potential ecological problems caused by mining and smelting activities (Tomasik and Warren 1996).

One contaminant of concern associated with mining and smelting activities is the trace metal Tl. Although found at low concentrations in most natural settings, in rivers adjacent to base metal mining activities in the USA and Canada Tl concentrations up to ~100 μg L^{-1} have been regularly recorded (USEPA 1980; Zitko and Carson 1975). Indeed, one report has even noted Tl concentrations in excess of 15 mg L^{-1} (Williams-Beam and Twidwell 2003). These concentrations exceed the CCME guidelines for Tl in surface waters, which recommend that surface water Tl concentrations not exceed 0.8 μg L^{-1} (CCME 2007). This CCME guideline is one of the few regulatory values that exist for Tl in aquatic environments, but is based only on the effects of Tl on growth of an aquatic plant (Brown and Rattigan 1979; CCME 2007, Kwan and Smith 1988).

The sensitivity of aquatic animals exposed to waterborne Tl has been previously characterized, but only for a limited number of endpoints. For example, 48 h LC_{50} values for Tl

toxicity to daphnids range between 1.66 and 1.86 mg L^{-1} (Chapter 2; Lin et al. 2005). Lowest observed effect concentrations for chronic Tl toxicity have been documented at environmentally relevant levels of 8.8 µg L^{-1} for *Daphnia magna,* using the endpoints of growth and reproduction (Chapter 3). Similarly, EC/LC_{50} values have been calculated for the aquatic invertebrate species *Hyalella azteca* for survival (4-week LC_{25}: 48 nmol L^{-1} = 9.8 µg L^{-1}), growth (6-week EC_{25}: 35 nmol L^{-1} = 7.2 µg L^{-1}), and reproduction (10-week EC_{25}: 10 nmol L^{-1} = 2.0 µg L^{-1}) (Borgmann et al. 1998). While these data indicate Tl concentrations at which risks to aquatic biota may occur, there remains a large gap in our knowledge of the underlying mechanisms of Tl toxicity to aquatic organisms.

In mammals, Tl is a neurotoxicant (e.g., Bramanti et al. 2019). The mechanisms by which Tl induces neurotoxicity are yet to be confirmed, but evidence exists for effects related to the promotion of oxidative damage, and inhibition of the basolateral Na^+/K^+-ATPase (Maya-López et al. 2018), the enzyme that drives cellular ionoregulation. This latter effect may relate to the known role of Tl in perturbation of potassium homeostasis (e.g., Hassler et al. 2007). However, a neurological mode of Tl toxicity has not been specifically examined in any freshwater organism.

One approach to investigating the neurotoxicity of Tl to *Daphnia magna* is to assess effects on phototactic behaviour. Phototaxis is a behavioural endpoint whereby the animal moves towards or away from a directed light stimulus. In daphnids this endpoint has been used to assess the toxicity of hydraulic fracturing flowback and produced waters (Delompré et al. 2019a), impairments induced by trace metals (e.g., Kolkmeier and Brooks 2013; Michels et al. 1999; Wu et al. 2008), and the effects of food scarcity (e.g., Johnsen and Jakobsen 1987; Michels and De Meester, 1998; Van Gool and Ringleberg 2003). Negative phototactic behaviour reduces potential ultraviolet (UV) damage and predation risk by avoiding the top of the water column

during daylight hours (e.g., McCoole et al. 2011), while positive phototaxis may facilitate feeding under predator-free conditions (Michels and De Meester 1998). Positive and negative phototaxis behaviours both exist in natural daphnid populations (e.g., De Meester 1993; Ringelberg 1999), and both responses have been used as indicators of potential adverse impacts of pollutants (e.g., Kolkmeier and Brooks 2013; Michels et al., 1999).

Changes in phototactic behaviour result from either impairment in the capacity of the organism to detect the stimulus (i.e., a sensory effect), or from a failure to respond appropriately to the stimulus (i.e., a motor effect). In daphnids, phototactic responses are driven by a number of different neurotransmitter systems, including dopaminergic, GABAergic and histaminergic signaling pathways (Barrozo et al. 2015; Bedrossiantz et al. 2021; McCoole et al. 2011). For example, McCoole and colleagues (2011) inhibited a negative phototactic response by exposing daphnids to the histamine receptor 2 (H2) antagonist cimetidine, which blocked the sensory stimulus. The motor responses of daphnids are linked to the activity of the enzyme acetylcholinesterase (AChE; Printes and Callaghan 2004). Acetylcholine is a critical signaling molecule in transmitting sensory information to nerves and muscles, and its activity is regulated by AChE. Consequently, changes in AChE activity can be informative of a toxicant effect on motor activity. Indeed, studies have shown that changes in swimming behaviour correlate with changes in AChE activity in daphnids (Ren et al. 2017), that these effects can be observed at sublethal toxicant concentrations (Ren et al. 2017), and are toxicant-specific (Guilhermino et al. 1996). A previous study has noted that AChE is a target of Tl toxicity in mouse neuroblastoma cells *in vitro* (Repetto et al. 1994).

This study aims to determine the effects of Tl on *D. magna* phototactic behaviour. These studies were conducted using naïve animals (i.e., not previously exposed to Tl) only subjected to Tl in

the assay water. This experimental design was used to minimize any effect of Tl on energy metabolism (e.g., Li et al. 2020), which could affect responses to light stimuli through mechanisms other than via the nervous system. It was hypothesized that neurological effects of Tl are conserved between mammalian and aquatic species, and that Tl would therefore affect the capacity of daphnids to respond to light. This was assessed using behavioural assays to measure phototactic responses, coupled with biochemical assays to determine whether the effects of Tl on daphnid behaviour were mediated by sensory or motor impairment.

4.2. Materials and methods

4.2.1. *Daphnia magna*

Daphnia magna were initially obtained from Aquatic Research Organisms (Hampton, NH, USA), and thereafter maintained in the Department of Biological Sciences at the University of Alberta. *Daphnia* were reared in International Organisation for Standardisation (ISO) test water 1 (hereafter referred to as ISO water): $CaCl_2.2H_2O$ (2 mM), $MgSO_4.7H_2O$ (0.5 mM), $NaHCO_3$ (0.77 mM), and KCl (0.08 mM), reconstituted in ultrapure water (OECD 2004). Feeding consisted of a combination of YCT (a yeast, cereal leaf, trout chow mix; ~0.5 mL L^{-1}), algae (*Raphidocelis subcapitata*; ~ 500 000 cells L^{-1}), and Roti-Rich liquid invertebrate food (~ 3 drops L^{-1}) once daily. Neonates (< 24 h old) used for experiments were removed from culture beakers and transferred immediately into treatment waters for testing. Adult daphnids were separated after birth and maintained in individual 50-mL beakers for 15 days, under the feeding regime described above for the source culture. All *Daphnia* were maintained at room temperature (22 ± 1°C) under a 16:8-h dark:light cycle.

4.2.2. *Vertical phototaxis assay*

Phototaxis was initially assessed via a vertical chamber method, modified from that described by De Meester (1989). A 9 cm^2 hole was cut in the top of a cardboard box (30 x 15 x 30 cm) which housed the test chamber. The test chamber (100 mL graduated glass cylinder; 25 cm height) was marked in 20-mL increments (upper, U; medial, M_1, M_2, M_3; lower L), to allow for quantification of phototactic response. Test solutions consisted of ISO test water 1 with Tl added from a $TlNO_3$ (Sigma-Aldrich, Oakville, ON, Canada) stock solution to achieve nominal concentrations of 0, 0.8, 700, 1860, and 8000 µg Tl L^{-1}. These concentrations represent a Tl-free control; the CCME regulatory limit (CCME 2007); an elevated environmental concentration; the 48-h LC_{50} value in this water chemistry (Chapter 2), and a 48-h LC_{100}, respectively. Ten naïve daphnids (i.e., not previously exposed to Tl) were transferred into the chamber, which was then placed into the cardboard box. The box was closed, and a light source was placed over the opening at the top of the box (5.5 cm from the waterline). The light source only generated visible light. Daphnids were not exposed to UV light during the experiment. After 5 min the box was opened, the chamber removed, and the number of daphnids in each zone was counted. After the data were collected, the following equation was used to calculate I_p, the 'Phototaxis Index' (De Meester 1993): where the letters represent the number of daphnids in each section of the test chamber, as defined above. The I_p value always lies between -1 and +1.

Equation 4.1:

$$I_p = \frac{U-L}{U+M_1+M_2+M_3+L}$$

The vertical phototaxis behavioural assay was used to test naïve neonate (<24 h old) and naïve adult (10-15 d old) *Daphnia* in both fed and fasted states. For fed exposures, daphnids were given YCT, at a concentration approximating a normal daily YCT ration, ten minutes prior

to the test. For fasted exposures, food was withheld from daphnids for 24 h prior to experimentation. To account for the possibility of behavioural variation over the course of a day, all vertical chamber behavioural trials were performed by testing a new group of daphnids every hour between 8 am and 8 pm. This was repeated over 8 experimental days (i.e., n = 8 for each time of day). For all vertical assay assessments, a "no light" control was conducted to verify that positive phototaxis behaviour occurred in response to the light stimulus rather than a consequence of disturbance associated with the movement of animals to the test chamber. No measures of daphnid Tl accumulation were conducted, owing to the short nature of the actual exposure to Tl (5 min.).

4.2.3. *Horizontal phototaxis assay*

This assay was used to assess the speed at which daphnids moved along a horizontally placed tube towards a light source, providing an additional measure of the phototactic response. The system used was identical to that described in Delompré et al. (2019a). Individual fasted naïve adults (10-15 d old) were placed in the test apparatus and exposed to one of 5 Tl treatments (nominal concentrations: 0, 0.8, 700, 1860, and 8000 µg Tl L^{-1}). A positive response was one where the daphnids appeared in the clear, illuminated portion of the tube. Speed was calculated as the length of distance travelled (from entry point to lit end), divided by the time to traverse that distance (cm s^{-1}). If the daphnid did not appear after 5 minutes, then it was assigned a score of 300 s. Again, due to the short duration of the actual Tl exposure no measures of daphnid Tl accumulation were taken.

4.2.4. Histamine receptor inhibitor assay

A histamine receptor inhibitor assay was used to determine the effects of Tl on phototactic behaviour and was conducted as described by McCoole et al. (2011). Prior to exposures, a

freshly made 1 M cimetidine (an inhibitor of the H2 receptor; Sigma-Aldrich, Oakville, ON, Canada) stock solution was prepared by dissolving cimetidine salt in DMSO. Test conditions included a control group without either cimetidine or Tl, a vehicle control (DMSO only, at 0.2%), a Tl control (nominally, 1860 µg L^{-1}), a cimetidine control (2 mM), and a Tl + cimetidine treatment (1860 µg TI L^{-1} + 2 mM cimetidine). The concentration of cimetidine used has been previously shown not to impair swimming behaviour (see Fig. 5 in McCoole et al. 2011). Each replicate represented ten naïve juvenile *Daphnia magna* (7-8 d old), that were placed in each test solution and observed in the vertical phototactic chamber as described above.

4.2.5. *Acetylcholinesterase assay*

A colorimetric assay (Ellman et al. 1961) was used to assess AChE activity. Briefly, naïve adult daphnids (10-15 d old) were exposed to control conditions (0 µg L^{-1} Tl) or the median acute lethal concentration (nominally, 1860 µg L^{-1} Tl) in ISO water. Following a 5-min exposure, daphnids (three per replicate) were removed, gently blotted dry and immediately homogenized using a motorized mortar and pestle in 500 µL of ice-cold phosphate buffer (pH 7.4), before being stored at -80°C until analysis. Using a 96 well plate, 50 µL of standard (i.e., AChE as a positive control) or sample was pipetted into the well followed by 100 µL of 5,5′-dithiobis-(2-nitrobenzoic acid) and 20 µL of acetylcholine iodide. The plate was then read at a wavelength of 412 nm once per minute for 6 minutes using a microplate reader (VersaMax Plate Reader). Bradford assays were conducted to quantify protein content within samples (Bradford 1976). Acetylcholinesterase activity is presented as moles of substrate hydrolyzed per minute per µg protein.

4.2.6. *Tl analysis*

Immediately following the 5-min behavioural assay, water samples (10 mL) were collected and passed through a 0.45 μm syringe filter and acidified with 1% trace metal grade nitric acid. Concentrations of dissolved Tl were determined using ICPMS. Multi Element Standard-1 (MES-1; Spex CertiPrep, Metuchen, NJ, USA), surface water standard reference materials SPS-SW2 (diluted 10 - and 500-fold; Spectapure Standards, Oslo, Norway), and NIST 1640a (diluted 10- and 100-fold; National Institute of Standards and Technology, Gaithersburg. MD, USA) were used for quality assurance. Blank values for the analysis were determined by calculating the average of three 2% nitric acid replicates. To account for drift in ICPMS sensitivity, an internal standard (10% nitric acid solution spiked with 5 μg L^{-1} indium and bismuth) was used. Limit of detection (LOD) and limit of quantification (LOQ) for the analysis were 0.11 and 0.76 ng L^{-1}, respectively. Any concentrations measured below the LOQ were assigned a value halfway between the LOQ and zero.

4.2.7. *Calculations and statistics*

Prior to statistical analysis, Grubb's test was employed for detection and removal of outliers. One outlier was subsequently removed from the adult swimming speed assessment at the highest Tl test concentration. For all analyses, assumptions of parametric analysis were tested using the Shapiro-Wilk test for normality and the Brown-Forsythe test for homogeneity of variance. Initially, a two-way ANOVA (with time of day and Tl concentration as the two factors) was conducted on assays conducted at distinct times of the day and showed that time of day did not have a significant effect on response. This allowed data to be pooled across the different test times. Subsequently, the phototactic responses of daphnids in the vertical assay were analysed using a two-way ANOVA (where the two factors were Tl concentration and the presence/absence of light), followed by a post hoc Tukey's test. Swim speed data were not

normally distributed, and therefore were analyzed using a non-parametric Kruskal-Wallis test. Effects of the H2 receptor antagonist cimetidine on phototaxis were analyzed by one-way ANOVA with a post hoc Tukey's test. The activity of AChE was analyzed using an unpaired t-test. All reported values represent the mean ± standard deviation. All statistical analyses were conducted using Prism GraphPad.

4.3. **Results**

4.3.1. *Thallium exposure concentrations*

Measured Tl concentrations were slightly higher than, but close to, nominal values (Table 4.1). Background concentrations of Tl in ISO water were below the LOQ (i.e., < 0.76 ng L^{-1}). From this point forward in this chapter, measured concentrations will be referred to in the text.

Table 4.1. Nominal and measured dissolved Tl concentrations.

Nominal Concentration (µg L^{-1})	Measured Concentration (µg L^{-1})
0	< LOQ
0.8	0.82 ± 0.07
700	917 ± 34
1860	2099 ± 54
8000	8395 ± 59

Values represent mean ± standard deviation, n = 6.
LOQ = 0.76 ng L^{-1}.

4.3.2. *Behavioural assay*

Daphnids in the vertical test chamber displayed a positive phototaxis response. Significant differences were noted between the "light" and "no light" treatments for all test conditions (two-way ANOVA, p-value < 0.05; Figure 4.1). No significant effect of test water Tl concentration on daphnid behaviour was determined in any of the "no light" treatments. There were no differences in phototactic responses as a function of time of day (data not shown; two-way ANOVA, p-value range 0.11 – 0.28). Because of this lack of effect, data examining the

effect of test water Tl on phototaxis were pooled independent of the time of day the tests were conducted. Subsequently, no significant differences in phototactic behaviour (i.e., in the presence of light in the test chamber) were observed in neonates (both fed and fasted) and fed adult *Daphnia magna* as a function of test water Tl concentration (Fig. 4.1a, 4.1b, 4.1d). However, adult fasted daphnids tested in 917 or 2099 µg Tl L^{-1} exhibited positive phototactic responses that were significantly greater relative to the phototactic responses observed at all other test Tl concentrations (Fig. 4.1c).

Effects on adult swim speed in the horizontal test chamber were observed at a test concentration of 2099 µg Tl L^{-1} (p-value = 0.01; Figure 4.2). Adult daphnids exposed to this concentration of Tl exhibited a swimming speed approximately 40% of that recorded in the control group daphnids. No significant differences in swim speed relative to the Tl-free control were observed in any of the other treatment groups.

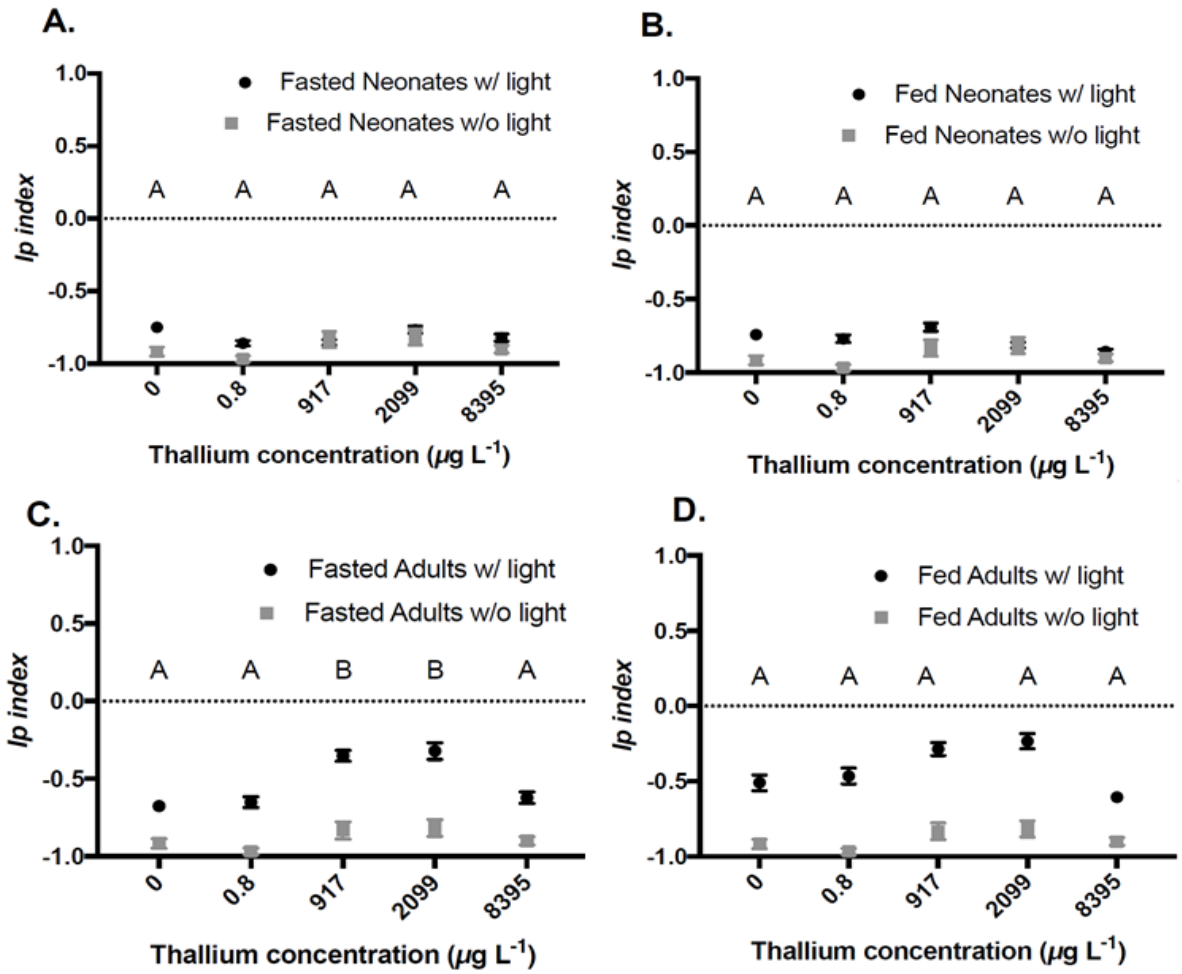

Figure 4.1. Effect of waterborne Tl exposure on phototactic behaviour of fed (A) and fasted (B) neonate (<24-h); and fed (C) and fasted (D) adult (10-15 day) *Daphnia magna*. Plotted points represent means (± standard error) of 96 replicates. Letters represent data points collected in light exposures. Plotted values not sharing letters are statistically significantly different ($\alpha = 0.05$).

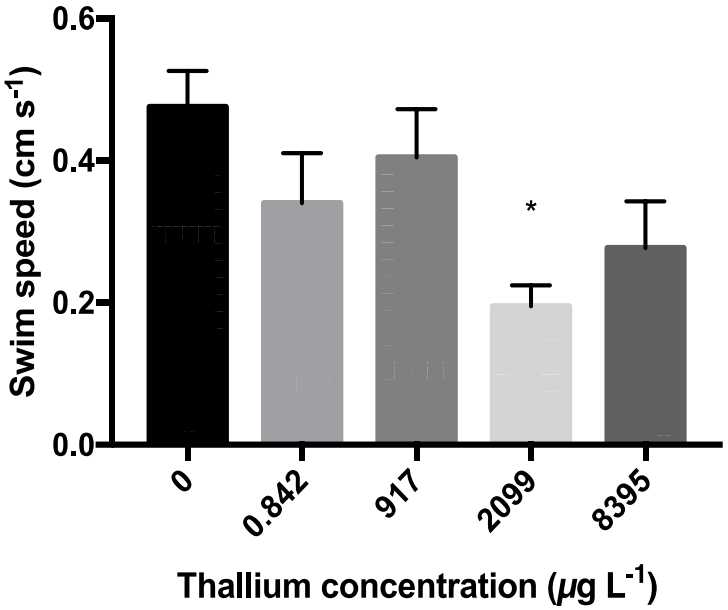

Figure 4.2. Effect of waterborne Tl exposure on fasted adult (10-15 day) *Daphnia magna* swim speed. Plotted points represent means (± standard deviation) of 7-8 replicates. Asterisk (*) indicate a significant difference relative to the control (0 µg L^{-1} Tl).

4.3.3. *Acetylcholinesterase assay*

There was a trend towards an increase in AChE activity in adult daphnids exposed to 2099 µg Tl L^{-1} (Figure 3). However, this effect was not statistically significant (t-test, $p = 0.10$).

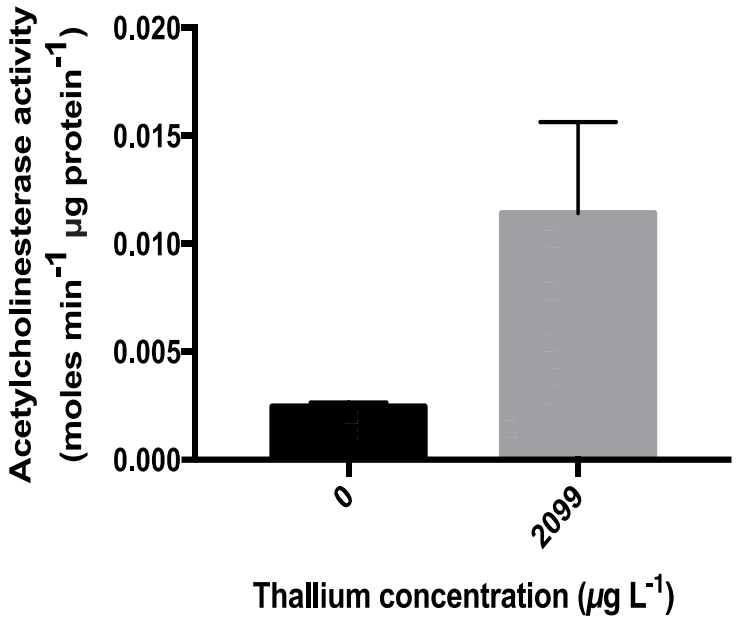

Figure 4.3. Acetylcholinesterase activity (moles min^{-1} µg $protein^{-1}$) in fasted adult (10-15 d) *Daphnia magna* exposed to 2099 µg L^{-1} Tl. Plotted points represent the mean (± standard deviation) of 6 replicates.

4.3.4. *Histamine receptor inhibition assay*

The effects of the H2 receptor antagonist, cimetidine, on daphnid phototactic behaviour in a vertical test chamber are exhibited in Figure 4.4. Cimetidine exposure resulted in a significantly more positive phototactic response than the Tl-free control ($p = 0.001$), an effect was statistically identical to the response induced in the presence of Tl alone. When Tl and cimetidine were both present, the stimulatory effect of each component was abolished, and the phototactic response observed was not significantly different from the control ($p = 0.99$).

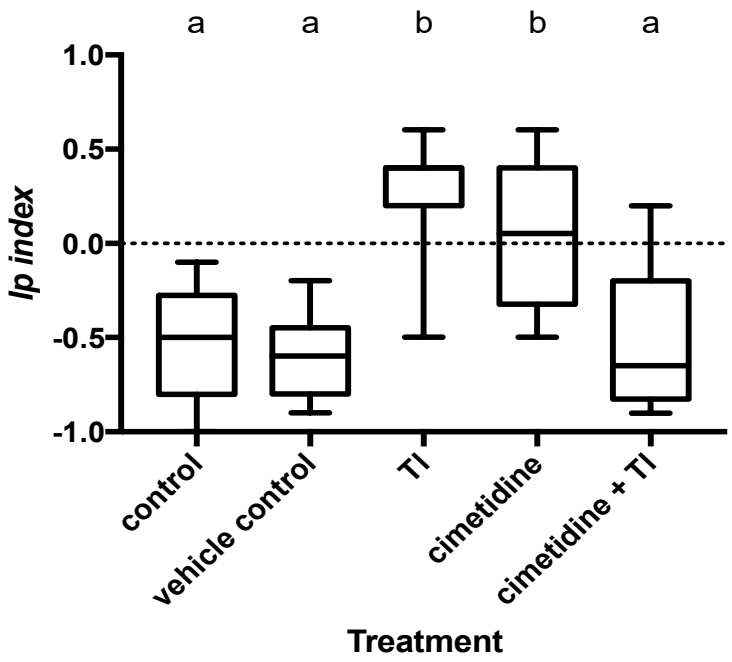

Figure 4.4. I_P following 5-minute exposure of fasted adult (7-8 day) *Daphnia magna* to 2099 µg L^{-1} Tl in the absence or presence of 2 mM cimetidine. Plotted points represent the median, lower and upper quartiles (± minimum and maximum values) of ten replicates. Plots sharing letters are not statistically significantly different ($\alpha = 0.05$).

4.4. Discussion

The presence of Tl in the test water resulted in effects on daphnid phototactic behaviour. These effects were observed only for fasted adult daphnids, which exhibited a significantly more positive phototactic response in the presence of 917 and 2099 µg Tl L^{-1} than in the Tl-free control. The phototactic responses of daphnids are hypothesised to mediate diel vertical migrations. As such, the predicted response to light exposure would be a negative phototaxis, avoiding potentially harmful effects of UV irradiation and reducing exposure to visual predators (Ringelberg 1999). In the current study, however, the basal response of daphnids to light was a movement towards the light source. In natural settings, the negative phototactic response is likely reinforced through the presence of fish kairomones. Under laboratory culture conditions, where

daphnids are raised for multiple generations in the absence of predatory cues and the absence of other negative stimuli such as UV exposure, then a positive phototaxis is not unexpected (De Meester 1993). Indeed, even in natural environments, clones of *D. magna* occur that display positive phototaxis (De Meester 1991). A positive phototactic response has been observed previously for the daphnid culture that was used in the current experiments (Delompré et al. 2019a). In the current study, Tl enhanced this phototactic response, suggesting a disruption of the mechanisms that regulate daphnid responses to light.

It was notable that effects of Tl on the phototactic response were observed at 917 and 2099 µg Tl L^{-1}, but not the highest test concentration of 8395 µg Tl L^{-1}. This test concentration is approximately four times the LC_{50} value (Chapter 2; Lin et al. 2005) and thus represents an extreme scenario, if even only for the 5 min of Tl exposure. Therefore, it is likely that the lack of response at the highest test concentration is a consequence of daphnids being functionally immobilized. There is some evidence to support this from the horizontal phototaxis assay. In that experiment, the presence of 2099 µg Tl L^{-1} reduced swimming speed (Fig. 4.2). In the vertical phototaxis assay this reduced speed was insufficient to affect the capacity of the 2099 µg Tl L^{-1} daphnids to respond towards the light (i.e., although swimming speed was reduced, over the 5-min exposure interval of the vertical behavioural assay, daphnids were still capable of exhibiting an enhanced capacity to move towards the light source). Swimming speed in the 8395 µg Tl L^{-1} group trended towards inhibition but was not significant (Fig. 4.2). This suggests that daphnids tested at 8395 µg Tl L^{-1} can reach the light source in the horizontal assay before the effects of immobilization are induced, whereas the 5-min exposure in the vertical assay is sufficiently long to induce an incapacity to enact a Tl-mediated response to the light stimulus. A non-monotonic pattern of toxicity where effects are seen at lower concentrations and not at higher

concentrations, is not uncommon in studies of neurotoxicant effects in crustaceans (Fong and Ford 2014).

An impairment in phototactic behaviour could be mediated by an effect on the capacity of the animal to sense the stimulus or through disruption of the appropriate motor response enacted in response to the stimulus. These possibilities were examined in fasted adult daphnids tested in waters with 2099 μg Tl L^{-1}, the concentration where an increase in the positive phototactic response was observed. Phototactic behaviour in daphnids is controlled in part by the histaminergic signaling system (McCoole et al. 2011). Cimetidine, an H2 receptor antagonist, blocks histamine signaling pathways and subsequently inhibits negative phototactic behaviour (McCoole et al. 2011). In our study, the increase in positive phototaxis upon cimetidine exposure is consistent with this previous work and closely matched the response induced by Tl (Figure 4.4). Intriguingly, in tests where Tl and cimetidine were both presented to daphnids, the significant effect of each component on positive phototaxis was abolished. This suggests that Tl and cimetidine act on different components of the histaminergic signaling pathway (i.e., the effect of Tl is not mediated by blockade of the H2 receptor), and it also indicates that the presence of cimetidine inhibits the mechanism of Tl effect on this pathway. On this basis, the most obvious explanation for the Tl effect is that it involves inhibition of nerve function. Thallium is well characterized as a mimic of K^+ and can interfere with K^+ transporter conductance (e.g., Matteson and Swenson 1986). It is therefore hypothesized that Tl interferes with histaminergic signaling by impeding K^+ conductance in daphnid sensory neurons. In the absence of H2 receptor activation (i.e., in the presence of cimetidine), this effect is ameliorated (i.e., there is no conductance to inhibit). In general, Tl has a very low binding affinity for organic

ligands (Chapter 2), so it is doubtful that the lack of effect in mixed Tl/cimetidine test waters is due to complexation and consequent nullification of Tl reactivity.

As noted above, altered responses to a stimulus could be a consequence of an effect on the motor system. In the current study, we examined whether AChE activity was altered when daphnids were tested in the presence of Tl and whether this could therefore explain the effect of Tl on positive phototaxis in adult daphnids. In general, exposures to trace metals cause inhibition of AChE activity, an effect that correlates with impaired locomotion (Xuereb et al. 2009). This is also true specifically for insecticide-exposed *D. magna*, where increased immobility and swimming behaviour in general, are directly related to reduced AChE activity (Printes and Callaghan 2004; Ren et al. 2017). In the current study, at Tl concentrations where a more positive phototaxis was recorded, a non-significant trend towards elevated AChE activity was observed, which is generally consistent with a role for this enzyme in daphnid locomotion. There is, however, insufficient statistical support to attribute the change in daphnid phototactic behaviour in response to Tl to a change in the capacity of the animal to enact a motor response to the stimulus. Given the lack of effect of Tl on AChE, and concomitantly the significant effect of the cimetidine exposure, it can be concluded that the Tl-induced change in phototaxis is mediated through a sensory mechanism of action.

There were no significant effects of Tl on positive phototaxis in neonates. Relative to adults, neonate daphnids have a less well-developed phototaxis response, a pattern that is obvious in Figure 4.1, where the *Ip* value is lower in neonate tests than in adult tests. This is consistent with previous studies. For example, De Meester (1992) studied *D. magna* clones that display positive phototaxis, and showed that juveniles (1-4 d old) had a reduced positive phototactic response compared to older individuals of that clonal group. Other authors have noted that relative to

adults, daphnid neonates display higher variability in their responses to light (Delompré et al. 2019a; Whitman and Miller 1982), which is a factor that might also contribute to their lesser response, and thus a reduced scope to delineate an effect of Tl.

In the current study, effects of Tl on positive phototaxis were only observed in fasted adults. One explanation for the lack of effect in fed animals is that Tl complexation to food may reduce its bioavailability and thus minimize its effects. However, as noted above, Tl does not have a high affinity for waterborne ligands (Chapter 2), and thus this is unlikely to explain the lack of effect of Tl on fed animals. Instead, the response is likely a consequence of the fed state of the animal. For example, previous studies have shown that culture conditions can influence phototactic behaviour. In contrast to the effects we observed (i.e., a more pronounced positive phototaxis in response to a lack of food), De Meester and Dumont (1989) tested the influence of different culture food concentrations on photobehaviour in *D. magna* and showed a reduced positive phototaxis in response to long-term food restriction. However, because of the long-term nature of the food restriction in that study, an effect due to behaviour or one due to a lack of physiological capacity to respond could not be distinguished. Similarly, reports of a reduced positive phototaxis in *Daphnia* in response to short-term fasting exist (Van Gool and Ringleberg 1995; 1998). Conversely, some authors have found results similar to ours, where short-term food deprivation increased positive phototaxis in daphnids (Clarke 1932). Differences between studies are likely due to factors such as the nature of the phototactic stimulus (Pearre 2003), food quality (Michels and De Meester 1998), and the ingrained response (i.e., positive or negative) of a specific daphnid clone to a light stimulus (De Meester 1993). It is hypothesized that the lack of effect of Tl on fed adults is due to the availability of dietarily-sourced K^+, which could be

mobilized to offset the Tl-induced effects on K^+ handling that may contribute to the sensory impairment.

The modification of daphnid phototactic behaviour by toxicants has important utility in environmental monitoring. For example, automated systems have been developed that facilitate the continuous recording of daphnid behaviour following a toxicant exposure (Gerhardt et al. 2006; Lechelt et al. 2000). The most refined approaches are capable of deployment in field settings, where they can provide continuous, real-time data that reflect the extent of water pollution (Dyomin et al. 2020). Such techniques offer several advantages over traditional laboratory-based biomonitoring including high sensitivity, rapid identification of a hazardous pollution event, environmental relevance, and the avoidance of issues associated with the ethical use of vertebrates in research (Dyomin et al. 2020; Gerhardt et al. 2006; Lechelt et al. 2000). The current study suggests that daphnids are responsive to elevated water Tl concentrations, and as such behaviour-based biomonitoring may be applicable to receiving waters at risk of Tl contamination.

4.5. Conclusion

The current study shows that the presence of a very high concentration of waterborne Tl disrupts the phototactic response of fasted adult *D. magna*. It appears that this response is mediated through an effect on the histaminergic signaling pathway, thus representing the first mechanistic demonstration of an effect of Tl on the nervous system of a freshwater organism. It is important to note that all significant changes in phototaxis were observed at Tl concentrations of 917 or 2099 μg L^{-1}, representing very high environmental scenarios. No significant effects were observed at the regulatory threshold (0.8 μg L^{-1}: CCME 2007). In the current work, the effects of water Tl were tested in a *D. magna* clone that exhibits a positive phototactic response,

in contrast to most natural *Daphnia* populations, which display negative phototaxis. The effects of Tl on daphnids that naturally exhibit a negative phototactic response remain unexplored.

As noted above, behavioural responses to toxicants by invertebrate species such as *D. magna* have potential value as a biomonitoring tool. Such approaches allow for continuous evaluation of an at-risk watershed, can be sensitive and rapid, and avoid ethical issues associated with more invasive methods of assessment (e.g., Dyomin et al. 2020; Gerhardt et al. 2006; Lechelt et al. 2000). Our data provide preliminary support for the implementation of daphnid photobehaviour as an endpoint for monitoring waterborne Tl toxicity.

5. Mechanistic examination of thallium and potassium interactions in *Daphnia magna*

5.1. Introduction

Traditional endpoints in aquatic toxicology include mortality, reproduction and growth. These are all metrics that have consequences at the population level, and are thus of high ecological relevance (Adams et al. 1992). However, effects on these endpoints may take time to manifest, may occur only after prolonged exposure to relatively high toxicant concentrations, and may therefore lack sensitivity (Forbes and Calow 2002). In contrast, examination of sub-lethal effects at an individual level can identify toxicant effects more rapidly, and at lower environmental concentrations (Van der Oost et al. 2003; Barata et al. 2008). Mechanistic knowledge of toxicant-organism interactions, such as uptake at epithelia and effects on molecular, biochemical and physiological pathways, have significant utility in risk assessment (Di Toro et al. 2001; Ankley et al. 2010). For example, mechanistic understanding is useful for the identification of biomarkers, which can aid in detecting environmental issues of concern (De Schamphelaere and Janssen 2002; De Schamphelaere et al. 2009). More importantly, a mechanistic understanding allows prediction of how toxicity changes with environmental factors such as water chemistry and the presence of other toxicants (Glover 2018). Such predictions are the basis of state-of-the-art risk assessment tools.

The mechanisms of Tl toxicity are not completely understood. However, several studies across a number of different species suggest that Tl can mimic K^+, and that this might be a key step in a toxic mechanism that results in the disruption of K^+ homeostasis (Cvjetko et al. 2010). Evidence for the mimicry of K^+ by Tl^+ is provided by both physicochemical data and experimental biology. In terms of the former, there are close similarities in charge (+1) and size (ionic radii: K^+ = 137 pm; Tl^+ = 150 pm; Shannon 1976) between the two ions, which would

theoretically facilitate substitution of K^+ by Tl in biological processes. Experimental confirmation of this interaction is provided by several studies that have shown Tl interactions with K^+ transporters. For example, Tl was found to have a 10 times greater affinity than K^+ for the K^+ binding site of NKA in rabbit kidney (Britten and Blank 1968). Similarly, in oocytes of lamprey Tl can substitute for K^+ at the Na^+, K^+, $2Cl^-$ (NKCC) cotransporter (Sherstobitov et al. 2010), and in gastric epithelia of hogs Tl has a 10-fold greater affinity for transport through K^+,H^+-ATPase than K^+ (Rabon and Sachs 1981). Since the cellular transport of Tl seems to be linked with K^+, and cellular Tl accumulation is linked to toxicity of Tl (Kwan and Smith 1988), it is possible that the mechanism of cellular Tl uptake may play a role in Tl toxicity.

Supporting this hypothesis, several studies suggest that K^+ can modify Tl toxicity to aquatic organisms. For example, exposure of *Ceriodaphnia dubia* to a K^+-depleted medium reduced the 48-h LC_{50} of Tl from >400 to 71 μg L^{-1} (Rickwood et al. 2015). In a study on two other daphnid species, Tatsi et al. (2015) showed that median effect concentrations of Tl were dependent on water K^+. These same authors also attributed effects of Tl on zebrafish heart rate to altered K^+ homeostasis (Tatsi et al. 2015). Effects of K^+ on Tl toxicity have also been observed in microalgae (Hassler et al. 2007). For example, growth of *Chlorella* was inhibited at Tl concentrations of 40 to 400 nM in low K^+ media (0.5 μM K^+; Hassler et al. 2007), but at media K^+ concentrations greater than 10 μM, no effects of Tl on growth rate were observed (Hassler et al. 2007). Modification of Tl uptake by K^+ has also been reported. For example, uptake of Tl in *Chlorella* was significantly lower when exposure occurred in waters collected from Lake Erie than in waters collected from Lake Superior (Twiss et al. 2004). This difference was attributed to greater K^+ concentrations in the Lake Erie water relative to the Lake Superior water.

The modifying effects of K^+ on Tl toxicity are reminiscent of similar effects of Na^+ ions on the toxicity of the trace metals Cu and Ag to aquatic biota. In both of these cases, the presence of Na^+ reduces accumulation of the toxic metal, and subsequently reduces toxicity (Erickson et al. 1996; Dethloff et al. 2007). These interactions form the basis of the BLM (Di Toro et al. 2001), a predictive risk assessment tool for the protection of aquatic ecosystems against trace metal toxicity. The BLM is based upon the gill surface interaction model and incorporates mechanistic understanding of three key elements that affect toxicity: trace metal uptake; the relationship between accumulation and toxicity; and interactions between the trace metal and water chemistry. Combined, this knowledge can be used to predict toxicity on a site-specific basis (Di Toro et al. 2001; Niyogi and Wood 2004). For example, it is known that Cu is taken up across the gills of aquatic animals as a mimic of Na^+. Therefore, ligands such as DOC bind Cu, prevent it from using branchial Na^+ transporters, thus reducing Cu toxicity (De Schamphelaere et al. 2009). Similarly, elevated water Na^+ will effectively outcompete Cu for uptake, also reducing toxicity (De Schamphelaere and Janssen 2002). Thus, knowledge of water chemistry components such as Na^+ and DOC can be used to develop a site-specific prediction of toxic impact for a given water Cu concentration. The BLM is a tool that has been integrated into freshwater guidelines for trace elements worldwide (De Schamphelaere and Janssen 2002; USEPA 2007; Rüdel et al. 2015; Gondek et al. 2017). If K^+ has a similar effect on Tl toxicity as Na^+ does on Cu toxicity, then it may be possible to develop a BLM for Tl that accounts for water K^+ concentration.

As noted above, predictive risk assessment approaches such as the BLM rely on mechanistic understanding of toxicity, from knowledge of uptake pathways to molecular and cellular effects of the absorbed toxicant. While there is evidence for interactions between Tl and

K^+ transporters, it is not known if, and how, Tl exposure affects function of these transporters. Of particular interest are K^+ channels. These represent pathways by which Tl could enter a cell, and are also targets for therapeutic drugs. As such they are amenable to manipulation in order to investigate their role in mediating Tl toxicity. Potassium channels are categorized into four major classes: voltage gated (K_v), inwardly rectifying (K_{ir}), calcium-activated, and tandem pore domain (Buckingham et al. 2005), and in mammals there are a total 70 K^+ channel-encoding genes (González et al. 2012). A variety of drugs have been developed that block specific K^+ channels involved in human diseases. For example, clozapine binds the voltage gated K_v11.1 K^+ channel, which mediates cardiac action potentials and has a role in heart disease (Hill et al. 2014). The pharmaceutical chlorpropamide inhibits ATP-sensitive inwardly rectifying K^+ channels which depolarize cell membranes (Hibino et al. 2010; González et al. 2012; Hill et al. 2014). Additionally, K^+ blockers such as amiodarone can bind delayed rectifier and voltage gated K^+ channels that allow K^+ efflux after membrane depolarization (Colatsky et al. 1990; Sato et al. 1994; Komada et al. 1999; Chen et al. 2016). These drugs, and their capacity to alter cellular K^+ handling, may provide insight into the mechanisms of Tl uptake and toxicity.

The current chapter incorporates three experiments that aimed to provide fundamental information about the nature of the Tl/K^+ interaction, and which could ultimately contribute to the development of a Tl BLM for *Daphnia magna*. First, an experiment assessing the modifying effects of K^+, Na^+, rubidium (Rb^+), and Cs^+ on Tl toxicity was performed. This sought to provide evidence for an interaction between Tl and K^+ in terms of toxic impact. If Tl enters cells via K^+ channels and/or disrupts K^+ transport, then modifying water K^+, or the addition of trace elements with known interactions at K^+ channels (Rb^+ and Cs^+; Kernan 1969), will likely modify Tl toxicity. Since there is limited evidence of Tl interaction with Na^+, this ion was used as a positive

control to determine the specificity of Tl effects. Second, pharmaceuticals (amiodarone, clozapine, and chlorpropamide) were used in exposures of daphnids, both in the presence and absence of Tl, to identify putative pathways by which Tl may interfere with K^+ handling, using whole-body K^+ as an endpoint. Lastly, Tl-dependent changes in K^+ uptake were measured, using Rb^+ as a proxy for K^+ (West and Pitman 1967; Carmosino et al. 2013). Whole-body K^+ is a convenient endpoint but reflects effects of multiple processes (i.e., uptake, cellular handling, loss), whereas the use of Rb^+ allowed isolation of Tl effects on K^+ uptake. Overall, by better understanding Tl/K^+ interactions in a key regulatory organism (*Daphnia magna*), data for the development of more robust regulations of trace metals in freshwater environments can be derived.

5.2. Methods

Methodological details regarding experimental animals, Tl burden analysis, water chemistry and statistical analysis can be found in Sections 3.2.1, 3.2.4, and 3.2.5. In contrast to Chapter 3, in this chapter Dunn's test was used as the post hoc test following analysis via a non-parametric ANOVA.

5.2.1. *Major ion manipulation lethal toxicity test*

To understand how Tl toxicity may change under various water chemistries, 48-h median lethal toxicity tests were conducted under conditions where water ion composition was modified. Ten neonate daphnids in each of 8 replicates were exposed to 1.86 mg L^{-1} Tl (9 µM; the 48-h LC_{50}; see Chapter 2) in waters where K^+, Na^+, Rb^+, or Cs^+ concentrations were independently varied. Treatments involving K^+ or Na^+ were made by spiking these ions into an OECD medium free of the ion of interest. For K^+ treatments the base medium was 2 mM $CaCl_2{\cdot}2H_2O$, 0.5 mM $MgSO_4{\cdot}7H_2O$, 0.77 mM $NaHCO_3$, with K^+ added from a 50 mM KCl stock solution to achieve

final concentrations of 0.007, 0.01, 0.02, 0.06, 0.1, 0.2, 0.6, 1.2, and 2.5 mM K^+. For Na^+ treatments the base medium was 2 mM $CaCl_2 \cdot 2H_2O$, 0.5 mM $MgSO_4 \cdot 7H_2O$ and 0.08 mM KCl., with Na^+ added from a 50 mM NaCl stock to give final Na^+ concentrations of 0.05, 0.11, 0.22, 1.1 and 2.2 mM. For water chemistry treatments with Rb^+ and Cs^+, the respective metals were added to standard OECD water (see Section 3.2.1). Rubidium treatments (0.3, 0.6, 1.2, 2.9, 5.9 µM Rb^+) were dosed from a 50 µM RbCl stock solution. Caesium treatments (0.2, 0.4, 0.8, 1.9, 38, 75 µM Cs^+) were dosed from a 500 µM CsCl stock solution. Dosing occurred 24-h prior to daphnid addition, to allow for speciation equilibration. All treatments were paired with time-matched Tl-free controls that were identical in composition but had no added Tl. These were used to account for any toxicity associated with the ion amendments. Following the 48-h exposure, daphnids were assessed for mortality as defined by the absence of all movement.

5.2.2. *One-hour median lethal toxicity test*

To measure changes in K^+ handling over a 1-h exposure a median lethal toxicity test was conducted. In Chapter 3, a 21-d exposure of daphnids to Tl did not result in a significant change in whole-body K^+ concentration. In that chapter it was hypothesized that compensation may have occurred, which eliminated any effect of Tl on whole-body K^+. In the current study it was hypothesized that a short exposure would reduce the possibility of compensatory mechanisms being enacted, thus unveiling an effect of Tl on K^+ handling. Neonate daphnids (10 in each of 6 replicate beakers) were exposed to concentrations of 0, 100, 200, 300, 400, 450, 500, 550, 600, 650, 700, 750 mg L^{-1} Tl in 40 mL of OECD water for 1-h. To determine mortality daphnids were examined under a dissection microscope, and mortality was defined as the absence of heartbeat for 3 seconds.

5.2.3. *Pharmaceutical blocker additions*

Exposure of daphnids to K^+ channel-blocking pharmaceuticals was used to determine whether K^+ transporters were either directly (i.e., Tl inhibits the transporter) or indirectly (i.e., Tl uses the transporter to gain access to the cell and subsequently cause toxicity) loci of Tl toxicity. Adult *D. magna* (10-15 d old) were used in this experiment to better facilitate measurement of whole-body K^+. Daphnids were exposed to the K^+ channel-blocking pharmaceuticals amiodarone (A), clozapine (Cl) and chlorpropamide (Ch) both alone and in combination with Tl to observe changes in whole-body K^+. All pharmaceuticals were purchased from Sigma-Aldrich. A 10% methanol solution was used to prepare all pharmaceutical stock solutions, and therefore a vehicle control of 0.15% methanol (representing the highest spiked volume of methanol) was used to account for any toxicity associated with the solvent.

The initial series of studies were conducted over 1-h exposure periods. Ten adult daphnids were placed into 50-mL beakers containing 20 mL of OECD water spiked with the pharmaceutical and Tl. Pharmaceuticals were added immediately prior to daphnid addition, and Tl (1-h LC_{50}: 572 mg L^{-1}) was added 24-h prior. Final exposure concentrations for amiodarone, clozapine and chlorpropamide were 0.8, 0.1 and 1 μM, respectively. Exposure concentrations for amiodarone and clozapine were based on LC_{50} concentrations to fathead minnow larvae (Overturf et al. 2012), while chlorpropamide concentrations were based on levels that inhibited K_{ATP} channels in patch clamp experiments (Lang et al. 2012). The mixed exposure group was spiked with all three pharmaceuticals at the previously mentioned concentrations. Following the 1-h exposure, daphnids were transferred into a series of two beakers containing ultrapure water to exchange the water trapped in the carapace (5 s each wash), and thus minimize carry over of K^+ for subsequent analyses. Daphnids were then gently blotted dry, and weighed using a microbalance, before being placed into 1.5 mL Eppendorf tubes. Tissue digestion was adapted

from Gillis and colleagues (2005). Daphnids were dried at 65°C until constant weight was reached, and then digested in 1 mL 10% trace grade HNO_3. The Eppendorf tubes containing the digests were placed back into the drying oven for another 72-h , then diluted into 9 mL ultrapure water for a final volume of 10 mL. Digests were measured for whole-body K^+ using FAAS as described in Section 3.2.4.

Because no significant changes in K^+ concentration were observed following the 1-h exposures to Tl with/without the pharmaceutical blockers, the blocker experiment was redesigned, to find an exposure length/Tl concentration combination that might more effectively affect whole-body K^+. Adult 10–15 day old daphnids were exposed to 0, 100 or 200 mg Tl L^{-1} for 8-h, rinsed and digested as described above, before being analyzed for whole-body K^+. Based on results from this study, an 8-h exposure of daphnids to pharmaceuticals in a medium containing 100 mg L^{-1} Tl was conducted, where exposure, sampling and analysis were identical to the description provided above for 1-h exposures.

5.2.4. *Potassium uptake*

Rubidium was used to measure the effects of Tl on K^+ uptake (Sanders and Kirschner 1983). A preliminary study was conducted where either 1 or 3 daphnids were exposed to 100 µg L^{-1} Rb^+ for up to 8-h (0.17, 0.5, 1, 2, 4, 8-h). Following exposure, daphnids were prepared and analyzed via ICPMS as described in Section 3.2.4. Based on daphnid Rb^+ concentration, an exposure scenario of 8-h incubations with 3 daphnids was considered optimal (data not shown). Subsequently, three adult daphnids were exposed to 100 µg L^{-1} Rb^+ and 8 different concentrations of Tl for 8-h (0, 1.2, 12, 32, 77, 152, 294, 588 µg L^{-1}). All treatments were dosed 24-h prior to daphnid addition. Following exposure, daphnids were rinsed in clean OECD water,

gently blotted dry with absorbent tissue paper, weighed and prepared for whole-body Rb^+ analysis via ICPMS, with operating conditions as described in Section 3.2.4.

5.3. Results

5.3.1. *Toxicity modification*

There was no mortality in any manipulation of water K^+, Na^+, Cs^+, or Rb^+ in the absence of Tl (data not shown). However, when 1.86 mg L^{-1} (9 μM) Tl was present, significant differences in mortality occurred when water K^+, Cs^+, and Rb^+ concentrations were modified (P-value$_{ANOVA}$: 0.0001, Figure 5.1a; P-value$_{Kruskal\text{-}Wallis}$: 0.004, Figure 5.1c; P-value$_{Kruskal\text{-}Wallis}$: 0.0001, Figure 5.1d). When K^+ concentrations were lower than 0.02 mM, increased mortality was observed (P-value$_{Tukeys}$: 0.0001), relative to treatments where water K^+ was in the range of 0.02 to 0.06 mM. Alternatively, when K^+ concentrations exceeded 0.06 mM mortality decreased (P-value$_{Tukeys}$: 0.046- 0.0001). There were, however, no significant effects of manipulating water Na^+ on Tl-related daphnid mortality (P-value$_{ANOVA}$: 0.2186, Figure 5.1b). Treatments where Rb^+ concentrations were varied in the presence of 1.86 mg L^{-1} Tl resulted in significant differences in mean mortality (P-value$_{Kruskal\text{-}Wallis}$: 0.004, Figure 5.1c). Specifically, exposures containing 1.2 and 2.9 μM Rb^+ had significantly decreased Tl mortality when compared to Rb^+-free treatments (P-value$_{Dunn}$: 0.008 and 0.027 respectively). In Cs^+-exposed daphnids mean mortality in the presence of Tl differed as a function of Cs^+ concentration (P-value$_{Kruskal\text{-}Wallis}$: 0.0001, Figure 5.1d). Mortality was greater when daphnids were exposed to 38 and 75 μM Cs^+-spiked treatments than in Cs^+-free treatments (P-value$_{Dunn}$: 0.0005).

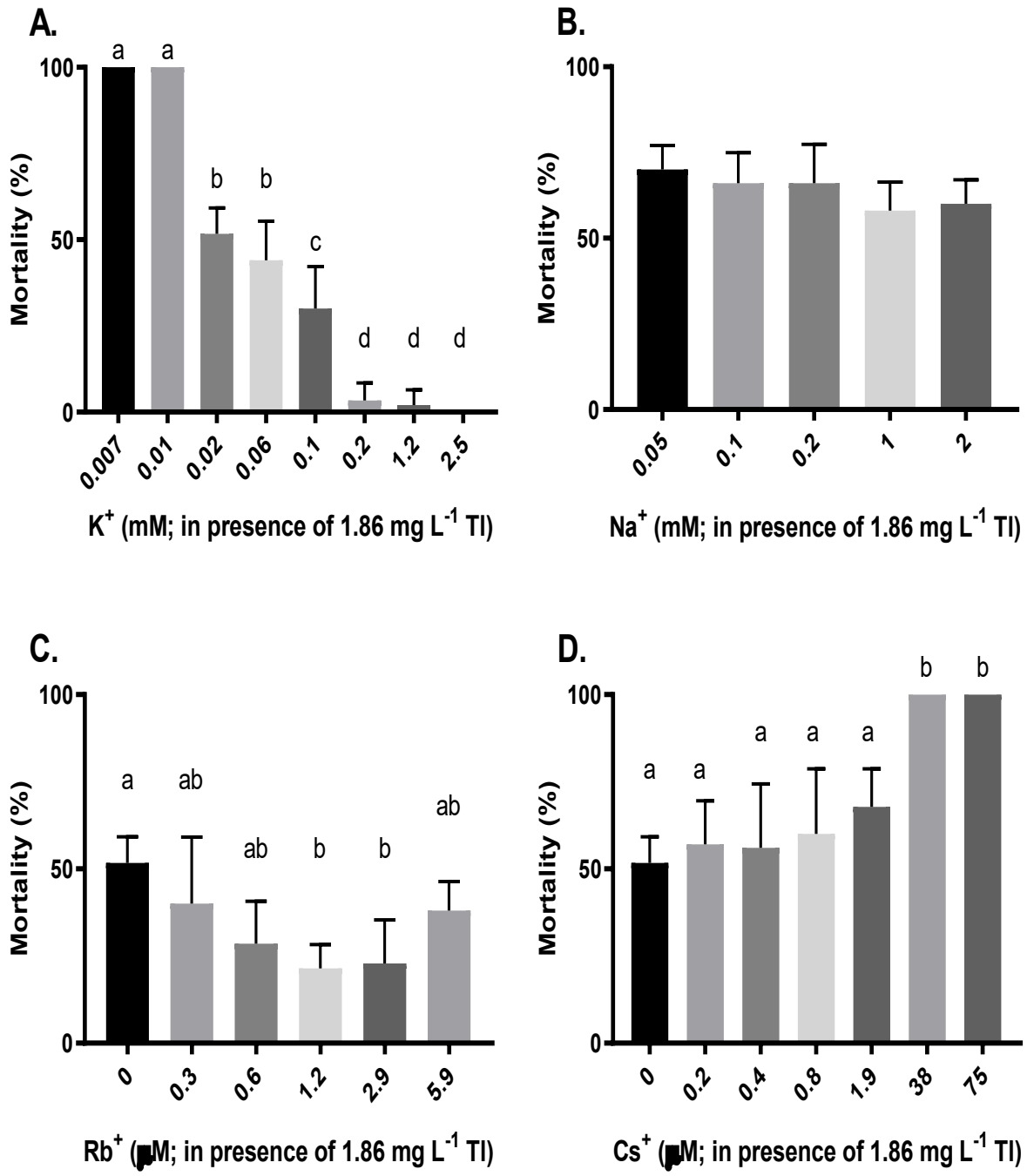

Figure 5.1. Effects of water ionic composition (K^+, A; Na^+, B; Rb^+, C; Cs^+, D) on acute toxicity of *Daphnia magna* in the presence of Tl (1.86 mg L^{-1}; 9 µM). Plotted points represent means (± standard deviation) of 8 replicates. Bars sharing letters are not statistically different from one

another. No mortality was observed in control experiments where *Daphnia* were exposed to the noted concentrations of K^+, Na^+, Cs^+, and Rb^+ but in the absence of Tl.

5.3.2. *One-hour median lethal toxicity and K^+ transport blocker initial study*

The calculated 1-h median lethal toxicity concentration (1-h LC_{50}) was 572 mg L^{-1} (95% CI 563-581; Figure 5.2). For the subsequent experiment conducted over 1-h, no significant differences were observed between control whole-body K^+ concentrations and the methanol solvent control (data not shown). Thus, the control group in all K^+ pharmaceutical experiments is represented by the pooled outcomes of the OECD and methanol solvent control groups. No significant differences in whole-body K^+ concentration were observed in amiodarone, chlorpropamide or mixed treatments (P-$value_{Kruskal\text{-}Wallis}$: 0.232, Figure 5.3a; 0.088, Figure 5.3c; 0.342, Figure 5.3d respectively). Significant differences in mean whole-body K^+ concentration occurred after 1-h exposure to clozapine (P-$value_{Kruskal\text{-}Wallis}$: 0.027, Figure 5.3b). Following a Dunn's test, the only significant difference was a reduced whole-body K^+ concentration in the Tl + clozapine group relative to daphnids exposed to Tl alone (P-$value_{Dunn}$: 0.029).

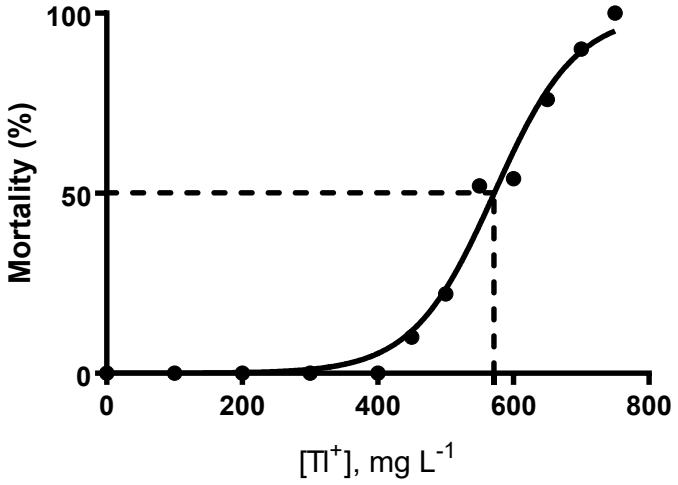

Figure 5.2. Calculated 1-h median lethal concentration of Tl to *Daphnia magna* in OECD water. Plotted points represent the means (± standard deviation) of 6 replicates

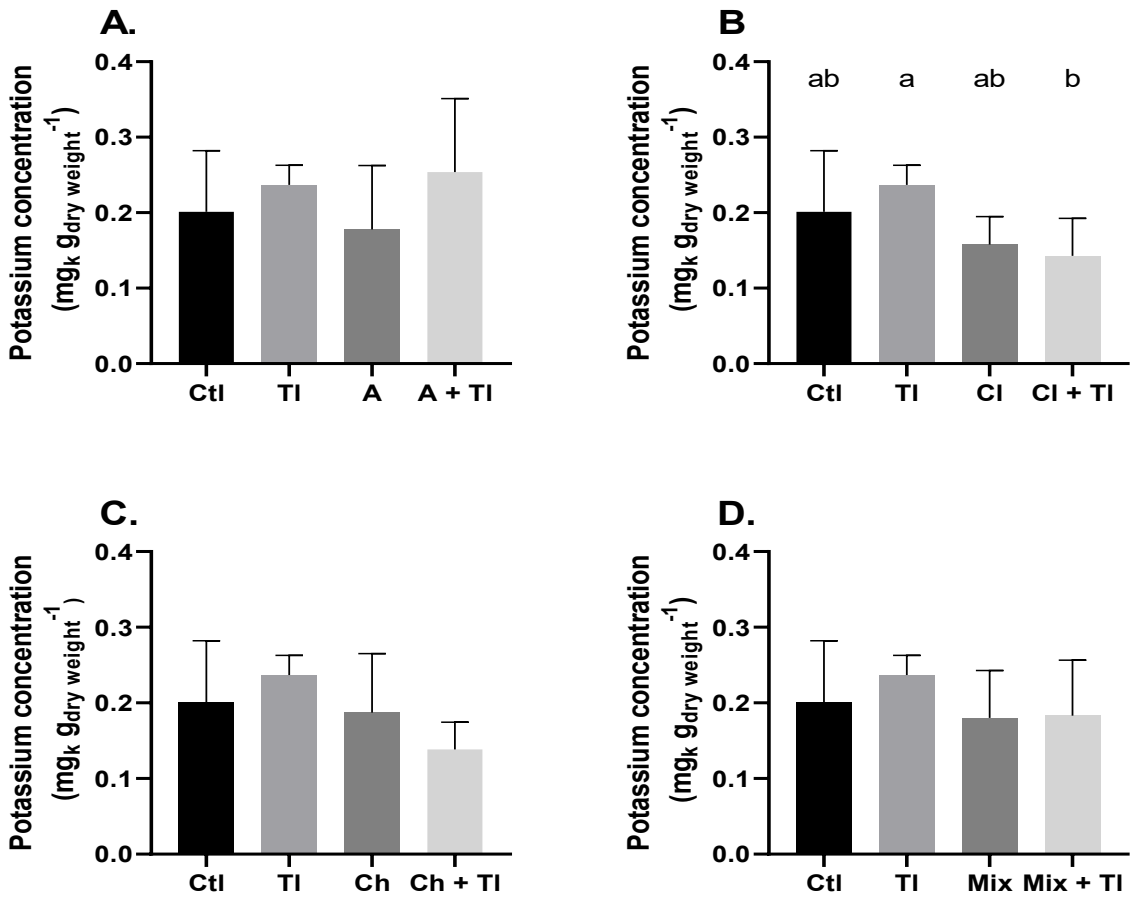

Figure 5.3. Effects of 1-h exposure to 572 mg L^{-1} Tl on *Daphnia magna* whole-body potassium concentration in the absence or presence of putative potassium channel blockers: a, amiodarone (A, 0.8 µM); b, clozapine (Cl, 0.1 µM); c, chlorpropamide (Ch, 1 µM); d, all three pharmaceuticals at stated exposure concentrations (Mix). Control (Ctl) represents pooled responses of unexposed daphnids and daphnids exposed to the vehicle control (0.15% MeOH). Plotted points represent means (± standard deviation) of 5-7 replicates. Bars sharing letters are not statistically different from one another.

5.3.3. *Pharmaceutical effect on whole-body K^+ in 8-h exposures*

Exposure of daphnids to either 100 or 200 mg L^{-1} Tl over 8-h in a medium with 0.8 mM K^+ resulted in significant changes in whole-body K^+ ($P\text{-value}_{Kruskal\text{-}Wallis}$: 0.016, Figure 5.4). In daphnids exposed to 100 mg L^{-1} Tl, whole-body K^+ was significantly reduced relative to the control ($P\text{-value}_{Dunn}$: 0028). Subsequently, the study described in Section 5.2.3 above, was rerun, over an 8-h exposure period to a Tl concentration of 100 mg L^{-1}.

Significant effects on whole-body K^+ occurred for all pharmaceutical exposures ($P\text{-value}_{Kruskal\text{-}Wallis}$: 0.0001, Figure 5.5a-c; 0.0002, Figure 5.5d respectively). However, in contrast to the results of the initial study where 100 mg L^{-1} Tl caused a significant reduction in whole-body K^+, the effect of Tl in this study was to reduce whole-body K^+, but only to 45% of the control value, an effect that was not statistically significant ($P\text{-value}_{Dunn}$: 0.075). In the amiodarone treatments a significant difference in whole-body K^+ was observed between control and amiodarone groups, with the latter displaying a significantly higher value than the former ($P\text{-value}_{Dunn}$: 0.0001). The whole-body K^+ value for the Tl-exposed daphnids was significantly lower than for daphnids exposed to both amiodarone and amiodarone + Tl ($P\text{-value}_{Dunn}$: 0.0001 and 0.011 respectively). Similarly, Tl-exposed daphnids displayed a lower whole-body K^+ than both the clozapine and clozapine + Tl groups ($P\text{-value}_{Dunn}$: 0.035 and 0.0001), and an identical pattern was also observed for chlorpropamide ($P\text{-value}_{Dunn}$: 0.0002 and 0.0002). Daphnids exposed to chlorpropamide (both alone and in combination with Tl) displayed whole-body K^+ values that were significantly higher than the control ($P\text{-value}_{Dunn}$: 0.001 and 0.0008). In the mixed treatment, which contained all 3 drugs, there were significant differences in whole-body K^+ between groups ($P\text{-value}_{Kruskal\text{-}Wallis}$: 0.0002), with the exposure group experiencing all three drugs + Tl exhibiting a significantly higher whole-body K^+ than the Tl only daphnids ($P\text{-value}_{Dunn}$: 0.0001).

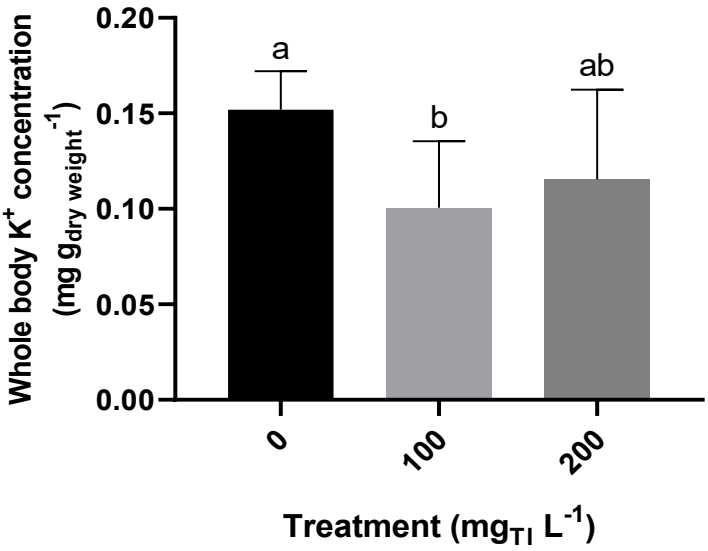

Figure 5.4. Measured whole-body potassium in *Daphnia magna* following an 8-h exposure to sublethal concentrations of Tl in the presence of 0.08 mM K^+. Plotted points represent the means (± standard deviation) of 6 replicates. Bars sharing letters are not statistically different from one another.

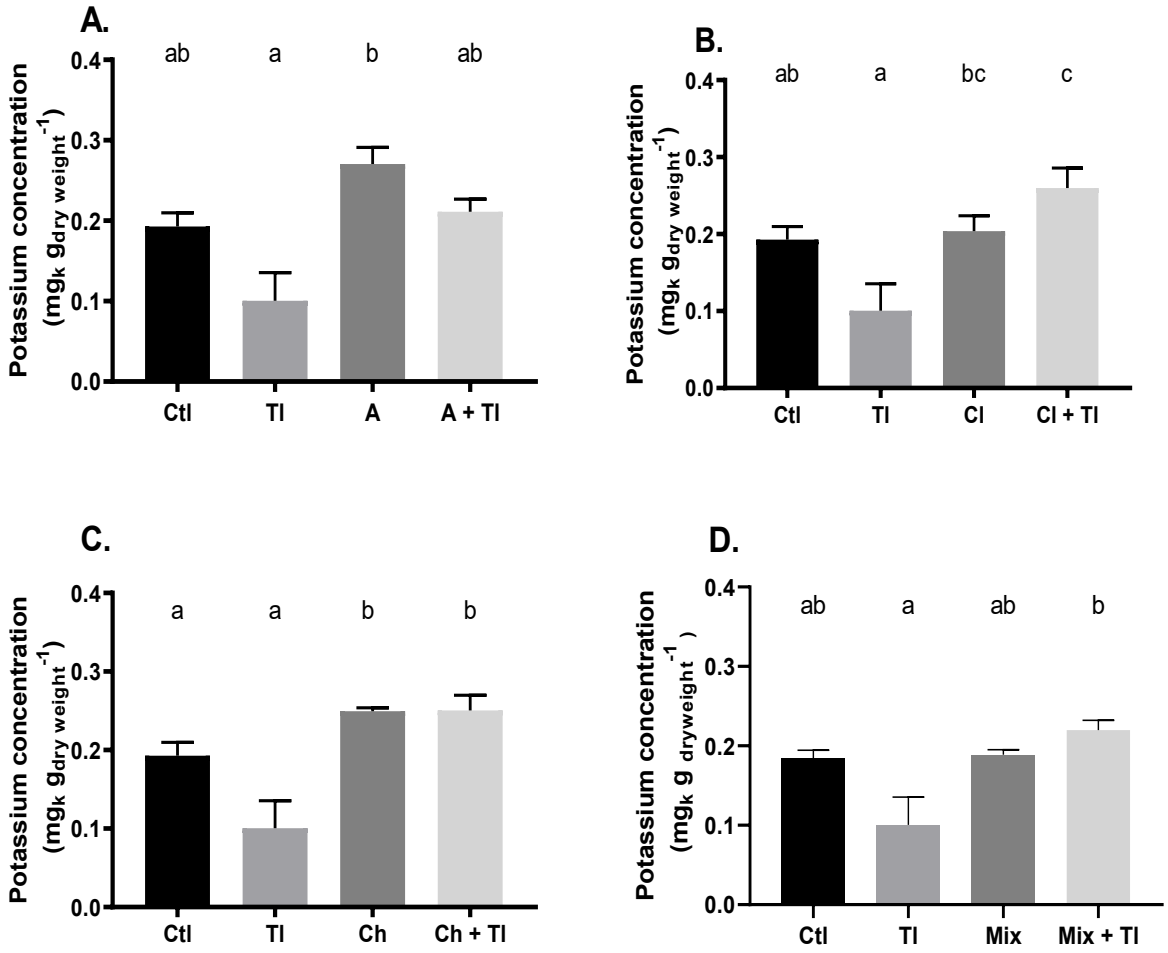

Figure 5.5. Effects of 8-h exposure to 100 mg L^{-1} Tl on *Daphnia magna* whole-body potassium concentration in the absence or presence of putative potassium channel blockers: A, amiodarone (A, 0.8 µM); B, clozapine (Cl, 0.1 µM); A, chlorpropamide (Ch, 1 µM); D, all three pharmaceuticals at stated exposure concentrations (Mix). Control (Ctl) represents pooled responses of unexposed daphnids. Plotted points represent means (± standard deviation) of 6- 12 replicates. Bars sharing letters are not statistically different from one another.

5.3.4. *Potassium uptake*

Using Rb^+ as a K^+ analogue, significant effects of Tl on K^+ uptake were observed (P-value$_{ANOVA}$: 0.0001; Figure 5.6). Potassium uptake was significantly reduced following exposure

to Tl concentrations as low as 32 µg L^{-1} (P-value$_{Tukey}$ 0.037). Between control and 588 µg L^{-1} Tl concentrations a 2.2-fold inhibition in K^+ uptake was observed.

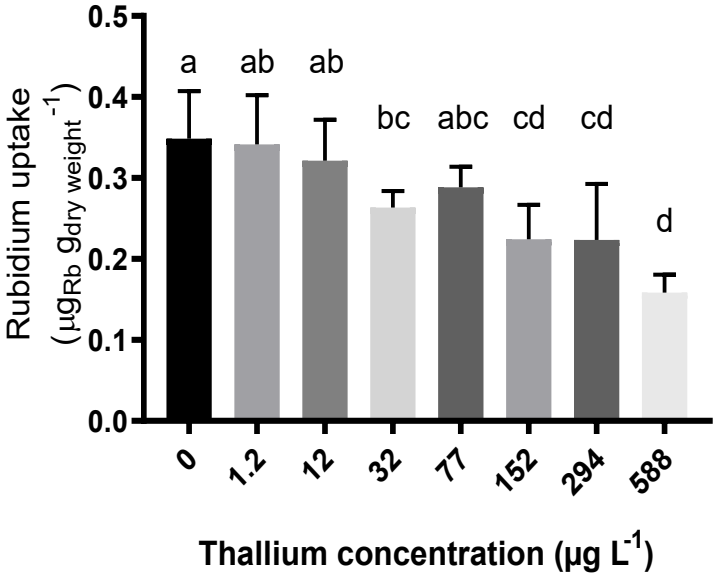

Figure 5.6. Effect of graded Tl exposure on Rb^+ (100 µg L^{-1}) uptake. Plotted points represent the means (± standard deviation) of 6 replicates. Bars sharing letters are not statistically different from one another.

5.4. Discussion

5.4.1. *Modification of thallium toxicity by cations*

In the present work K^+ concentrations less than 0.02 mM increased mortality associated with Tl, but at K^+ concentrations greater than 0.06 mM, mortality significantly decreased. These results therefore confirm the hypothesis that in daphnids Tl toxicity is dependent on water K^+ concentration. This finding seems to be consistent across phyla, as similar outcomes have been noted in the algae *Chlorella* (Hassler et al. 2007), and the crustaceans *Hyalella azteca, Ceriodaphnia dubia, Daphnia pulex* and *Daphnia magna* (Borgmann et al. 1998; Rickwood et al. 2015; Tatsi et al. 2015). The dependence of Tl toxicity on K^+ concentration has also been

observed in rats, where increased dietary K^+ increased the median lethal dose of Tl (Gehring and Hammond 1967).

To provide environmental context for these findings, it should be noted that global freshwaters exhibit K^+ concentrations ranging from 8 to 512 µM (Rowan and Rasmussen 1994). In Canadian lakes where endemic populations of *Daphnia magna* are likely, K^+ concentrations range from 11 to 57 µM. In the current study, significant increases in mortality were observed below 20 µM K^+, and amelioration of Tl toxicity occurred above 60 µM K^+. This suggests that only at the edges of the natural freshwater K^+ range, would K^+ be likely to affect Tl toxicity. However, as noted in Hassler et al. (2007), the ratio of K^+ to Tl^+ may be the more informative metric, and one that can be used as a predictor of aquatic Tl toxicity. Based on the data in the current study, a K^+ to Tl^+ molar ratio of 6:1 protects *D. magna* against Tl mortality. Taking the worst-case scenario of a freshwater K^+ concentration of 11 µM, then water K^+ would protect against Tl-induced mortality in all but the most contaminated mining wastewater samples (see Table 1.1). Conservatively assuming that the same K^+ to Tl^+ ratio of 6:1 mitigates sublethal effects of Tl, then freshwater K^+ concentrations of 0.25 and 12 µM would protect against impacts on growth (LOEC = 8.8 µg Tl L^{-1} (0.04 µM); Table 3.2) and reproduction (LOEC = 424 µg Tl L^{-1} (2 µM); Table 3.2), respectively. Notably, the protective ratio of 6:1 derived in the current study is significantly smaller than the ratio that protects against effects of Tl on growth of microalgae and mortality of rotifers (40-160-fold; Hassler et al. 2007). This likely reflects differences in sensitivity to Tl. This difference also emphasizes that further studies involving experimental manipulation of water K^+ and Tl, in concert with measures of short-term bioaccumulation in a wider range of aquatic biota, would be useful to further establish relationships between water chemistry and eventual toxicity of Tl to freshwater animals. If strong

relationships could be established, then this would be the basis for the development of a BLM that could use site-specific measures of water K^+ and Tl and predict risk of Tl toxicity to local fauna.

It is notable that in the current chapter a K^+:Tl^+ ratio of 6:1 was protective, but in Chapter 2 of this thesis, a 15:1 ratio was not sufficient to generate a significant protective effect against Tl toxicity to daphnids (see Figure 2.2). These studies were done under identical conditions, with neonate daphnids of the same age, from the same clonal strain, but were separated in time by approximately 2 years. It has been shown that significant differences in sensitivity to toxicants can occur in *Daphnia* as a function of physiological differences related to season or even minor variations in the density of the origin culture (Olkova et al. 2018). It is therefore possible that differences in the protective effects of K^+ on Tl^+ toxicity result from physiological differences in K^+ homeostasis and/or Tl sensitivity. For example, in a field study examining the effects of exogenous K^+ on growth and reproduction in *Daphnia dentifera* it was observed that stimulation of these endpoints was variable, but was independent of environmental K^+ concentration and other environmental factors (Civitello et al. 2014). These authors therefore suggested that seasonal variation in the physiology of the daphnids was responsible for governing differences in K^+-mediated responses.

In contrast to manipulations of water K^+, Na^+ modifications to water chemistry had no effect on Tl-induced mortality in daphnids. This suggests that the interactions between Tl and monovalent cations are specific to K^+ (and its analogs; see below). In cells, the transport of Na^+ and K^+ is strongly linked (Morris et al. 2006). In part this is because of the actions of NKA, which exchanges Na^+ and K^+ across the basolateral membranes of all cells (Suhail 2010). Although there is some evidence of Tl^+ interactions with Na^+, notably in rat retinal cells in vitro

(Tao et al. 2008), there is no literature support for an effect of Tl on Na^+ homeostasis, or for a role for Na^+ in protecting against Tl toxicity. The data presented in this chapter also fail to provide evidence of this latter effect.

In contrast, the supplementation of exposure water with K^+ analogs resulted in changes in Tl-induced mortality. At Rb^+ exposure concentrations of 1.2 and 2.9 µM, toxicity of Tl to daphnids was reduced. Rubidium has very similar properties to K^+, and as noted in Section 5.1, can be used as an analog of K^+ in transport studies. This is likely due to similarities in both charge (+1) and ionic radii (Rb^+: 152, K^+: 137 pm; Shannon 1976). Therefore, it is likely that the protective effects of Rb^+ on Tl toxicity are mediated by the same mechanisms as the protective effects of K^+ on Tl toxicity. Once a certain threshold concentration of K^+ transporter-permeant ions is present to outcompete Tl for uptake, this reduces the capacity of Tl to enter the cell, ameliorating the toxic effect. Because of the higher affinity of Tl ions for transport relative to both K^+ and Rb^+ (NKA K_m: Tl^+: 0.15, Rb^+: 0.74, K^+: 0.80; Robinson 1970; Robinson 1975), relatively higher concentrations of K^+/Rb^+ are required to modify Tl uptake (and thus toxicity). In the Rb^+ exposures, K^+ was present in the base medium, thus likely explaining the lower effective concentration of Rb^+ required to initiate this effect relative to K^+ (1.2 versus 20 µM). At the highest tested Rb^+ concentration (5.9 µM), the rate of Tl mortality was no longer significantly reduced relative to Rb^+-free controls. There is some evidence that Rb^+ can itself be toxic (Abdollahi et al. 1998), and so it is possible that this slight reduction in toxicity amelioration may relate to a negative effect of Rb^+ in combination with Tl on K^+ homeostasis. However, Rb^+ treatments in the absence of Tl caused no toxic effect (data not shown), and toxic effects in rats have only been observed when Rb^+ exposure concentrations were in the mM range (Abdollahi et al. 1998).

In the current study Cs^+ had no effect on Tl toxicity to daphnids until water Cs^+ concentrations reached 38 µM. At this, and the higher tested Cs^+ concentration of 78 µM, Cs^+ exacerbated Tl toxicity causing complete mortality over the course of the 48-h exposure. Again, this effect was not due to the toxicity of Cs^+ alone, as the Tl-free control exhibited no toxicity (data not shown). Unlike both Tl^+ and Rb^+, which mimic K^+ and move freely through K^+ transporters (Sessler et al. 1986; Omay and Schwarz 1992), Cs^+ is a K^+ channel blocker (Clay and Shlesinger 1984). If Tl^+ requires K^+ channels to enter cells, and thus cause toxicity, then the prediction might be that as Cs^+ concentrations increase, the passage of Tl into the cell might reduce, thus ameliorating toxicity. In fact, the opposite effect occurred. This therefore argues against a role for K^+ channels in cellular Tl uptake (in that Cs^+ would block Tl uptake, but toxicity of Tl is enhanced), but does suggest a role of K^+ channels in promoting Tl toxicity. Under this scenario Tl impairs function of a K^+ channel, the effect of which is exacerbated by K^+ channel blockade by Cs^+. The exact nature of this effect is not known, but if Tl were capable of blocking cellular K^+ efflux, or disrupting mitochondrial K^+ handling, then this could cause changes in electrochemical gradients and/or altered cellular energy metabolism. These possibilities are discussed in more detail in Section 7.4.1. Measures of Tl accumulation would be of value to further address the interactions between Tl and Cs^+.

5.4.2. *Pharmaceutical effect on whole-body K^+ following a 1-h exposure*

The overall goal of this experiment was to determine if Tl disrupts whole-body K^+, and if this effect is mediated by the interactions of Tl with K^+ channels. The initial step in this study was to determine an effect concentration of Tl, based on a 1-h exposure. Data in Section 3.3 showed no effect of chronic Tl exposure on whole-body K^+ in daphnids, with the working hypothesis being that compensation occurred to restore K^+ concentration over long-term

exposures. Thus, a shorter exposure period was desirable to reduce the possibility of compensation occurring. However, the outcomes of this study showed that a 1-h exposure to Tl was insufficient to change whole-body K^+, despite mortality. This suggests that whole-body K^+ is either not a sensitive endpoint of Tl toxicity to daphnids, or that it takes a longer time for effects of Tl on the whole-body K^+ status to become apparent. One possible mechanism that may explain toxicity in the absence of a change in whole-body K^+, is that Tl effects are initially manifested in the nervous system. In mammals, the nervous system is well characterized as a target tissue for Tl toxicity (Osorio-Rico et al. 2017). Indeed, a variety of effects of Tl on neural tissue have been described, including disruption of energy metabolism, generation of oxidative stress, and impairment of ion transport processes through inhibition of NKA (Osorio-Rico et al. 2017; Maya-López et al. 2018). In fact, Tl concentrations as low as 5 µM are sufficient to cause damage in isolated synaptosome preparations from rat brain (Maya-López et al. 2018). Evidence for a role of Tl in neurological function in daphnids was provided by data presented in Chapter 4 of this thesis, where Tl was suggested to impair phototactic behaviour by disrupting the sensory system. If the mortality indicated in a 1-h exposure was mediated through neurological effects, this would be unlikely to show as a change in whole-body K^+ even if disruption of K^+ homeostasis was the root cause of toxicity, because of the relatively small contribution of this tissue to total body mass.

Despite the lack of effect of Tl on whole-body K^+, 1-h exposures to pharmaceuticals did result in some effects on daphnid whole-body K^+. Specifically, a reduction in whole-body K^+ concentration was observed in daphnids exposed to clozapine + Tl compared to the Tl treated group (Figure 5.3b). Clozapine binds to, and inhibits the function of, the $K_v11.1$ channel, a voltage gated K^+ channel, which in humans contributes to repolarization of cardiac action

potentials (Vandenberg et al. 2012; Hill et al. 2014). The gene that codes for this channel is present in the *Daphnia magna* genome (Genbank accession number: XP_032780879.1). The reduction in whole-body K^+ in the presence of both Tl and clozapine suggests that there may be an interaction between these two agents that is not present when either one of them is present alone. Because of the multiple distinct K^+ channels that are likely responsible for cellular K^+ homeostasis, blockage of any one specific route of entry/exit may be insufficient to cause a change in K^+ status. These data would therefore suggest that clozapine and Tl are affecting distinct pathways of K^+ handling, and that only the blockade of both of these pathways is sufficient to disrupt K^+ handling.

5.4.3. *Pharmaceutical effect on whole-body thallium and K^+ following an 8-h exposure*

In order to find a more effective experimental protocol in which to study impacts of Tl on K^+ homeostasis, an 8-h study was performed, which initially examined the effects of two Tl concentrations on daphnid whole-body K^+ (Figure 5.4). This study showed that 100 mg L^{-1} Tl could be effective in reducing daphnid K^+ status. Although the exact mechanisms by which K^+ homeostasis is affected by Tl have not been described, there are several studies that support this finding. For example, Tl inhibits gut K^+ transport in *Chironomus riparius* (Belowitz and O'Donnell 2013), and also impairs both influx and efflux of K^+ across the mitochondrial membranes of rat liver (Barrera and Gómez-Puyou 1975). It is noteworthy that no change in K^+ homeostasis was found after a 1-h exposure to a lethal Tl concentration (Section 5.4.2), and it took 8-h of exposure to induce a downwards trend in whole-body K^+ in the current experiment. This suggest that it takes time for the effects of Tl on this endpoint to develop. This would argue against a direct effect of Tl at an apical epithelial surface, as has been noted for ionoregulatory

impacts of other trace metals in aquatic biota (e.g., Hogstrand et al. 1994; Grosell and Wood 2002; Bianchini and Wood 2003).

In the 8-h exposure study incorporating pharmaceuticals, there was a trend towards decreasing whole-body K^+ in the presence of Tl alone, but this effect was not significant (P-value$_{Dunn}$: 0.075 – 0.300), as it had been in the preliminary studies without pharmaceuticals (Fig. 5.4). However, the presence of K^+ channel-blocking drugs did affect whole-body K^+, although not in the manner that may have been predicted. None of the pharmaceuticals tested reduced daphnid whole-body K^+. In fact, the only significant effect of a pharmaceutical agent alone was chlorpropamide, which increased whole-body K^+ relative to the unexposed control. There are several potential explanations for the lack of observed effect. For example, it is possible that the effectiveness of the drugs may have been limited. The pharmaceutical exposure concentrations were chosen based on data from studies in other systems, and thus may not have been sufficiently high to cause effects in daphnids. However, since the clozapine and amiodarone concentrations were based on lethal doses of the drugs to fathead minnows, and fathead minnows are generally less sensitive to toxicants than *Daphnia magna* (Maki 1979; Overturf et al. 2012), this was unlikely to be the cause of the observed pattern. It is also possible that the efficacy of the drugs may have been limited by degradation over time. In human systems plasma half-lives for chlorpropamide, clozapine and amiodarione are 34, 8, and 80-h respectively (Sartor et al. 1980; Latini et al. 1984; Mahoney et al. 1999). It is therefore unlikely that exposure of these drugs via the water, in the absence of metabolizing enzymes and lower temperatures than in human systems, would have resulted in complete degradation. Finally, given the multitude of possible K^+ channels involved in cellular transport of K^+ (Buckingham et al. 2005), it is possible that blockade of single (or in the case of the mixed exposure treatment, several) pathways,

simply results in the diversion of transport through other pathways that are not blocked. This would result in no net change in transport and thus no net change in whole-body K^+ status. A similar outcome has been observed in blocker studies of epithelial Ca^{2+} uptake in whole tissue preparations (Glover and Goss 2020).

It is clear, however, that chlorpropamide generated a significant effect, raising whole-body K^+ status. In mammals, chlorpropamide blocks inwardly rectifying K^+ channels in tissues such as human kidney and guinea pig intestine (Zini et al. 1991; Lang et al. 2012). A gene for the chlorpropamide target (KIr6) is found in the *D. magna* genome (Genbank accession number XP_032790563.1). Although the target for chlorpropamide is an inwardly rectifying channel, it nevertheless conducts K^+ in either direction depending on the prevailing concentration gradient (Lang et al. 2012). In most cells this would result in efflux of K^+ (intracellular K^+ concentration is approximately 135 mM, extracellular K^+ concentrations approximately 12 mM; Wright 2004). If chlorpropamide was blocking K^+ efflux from cells, then this could ultimately result in an increase in cellular and whole-animal K^+.

Chlorpropamide, amiodarone (a blocker of K_v and K_{ATP}), clozapine (a blocker of K_v) and the mixture of all three pharmaceuticals also significantly modified the effect of Tl on whole-body K^+. In all these cases the whole-body K^+ status of daphnids was significantly elevated in the presence of the drug and Tl compared to daphnids exposed to Tl alone. This indicates that all three blocking agents likely ameliorated the capacity of Tl to alter K^+ handling. This therefore suggests that Tl is capable of uptake through multiple K^+ channels. Indeed, although Tl uptake through the chlorpropamide-inhibited KIr6 channel has not been determined, Tl flux has been measured through other inwardly rectifying K^+ channels (Wydeven et al. 2014). Just as K_{ir} and $K_v11.1$ homologues (targets of chlorpropamide and clozapine, respectively) are present in the *D.*

magna genome so too are targets for amiodarone (Genbank accession numbers: XP_032780879.1, XP_032790563), lending circumstantial support for the hypothesis that these channels are potential pathways of Tl uptake in *D. magna*. Of course, this conclusion contrasts with those drawn from the effects of Cs^+ on Tl toxicity (discussed in Section 5.4.1, above). The presence of Cs^+, a generalized K^+ channel blocker, exacerbated Tl toxicity, which would be inconsistent with passage of Tl through a K^+ channel and inconsistent with the ameliorative effects of Tl toxicity seen in the presence of pharmaceutical K^+ blockers. This inconsistency requires further exploration.

The other key conclusion that can be drawn from the pharmaceutical data is that the mode of action of Tl is clearly distinct from the mode of action of the blocking agents themselves. If Tl and pharmaceuticals were having similar actions, then their effects on whole-body K^+ status would be similar. This lends support to the concept that while Tl likely enters cells via K^+ transporters, its effects on K^+ homeostasis appear to be mediated at distinct loci. This is consistent with previous studies showing that Tl has a high permeability through K^+ transporters (Brismar 1998), but does not block transport of K^+ (Belowitz and O'Donnell 2013).

5.4.4. *Potassium uptake*

The use of Rb^+ as a tracer for uptake of K^+ is a common practice due to the physicochemical similarity of the two ions, a property that translates to similar cellular handling (Brismar 1998; Carmosino et al. 2013). In the current study, Tl was shown to decrease K^+ uptake in daphnids. This indicates that at least part of the changes in whole-body K^+ observed upon Tl exposure are mediated by an inhibition of cellular K^+ uptake. In neonate *D. magna*, K^+ uptake from the environment can be achieved by the nuchal organ (Morris and O'Donnell 2019), a tissue specialized for ion transport located in the "neck" region of the animal. Later in

development, the nuchal organ disappears and epipodites take over ionoregulation (Aladin and Potts 1995). The specific transporters that achieve K^+ uptake have not been characterized, but these are likely targets for the effects of Tl on K^+ uptake identified in the current study.

It should be noted, however, that K^+ uptake rates as determined in the current study are relatively low. The basal K^+ uptake rate in the absence of Tl was 0.044 µg g^{-1} h^{-1}, with Tl at 588 µg L^{-1} reducing K^+ uptake by 45%. Assuming no effect of Tl on K^+ efflux rates, and assuming complete inhibition of K^+ uptake by 100 mg L^{-1} Tl (Fig. 5.4), then a decrease in whole-body K^+ of 0.025 mg g^{-1} over 8-h would be predicted. Whole-body K^+ concentrations of control daphnids as measured in the current study are in the order of 0.2 mg kg^{-1}. Therefore, it is unlikely that the effects on whole-body K^+ mentioned in Section 5.4.3 are solely based on inhibition of uptake by Tl.

5.5. Conclusion

The presented work shows that interactions between K^+ and Tl are, at least in part, responsible for Tl toxicity. These effects are K^+-specific as Na^+ did not modify Tl toxicity. Based on studies with pharmacological blockers of K^+ channels, evidence was provided that Tl uses such channels to induce toxicity, but toxicity is not mediated by interactions at the uptake locus. The interaction between K^+ and Tl may ultimately provide a mechanism for site-specific risk assessment of Tl in natural waters.

6. Accumulation of thallium in rainbow trout (*Oncorhynchus mykiss*) following acute and sub-chronic exposure

6.1. Introduction

Trace metals are widely distributed throughout freshwater ecosystems (Meena et al. 2018), and their presence poses potential risks to aquatic animals such as fish. However, in order for metals to exert effects on organismal biology, they first must be accumulated (DeForest et al. 2007). To characterize accumulation of toxicants from the environment, two metrics are commonly used: BCF and BAF. The BCF refers to the ratio of chemical accumulated in the organism relative to the water exposure concentration (DeForest et al. 2007). The BCF is most commonly applied to laboratory studies where the diet is not a factor that contributes meaningfully to accumulation. In contrast, BAF is the ratio of organism accumulation to the chemical concentrations in the surrounding medium from all possible exposure routes (i.e., both dietary and waterborne) (Gobas and Morrison 2000). As such, BAF is mostly applicable to field studies. Measures of accumulation are important as it has been shown that accumulation of metals in freshwater organisms often equates to sub-lethal toxic effects. For example, following exposure of gilthead bream (*Sparus aurata*) to Cd, a relationship between Cd burden and oxidative stress was observed (Souid et al. 2013). Similar relationships have been observed linking effects on ionoregulatory enzymes with Cu burden in kidney tissue of goldfish (Moyson et al. 2016).

Due to the relationship between accumulation and toxic effect, measuring accumulation can be critical for regulatory approaches. One approach that utilizes the relationship between acute toxicity and trace metal bioaccumulation in aquatic systems is the BLM (Di Toro et al. 2001). Briefly, this is a regulatory tool that takes measures of water chemistry to determine trace

metal bioavailability to an aquatic organism (or a metal-sensitive tissue (i.e., biotic ligand) of an aquatic organism, such as the fish gill). Bioavailability, or short-term bioaccumulation, which is considered to reflect bioavailability, can then be used to predict toxic effects (Di Toro et al. 2001). Accordingly, this model has been applied globally in the development of guidelines for the protection of aquatic biota against trace metal toxicity (De Schamphelaere and Janssen 2002; USEPA 2007; Rüdel et al. 2015; Gondek et al. 2017). Another model that considers bioaccumulation in risk assessment is the tissue residue approach (TRA) (Meador et al. 2008). The TRA uses critical body residue (CBR), the concentration of chemical bioaccumulated (in the whole body or in a specific tissue) corresponding to measured toxicity, to correlate bioaccumulation with mortality to predict toxicity within and across species (Barron et al. 1997; Leonard et al. 2014). One benefit of the TRA model over the BLM is that it considers the biologically effective dose, which relates to the internally bioavailable portion of the concentration of the chemical. This is important, as it provides a mechanism for differentiating risk in scenarios where the toxicity of chemicals does not correlate to gross measures of tissue toxicant burden (Barron et al. 1997). The application of TRA to ecological risk assessment has facilitated an improved assessment of bioavailability for metals and organic compounds (Sappington et al. 2011). For example, the TRA has been used by the USEPA to develop guidelines for new pesticides that show bioaccumulative potential (USEPA 2009b).

In fish, the gills are the primary route of waterborne metal uptake from the environment (Zia and McDonald 1994). Metals are absorbed from the water principally as free metal ions (Cuss et al. 2020). This occurs either through dedicated metal transporters for those elements that are essential (Bury et al. 2003), or in the case of non-essential metals, via mimicry of major ions such as Na^{+} or Ca^{2+} (Olsson et al. 1998). Once absorbed, metals may be sequestered in the gill

tissue, through association with metal-binding ligands such as the cysteine-rich protein metallothionein (MT; Olsson and Hogstrand 1987). In some invertebrate species, trace metals may also be sequestered in tissues as insoluble granules (Rainbow 2002). Following accumulation in the gill, labile metals may be released across the basolateral surface into the blood, which delivers metals to other tissues where they are sequestered or excreted (Olsson et al. 1998). A trace element accumulates in a given tissue, depending on that elements ultimate disposition (i.e., sequestration or excretion) (Calamari et al. 1982), its physicochemical properties (Veltman et al. 2008), and biological factors such as exposure history and physiological status (Cain et al. 2006; Urien et al. 2017). Ultimately, metal accumulation in specific tissues can be of importance for a number of different applications. As noted above, branchial accumulation is of value for regulatory risk assessment, while accumulation of metals in fish muscle tissue is important in assessing risk to human health (Ali and Khan 2019), and metal accumulation in otoliths is useful for determining the metal exposure history of fish (Hüssy et al. 2020).

As introduced in Sections 1.1.7 and 1.1.8, Tl is a trace metal that is known to accumulate and cause toxic effects in aquatic organisms (Couture et al. 2011). While dissolved concentrations in uncontaminated surface water are generally low (e.g., 3 ng L^{-1}; Shotyk et al. 2019), field studies have measured Tl accumulation in several aquatic species (Table 6.1). Near the Wengjiang River, a water body impacted by activities at the Dabaoshan mine, measured total water concentrations of Tl average 0.1 µg L^{-1}. In a study examining Tl bioaccumulation in 19 species of freshwater organisms collected from this watershed, BAF values in muscle tissue from the fishes ayu (*Plecoglossus altivelis)* and Chinese false gudgeon (*Abbottina rivularis)* were 8750 and 3548, respectively (Chan et al. 2021). Interestingly, Tl even appears to accumulate in

biota collected from waters where there is no known anthropogenic source of the metal. For example, in the Athabasca River, Tl concentrations in otoliths of trout perch (*Percopis omiscomaycus*) were 6071 times greater than the Tl concentration dissolved in the river (Shotyk et al. 2019).

Table 6.1. Bioaccumulation factors for Tl of field collected fish.

Common name	Latin name	Exposure concentration (µg L^{-1})	Tissue	Tissue concentration (µg kg^{-1})	BAF	Source
Bitterling	*Acheilognathus macropterus*	0.03[t]	Gill	34	1140	Chan et al. 2021[a]
			Muscle	23	760	
Goldfish	*Carassius auratus*		Gill	19	640	
			Muscle	30	1000	
Common carp	*Cyprinus carpio*		Gill	25	840	
			Muscle	39	1300	
Spotted steed	*Hemibarbus maculatus*		Gill	18	600	
			Muscle	14	460	
Sichuan taimen	*Hucho bleekeri*		Muscle	19	640	
Mozambique tilapia	*Oreochromis mossambicus*		Gill	51	1700	
			Muscle	78	2600	
Yellowhead catfish	*Pseudobagrus fulvidraco*		Gill	42	1400	
			Muscle	53	1760	
Chinese perch	*Siniperca chuatsi*		Gill	35	1160	
			Muscle	50	1660	
Yellowfin	*Xenocypris argentea*		Gill	43	1440	
			Muscle	35	1160	

Table 6.1 cont.

Common name	Latin name	Exposure concentration (µg L^{-1})	Tissue	Tissue concentration (µg kg^{-1})	BAF	Source
Topmouth gudgeon	*Pseudorasbora parva*	0.1[t]	Muscle	26	264	Chan et al. 2021[a]
Rainbow gudgeon	*Sarcocheilichthys nigripinnis*		Muscle	31	308	
Topmouth culter	*Erythroculter ilishaeformis*		Muscle	26	264	
Ayu	*Plecoglossus altivelis*		Muscle	875	8750	
White seabass	*Atractoscion nobilis*	0.11[t]	Gill	196	1779	
			Muscle	43	395	
Sharpbelly	*Hemiculter leucisculus*		Muscle	87	791	
Chinese false gudgeon	*Abbottina rivularis*		Muscle	390	3548	
Shiner	*Notropis* spp.	0.01[d]	Muscle	10	900	Jardine et al. 2019
Walleye	*Sander vitreus*		Muscle	30	2500*	
Northern pike	*Esox lucius*					
Lake whitefish	*Coregonus clupeaformis*					
Trout-perch	*Percopis omiscomaycus*	0.003[d]	Otolith	17	6071	Shotyk et al. 2019
Lake trout	*Salvelinus namaycush*	0.01[ns]	Whole body	141	10071	Lin et al. 2001

*: Pooled samples
[a]: Values from Chan et al. (2021) were recalculated from reported water and tissue Tl concentrations.
[t]: Total concentration
[d]: Dissolved concentration
[ns]: Total or dissolved not specified

Thallium bioaccumulation in aquatic species has also been shown experimentally under controlled laboratory conditions, indicating waterborne Tl bioavailability (Table 6.2). For example, Zitko et al. (1975) exposed juvenile Atlantic salmon (*Salmo salar*) for 12.5 days to concentrations of Tl ranging from 17.9 to 200 μg L^{-1} and measured significant Tl accumulation in gill and muscle tissue. Accumulation of Tl has also been observed in larvae of fathead minnows (Lapointe and Couture 2010), where whole-body Tl accumulation over a 21-day exposure to 0.9 μg Tl L^{-1} was significantly elevated relative to control fish. The BCF values calculated from these studies range from 7 to 1430. However, under Canadian guidelines that consider BCF values >5000 to be of concern (Environment Canada 2000a), Tl is not classified as a priority environmental toxicant. However, the data to date are insufficient to identify whether there are specific tissues in which Tl preferentially accumulates, an outcome that has implications for risk assessment.

Table 6.2. Bioconcentration factors for Tl in laboratory-exposed aquatic organisms.

Organism	Common name	Latin name	Exposure length (d)	Exposure concentration (µg L^{-1})	Tissue	Tissue concentration (mg kg^{-1})	BCF	Source
Plant	Common duckweed	*Lemna minor*	10	0.01[at]	Fronds	880[c]	88000	Kwan and Smith 1988
				0.75[at]		4426[c]	5901	
Invert.	Amphipod	*Hyalella azteca*	7	30[ns]	Whole body	174	5800	Borgmann et al. 1998
	Harlequin fly	*Chironomus riparius*	14	1000[bt]	Whole body	0.6	0.6	Dumas and Hare 2008
	Annelid	*Tubifex tubifex*	14			0.3	0.3	
	Crustacean	*Daphnia magna*	21	0.9[d]		8	8889	Chapter 3
				9[d]		26	2889	
				83[d]		188	2265	
				424[d]		394	929	

[a]: nmol cm^{-3}
[b]: µg kg^{-1}
[c]: nmol g^{-1}
[m]: mg L^{-1}
[t]: Total concentration
[d]: Dissolved concentration (filtered through 0.45 micron membrane filter)
[ns]: Total or dissolved not specified
[e] ± standard deviation

Table 6.2 cont.

Organism	Common name	Latin name	Exposure length (d)	Exposure concentration (µg L^{-1})	Tissue	Tissue concentration (mg kg^{-1})	BCF	Source
Fish	Atlantic salmon	*Salmo salar*	12.5	17.9[ns]	Muscle	2	130	Zitko et al. 1975
				17.9[ns]	Gill	26	1430	
				45[ns]	Muscle	5	114	
				45[ns]	Gill	1	27	
				100[ns]	Muscle	15	146	
				100[ns]	Gill	30	300	
				200[ns]	Muscle	27	135	
				200[ns]	Gill	32	161	
	Rainbow trout	*Oncorhynchus mykiss*	28	0.9[d]	Gill	15	16783 ± 5875[e]	Chapter 6
					Otolith	12	13114 ± 1536[e]	
					Muscle	7	7995 ± 1442[e]	
				141[d]	Gill	339	2771 ± 582[e]	
					Plasma	415[m]	2944 ± 1688[e]	
					Otolith	568	4029 ± 842[e]	
					Muscle	95	671 ± 154[e]	
	Fathead minnow	*Pimephales promelas*	21	0.08[t]	Whole body	0.0008	10	Lapointe and Couture 2010

By generating tissue-specific data for Tl accumulation, a greater understanding of interactions between body burden and toxic effects associated with Tl can be applied to risk management practices such as the BLM and TRA (Di Toro et al. 2001; Meador et al. 2008). This study therefore aimed to investigate Tl accumulation in the gill, plasma, muscle, and otolith of rainbow trout exposed to dissolved waterborne Tl. Accumulation in the gill and plasma provides insights into the uptake and subsequent distribution of Tl, while muscle Tl burden is of value for understanding the risks associated with human consumption of fish sourced from Tl-contaminated waters. Additionally, given its utility in field studies examining trace metal exposure history, otolith Tl concentration was measured to determine if burdens reflect exposure conditions in laboratory studies. In this chapter, K^+ concentration was also measured in muscle and plasma, in order to determine if Tl accumulation disrupted K^+ homeostasis in these tissues (Brismar 1998; Chapter 5). This study focused on rainbow trout, an important regulatory species (Dwyer et al. 1995), and one that is generally considered sensitive to trace metal toxicity (Environment Canada 2000c). Rainbow trout are also a surrogate species for cold-water fishes, providing an understanding of toxic mechanisms that can be applied to other fish species inhabiting cold freshwaters.

6.2. Methods

6.2.1. *Fish*

Rainbow trout (Strain: Trout Lodge Jumpers, TLTLJ) were acquired from Raven Creek Brood Trout Station (Caroline, Alberta, Canada), and maintained in the Department of Biological Sciences at the University of Alberta. Trout were grown to experimental size (19 - 55 g) in flow-through tanks supplied with aerated and dechlorinated facility water (hardness 160 mg

$CaCO_3$ L^{-1}; alkalinity 120 mg L^{-1}; K^+ 2 mg L^{-1}; pH 8.2; temperature 10 ± 1°C). Fish were fed dry commercial trout pellets (Purina trout chow) daily and maintained at a 14:10 photoperiod. All animal use was approved by the University of Alberta/Athabasca University Animal Care Committee under Protocol AUP2712.

6.2.2. *Exposure design*

Twenty-four hours prior to exposure, acid-washed glass treatment tanks (8 L) were placed in a water table and filled with 4 L of dechlorinated facility water. Tanks were then spiked with a pH 7.5 $TlNO_3$ stock (1000 mg L^{-1}) to the appropriate concentration for exposure, and aerated. The experiment was run with 8 replicates per treatment for either an acute (96-h; 0, 0.8, 2000, 4000 µg L^{-1}) or sub-chronic (28-d; 0, 0.8, 170 µg L^{-1}) exposure. Nominal exposure concentrations were based upon CCME water quality guidelines for Tl (0.8 µg L^{-1}), elevated environmental concentrations (170 µg L^{-1}; Williams-Beam and Twidwell 2003), a value 50% of the 96-h median lethal concentration (LC_{50}) of Tl to rainbow trout (2000 µg L^{-1}), and the acute LC_{50} value itself (4000 µg L^{-1}; Pickard 2001). After a 24-h equilibration period following Tl addition to facilitate steady state Tl speciation, trout were placed individually into tanks and exposed for either 96-h or 28-d. Acutely-exposed fish were fasted for the entirety of exposure, whereas sub-chronically-exposed fish were fed every 4 days to satiation immediately prior to a 100% water change (where the new exposure water had been allowed to equilibrate for 24-h prior to fish addition). Treatment conditions were monitored and measured once daily (temp = 11°C, pH = 7.7). Fish health was assessed at least twice daily. Following exposure, the fish were removed and immediately euthanized in 100 mg L^{-1} tricaine mesylate solution buffered to pH 7.5 with sodium bicarbonate. Blood samples were collected using a 1 mL syringe with a 20-gauge needle via caudal puncture, and transferred into a 1.5 mL Eppendorf tube. Plasma was obtained

by centrifuging freshly-collected blood samples at room temperature for 30-60 seconds at 10,000 g, or until a clear separation of cells and plasma was achieved. Plasma samples were transferred to clean 1.5 mL tubes. Immediately following plasma collection, and after severing of the spinal cord, heads of fish were removed with a razor blade, cutting behind the opercula to ensure no damage to gills. Second and third gill filaments were removed from each side of the fish and stored in separate Eppendorf tubes. Otoliths were carefully removed from both sides of the severed head by inserting curved tapered fine-point tweezers just behind the eye. White muscle was collected by taking two 1 x 1 cm tissue samples from between the pectoral and pelvic fins. Whole liver and trunk kidney were also dissected for uses described in other chapters. All collected tissues were flash frozen in liquid nitrogen and stored at -80°C. Processing of tissues is described in Section 6.2.4 (plasma, gill, muscle), in Sections 7.2.1 (gill and kidney), or in Section 8.2.1 (liver).

6.2.3. *Water sampling and Tl analysis*

Within each water change cycle, triplicate 10-mL water samples were taken at 0-h (immediately after water change) and 96-h (immediately before water change). To determine dissolved concentrations, collected samples were passed through a 0.45 μm syringe filter and acidified with 1% trace metal grade HNO_3. Samples were then analyzed for Tl via ICPMS. A detailed description of Tl analysis is located in Section 3.2.4. Reported acute exposure concentrations are the replicate mean values of 0 and 96-h measurements, then averaged across all replicates. Reported sub-chronic Tl concentrations represent mean values taken immediately before fish addition to a tank and immediately before a water change. All such values per replicate were averaged, and then these mean values were themselves averaged across all replicates.

6.2.4. *Tissue preparation and thallium analysis*

Plasma volumes were measured using a P1000 micropipette, before the plasma was transferred to a weighed Eppendorf tube. One mL of 70% trace metal grade HNO_3 was then added to the tube. Otolith tissues were weighed, dried at 65°C in a drying oven until stable weight, then digested in 1 mL of 70% trace metal grade HNO_3 and placed back into the drying oven for an additional 72-h. Prior to gill digestion for ICPMS, gill tissue was prepared and analyzed in ionoregulatory activity assays as described in Section 7.2.1. After activity analysis, gill homogenates were dried at 65°C until stable weight. The dried tissue was then digested following the same procedure used for otolith digestion. An UltraClave (Milestone, Shelton, Connecticut, USA) was used for muscle tissue digestion. Briefly, muscle tissue (0.2 g) was placed into a clean digestion tube containing 3 mL of twice distilled HNO_3 and 0.1 mL tetrafluoroboric acid. To prepare the digestion, 330 mL ultrapure water, 30 mL H_2O_2 and 3 mL H_2SO_4 were added to the Teflon bowl in the UltraClave system. The tube containing the sample was capped, placed into the UltraClave and digested for 2-3-h. Once completed, samples were transferred into 15 mL Falcon tubes and stored at 4°C until analyzed. For quality assurance of tissue digestions, a standard reference material (SRM) NIST 1566b (Oyster Tissue, National Institute of Standards and Technology, Gaithersburg, Maryland, USA) was used, and treated as described above for muscle tissue.

Following digestion, ICPMS was used to analyze samples for Tl concentration, as described in Section 3.2.4. The LOD and LOQ resulting from this analysis were 0.1 and 0.3 ng L^{-1}, respectively. For the purposes of statistical analysis, samples with concentrations below LOQ were assigned a value halfway between the LOQ and 0.

Muscle and plasma tissues were also analyzed for K^+ concentration. Gill tissues were not measured for K^+ concentration as the homogenization buffer used for enzyme analysis (which was conducted prior to bioaccumulation analysis) may have added K^+ to samples. Potassium concentration was measured using FAAS as described in Section 3.2.4.

6.2.5. *Bioconcentration factor*

A BCF was calculated for each fish exposed to Tl sub-chronically, as described by Veith et al. (1979). Measured Tl concentration for a given tissue (C_t; µg L^{-1} (plasma) or µg kg^{-1}) was divided by the measured Tl concentration in the exposure water (C_w; µg L^{-1}).

Equation 6.1:

$$BCF = \frac{C_t}{C_w}$$

Bioconcentration factors reported in Sections 6.3 and 6.4 are the calculated means of BCF values from each individual fish. Acute BCF values were not calculated based on the assumption that an equilibrium between accumulation and excretion had not been reached following 96-h of exposure (USEPA 2016).

6.2.6. *Statistics*

Prior to statistical analysis, Grubb's test was employed for detection and subsequent removal of outliers. Outliers were removed from acute plasma (one value removed from each of the 0 and 0.9 µg L^{-1} exposure concentrations), sub-chronic plasma (one removed from 0 µg L^{-1}), acute otolith (one removed from 0, 0.9 and 2004 µg L^{-1}), and sub-chronic otolith (one removed from 0.9 and 141 µg L^{-1}). For all analyses, assumptions of parametric analysis were tested using the Shapiro-Wilk test for normality, and the Brown-Forsythe test for homogeneity of variance. If assumptions were met, a one-way ANOVA was conducted to assess variance between treatments, followed by Tukey's multiple comparison test at an alpha level of 0.05. If

assumptions were not met, a non-parametric Kruskal-Wallis test was used, followed by Dunn multiple comparison test at an alpha level of 0.05. All reported values represent the mean ± standard deviation. All statistical analyses were conducted using Prism GraphPad. All tissue Tl concentrations are expressed on a dry weight basis.

6.3. Results

6.3.1. *Thallium exposure concentrations*

Measured exposure Tl concentrations were close to nominal values (Table 6.3). For the SRM NIST 1640a, measured Tl concentrations were 95 ± 0.2% of the certified value. From this point forward in this chapter, measured exposure concentrations will be referred to in the text. There was no certified Tl value in the tissue SRM (NIST 1566b). However, measured Tl concentration for NIST 1566b were similar to values reported in Park et al (2018).

Table 6.3. Dissolved thallium concentrations (μg L^{-1}) for acute and sub-chronic waterborne exposures.

Nominal concentration	Measured concentration[a]
0	0.12 ± 0.01
0.8	0.87 ± 0.01
170	141 ± 4
2000	2004 ± 73
4000	4200 ± 196

[a] Measured Tl values represent mean (± standard deviation) of 6 replicate water samples.

6.3.2. *Morbidity in thallium-exposed trout*

During acute exposures of rainbow trout, morbidity (loss of equilibrium) was observed in 7 fish. These fish were subsequently euthanized. In 2 cases morbidity was a result of a tank aeration failure. In general, morbidity was relatively evenly distributed across all treatments, and was therefore unlikely to be a consequence of Tl exposure itself. In total, 2 fish were euthanized from each of the control, 0.9 μg L^{-1} and 2004 μg L^{-1} exposure treatments, and a single fish was

euthanized from the highest exposure group (4200 µg L^{-1}). To ensure 8 replicates for each exposure concentration, additional animals were run immediately following the conclusion of the initial acute exposure study. No morbidity was observed in sub-chronic trout exposures.

6.3.3. *Thallium accumulation in gill*

Gill Tl concentrations were significantly different between treatment groups following acute Tl exposure ($P\text{-value}_{Kruskal\text{-}Wallis}$: 0.001; Figure 6.1a). Concentrations of Tl in gill tissue of trout exposed to 2004 and 4200 µg Tl L^{-1} were 142 and 243 times greater than gill Tl concentrations in control fish. Similarly, in the sub-chronic experiment, significant differences in mean gill Tl concentrations were also observed ($P\text{-value}_{Kruskal\text{-}Wallis}$: 0.0001; Figure 6.1b). In the 141 µg Tl L^{-1} treated fish, gill Tl concentrations were 109 times greater than those measured in control fish ($P\text{-value}_{Dunn}$: 0.001). Sub-chronic gill BCF values (mean ± standard deviation) were 16800 ± 11800 and 2770 ± 1300, for the 0.9 and 141 µg Tl L^{-1} treatments, respectively.

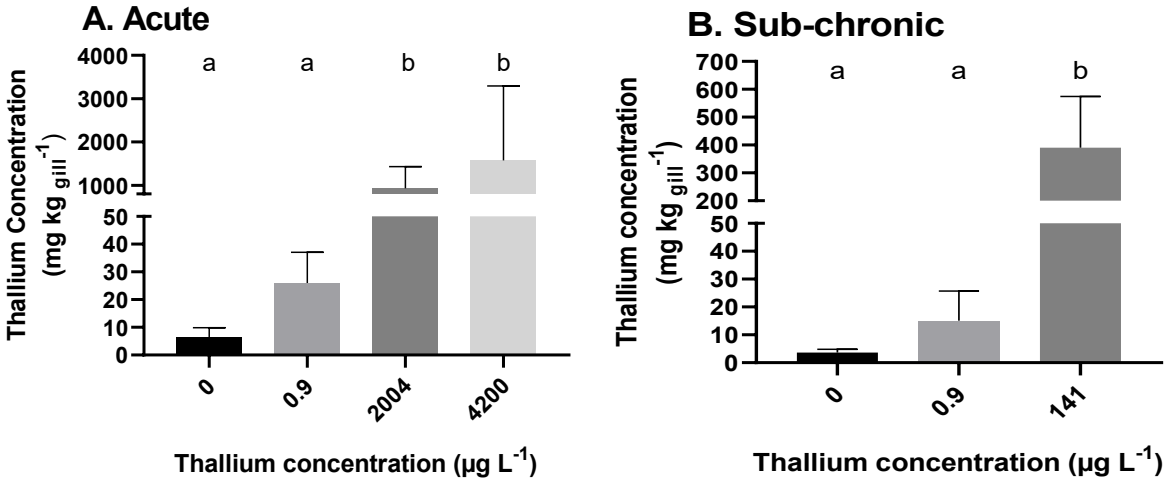

Figure 6.1. Branchial Tl concentration (mg per kg) in rainbow trout following an acute (96-h; A) or sub-chronic (28-d; B) exposure. Plotted points represent means (± standard deviation) of 8 replicates. Bars that share letters are not statistically different from one another.

6.3.4. *Thallium accumulation in plasma*

Concentrations of Tl in plasma for both 0 and 0.9 µg L^{-1} treatments in fish subjected to acute and sub-chronic Tl exposure were below LOQ values (0.3 ng L^{-1}). Mean Tl plasma concentrations in trout acutely-exposed to 2004 and 4200 µg L^{-1} Tl were 16.7 and 20.3 mg L^{-1}, values that were significantly greater than those of control fish (P-$value_{Tukeys}$: 0.047 and 0.002, Figure 6.2a). Similar findings were observed in sub-chronically-exposed trout where mean Tl concentration in plasma was 11.3 mg L^{-1} in fish exposed to 141 µg L^{-1}, a value significantly greater than that of control fish (P-$value_{Tukeys}$: 0.021, Figure 6.2b). A plasma BCF of 2940 ± 3380 was determined for fish exposed to 141 µg L^{-1} Tl for 28-d.

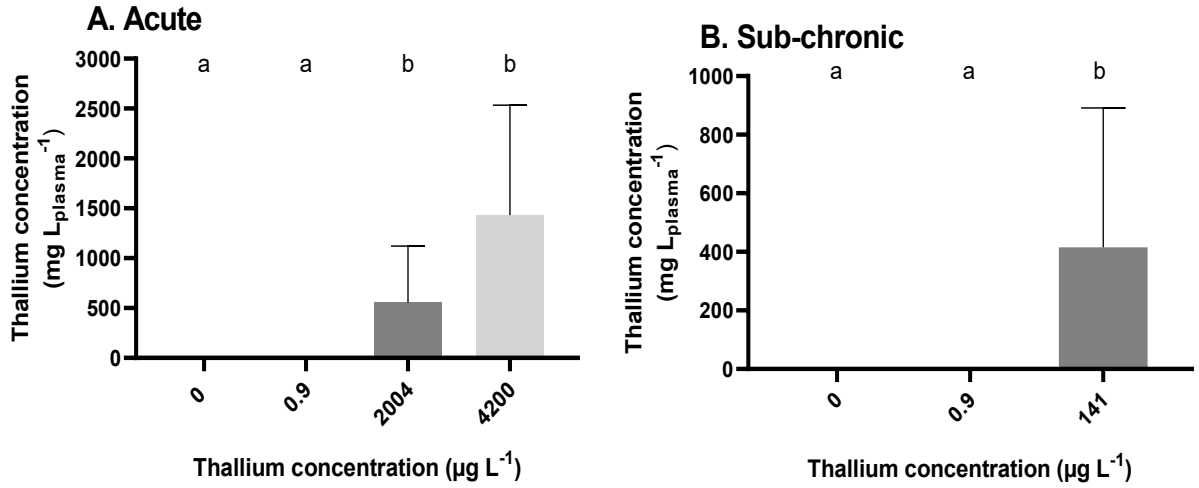

Figure 6.2. Plasma Tl concentration (mg per L) in rainbow trout following an acute (96-h; A) or sub-chronic (28-d; B) exposure. Plotted points represent means (± standard deviation) of 7-8 replicates. Bars that share letters are not statistically different from one another.

6.3.5. *Thallium accumulation in muscle*

Following acute exposure of rainbow trout to Tl, differences were observed in muscle Tl concentrations ($P\text{-value}_{ANOVA}$: 0.0001, Figure 6.3a). Tukey's multiple comparisons test showed that muscle tissue Tl burdens from fish exposed to 0.9 µg L^{-1} Tl were not significantly different from those of control fish, however accumulated Tl concentrations in the 2004 and 4200 µg L^{-1} groups were significantly greater than the control treatment ($P\text{-value}_{Tukeys}$: 0.0001). Similarly, sub-chronic exposure to Tl led to a significant difference between Tl concentrations in muscle tissue of rainbow trout ($P\text{-value}_{ANOVA}$: 0.0001, Figure 6.3b). Again, no significant differences were observed between control and 0.9 µg L^{-1} treatments, but trout exposed to 141 µg L^{-1} had significantly greater muscle Tl concentrations than both the control and 0.9 µg L^{-1} fish ($P\text{-value}_{Tukeys}$: 0.0003 and 0.0005, respectively). The sub-chronic BCF values for muscle tissue were 8000 ± 3530 and 671 ± 377, for Tl exposure concentrations of 0.9 and 141 µg Tl L^{-1}, respectively.

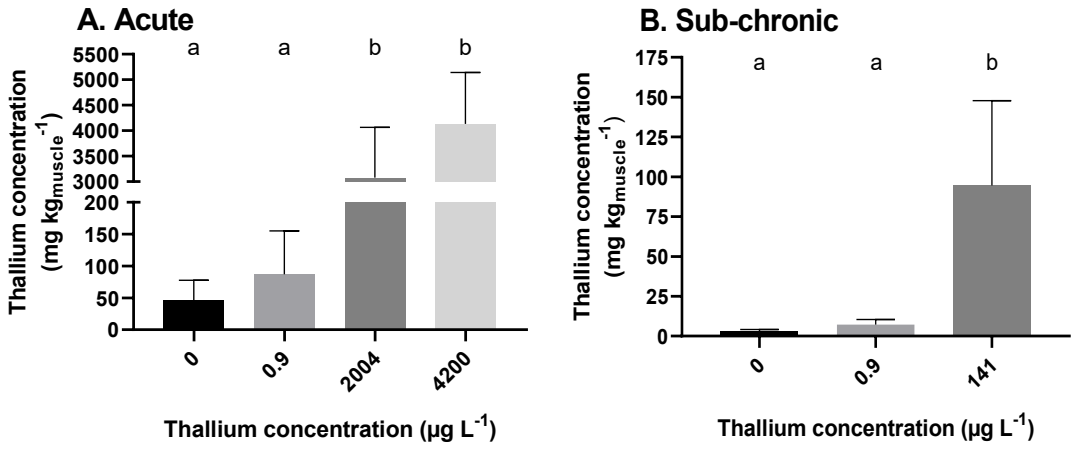

Figure 6.3. Muscle thallium concentration (mg per kg) in rainbow trout following an acute (96-h; A) or sub-chronic (28-d; B) exposure. Plotted points represent means (± standard deviation) of 8 replicates. Bars that share letters are not statistically different from one another.

6.3.6. *Thallium accumulation in otoliths*

Significant differences were observed in otolith Tl concentrations of acutely-exposed trout (P-value$_{Kruskal\text{-}Wallis}$: 0.0001). Otolith Tl was greater in fish exposed to 2004 and 4200 µg Tl L^{-1} versus the control group (P-value$_{Dunn:}$ 0.015 and 0.0004; Figure 6.4a). Likewise, significant differences in Tl otolith concentration were measured following sub-chronic exposure of trout to Tl (P-value$_{ANOVA}$: 0.0001). The Tl concentration in otoliths of trout exposed to 141 µg L^{-1} for 28 days was significantly greater than in otoliths of both control and 0.9 µg L^{-1} treatment groups (P-value$_{Tukeys}$: 0.0001; Figure 6.4b). For otoliths of sub-chronically-exposed fish, BCF values for trout exposed to 0.9 and 141 µg Tl L^{-1} were 13100 ± 3760 and 4030 ± 1880, respectively.

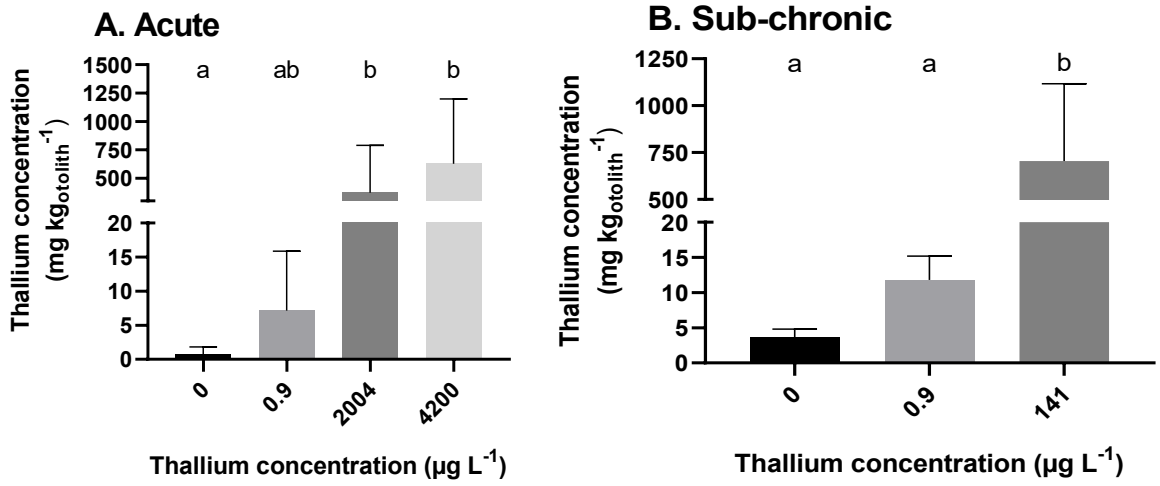

Figure 6.4. Otolith thallium concentration (mg per kg) in rainbow trout following an acute (96-h; A) or sub-chronic (28-d; B) exposure. Plotted points represent means (± standard deviation) of 7-8 replicates. Bars that share letters are not statistically different from one another.

6.3.7. Effect of thallium on muscle and plasma K^+ concentration

No significant differences in plasma K^+ concentrations were observed in trout acutely-exposed to Tl (P-value$_{ANOVA}$: 0.143; Figure 6.5a). Similarly, there were no significant differences in plasma K^+ concentrations of sub-chronically-exposed trout (P-value$_{ANOVA:}$ 0.714; Figure 6.5b). Potassium concentrations in muscle samples of trout undergoing acute (P-value$_{ANOVA}$: 0.160, Figure 6.5c) or sub-chronic Tl exposure (P-value$_{ANOVA}$: 0.621; Figure 6.5d), were also unaffected by Tl exposure.

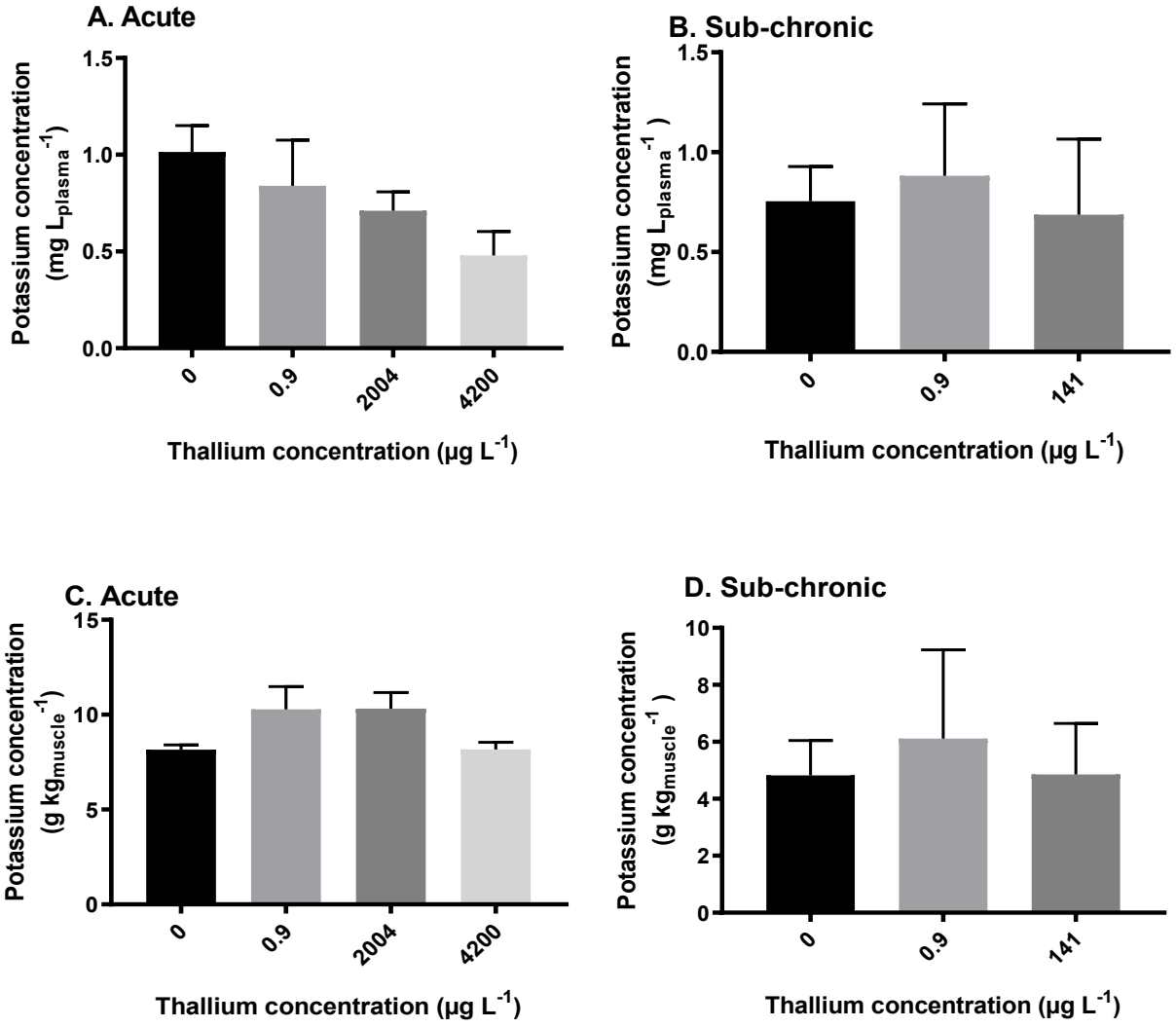

Figure 6.5. Potassium concentration in rainbow trout blood plasma (mg per L) following acute (96-h; A) or sub-chronic (28-d; B) exposure; and K^+ concentration in rainbow trout muscle tissue (g per kg) following acute (96-h; C) or sub-chronic (28-d; D) exposure. Plotted points represent means (± standard deviation) of 6-8 replicates.

6.4. Discussion

6.4.1. *Morbidity*

One notable outcome of the current study was the low morbidity in fish exposed to 4200 µg Tl L^{-1}. This concentration represented a value close to the reported 28-d LC_{50} value for rainbow trout (4300 µg Tl L^{-1}; Pickard et al. 2001), and thus mortality close to 50% might have been expected. Instead, just 1 of the 9 fish exposed to this concentration exhibited any morbidity. This may be a consequence of fish size. The fish in the current study ranged in size from 19 to 55 g, whereas the mean size of fish in the LC_{50} study of Pickard and colleagues was 0.36 g. This suggests a size-dependent sensitivity of rainbow trout to Tl toxicity. This is a commonly-reported phenomenon for trace metals. For example, Grosell and colleagues (2002), showed that sensitivity to waterborne Ag and Cu scaled closely with body size, with smaller organisms being more sensitive than larger organisms.

6.4.2. *Thallium accumulation in gills*

Gill tissue of rainbow trout exhibited a significantly elevated Tl burden after a 28-d exposure to 141 µg Tl L^{-1}, and following a 96-h exposure to Tl concentrations of 2004 µg L^{-1} or greater (Figure 6.1a-b). Furthermore, Tl accumulation in gill tissue was dose-dependent, in that as Tl exposure concentration increased, accumulation increased in both acute and sub-chronic exposures. This dose-dependent response contrasts with the findings of Zitko et al. (1975) in Atlantic salmon. These authors showed that Tl accumulation in gill tissue did not correlate to Tl

exposure concentration (r^2: 0.280; P-value: 0.471). For example, the Tl concentration in gills of salmon exposed to 45 µg Tl L^{-1} was lower than in those fish exposed to 17.9 µg Tl L^{-1} (Zitko et al. 1975). The other notable difference between the current study and that conducted in Atlantic salmon is the markedly higher tissue burdens in the current work. After a 28-d exposure to 141 µg Tl L^{-1}, branchial Tl was 10 times greater than that measured in gill tissue of salmon exposed to 200 µg Tl L^{-1} for 12.5-d (Zitko et al. 1975). Such differences are unlikely related to exposure time, as the branchial Tl burden of trout exposed to 141 µg Tl L^{-1} for just 96-h was also markedly greater (11-fold) than those measured in Atlantic salmon.

The factors contributing to these differences in burden between studies are unknown, but a number of possibilities exist. For example, salmon were exposed to waters that ranged in temperature between 7 and 17.5°C, whereas in the current study temperature was relatively constant at 11°C. Numerous studies have shown that metal accumulation in fish is temperature dependent. In carp, for example, higher burdens of Cu are observed at 10°C than at 20°C (Castaldo et al. 2021). The current study was performed using a static-renewal approach, whereas that of Zitko and colleagues used a continuous flow-through design. Because of the potential for the exposure concentration to change over time (e.g., through adsorption, evaporation, uptake by the test animal), static-renewal is considered a less robust approach than flow-through (USEPA 2002b). However, in the current study Tl concentrations were measured before and after renewal and were not found to differ (data not shown). Conversely, flow-through systems can be difficult to balance in order to achieve a constant tank toxicant concentration. In the study of Zitko et al. (1975) water Tl measurements were made only once a week, and reported concentrations were highly variable (see Figure 1 in Zitko et al. 1975). Therefore, variability in exposure concentration may have been a factor contributing towards

different patterns of gill Tl burden between the two studies. Lastly, as noted below, one potential source of branchial Tl is the gut, via the swallowing of contaminated water during feeding. In the study of Zitko et al. (1975) salmon were not fed over the duration of the exposure, whereas in the current work trout were fed every 4 days in the sub-chronic exposure. This may have generated an additional pathway of Tl uptake, and contributed to the higher branchial burdens observed for trout versus salmon. However, this phenomenon cannot explain the higher burden in acutely-exposed trout, which were not fed over the 96-h exposure period.

The gill is known to play an important role in K^+ handling (Lin and Lee 2005; Furukawa et al. 2011), and it is likely that Tl uptake and accumulation in the gill of rainbow trout is linked with K^+, as it is for other aquatic biota, including *Daphnia magna* (Chapter 5). However, the specific transport pathway by which Tl enters the gill cell has not been characterized. Some researchers have indicated the presence of apically-located branchial K^+ transporters in rainbow trout (e.g., Kerstetter and Kirschner 1972; Eddy 1985), but the uptake of K^+ across the gills is relative slow and small in magnitude (Gairdaire et al. 1991). Nevertheless, taking the maximal transport rate of K^+ characterised by Gairdaire and colleagues (7.5 μmol 100 g^{-1} h^{-1}), a calculation can be done to estimate the burden of Tl taken up by a rainbow trout across the gill. Assuming that Tl is absorbed across the gill equally as effectively as Tl (i.e, K^+ and Tl^+ share the same maximal transport rate value), then over the course of a 28-d exposure a 30-g fish (size of fish in the current study) would be capable of absorbing around 300 mg of Tl across the gill epithelium. This would be more than sufficient to account for the branchial Tl burden, and the accumulation of Tl in other studied tissues.

It is, however, possible that other routes of uptake could contribute towards branchial Tl. One such route is the skin, which has shown to be involved in K^+ uptake in medaka larvae,

through a paracellular transport pathway (Horng et al. 2017). Of greater relevance to the current study is the absorption of waterborne Tl via the gut through drinking or during feeding. While freshwater teleosts differ from marine teleosts in that they do not need to drink to maintain osmoregulation, some drinking in freshwater fish does occur (Fuentes and Eddy 1997). This would expose the gut epithelium to Tl, facilitating uptake through intestinal K^+ transporters (Rubino et al. 2019), before gaining entry into gill tissue through basolateral transporters via the blood. However, drinking alone could explain only a small proportion of tissue Tl burden. Taking the normal drinking rate of freshwater juvenile rainbow trout (0.9 mL kg^{-1} h^{-1}; Fuentes and Eddy 1998) and a 30 g fish, then over the course of a 28-d exposure, such a fish would imbibe only around 2.5 µg of Tl, insufficient to contribute substantially to tissue burden, even assuming complete assimilation from the diet. It is possible, however, that the swallowing of water containing Tl during feeding may also lead to gut Tl uptake, and eventual gill accumulation. However, this would also be unlikely to contribute markedly to tissue Tl burdens.

Intracellular metal-binding ligands can play an important role in the patterns of trace metal accumulation in tissues. For example, trace metals such as Zn, Cd and Cu bind to the cysteine-rich protein MT, an important intracellular ligand of fish tissues such as the gill (Hamilton and Mehrle 1986), and one which reduces the bioreactivity of metal ions (De Boeck et al. 2003; Klassen et al. 2009). These metals bind the thiol groups of cysteine with a high affinity. For example, calculated Log K values for Zn and Cu to MT thiol groups are 11.4 and 14.6, respectively (Krezel and Maret 2007; Banci et al. 2010). However, the binding affinity of Tl for thiol groups is very low (Log K = 2.40; Martin et al. 2020). This has also been shown experimentally, with several studies noting that Tl does not bind MT (Rosabal et al. 2016; Caron et al. 2017). Similarly, as described in Chapter 2, Tl speciation in freshwater is dominated by the

free Tl^+ ion and the formation of complexes in the presence of DOM (a complex organic molecule containing thiol groups) was negligible. This supports the idea that MT is unlikely to play an important role in the accumulation of Tl in the gill, or indeed, other tissues.

Instead, it is likely that mitochondria drive cellular Tl accumulation. For example, a study by Fukumoto and colleagues (1997) observed that the major sites of Tl localization in heart muscle tissue were mitochondria. Similarly, in tissues of rats injected with Tl, swelling of mitochondria was noted and attributed to Tl accumulation in this organelle (Herman and Bensch 1967). The accumulation of Tl in mitochondria is likely a consequence of K^+ mimicry, with the metal ion taking advantage of the high density of K^+ channels found on mitochondrial membranes (Laskowski et al. 2016). Gill chloride cells are especially rich in mitochondria, which provide the ATP required to drive energetically-expensive ion transport processes (Pisam and Rambourg 1991). It remains to be determined if mitochondrial Tl accumulation governs patterns of branchial Tl accumulation, and if there are different accumulation patterns of Tl according to branchial cell types with different mitochondrial densities.

6.4.3. *Thallium accumulation in plasma*

There was no detectable Tl in plasma at Tl exposure concentrations of 0.9 $\mu g\ L^{-1}$, regardless of exposure duration (Fig. 6.2a,b). As Tl^+ is known to mimic K^+, Tl handling would be expected to be closely linked to K^+ handling. Therefore, studies that detail the plasma handling of K^+ may help to explain the patterns of Tl accumulation observed in the current work. A study by Sanders and Kirschner (1983) showed that following injection of ^{86}Rb (a tracer of K^+; see Section 5.4.4), greater than 90% of the injected dose disappeared from blood of rainbow trout within 1-h. It is therefore likely that the undetectable levels of plasma Tl in low exposure concentrations reflect rapid mobilization of Tl from the blood to other tissues. This is supported by the fact that although

there are undetectable concentrations of Tl in plasma, under exposure to 0.9 µg Tl L^{-1}, Tl accumulates to a significant extent in muscle tissue and in the otolith. Transport via the blood is the most reasonable explanation for the accumulation of Tl in these tissues, thus the lack of detectable plasma Tl must be indicative of a rapid off-loading of plasma Tl burden.

Thallium concentration in blood plasma was significantly increased in trout acutely-exposed to 2004 and 4200 µg Tl L^{-1}, relative to lower Tl exposure concentrations. As for branchial Tl accumulation, there was no evidence for saturation of Tl accumulation in the plasma. This is consistent with findings that show Tl does not bind to plasma proteins (Talas et al. 1983), a factor that would ultimately limit accumulation. It is therefore probable that Tl remains unbound in the plasma, similar to K^+ (Palmer 2015). Thus, accumulation of Tl in the plasma is likely a consequence of Tl movement into the plasma being more rapid than its removal, resulting in a higher plasma Tl burden as Tl exposure concentration increases. The finding of an increased plasma Tl burden with increased exposure concentration also indicates that the gill of fish is not an effective barrier against Tl absorption. For many trace metals, the gill can effectively buffer the rest of the body against trace metal exposure (Zia and McDonald 1994). This lack of gill buffering is again likely to be a consequence of the ability of Tl to behave very similarly to K^+, which moves relatively freely across the basolateral membranes of gill epithelia in fish with limited loss across the apical membrane (Gardaire et al. 1991; Lin and Lee 2005).

Given the similarity in handling between Tl^+ and K^+, it is interesting that no changes in plasma K^+ concentrations were observed (Figure 6.5a-b). Similar findings were reported in Chapter 3 when assessing Tl accumulation and effects on whole-body K^+ concentration in *Daphnia magna.* In that chapter it was suggested that the effects of Tl on K^+ homeostasis are a function of exposure time, and that compensation in K^+ transport may occur correcting any Tl-induced

imbalance in tissue ion concentrations. Interactions between Tl accumulation and tissue K^+ concentration are discussed further in Section 6.4.4, below.

6.4.4. *Thallium accumulation in muscle tissue*

As noted by several previous field and laboratory studies (Tables 6.1, 6.2), and confirmed by the current work (Fig. 6.3ab), waterborne Tl accumulates in muscle tissue. Thallium accumulation in muscle tissue of trout exposed for 28-d to 141 µg Tl L^{-1} (98.7 mg kg^{-1}) was approximately three times greater than muscle Tl burden of Atlantic salmon exposed to 200 µg L^{-1} for 12.5-d (32 mg kg^{-1}). This would suggest that Tl burden accrues with time. However, in the current study muscle Tl decreased between the 96-h and 28-d exposure. This suggests that there must be mechanisms that act to either limit Tl accumulation, and/or increase Tl excretion, in muscle over time. The specific mechanisms remain unknown. However, there is evidence for acclimation of major ion uptake pathways that are shared with trace metals. For example, rainbow trout exposed to waterborne Zn exhibit a decrease in the affinity of transport pathways for Ca^{2+}, the ion that Zn mimics to gain access to the cell (Hogstrand et al. 1994). The effect of this decreased affinity is to reduce Zn influx, while maintaining Ca^{2+} influx, and is considered to be an important mechanism that facilitates acclimation to elevated waterborne Zn. It is possible that a similar mechanism exists for K^+ transport pathways in response to extended exposure to waterborne Tl.

It should be noted that the general patterns of Tl accumulation in the muscle were similar to those of the gill (i.e., a decrease in burden with length of exposure; general concentration-dependence of accumulation). This may reflect similarities in cellular Tl handling, the possible mechanisms of which were discussed in Section 6.4.2, above.

As mentioned in Chapter 5, cellular uptake of Tl occurs via K^+ transporters, raising the possibility that direct competition between Tl and K^+ could alter K^+ homeostasis (Britten and

Blank 1968). This has been experimentally confirmed by several studies (e.g., Siegel and Siegel 1976; Belowitz and O'Donnell 2013). For example, in midgut of *Chironomus riparius* larvae exposed to 60 mg Tl L^{-1} for 48-h, K^+ fluxes in the anterior and posterior midgut were impaired (Belowitz and O'Donnell 2013). However, in muscle tissue of trout exposed to Tl, there were no changes in K^+ concentration (Figure 6.5c-d). Similar findings have been observed for another K^+ mimic, Rb^+, in rat muscle (Kernan 1969). In that study, a 2-week exposure of rats to Rb^+-spiked drinking water, resulted in Rb^+ accumulation in various muscles (soleus, diaphragm, extensor digitorum longus, vastus lateralis, and gastrocnemius), but there was no effect of this accumulation on muscle K^+ concentration. Similarly, taking the values of muscle Tl and K^+ obtained by a long-term field study of Artic char (Gantner et al. 2009), a linear regression analysis failed to show a relationship between K^+ and Tl (r^2: 0.296; P-value: 0.265). Therefore, although there are reports that Tl does impair K^+ homeostasis, this does not appear to occur at the level of the muscle tissue in rainbow trout exposed to waterborne Tl, even for extended periods of 28-d. This may be a function of the fact that Tl uses K^+ transporters without blocking them (Britten and Blank 1968; Rabon and Sachs 1981; Carmosino et al. 2013), but it also indicates the lack of indirect effects of Tl on K^+ handling (i.e., those that are not related to direct competition for uptake).

Metal accumulation in fish muscle tissue has relevance to human health. Indeed, consumption of metal-contaminated fish has been associated with a number of significant public health issues, most notably in Japan with Minamata disease resulting from methylmercury contamination in an aquatic food chain (Harada 1995). While effects of Tl consumption are well-described from multiple cases of intentional poisoning (ATSDR 1992), there are few regulatory guidelines for consumption of Tl in food. The USEPA (1980) generated an acceptable daily intake (ADI) value of 37.3 µg Tl for a 70 kg man. This value was based on an ADI generated for

rats (533 µg kg^{-1}), and applying a safety factor of 1000. Based on fish consumption values from a Canadian survey (~100 g day^{-1}; Hu and Chan 2021), and taking the highest Tl muscle burden measured in the current study (4131 mg kg^{-1} in fish exposed acutely to 4200 µg L^{-1}), the daily intake of Tl from a worst-case exposure scenario would be 413,100 µg, a dose that far exceeds the suggested ADI value. Muscle obtained from fish exposed to 141 µg Tl L^{-1} for 28-d would also exceed the ADI value (9500 µg). However, these scenarios represent rather extreme environmental exposure scenarios. For example, Tl concentrations comparable to those used in the chronic exposures in this study are only found in wastewaters or surface waters collected in close proximity to mining areas (Table 1.1). Muscle Tl burdens from field studies (Table 6.1), indicate that in most situations fish would be safe for human consumption. However, consumption of muscle from ayu (875 µg Tl kg^{-1}) and Chinese false gudgeon (390 µg Tl kg^{-1}) collected downstream of the Dabaoshan mine, in waters with a Tl concentration of 0.1 µg L^{-1} (Chan et al. 2021), would also exceed the ADI (116 and 52 mg kg^{-1}, respectively). These ADI values account for the higher fish consumption rates of the population of Guangdong province where the Dabaoshan mine is located, relative to Canadian consumers (Li et al. 2013). This does, therefore, suggest that there may be some risk to human health associated with the consumption of fish sourced from waters moderately-contaminated with Tl.

6.4.5. *Thallium accumulation in otoliths*

Field-collected otoliths are a useful indicator for determining the age of fish, as well as for identifying previous exposure to trace metals (Arai et al. 2007). The data presented in this chapter show that rainbow trout otoliths can also accumulate Tl following acute and sub-chronic laboratory exposure (Figure 6.4a-b). For example, accumulation of Tl in otolith tissues following acute exposure to elevated Tl concentrations (2004, 4200 µg L^{-1}) resulted in mean otolith Tl

concentrations of 211 and 628 mg kg^{-1}, respectively. In otoliths of field-collected trout perch, Tl concentrations averaged 0.017 mg kg^{-1} under environmental exposure concentrations averaging 3 ng L^{-1} of dissolved Tl (Shotyk et al. 2019). Although Tl concentrations in otoliths of field-collected fish are significantly lower than those in laboratory-exposed trout, these findings provide further evidence that Tl readily accumulates in otoliths, at concentrations that reflect exposure concentrations. This finding supports work by Hansson et al. (2020), which suggests otoliths can be used in biomonitoring of mining areas to identify long-term exposure and serve as a record of contamination in the surrounding environment.

Of the tissues assessed in this study, only the otoliths exhibited Tl concentrations that increased markedly with exposure duration. In all other sampled tissues, there was either a decrease in Tl concentration when comparing 96-h and 28-d exposures, or Tl concentrations remained approximately the same. This lack of lability of otolith-associated Tl adds further confidence to the concept that metal accumulation in otoliths can be a robust reflection of past and present exposure history.

6.4.6. *Bioconcentration factor*

The BCF represents the magnitude of accumulation in a tissue or organism relative to the exposure concentration. This is a measure that has been used in regulatory guidelines for hazard assessment by Environment Canada (2000a). As mentioned in Section 6.1, Environment Canada guidelines consider a BCF value greater than 5000 to indicate a toxicant that is bioaccumulative (Environment Canada 2000a). Based on this guideline, the data presented in the current chapter indicate that Tl is bioaccumulative (Table 6.2). This finding is largely distinct from studies that have previously calculated BCF or BAF values for fish (Table 6.1 and 6.2), with a couple of exceptions. For example, data from Shotyk and colleagues (2019) results in a BAF value for

otolith tissue of 6071. This magnitude of accumulation is interesting, as fish in Shotyk et al. (2019) were not collected from an area with elevated concentrations of Tl in surface water. It is, however, important to highlight that in trout exposed for 28-d to 141 µg Tl L^{-1}, a more environmentally-realistic, albeit high, exposure scenario, BCF values were below regulatory concern. In their review of BAF and BCF values, McGeer and colleagues (2003) noted that these metrics are extremely variable and are not related to toxic impacts. Moreover, variability in BCF/BAF values across studies can be attributed to exposure length, changes in exposure concentration over time, life history and other variables. Consequently, even though BCF and BAF values do provide some insight to Tl exposure and accumulation, and can help identify the potential for toxic effects to occur in aquatic biota, actual measures of metal accumulation in tissues may serve as a better indicator of exposure and risk.

6.5. Conclusion

The present study assessed the accumulation of Tl on a tissue-specific basis following the waterborne exposure of rainbow trout to Tl. At concentrations near the CCME regulatory limit of 0.8 µg L^{-1} (i.e., 0.9 µg L^{-1}) no significant elevation in tissue Tl burden was observed in gill, plasma, muscle or otolith tissues, relative to unexposed controls. However, Tl accumulated in gill, plasma, muscle and otolith tissues when trout were exposed acutely to 2004 and 4200 µg L^{-1}, and sub-chronically to 141 µg L^{-1}. Although Tl is a K^+ mimic, results from this study suggest that Tl exposure to rainbow trout does not affect K^+ homeostasis, as supported by the lack of change in tissue K^+ concentration. However, despite significant Tl accumulation in muscle tissue of trout exposed to 141 µg L^{-1}, under regulatory guidelines the Tl BCF in this scenario would not be considered of environmental concern. This contrasts with the finding that the muscle Tl burden in this exposure scenario does exceed concentrations considered safe for human

consumption. This suggests that advisories for human consumption may be warranted for fish collected in surface waters where Tl concentrations are elevated, such as near mining areas.

7. Effects of acute and sub-chronic waterborne thallium exposure on ionoregulatory transporters in the gill and kidney of rainbow trout.

7.1. Introduction

A freshwater teleost is hyperosmotic to its surrounding environment. As such it will constantly lose ions via diffusion from its more concentrated body to the more dilute environment. In order to maintain ionic and osmotic homeostasis a freshwater fish therefore relies absolutely on epithelial ion transporters to recover lost ions (Perry et al. 2003; Horng et al. 2017; Takvam et al. 2021). Any disruption in ion regulation by, for example, environmental toxicants, may cause changes in ionoregulatory transporter function, leading to an inability to maintain ionic balance. This can ultimately result in mortality (Griffith 2016).

The gill epithelia of freshwater teleosts maintain cellular concentrations of major ions such as Na^+, K^+, Cl^- through transporters located on their apical and basolateral surfaces (Horng et al. 2017). As depicted in Figure 7.1a (adapted from Evans et al. 1999 and Horng et al. 2017), branchial transporters mediate exchange of ions between the cell, interstitial fluid and the surrounding freshwater environment, maintaining intracellular ion concentrations and an inside negative electrical potential. For example, proton ATPase (H^+-ATPase) actively translocates H^+ from inside the cell to the external environment, contributing to an electrochemical gradient that helps to facilitate the uptake of Na^+ from freshwater (Randall and Lin 1993; Lin et al. 2004). However, the greatest contributor to the electrochemical gradient that promotes the uptake of Na^+ is NKA (Moller et al. 1996; Lin et al. 2004). Located on the basolateral membrane in all cells, NKA transports 3 Na^+ out of, and 2 K^+ into, the cell for every molecule of ATP hydrolyzed. This creates an electrochemical gradient that then becomes the driving force for other cellular ion exchanges (Borgatti et al. 1992; Hwang et al. 2011; Shui et al. 2018). For example, electroneutral NKCC cotransporters utilize the gradient created by NKA to move Na^+,

K^+ and Cl^- into the epithelial cell (Katoh et al. 2008; Carmosino et al. 2013). There are two isoforms of the NKCC co-transporter; the secretory isoform NKCC1 located on the basolateral surface and the absorptive isoform NKCC2 located on the apical surface (Haas and Forbus III 1998). While the former isoform is located in many epithelia, NKCC2 is primarily associated with the reabsorption of Na^+ and Cl^- at the renal epithelium (Katoh et al. 2008). While NKCC is a vector for the basolateral uptake of K^+ into the cell, physiological evidence in the freshwater fish gill exists for the presence of an apical K^+ channel that achieves uptake of K^+ from the environment (e.g. Kerstetter and Kirschner 1972; Eddy 1985; Gairdaire et al. 1991). Branchial K^+ uptake is characterised as being of low magnitude (Gairdaire et al. 1991), possibly because it occurs despite a significant electrochemical gradient that appears to favor K^+ loss across the apical surface. This channel has not been structurally characterized and its identity remains unknown.

As noted in Figure 7.1b (adapted from Katoh et al. 2008 and Takvam et al. 2021), the general scheme of ion transport in the kidney is similar to that of the gill. However, to compensate for the influx of K^+ through the apical NKCC, efflux of K^+ through a K^+ channel occurs (Takvam et al. 2021). Although the specific K^+ channel is unidentified, in freshwater teleosts a number of apically-located candidates have been suggested. These include the big potassium (BK) channel and hyperpolarization-activated cyclic nucleotide-gated sodium potassium channels (HCN) (Tse et al. 2006; Loncoman et al. 2015; Fehsenfeld and Wood 2020).

Trace metals can inhibit the function of ion transporters (Kramer et al. 1986). One mechanism by which this can occur is through metal ion mimicry of major ions such as Na^+, Ca^{2+}, and K^+ (Wright 1995). Thallium, for example, is known to as act as a K^+ mimic in mammalian systems (Britten and Blank 1968; Cavieres and Ellory 1974; Hunter et al. 1986;

Carmosino et al. 2013), and multiple studies have shown that Tl can enter cells through NKA and NKCC ion transporters (Hunter et al. 1986; Lu et al. 2001; Sherstobitov et al. 2010; Carmosino et al. 2013). For instance, the transport of K^+ through NKCC in kidney cells can be completely replaced by Tl^+ (Carmosino et al. 2013), while 93% of Tl influx into freshwater lamprey (*Lampetra fluviatilis*) oocytes is thought to be achieved by NKA and NKCC (Sherstobitov et al. 2010). Similar findings have been reported in human blood cells (Cavieres and Ellory 1974), and rabbit kidney (Britten and Blank 1968). For example, in rabbit kidney cells, Tl was shown to have a 10 times greater affinity for the NKA K^+ binding site than K^+ itself (Britten and Blank 1968). Evidence also shows that Tl^+ transport into cells can occur at rates significantly greater than those of K^+. In human glioma cells, Tl^+ permeability through inwardly rectifying K^+ channels is 3.5 times greater than that of K^+ (Brismar et al. 1989). Similarly, the rate of Tl permeability through NKCC of mouse ascites tumor cells is 6.4-fold greater than that of K^+ (Sessler et al. 1986). The mimicry of K^+ by Tl^+ is likely a function of similarities in charge (+1) and ionic radii (K^+ = 137 pm; Tl^+ = 150 pm; Shannon 1976).

The use of K^+ transporters by Tl raises concerns about the effects of Tl exposure on K^+ homeostasis. For example, following exposure of *Chironomus riparius* to 50 µmol Tl L^{-1}, K^+ transport was inhibited at the anterior and posterior midgut (Belowitz and O'Donnell 2013). Such disruptions could ultimately account for Tl toxicity in aquatic organisms (Chapters 2, 3; Nehring 1962; Pickard et al. 2001). There is also significant evidence for a protective effect of K^+ on Tl toxicity. For example, suppression of Tl toxicity at high K^+ concentrations (and increased Tl toxicity at low K^+ concentrations), has been observed in *Ceriodaphnia dubia, Daphnia magna* and *Raphidocelis subcapitata* (Rickwood et al. 2015; Section 4.3.1). However, the specific mechanism underlying the interactions between Tl toxicity and K^+ is still unclear.

Evidence of interactions between Tl and K^+, coupled with the interdependence of the various cellular ion transporters (Figure 7.1a,b), suggests the potential for effects of Tl on ion transport more generally. If Tl is capable of inducing changes in K^+ handling, then this may be reflected in changes in entities that achieve K^+ transport, but also in transport pathways that are indirectly dependent on K^+ transport and the maintenance of cellular electrochemical gradients. This study sought to determine if Tl exposure caused changes in enzyme activity or gene expression of key epithelial ionoregulatory transporters. The effects of Tl on NKA and H^+-ATPase activity were assessed via enzyme assay. As there is no readily available activity assay for NKCC, real time quantitative polymerase chain reaction (RT-qPCR) was used to assess changes in gene expression of the NKCC1 isoform following Tl exposure. As the apical K^+ channel remains uncharacterized, effects of Tl on this transporter were not examined. This work aims to address potential mechanisms by which Tl may impair K^+ homeostasis, and thus generate toxicity in rainbow trout, an important regulatory species.

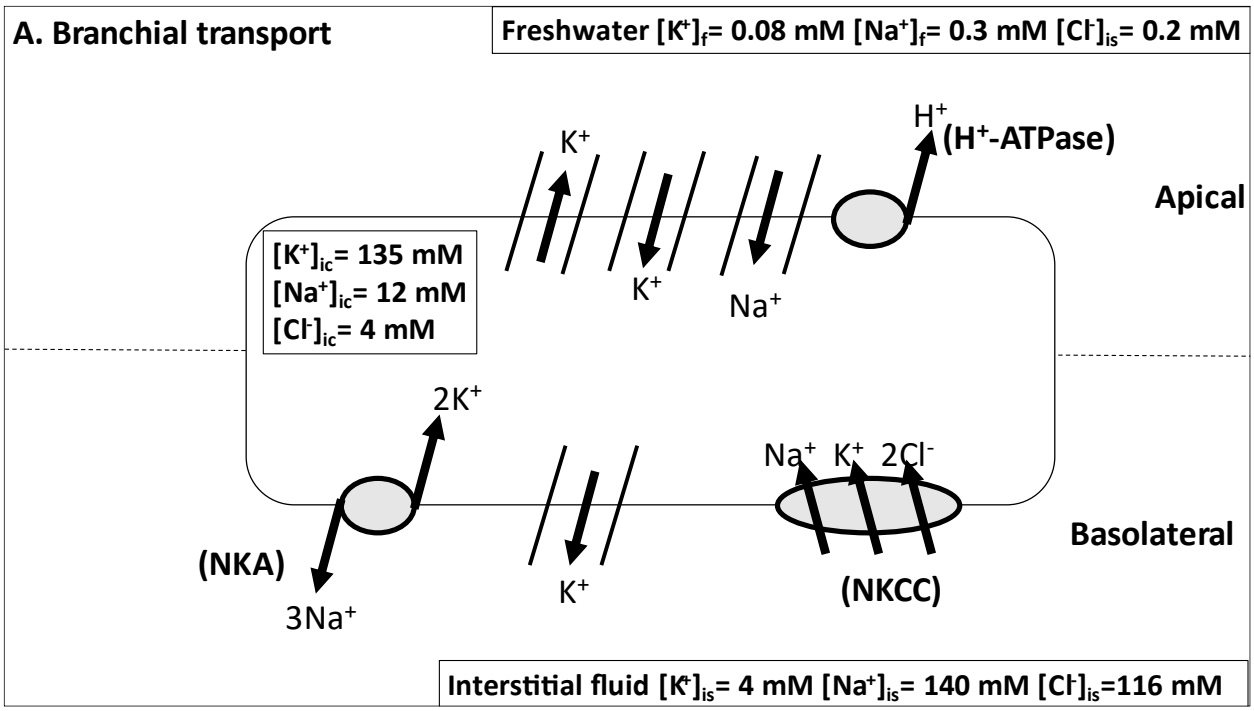
A. Branchial transport
Freshwater $[K^+]_f$= 0.08 mM $[Na^+]_f$= 0.3 mM $[Cl^-]_{is}$= 0.2 mM
H^+
(H^+-ATPase)
Apical
K^+
K^+
Na^+
$[K^+]_{ic}$= 135 mM
$[Na^+]_{ic}$= 12 mM
$[Cl^-]_{ic}$= 4 mM
$2K^+$
Na^+ K^+ $2Cl^-$
Basolateral
(NKA)
$3Na^+$
K^+
(NKCC)
Interstitial fluid $[K^+]_{is}$= 4 mM $[Na^+]_{is}$= 140 mM $[Cl^-]_{is}$=116 mM

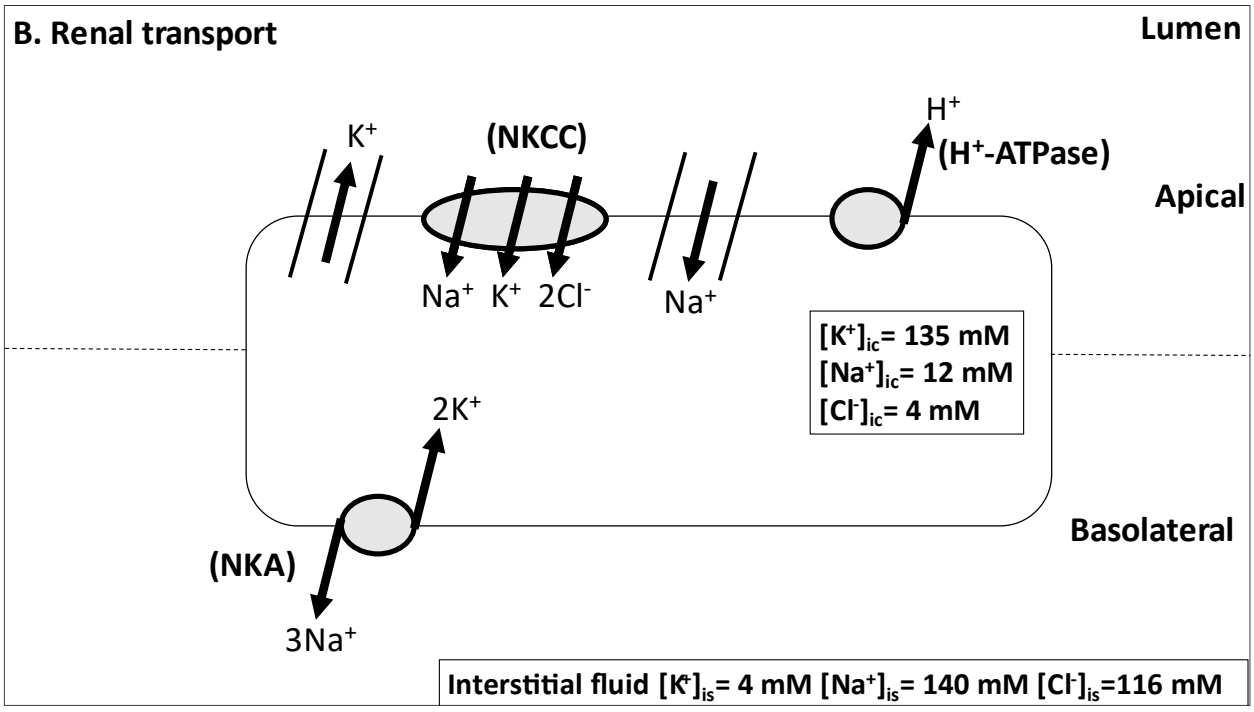
B. Renal transport
Lumen
H^+
(H^+-ATPase)
Apical
K^+
(NKCC)
Na^+ K^+ $2Cl^-$
Na^+
$[K^+]_{ic}$= 135 mM
$[Na^+]_{ic}$= 12 mM
$[Cl^-]_{ic}$= 4 mM
$2K^+$
Basolateral
(NKA)
$3Na^+$
Interstitial fluid $[K^+]_{is}$= 4 mM $[Na^+]_{is}$= 140 mM $[Cl^-]_{is}$=116 mM

Figure 7.1. A proposed model for branchial and renal ion regulation. A. is an overview of ion transport across gill epithelia (adapted from Evans et al. 1999; Horng et al. 2017). B. is an overview of ion transport across kidney epithelia (adapted from Katoh et al. 2008 and Takvam et al. 2021). Nominal intracellular and interstitial fluid ion concentrations adopted from Wright (2004). f = freshwater; ic = intracellular; is = interstitial. See Section 7.1 for description. The model shows 4 mM for intracellular [Cl^-], however some researchers suggest a value of 75 mM is more realistic (Wood and LeMoigne 1991)

7.2. Methods

Methodological details regarding experimental animals, exposure design, and water chemistry analysis can be found in Sections 6.2.1 and 6.2.2.

7.2.1. *Tissue preparation and enzyme analysis*

Following euthanasia, rainbow trout trunk kidney and second and third gill arches were removed, placed into separate 1.5 mL Eppendorf tubes and flash frozen in liquid nitrogen. Tissues subjected to enzyme analysis (approximate mass range: 250-500 mg) were homogenized using a handheld homogenizer in 1 mL SEID-EGTA buffer (125 mM sucrose; 5 mM EGTA; 50 mM imidazole; 0.05 g 50 mL^{-1} Na deoxycholate, pH = 7.3), and then centrifuged at 5000 g at 4ºC for 3 minutes. The resulting supernatant was then transferred into a new Eppendorf tube and stored at -80ºC until used in NKA and H^+-ATPase enzyme assays.

The activity of NKA and H^+-ATPase was measured using assay protocols of McCormick (1993) and Lin and Randall (1993), respectively, as modified by Delompré et al. (2019b). In both assays, ATP hydrolysis was coupled to the oxidation of nicotinamide adenine dinucleotide (NADH), with the disappearance of NADH monitored over time. The differences between uninhibited reactions, and those conducted in the presence of specific ATPase inhibitors were

used to determine activity. The inhibitors used were ouabain (an NKA-specific inhibitor), and N-ethylmaleimide (NEM) and sodium azide (which are inhibitors of plasma membrane and mitochondrial H^+-ATPase activity, respectively). More specifically, to measure uninhibited activity, triplicate 10 μL aliquots of supernatant were added to 200 μL of a master mix solution containing 2.8 mM phosphoenolpyruvate (PEP); 3.5 mM ATP; 0.22 mM NADH; 4 U mL^{-1} lactate dehydrogenase (LDH); 5 U mL^{-1} pyruvate kinase (PK); 189 mM NaCl; 10.5 mM $MgCl_2.6H_2O$; 42 mM KCl; 50 mM imidazole, in a 96-well microplate. A standard curve was generated from a 4 mM adenosine diphosphate (ADP) stock. Disappearance of NADH was measured at a wavelength of 340 nm on a VersaMax microplate reader (Molecular Devices, Sunnyvale, California, USA). The assay plate was re-read until the slope of the standard curve reached -0.01 to -0.04. At the same time activity was measured in wells where 0.65 mM ouabain was added to triplicate samples to inhibit NKA, and 500 mM sodium azide and 100 mM NEM were added to triplicate samples to inhibit H^+-ATPase. Enzymatic activity was normalized to sample protein content via Bradford protein assay (Bradford 1976).

7.2.2. *RT-qPCR tissue preparation and analysis*

Total RNA for analysis of NKCC1 (the target gene) and 18s rRNA (the housekeeping gene) was extracted from gill and kidney tissues using TRIzol RNA isolation, followed by RT-qPCR. Briefly, in safe-lock Eppendorf tubes, 50 mg of tissue along with 0.75 mL of TRIzol reagent were homogenized using a handheld homogenizer. Chloroform (0.15 mL) was then added to the tubes, which were vigorously mixed, and then spun at 12000 g at 4°C for 15 minutes. The upper aqueous phase, which contained RNA, was then transferred to a clean 1.5 mL Eppendorf tube. Precipitation of RNA was conducted by the addition of 1 mL of ice cold 99.5% isopropanol followed by a 30-minute incubation at -20°C. Following incubation, tubes

were spun at 12000 g for 10 minutes at 4°C, and the supernatant was then discarded. The pellet was then washed 3 times by adding 1 mL 75% ethanol, inverting, and spinning at 10000 g for 5 minutes at 4°C, with the liquid removed after each spin. The RNA pellet was then dried and resuspended in 30 µL of nuclease-free water. To determine RNA quality, purified RNA was analyzed using a NanoDrop spectrophotometer (ND-1000; Nanodrop Technologies, Wilmington, Delaware, USA). Samples with 260:280 nm absorbance ratios of ~1.80 were deemed of sufficient purity for RT-qPCR analysis. Additionally, only samples with RNA concentration greater than 100 ng μL^{-1} were used. Subsequently, RNA was diluted as needed and analyzed for gene expression using iTaq Universal SYBR® Green One-Step Kit (Bio-Rad Laboratories, Hercules, California, USA), according to the manufacturer's 10 µL reaction thermal cycling protocol specifications. First, a reverse transcription reaction was performed at 50°C for 10 minutes. Second, a polymerase activation and DNA denaturation reaction occurred for 1 minute at 95°C. Amplification then was carried out by 40 thermal cycles of denaturation at 95°C for 15 seconds followed by an annealing/extension and plate read at 60°C every 60 seconds. All RT-RT-qPCR analysis was performed using an Applied Biosystem 7500 Real-Time PCR System (Applied Biosystems, Waltham, Massachusetts, USA). To ensure purity and specificity of the RT-qPCR products a melt curve analysis was conducted, where a single peak confirmed successful primer amplification. Melt-curve analysis was performed by ramping up temperature from 65 to 95°C at 0.5°C increments with a 5 second holding step between each ramp. Calculated ΔΔCT values for the housekeeping gene 18s rRNA showed no significant difference between treatments and these values were therefore grouped and averaged by tissue and exposure length. Relative levels of NKCC1 target transcript were normalized by the mean expression of 18s rRNA from the same tissue and exposure length (e.g., gill tissue, acute

exposure). Calculated fold-change in expression for treatment groups is expressed relative to fold-change of gene expression in control groups. Fold changes were calculated via the $2^{-\Delta\Delta CT}$ method (Livak and Schmittgen 2001). Primers were designed using Prime Express Software v3.0.1 (Thermo Fisher Scientific, Waltham, Massachusetts, USA). For optimization, primers were designed manually with primer length set at 20 and amplicon length set at 200 for optimum SYBR PCR efficiency (Table 7.1).

Table 7.1. Primers for RT-qPCR analysis.

Gene	GenBank #	Forward primer	Reverse primer	Efficiency
18s rRNA	AF243428.2	CACGCGCGCCACACT	TAATTGCAATCCCCAATCCCTAT	2.01
NKCC1	AJ417890	GTCGTCACCACCATCACAG	CCAATAGCTCCTCCAAATTCAG	1.86

7.2.3. *Relationship between NKA and thallium burden*

Analyses were conducted to assess the relationship between branchial NKA activity (this chapter) and the Tl gill burden data (Figure 6.1a,b; Section 6.3.3). Three analyses were performed using a simple linear regression (Prism Graph Pad), where NKA activity was plotted against Tl burden for acute, sub-chronic, and combined (acute + sub-chronic) datasets.

7.2.4. *Statistics*

Details of statistical analysis can be found in Section 6.2.6. Following analysis, a single outlier was removed from the acute gill NKA dataset (at the 0.9 µg L^{-1} exposure concentration), and 2 outliers were removed from acute kidney H^+-ATPase replicates (both at 2004 µg L^{-1}).

7.3. Results

7.3.1. *Water chemistry analysis*

Results of the exposure water chemistry analysis can be found in Section 6.3.1. From this point on in this chapter, treatment concentrations are reported as measured values.

7.3.2. *NKA enzymatic activity*

No significant differences in branchial NKA activity were found between treatment groups following a 96-h exposure of rainbow trout to waterborne Tl ($P\text{-value}_{ANOVA}$: 0.355, Figure 7.2a). In contrast, significant effects on branchial NKA activity were observed after a 28-d exposure. Specifically, NKA activity was reduced in the 141 µg L^{-1} treatment relative to the control group ($P\text{-value}_{Tukeys}$: 0.043, Figure 7.2b). No significant differences were observed in renal NKA activity following either acute ($P\text{-value}_{ANOVA}$: 0.126, Figure 7.2c), or sub-chronic ($P\text{-value}_{ANOVA}$: 0.229, Figure 7.2d) Tl exposure.

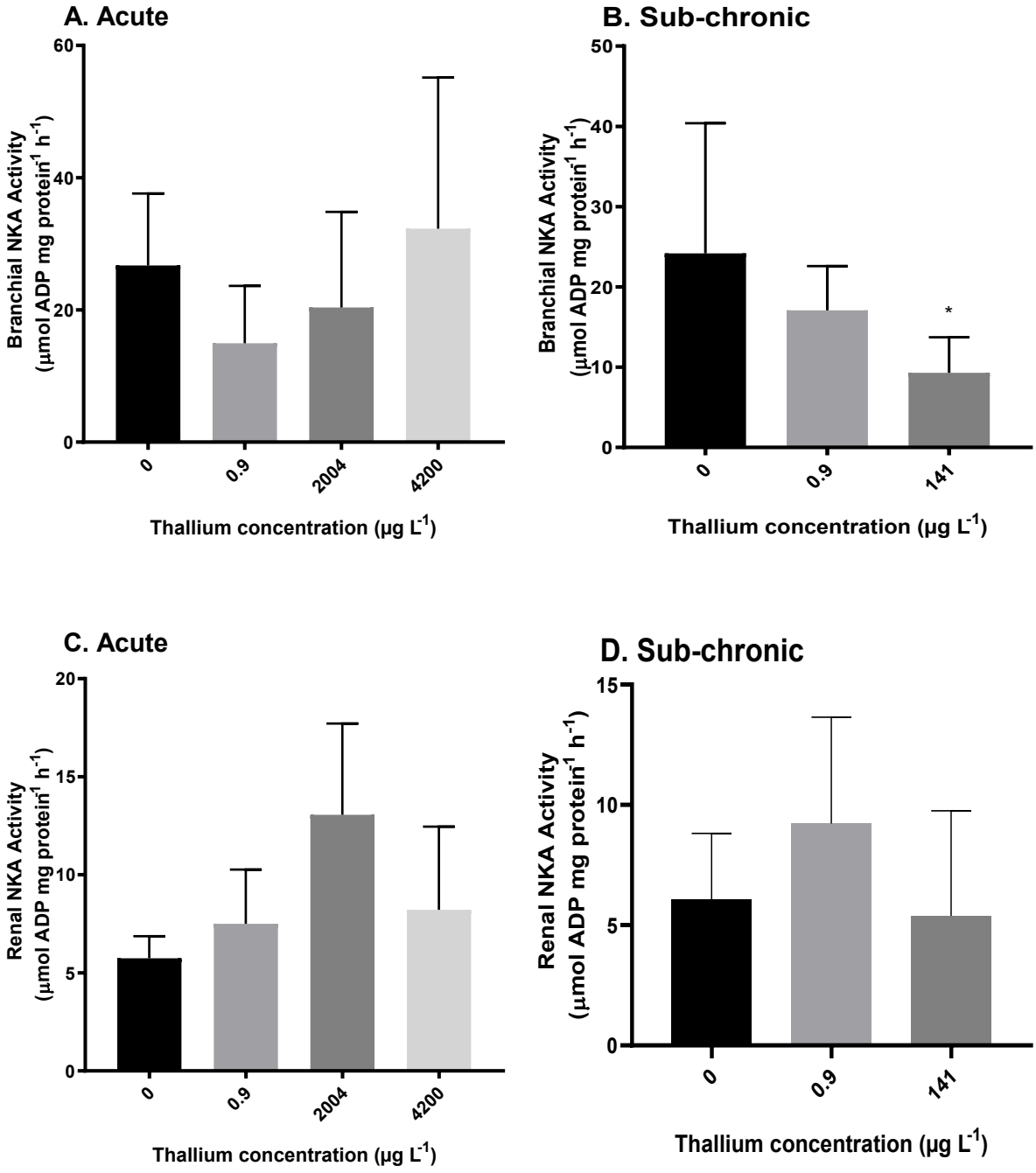

Figure 7.2. NKA activity for rainbow trout gill tissue following acute (A) and sub-chronic (B) Tl exposure and kidney tissue following acute (C) and sub-chronic (D) Tl exposure. Plotted points represent means (± standard deviation) of 7-8 replicates. Asterisk represents significant differences from the control.

7.3.3. *H^+-ATPase enzymatic activity*

No significant differences were observed in branchial H^+-ATPase activity following acute ($P\text{-value}_{ANOVA}$: 0.642, Figure 7.3a) or sub-chronic ($P\text{-value}_{ANOVA}$: 0.658, Figure 7.3b) Tl exposure. However, a significant increase in renal H^+-ATPase activity was observed in trout acutely exposed to 4200 µg Tl L^{-1}, relative to control kidney ($P\text{-value}_{Tukeys}$: 0.007, Figure 7.3c). In contrast, no differences were observed in renal H^+-ATPase activity following sub-chronic Tl exposure ($P\text{-value}_{ANOVA}$: 0.299, Figure 7.3d).

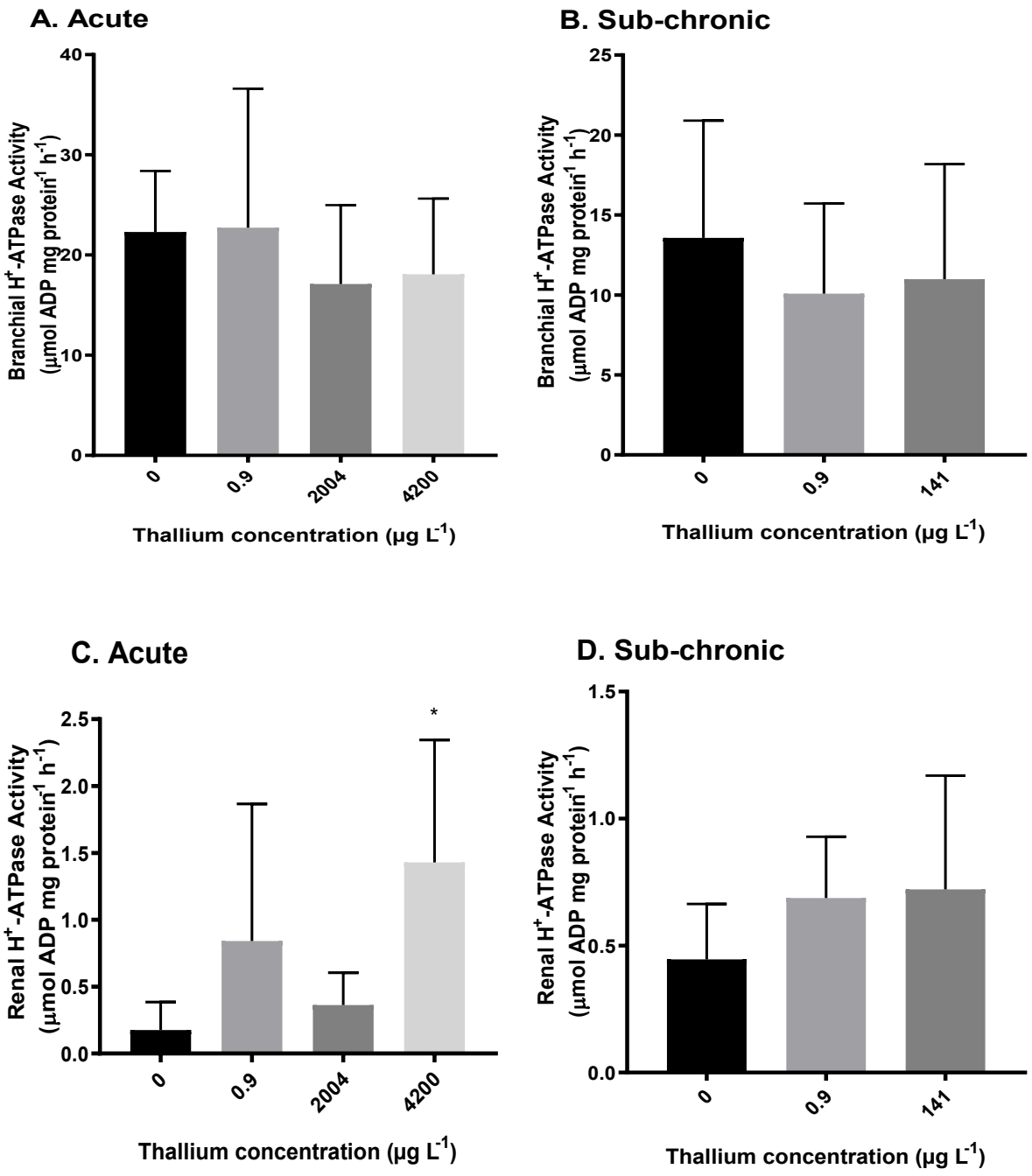

Figure 7.3. H^+-ATPase activity for rainbow trout gill tissue following acute (A) and sub-chronic (B) Tl exposure and kidney tissue following acute (C) and sub-chronic (D) Tl exposure. Plotted points represent means (± standard deviation) of 6-8 replicates. Asterisk represents significant differences from the control.

7.3.4. *RT-qPCR*

There were no significant differences in NKCC1 gene expression in branchial tissues following either acute ($P\text{-value}_{ANOVA}$: 0.093, Figure 7.4a) or sub-chronic ($P\text{-value}_{ANOVA}$: 0.138, Figure 7.4b) exposure of rainbow trout to Tl. Likewise, no significant differences were observed in kidney NKCC1 expression following both acute ($P\text{-value}_{Kruskal\text{-}Wallis}$: 0.070, Figure 7.4c) and sub-chronic ($P\text{-value}_{Kruskal\text{-}Wallis}$: 0.063, Figure 7.4d) Tl exposures.

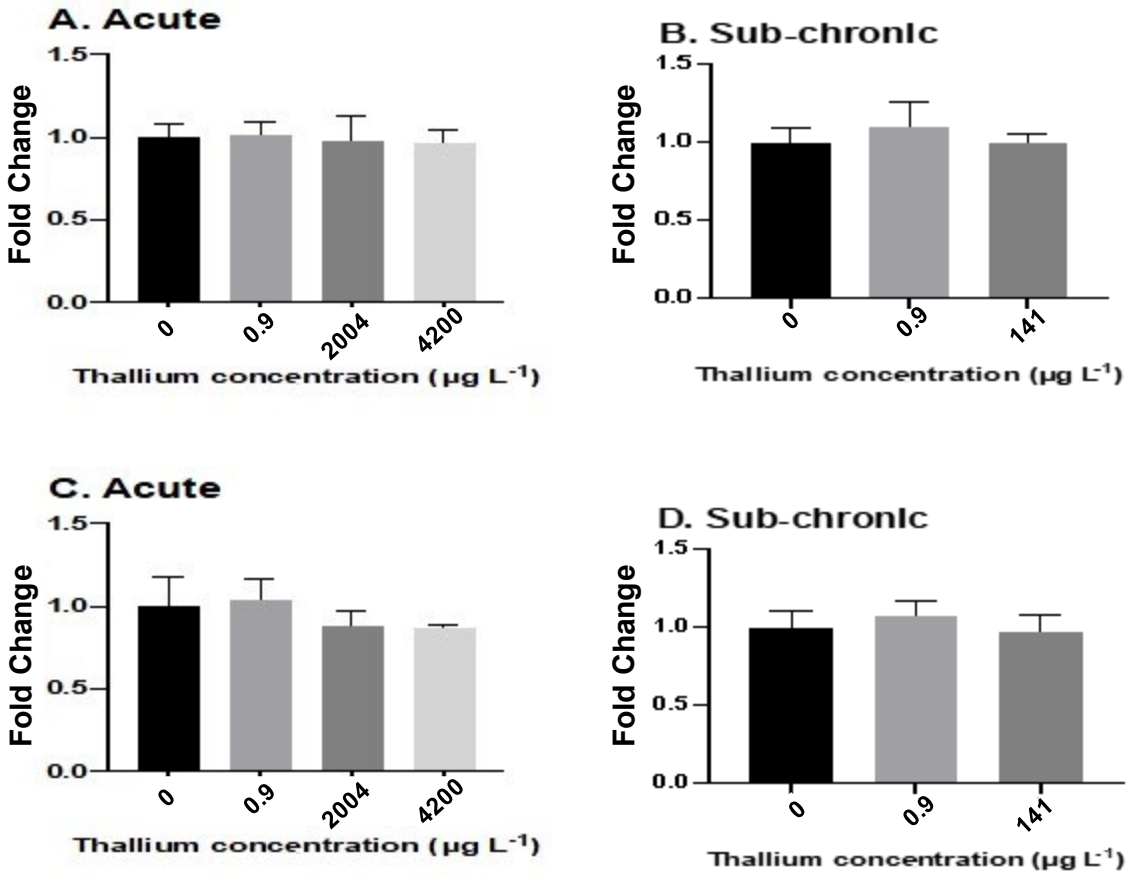

Figure 7.4. NKCC1 gene expression for rainbow trout gill tissue following acute (A) and sub-chronic (B) Tl exposure and kidney tissue following acute (C) and sub-chronic (D) Tl exposure. Plotted points represent means (± standard deviation) of 8 replicates.

7.3.5. *Branchial Tl burden and NKA activity*

Linear regression of NKA activity and Tl burden for 96-h-exposed rainbow trout showed the two variables were not significantly related (r^2: 0.003, P-value: 0.830, Figure 7.5a). Similarly, in sub-chronically-exposed trout, there was no significant relationship between gill Tl burden and branchial NKA activity (r^2: 0.118, P-value: 0.210, Figure 7.5b). The linear regression analysis for the combined acute and sub-chronic datasets also showed no significant relationship between the two variables (r^2: 0.007, P-value: 0.639, Figure 7.5c).

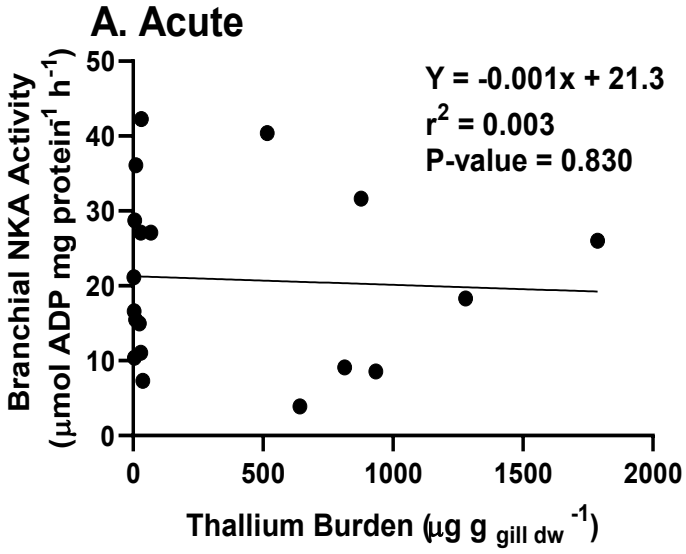

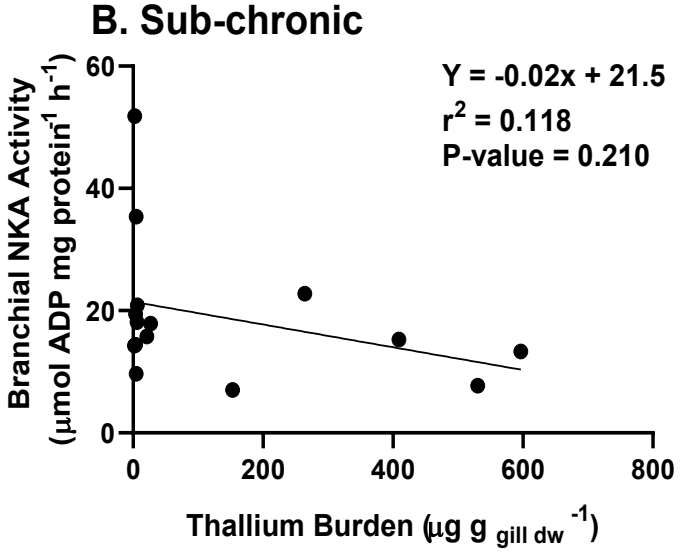

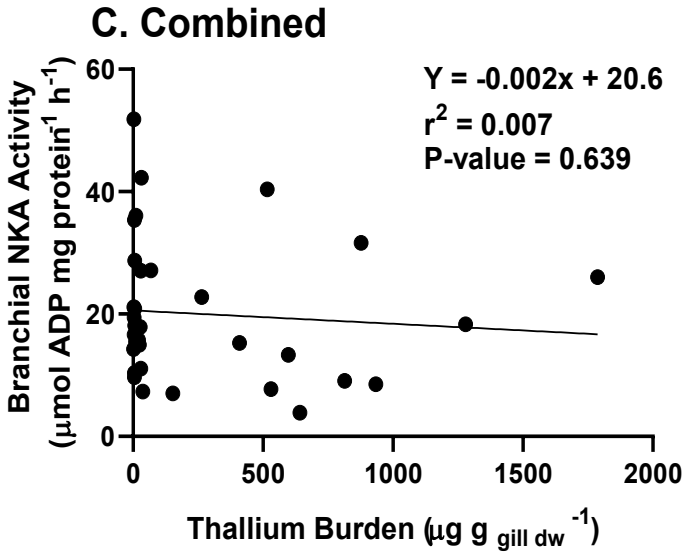

Figure 7.5. The relationship between branchial NKA activity and gill Tl burden of rainbow trout following acute and sub-chronic Tl exposure. Acute (A) sub-chronic (B) or combined (both acute and sub-chronic) (C) data sets were fitted to a linear regression. Values for r^2 and p are reported for a total of 15-34 individuals.

7.4. Discussion

7.4.1. *Effect of thallium on ionoregulatory ATPases*

In the present study, Tl exposure caused an inhibition of branchial NKA activity after a 28-d waterborne exposure to 141 µg Tl L^{-1} (0.7 µM; Figure 7.2b). Interactions between Tl and NKA have been well documented in mammalian models (Britten and Blank 1968; Cavieres and Ellory 1974; Appenroth et al. 1995). For example, Tl can substitute for K^+ and subsequently stimulate NKA activity in rabbit kidneys (Britten and Blank 1968). Similar stimulatory effects on NKA are observed in human blood cells exposed to Tl concentrations below 0.1 mM (Cavieres and Ellory 1974), while exposure of zebrafish to Tl concentrations of 0.02 to 1 µg L^{-1} (0.1 to 5 nM) for 96 d, caused an increase in branchial NKA activity (Hou et al. 2017). Inhibitory effects of Tl on NKA, similar to those reported in the current work, have also been observed. For

example, Tl inhibits red blood cell NKA activity at concentrations greater than those that cause stimulation of activity (Cavieres and Ellory 1974; Skulski et al. 1975).

These data suggest that, at least in mammalian systems, the effects of Tl on NKA activity are dependent upon exposure dose. However, dose alone is unlikely to explain the inhibition of NKA in the current work, as this effect was only observed in the gill after a 28-d exposure to 0.7 µM, while acute exposures to concentrations more than an order of magnitude higher had no effect. Furthermore, effects of Tl on NKA did not correlate with whole gill Tl burden (Figure 7.5a-c). A fundamental assertion of regulatory approaches based on bioaccumulation, such as the BLM, is that accumulation can be informative of toxicological impact (see Section 1.1.9; Di Toro et al. 2001). While this relationship holds for most trace metals (Niyogi and Wood 2004), it is dependent upon the toxic endpoint selected. For example, while inhibition of Na^+ uptake does correlate with short-term branchial Ag burden in rainbow trout, no such relationship exists for the inhibition of NKA by Ag (Morgan and Wood 2004). This latter finding is consistent with the outcome of the current study.

One explanation for the inhibition of NKA by Tl is through depletion of ATP. Mitochondria, which provide ATP to the cell, rely on the influx of K^+ for several critical processes. These include maintenance of matrix volume and membrane potential, which ultimately facilitate electron transport and ATP production (Laskowski et al. 2016). In a cell, 10% of intracellular K^+ is conserved in the mitochondria (Szabò et al. 2012), and several classes of K^+ channels exist on mitochondrial membranes to facilitate K^+ exchange. Mitochondrial K^+ channels generally have a higher conductance than their equivalents located on the plasma membrane (Kravenska et al. 2021). These characteristics indicate that mitochondria have a unique K^+ handling phenotype relative to the rest of the cell, and that the importance of K^+

handling in these organelles may make them an especially sensitive target of Tl toxicity. As noted in Section 5.3.3 of this thesis, there is strong evidence from the literature that Tl interacts with K^+ channels to gain access to a cell (or in this case an organelle). Indeed, studies in rats have shown the capacity for Tl flux through mitochondrial K^+ channels including the large-conductance Ca^{2+}-activated K^+ channel (BK; Testai et al. 2013) and the mitochondrial ATP-sensitive K^+ channel (mitoK_{ATP}; Foster et al. 2012). Evidence also exists for the accumulation of Tl in mitochondria, a phenomenon that causes mitochondrial swelling (Herman and Bensch 1967). Ultimately, Tl can impair mitochondrial function, resulting in a cellular depletion of ATP and therefore reduced substrate for ATPase enzymes (Melnick et al. 1976; Pourahmad et al. 2010; Jonckheere et al. 2012). Thus, based on the knowledge that Tl enters the mitochondria where it accumulates and reduces available ATP, prolonged exposure to Tl could cause an inhibition of the activity of NKA, which is, of course, ATP dependent. In the current study the presence of Tl effects on NKA occurred only after sub-chronic, and not acute, exposure. This may relate to differences in mitochondrial Tl burden; a failure of mechanisms that may protect against mitochondrial Tl toxicity over time; or a gradual depletion in the ATP pool with prolonged Tl exposure. Measures of mitochondrial Tl burden and/or cellular ATP would help to address the underlying mechanisms behind the effect of Tl on NKA.

The hypothesis that the effects of Tl on NKA activity are related to energy metabolism is supported by the finding that Tl inhibits PK (Kanye 1971). Pyruvate kinase catalyzes transfer of a phosphate group from PEP to ADP generating ATP (Israelsen and Vander Heiden 2015). Potassium is essential for PK activity (Oria-Hernández et al. 2005), but Tl has a 50 times greater affinity for PK than does K^+ (Kanye 1971). These differences in affinity translate to a much lower optimal concentration for Tl activation of the enzyme (3 mM for Tl versus 100 mM for

K^+; Kanye 1971). However, at concentrations greater than 10 mM Tl inhibits activity of PK purified from rabbit muscle (Kanye 1971). Although the experimental design is significantly different in the current study (i.e., 28-d in vivo whole animal waterborne exposure versus in vitro purified enzyme assay), it is possible that the inhibitory effect of Tl observed on branchial NKA activity results from the depletion of cellular ATP through PK inhibition, in addition to the more general effect of Tl on mitochondrial ATP production noted above.

While changes in the availability of ATP by Tl would explain effects on NKA, it does not account for the lack in response of branchial H^+-ATPase in sub-chronically-exposed trout. Differences in responses of the two ATPase enzymes are likely related to differences in their relative affinities for ATP. For example, if H^+-ATPase had a greater affinity for ATP binding than NKA, it could effectively function at cellular ATP concentrations that affected NKA activity. Knowledge of ATP binding affinities of ATPase enzymes in fish is scarce, but ATP-binding affinities have been well-characterized in other systems. For example, ATP binds NKA with an affinity constant (K_m) of ~200 μM, while the equivalent value for H^+-ATPase is in the range of 8 to 40 μM (Jorgensen and Pedersen 2001; Nakano et al. 2008; Tirtom et al. 2013). Although binding affinity depends significantly on experimental conditions and organism physiology (Antunes et al. 2017), the ATP binding affinities derived for fish NKA are similar to other values in the literature (210 -540 μM; Morrison et al. 2006). Assuming that binding affinities of ATP to H^+-ATPase are also similar, then this suggests that ATP has a greater affinity for H^+-ATPase than for NKA. This would mean that as cellular ATP depletes effects on NKA activity would be observed before H^+-ATPase activity would be impacted, consistent with the patterns observed in the rainbow trout gill in the current study.

As noted above, branchial H^+-ATPase activity was not affected by Tl exposure. In contrast, acute exposure to Tl concentrations of 4200 µg Tl L^{-1} resulted in an increase in renal activity of H^+-ATPase (Figure 7.3c). This effect may also be a consequence of ATP depletion, through effects of Tl on mitochondria. Depletion of ATP by trace metals is known to cause intracellular acidosis (e.g., Pourahmad and O'Brien 2000). In rainbow trout, acidosis results in an increase in H^+-ATPase expression in the kidney (Perry et al. 2000). Therefore, the observed stimulation in renal H^+-ATPase may be a response to a Tl-induced acidosis resulting from cellular ATP depletion. This effect would be transient (Perry et al. 2000), occurring only until acid-base homeostasis was restored, thus explaining why activity of this enzyme was only stimulated after acute exposure

In contrast to the Tl-induced stimulation of H^+-ATPase noted in the kidney after acute exposure, no effects of Tl on branchial H^+-ATPase activity were observed following either acute and sub-chronic Tl exposure (Figure 7.2c and 7.2d). Similarly, the inhibitory effects of Tl exposure on branchial NKA activity were not observed in the kidney. It is known that there are different assortments of ion transporters in the branchial and renal epithelia of trout (see Fig. 7.1), including transporters that are associated with Tl uptake (e.g., NKCC; Sherstobitov et al. 2010). Activities of key enzymes also differ between tissues (NKA ~4-fold higher in gill than kidney, Fig. 7.2; H^+-ATPase up to 126-fold higher in gill than kidney; Fig. 7.3). Such differences may ultimately be responsible for distinct response of the different tissues to Tl exposure. Further research is required to delineate the key factors affecting tissue sensitivity to Tl.

7.4.2. *Thallium effects on the NKCC cotransporter*

The hypothesis in the current study was that disruption of K^+ handling by Tl might directly or indirectly affect NKCC expression. Although changes in NKA and H^+-ATPase were observed, no effects of Tl on NKCC1 expression were seen. However, NKCC1 expression was detected in both gill and kidney tissues. This differs from the suggested pattern of NKCC isoform distribution proposed for rainbow trout. Work by Katoh and colleagues (2008) indicated that only NKCC2 is found in trout kidney. This conclusion was based on the binding of an antibody that recognizes both NKCC1 and NKCC2, but the apical localization of binding was used as evidence to indicate that binding was occurring to the absorptive isoform (i.e., NKCC2) rather than the secretory isoform (i.e., NKCC1). It is therefore possible that the amplification of NKCC1 in the kidney tissue in the current study is a consequence of trapped blood in this tissue, as NKCC is expressed in the erythrocytes of at least some fish species (Berenbrink et al. 2006).

Whether the NKCC1 expression was branchial or erythrocytic, it was clear that Tl had no effect on this endpoint. Previous research has shown that Tl acts as a substrate for NKCC, and its presence does not affect transporter activity (Sherstobitov et al. 2010; Carmosino et al. 2013). In the current study, therefore, any change in NKCC would be anticipated to occur indirectly, a result of changes in electrochemical gradients being driven by effects of Tl on other transporters. Although an inhibition in branchial NKA was observed after sub-chronic exposure, and an acute stimulation in renal H^+-ATPase activity was also seen, in neither of these treatments was there an effect of Tl on NKCC expression. This suggests that any changes in the electrochemical gradient resulting from these effects of Tl could have been compensated by other transporters. For example, changes in NKA activity in hypercapnic fish gill are compensated for by altered expression of the apical Na^+/H^+ exchanger (Deigweiher et al. 2008). However, because gene expression does not always correspond to protein expression or transporter activity (Maier et al.

2009), alternative techniques such as Western blotting would be required to confirm the lack of effect of Tl on NKCC noted in the current study.

7.5. Conclusion

In this chapter Tl was found to inhibit branchial NKA activity following sub-chronic exposure and enhance renal H^+-ATPase activity after an acute exposure. The effect of Tl on NKA activity occurred after exposure to 141 μg L^{-1} Tl, a concentration that can be exceeded in surface waters near base metal mining sites globally (Table 1.1). This study is the first to assess changes in ionoregulatory activity and gene expression following whole animal exposure to waterborne Tl.

8. Effects of Tl on hepatic antioxidant capacity and protein carbonylation in rainbow trout (*Oncorhynchus mykiss)*

8.1. Introduction

Oxidative stress is caused by an imbalance between ROS and cellular antioxidant capacity (Pizzino et al. 2017). In cells, ROS are generated through the interaction of oxygen and electrons that have leaked from the electron transport chain in the mitochondria (Zhao et al. 2019), and include superoxide ($O_2^{\cdot -}$) and hydroxyl ($OH^{\cdot}$) radicals (Tabassum and Jeong 2019). Additionally, ROS can be produced through the Fenton reaction, which involves the oxidation of Fe^{2+} to Fe^{3+} via H_2O_2, creating a hydroxide ion and $OH^{\cdot}$ (Tarfeño-Saldivia et al. 2018). Although ROS are created naturally, exposure to toxicants such as metals can increase ROS production (Lushchak 2011). This increase in ROS can cause the oxidation of proteins (protein carbonylation), DNA, and lipids, and alter cellular redox status (Livingstone 2003). Ultimately, these cellular changes can affect a wide range of physiological processes, including the capacity of an organism to adapt to environmental change and to mitigate infection (Lushchak 2011; Lee et al. 2019).

Within a cell, enzymatic and non-enzymatic antioxidants are important for the mitigation of toxic effects by ROS (see Figure 8.1). Ultimately, antioxidants transform ROS to non-toxic products such as water and oxygen (Cohen and Hochstein 1963), but in so doing can generate reactive intermediates. For example, the enzyme SOD catalyzes the dismutation of O_2^- (Alfonso-Prieto et al. 2009), where two O_2^- and two H^+ molecules react to produce hydrogen peroxide (H_2O_2) and oxygen. To further detoxify the resulting H_2O_2, the enzymatic antioxidants CAT and GPx degrade H_2O_2 to water and oxygen (Alfonso-Prieto et al. 2009), and water and alcohol (Jurković et al. 2008), respectively. Additionally, ROS can be scavenged by non-enzymatic

antioxidants. For example, GSH reduces H_2O_2 resulting in two water molecules and oxidized glutathione (GSSG) (Aquilano et al. 2014). Other non-enzymatic antioxidants include vitamin C and E, and MT (Chiaverini and De Ley 2010; Traber and Stevens 2011). Functionally, vitamin E protects against lipid peroxidation by reducing lipid hydroperoxyl radicals (Etsuo et al. 1982). Oxidized vitamin E is then reduced by vitamin C. Metallothionein effectively scavenges ROS through covalent bonding with the sulfhydryl groups in this cysteine-rich protein (Chiaverini and De Ley 2010).

Exposure to trace metals is associated with the generation of oxidative stress through a number of different mechanisms. For example, as noted above, ROS can be generated by the Fenton reaction. In this scenario, ROS are created by an increase in free cellular Fe, likely via displacement of Fe from cellular binding sites by other trace metals (Tarfeño-Saldivia et al. 2018). Other redox-active trace metals, such as Cu, can also generate ROS through Fenton-like reactions with H_2O_2 (Lloyd and Phillips 1999). The alternative mechanism by which trace metals induce oxidative stress is by interference with antioxidants. This can include binding non-enzymatic antioxidants thereby reducing their capacity to subsequently scavenge ROS (Lushchak 2011), or via inhibition of antioxidant enzymes, impairing their capacity to detoxify ROS (Atli and Canli 2007).

The trace metal Tl has been observed to cause changes consistent with oxidative stress in freshwater organisms. For example, Farag and colleagues (2021) noted a significant decrease in liver CAT and SOD activity following exposure of Nile tilapia to 42 µg Tl L^{-1} (0.2 µM) for 60-d, while zebrafish exposed to 0.1 nM Tl for 96-d exhibited an increase in hepatic SOD activity (Hou et al. 2017). In the freshwater annelid *Tubifex tubifex*, whole-body CAT activity increased following exposure to Tl concentrations of 0.25 µg L^{-1} (0.001µM) and greater for 7 days (Kiliç

and Kiliç 2017). These studies in aquatic biota are generally consistent with work in mammals that show effects of Tl on oxidative stress endpoints (e.g., Kiliç and Kutlu 2010; Villaverde et al. 2004). However, there are distinct differences between studies in terms of the specific effects observed. For example, in the study on Nile tilapia noted above, no effects of Tl on GSH were reported (Farag et al. 2021), while in rats injected with 0.12 mM Tl, a significant decrease in hepatic GSH was measured (Kiliç and Kutlu 2010). The distinct outcomes in studies of antioxidant responses following Tl exposure are likely the result of different exposure Tl concentrations, exposure lengths, test species, and differing antioxidant capacities of the studied tissues.

As mentioned in Chapters 5 and 7, Tl has the potential to disrupt mitochondria due to mimicry of K^+. One of the major functions of K^+ in the mitochondria is to trigger cell signaling cascades that result in increased mitochondrial ROS production, which ultimately facilitates cell growth (Garlid and Paucek 2003). Since mitochondrial K^+ handling is linked to ROS production, and previous studies show that K^+ transport and oxidative stress endpoints are affected by Tl exposure, the current study aims to determine if waterborne Tl exposure causes effects on oxidative stress endpoints in rainbow trout. This species was selected as the study organism because in addition to being an important regulatory model (Dwyer et al. 1995), it is also sensitive to metal ion-mediated oxidative stress (Thorgaard et al. 2002; Arabi and Alaeddini 2005; Shekh et al. 2020). The liver was chosen as the target tissue for investigation as it is known to accumulate Tl (Zitko et al. 1975), it is a tissue that because of its involvement in oxidative metabolism generates significant ROS (Risso-de Faverney et al. 2001), and it displays damage following Tl exposure (Hou et al. 2017). Although several studies have observed the effects of Tl on antioxidant capacity, to date there are limited studies in fish, and none in salmonids. The

current chapter sought to fill this knowledge gap by assessing the effects of sub-chronic and acute Tl exposure on antioxidant capacity (CAT and GPx activity, and total GSH) and oxidative damage (protein carbonylation) in liver of rainbow trout.

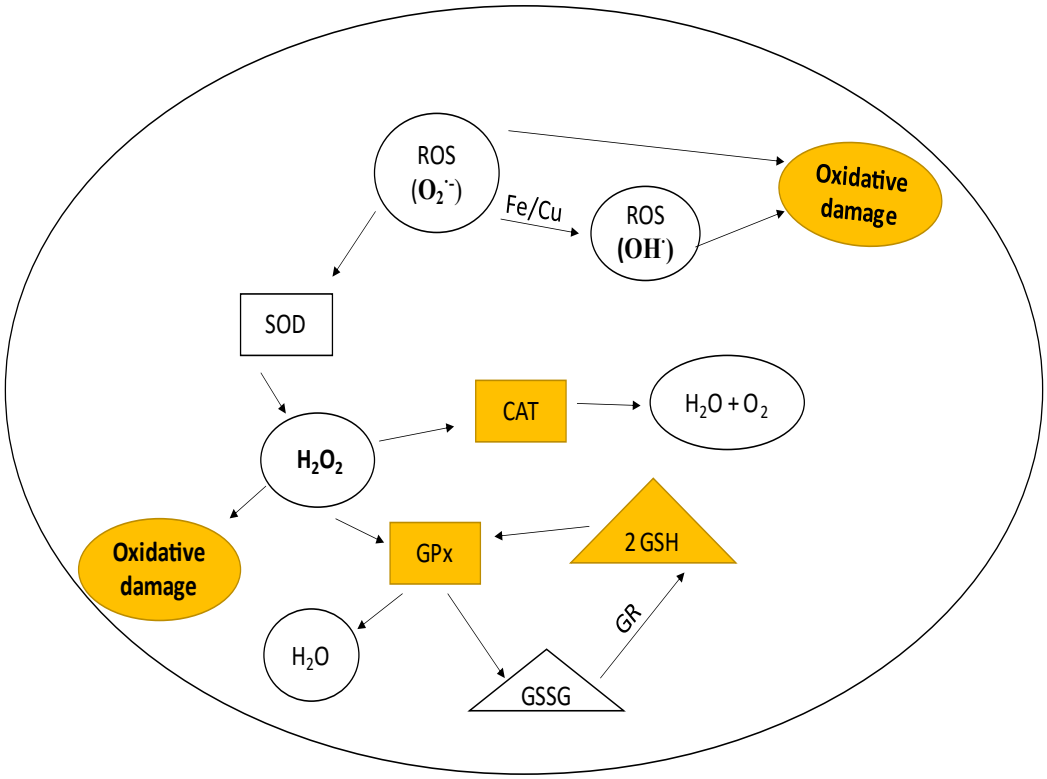

Figure 8.1. A cellular oxidative stress pathway. Antioxidant enzymes are illustrated as boxes and non-enzymatic antioxidants are illustrated as triangles. Components with orange fill are the antioxidants and oxidative stress endpoints that were assessed in this study. Bold text in circles indicates pro-oxidant molecules. In the current study protein carbonylation was used as a marker of oxidative damage. Abbreviations as follows: Reactive oxygen species (ROS), superoxide ($O_2^{\cdot-}$), hydroxide radical ($OH^{\cdot}$), superoxide dismutase (SOD), catalase (CAT), hydrogen peroxide (H_2O_2), glutathione peroxidase (GPx), oxidized glutathione (GSSG), reduced glutathione (GSH), glutathione reductase (GR). This model was adapted from Qu et al. 2014 and Avci et al. 2015.

8.2. Methods

Methodological details regarding experimental animals, exposure design, and water chemistry analysis can be found in Sections 6.2.1 and 6.2.2.

8.2.1. Tissue preparation

Following euthanasia, the whole liver was removed, placed into 1.5 mL Eppendorf tubes and flash frozen in liquid nitrogen. Tissues subjected to oxidative stress endpoint analysis (approximate mass range: 250-500 mg) were homogenized in 1 mL ice cold phosphate buffer saline using a handheld homogenizer and then centrifuged at 5000 g at 4ºC for 3 minutes. The resulting supernatant was then transferred into a new Eppendorf tube and stored at -80 ºC until used in CAT, GPx, GSSG, and protein carbonyl assays.

8.2.2. Catalase

The CAT activity assay was performed as described by Aebi (1984). Briefly, a sub-sample of liver homogenate was taken and diluted up to 100 times to a total volume of 2 mL, to meet working assay conditions that required an initial absorbance reading of ~0.5. The diluted sample was placed into a 3-mL glass cuvette and 1 mL H_2O_2 was added. Absorbance (A_i) was read at 240 nm using an Ultrospec 3000 UV-Visible light spectrophotometer (Pharmacia, Bridgewater, New Jersey, USA). A second reading was taken after 30 s (A_f). To calculate CAT activity, Equation 8.1 was used. The rate constant for CAT activity (2.3) was divided by the length of the assay (30 s) and multiplied by the log of A_i over A_f. Homogenate protein content was measured via Bradford (1976) protein assay and CAT activity was expressed as nmol min^{-1} g $protein^{-1}$.

Equation 8.1:

$$\text{CAT activity} = \left(\frac{\text{Reaction rate}}{\text{time}} * \log\frac{A_i}{A_f} * \text{sample dilution}\right) / \text{g protein}$$

8.2.3. Glutathione peroxidase

A GPx assay kit was purchased from a commercial supplier (Item No. 703102; Cayman Chemical, Ann Arbor, Michigan, USA), which measured activity indirectly by a coupled reaction with glutathione reductase (GR). The assay was initiated by the addition of 20 µL assay buffer, GPx control (bovine erythrocyte GPx), or sample to wells in a 96 well plate. Then each well received 50 µL assay buffer, 50 µL co-substrate mixture (reconstituted GSH and GR), and 50 µL nicotinamide adenine dinucleotide phosphate (NADPH). Twenty µL of cumene hydroperoxide was then added to each well. The plate was read at a wavelength of 340 nm on a VersaMax microplate reader (Molecular Devices, Sunnyvale, California, USA) once every minute for 5 minutes total. Activity was calculated using Equation 8.2. Time 1 and 2 are two points 1 minute apart, which were selected to best represent the linear portion of the curve. $Dilution_f$ represents the total volume per well, and sample V represents the volume of sample per well. The slope of the linear relationship between absorbance and time was divided by the extinction coefficient for NADPH (0.00373 μM^{-1}), and multiplied by the product of total well divided by sample volume. Data were normalized to homogenate protein content following a Bradford assay and final results are reported in nmol min^{-1} g $protein^{-1}$.

Equation 8.2:

$$\text{GPx activity} = \left(\frac{\text{slope}\left(\frac{|A_{340}(\text{Time 2}) - A_{340}(\text{Time 1})|}{\text{Time 2 (min.)} - \text{Time 1 (min.)}}\right)}{\text{extinction coefficient}} * \frac{\text{dilution}_f}{\text{sample V}} * \text{sample dilution} \right) / \text{g protein}$$

8.2.4. *Total glutathione*

A glutathione content assay kit was purchased from a commercial supplier (Item No. 703002; Cayman Chemical, Michigan, USA). Glutathione was quantified using a standard curve generated from a stock solution of 25 µM GSSG in MES buffer (0.4 M 2-(N-morpholino)ethanesulphonic acid, 0.1 M phosphate, 2 mM EDTA, pH 6.0.). The assay was

conducted by the initial addition of 50 µL of GSSG standard (0, 0.5, 1, 2, 4, 8, 12, or 16 µM), or sample, to wells in a 96 well plate. Then each well received 150 µL of assay cocktail that contained MES buffer, high-performance liquid chromatography grade water, reconstituted cofactor ($NADP^+$ and glucose-6-phosphate), GSH enzyme mixture (GR and glucose-6-dehydrogenase) and Ellman's reagent (5,5-dithio-bis-(2-nitrobenzoic acid); DTNB). Immediately following the addition of assay cocktail, the plate was covered to exclude light and placed on an orbital shaker for 25 minutes. After the incubation period the plate was read at a wavelength of 405 nm on a microplate reader. Glutathione content was calculated from the standard curve and normalized to homogenate protein content via Bradford assay. Final GSSG concentrations are reported as µmol g $protein^{-1}$.

8.2.5. *Protein carbonylation*

A protein carbonyl colorimetric assay kit was purchased from a commercial supplier (Item No. 100005020; Cayman Chemical, Michigan, USA). Carbonyl content was measured through the reaction of carbonyl moieties with 2,4-dinitrophenylhydrazine (DNPH). The assay was conducted by transferring 200 µL of sample into two separate Eppendorf tubes, one designated the sample, the other control. Then 800 µL of 2.5 M DNPH was added to the sample tube and 800 µL 2.5 M HCl to the control tube. Tubes were then incubated for 1-h in the dark with a brief vortex every 15 minutes. After incubation, 1 mL of 20% trichloroacetic acid (TCA) solution was added to each tube, vortexed and placed on ice for 15 minutes. Both control and sample tubes were then centrifuged at 10000 g for 10 minutes at 4°C. The supernatant was discarded and the remaining pellet was resuspended and washed in 1 mL of 1:1 ethanol/ethyl acetate. The pellets were centrifuged again at 10000 g for 10 minutes at 4°C, and this step was repeated two more times. Following the final wash, the pellets were resuspended in 500 µL

guanidine hydrochloride, vortexed and centrifuged once more under the same settings. To measure the carbonyl concentration, 220 µL of sample/control were added to a 96 well microplate and read at 360 nm on a microplate reader. Carbonyl content was calculated using Equation 8.3 and normalized by protein content.

Equation 8.3:

$$\text{Protein carbonyl content} = \left(\left[\frac{(\text{sample absorbance-control absorbance})}{\text{extinction coefficient DNPH}(0.011)} \right] * \frac{\text{dilution}_f}{\text{sample V}} \right) / \text{g protein}$$

8.2.6. *Statistics*

Details of statistical analysis can be found in Section 6.2.6. Following analysis, a single outlier was removed from the acute protein carbonyl dataset (at the 0 µg L^{-1} exposure concentration), and 1 outlier was removed from acute GSSG replicates (at 2004 µg L^{-1}). One outlier was removed from the acute CAT dataset (at 2004 µg L^{-1}) and two from the acute GPx dataset (one each at 0.9 and 2004 µg L^{-1}).

8.3. Results

8.3.1. *Antioxidant capacity*

No significant differences in hepatic CAT activity were observed following acute (P-$value_{Kruskal\text{-}Wallis}$: 0.450, Figure 8.2a) or sub-chronic (P-$value_{Kruskal\text{-}Wallis}$: 0.955, Figure 8.2b) exposures of rainbow trout to Tl. Glutathione peroxidase activity was also not statistically different in acute (P-$value_{Kruskal\text{-}Wallis}$: 0.265, Figure 8.3a) or sub-chronic (P-$value_{Kruskal\text{-}Wallis}$: 0.711, Figure 8.3b) Tl exposures. Following a Kruskal-Wallis test, no significant differences were observed in total glutathione concentration in either the acute (P-$value_{Kruskal\text{-}Wallis}$: 0.737, Figure 8.4a) or sub-chronic (P-$value_{Kruskal\text{-}Wallis}$ 0.938, Figure 8.4b) Tl exposure treatments.

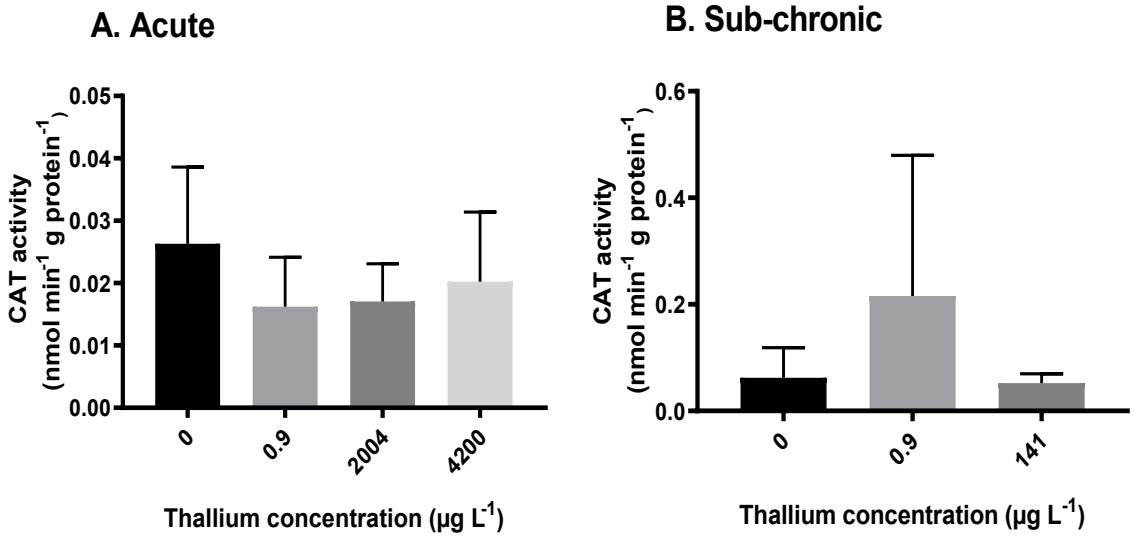

Figure 8.2. Catalase activity in rainbow trout liver tissue following acute 96-h (A) and sub-chronic 28-d (B) Tl exposure. Plotted points represent means (± standard deviation) of 7-8 replicates.

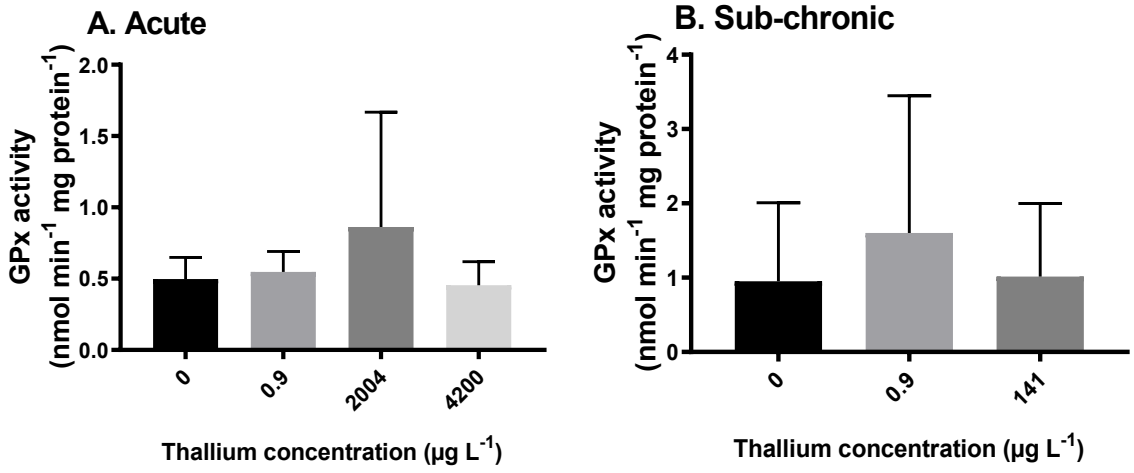

Figure 8.3. Glutathione peroxidase activity for rainbow trout liver tissue following acute 96-h (A) and sub-chronic 28-d (B) Tl exposure. Plotted points represent means (± standard deviation) of 6-8 replicates.

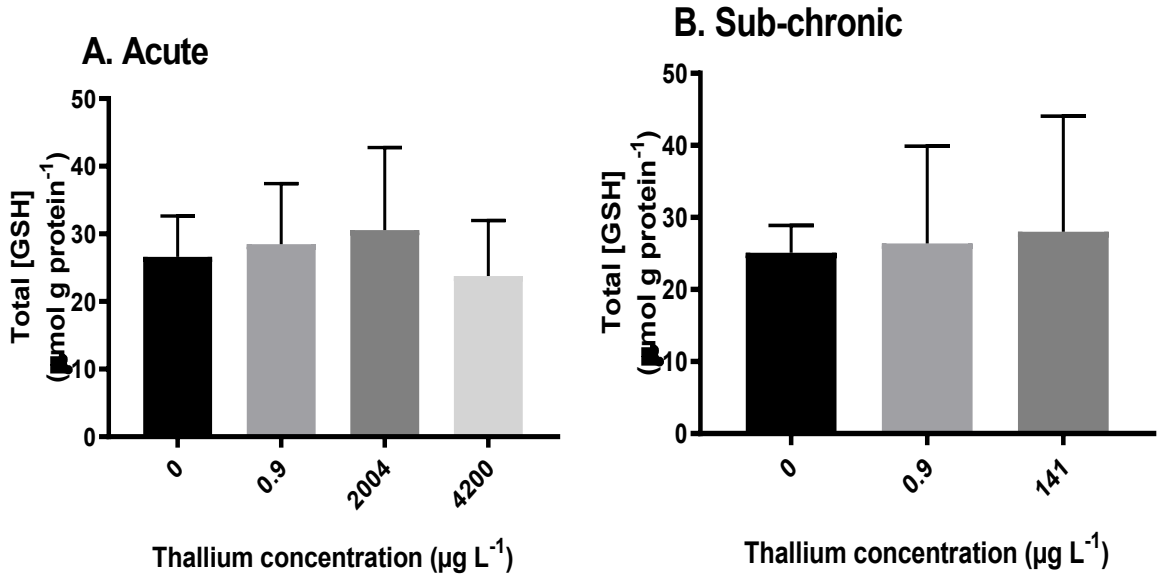

Figure 8.4. Total glutathione concentration for rainbow trout liver tissue following acute 96-h (A) and sub-chronic 28-d (B) Tl exposure. Plotted points represent means (± standard deviation) of 7-8 replicates.

8.3.2. *Protein carbonylation*

No significant differences were observed in protein carbonyl content in juvenile rainbow trout liver following acute 96-h Tl exposures ($P\text{-value}_{ANOVA}$: 0.462, Figure 8.5a). In sub-chronic exposures no significance in protein carbonyl content were observed in Tl-treated fish compared to controls ($P\text{-value}_{ANOVA}$: 0.218, Figure 8.5b).

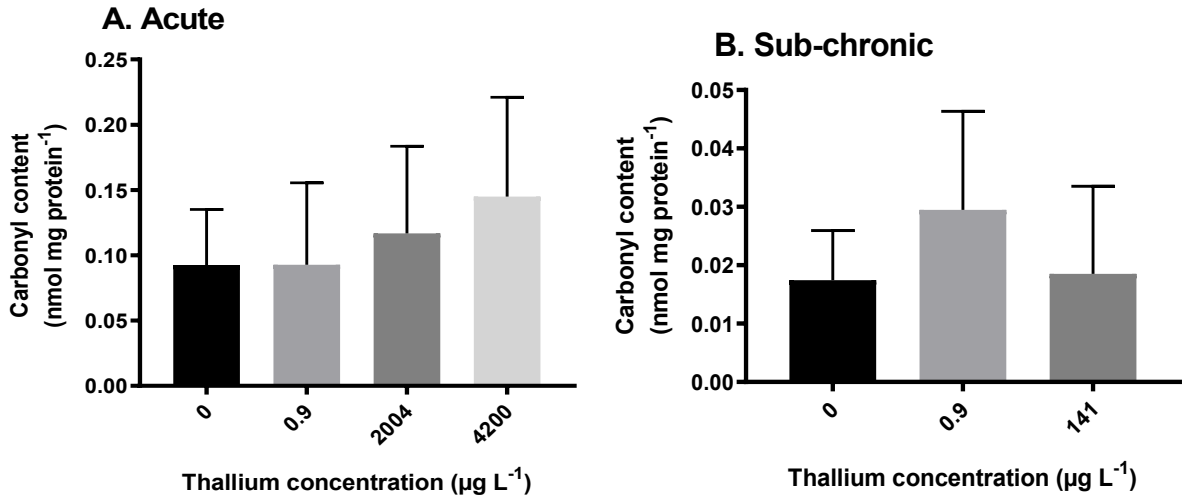

Figure 8.5. Protein carbonyl content for rainbow trout liver tissue following acute 96-h (A) and sub-chronic 28-d (B) Tl exposure. Plotted points represent means (± standard deviation) of 7-8 replicates.

8.4. Discussion

8.4.1. *Effects of thallium on antioxidant capacity*

There were no significant changes in any measured antioxidant endpoint following the exposure of rainbow trout to waterborne Tl, either acutely (96-h) or sub-chronically (28-d) (Figures 8.2-8.4). Although Tl can influence the activity of CAT, GPx, and the concentration of GSH in different tissues across several phyla (Babić et al. 2009; Osorio-Rico et al. 2015; Kiliç and Kiliç 2017), its effect on antioxidant capacity is not consistent.

A study by Babić and colleagues (2009) observed a decrease in CAT activity in the aquatic plant *Lemna minor* following exposure to 400 µg L^{-1} (2 µM) Tl for 14-d, a finding supported by Farag and colleagues (2021) who showed waterborne exposure to 42 µg L^{-1} (0.2 µM) Tl decreased CAT activity in liver of Nile tilapia. Conversely, CAT activity was found to increase in whole-body samples of *Tubifex* following a 7-d exposure to 0.25 µg L^{-1} (1.2 nM) Tl

(Kiliç and Kiliç 2017). Decreases in CAT activity have been attributed to inhibition of the enzyme by Tl (Babić et al. 2009), whereas increases in activity are likely to represent induction in response to enhanced ROS generation or deficits in other ROS scavenging mechanisms (Kiliç and Kiliç 2017). In the current work no changes in CAT were observed, suggesting Tl does not affect ROS generation or antioxidant capacity, or that any such effects offset. Because of the variability in literature studies of Tl toxicity (e.g., in terms of factors such as exposure concentrations, species and exposure duration), comparison of effects between studies are difficult. Nevertheless, the different responses of CAT to Tl exposure across studies is similar to the patterns observed for other trace metals on this endpoint. For example, in galaxiid fish Zn exposure increases hepatic CAT activity (McRae et al. 2016), but in killifish Zn causes the opposite effect (Loro et al. 2012). In galaxiid fish exposed to waterborne Cd, liver CAT activity decreased (McRae et al. 2018), but exposure of mosquitofish to Cd induces CAT activity (Nunes et al. 2015). Further work is required to delineate the specific factors responsible for the distinct patterns of CAT activity following Tl exposure. However, measures of tissue burdens may be informative as some studies in fish have suggested that effects on CAT are related to the extent of trace metal accumulation (McRae et al. 2018).

Similar to the pattern observed for CAT, no significant differences in GPx activity were observed in rainbow trout liver following waterborne Tl exposure. This finding is also similar to results reported for rats 24-h post injection of 39 mg L^{-1} (190 µM) Tl. In that study, no changes in GPx activity in the brain were observed (Osorio-Rico et al. 2015). In contrast, GPx activity was found to be a highly sensitive and responsive endpoint following the exposure of *Tubifex* to Tl. A 7-day exposure to 0.5 µg L^{-1} (2 nM) Tl caused an increase in GPx activity (Kiliç and Kiliç 2017), but at a slightly higher Tl concentration of 1 µg L^{-1} (5 nM), over a more prolonged

exposure period (15-d), GPx activity significantly decreased. Exposure concentrations of Tl in the presented data (4200 μg L^{-1}; 21 μM) are markedly greater than the concentrations used in Kiliç and Kiliç (2017), and thus might be expected to have induced a response. The lack of response in GPx activity in rainbow trout may reflect the greater tolerance of this species to Tl. For example, 96-h LC_{50} values for waterborne Tl in rainbow trout are 4.3 mg L^{-1} (Pickard et al. 2001), several orders of magnitude greater (i.e., more tolerant) than the equivalent values for *Tubifex* (0.018 mg Tl L^{-1}; Kiliç et al. 2011). The mechanisms underlying the differences in sensitivity are not known, however smaller animals are considered more vulnerable to toxicants that enact effects through disruption of ion handling (Grosell et al. 2002). This is a function of higher ion turnover rates and a lesser capacity to buffer against ion loss. If effects of Tl on oxidative stress are mediated through disruption of K^+ homeostasis, then this could explain the lack of impact of Tl in rainbow trout versus the much smaller *Tubifex*.

Inconsistent effects of Tl on non-enzymatic antioxidant capacity have also been observed. In the current study there were no significant changes in total GSH concentration between treatment groups (see Figure 8.4a-b). Similarly, in rats injected with 20 mg L^{-1} (100 μM) Tl, no significant changes in kidney GSH occurred after 48-h (Appenroth and Winnefeld 1999). However, this study contrasts with other results for the effects of Tl exposure on rat kidney. For example, an intraperitoneal dose of 16 mg kg^{-1} Tl resulted in a significant decrease in renal GSH after 5-d (Anaya-Ramos et al. 2021). Effects of Tl on GSH have also been observed in rat brain, where an intraperitoneal dose of 32 mg kg^{-1} resulted in an increase in hypothalamus GSH after 24-h (Osorio-Rico et al. 2015). It is possible the lack of effect of Tl on antioxidant capacity in rainbow trout is the result of basal concentrations of antioxidants in liver tissue being greater than in measured tissues in other studies. For example, total GSH concentration in control

rainbow trout was 27 μmol g^{-1}. In rat brains, where Tl exposure significantly increased GSH, the mean concentration of GSH was approximately 2 μmol g^{-1} (Osorio-Rico et al. 2015), while basal GSH concentrations in the study of Anaya-Ramos and colleagues (2021) conducted in rat kidney were ~1.2 μmol g^{-1}. However, this correlation is not perfect as similar concentrations of GSH are reported in other brain regions (Osorio and Rice et al. 2015) and in other rat kidney studies (Appenroth and Winnefield 1999), where there was no change in GSH recorded upon Tl exposure.

In the current study none of the measured antioxidant endpoints were affected by Tl exposure, despite Tl exposure concentrations higher than those that cause changes in antioxidant profiles in other studies. Since only a selection of antioxidants was examined, it is possible that changes may have occurred in antioxidants that were not assessed. For example SOD, which is one of the first defense mechanisms against ROS (Figure 8.1), is known to be sensitive to Tl exposure (Babić et al. 2009; Kiliç and Kutlu 2010; Hou et al. 2017; Farag et al. 2021; Varão et al. 2021). However, if SOD activity increased this would be likely to increase H_2O_2 production, which in turn would be expected to increase CAT and GPx activity. Indeed, linkages between different components of the antioxidant defenses have been observed upon Tl exposure, with reductions in SOD activity associated with similar changes in CAT in Tl-exposed tilapia (Farag et al. 2021). Therefore, the lack of change in CAT activity suggests that SOD activity was also likely to be unaffected by the Tl exposure regimes in the current study. Similarly, activity of the important antioxidant enzyme GR (see Fig. 8.1) tends to be linked to activity of GPx (Villaverde et al. 2004; Couto et al. 2016). The lack of change in hepatic GPx upon Tl exposure in rainbow trout thus argues against an unmeasured change in GR.

A further possibility is that antioxidants not associated with the pathways described in Figure 8.1 were altered. Metallothionein, in addition to binding trace metals, is also known to be an effective cellular scavenger of ROS (Chiaverini and De Ley 2010; Hauser-Davis et al. 2014). Studies have indicated that MT protects against Tl-induced oxidative stress in mammal models, and prevents changes in other antioxidant pathways (Kiliç and Kutlu 2010; Anaya-Ramos et al. 2021). Similar roles have been noted for vitamin E in Zn-induced oxidative stress in fish (Alkaladi 2019). There is also evidence that vitamin E and C are protective against Tl-induced nephrotoxicity in rats, although this effect could not be attributed specifically to roles of these vitamins as antioxidants (Appenroth and Winnefeld 1998). Work assessing the protective effects of vitamin E and C, and MT on Tl-induced oxidative stress is needed to confirm roles for these antioxidants in protecting against Tl toxicity in rainbow trout.

8.4.2. *Effects of thallium on protein carbonylation*

In the presented work, protein carbonyl content was used as an indicator of protein damage following exposure to Tl. Protein damage results from the oxidation of protein by ROS, and can result in loss or modification of protein function, and cellular death (Sitte 2003; Pickering and Davies 2013). In the current study, no significant changes in protein carbonyl content were observed in trout acutely or sub-chronically exposed to Tl (Figure 8.5a-b). Given the lack of effect of Tl exposure on antioxidant capacity, this outcome is perhaps not surprising. These data suggest that either Tl is not generating significant ROS in the liver, or the basal levels of antioxidants in the liver are sufficiently high to transform ROS without any induction in enzyme activity or depletion in GSH occurring. Protein carbonylation following Tl exposure has, however, been shown previously. In a study by Radić and colleagues (2009), increased protein carbonylation was shown in broad bean (*Vicia faba)* exposed to waterborne Tl at concentrations

of 1 mg Tl L^{-1} (5 µM) and higher. Thallium has also been observed to affect other oxidative damage endpoints. For example, induction of lipid peroxidation occurred in the brains of rats exposed to 1.6 mg kg^{-1} (8 µmol kg^{-1}) Tl (Galván-Arzate et al. 2000). While it is clear that Tl can induce oxidative stress, these effects may be more common in tissues where basal concentrations of antioxidants are lower.

8.5. Conclusion

In this study Tl exposure did not result in significant effects on antioxidant capacity and protein damage in livers of rainbow trout. This is despite exposure concentrations in the acute and sub-chronic experiments being greater than those of other studies that had observed changes in antioxidant capacity (Hou et al. 2017; Kiliç and Kiliç 2017). The mechanisms underlying this lack of effect are unknown, but under these exposure conditions oxidative stress is not a significant mechanism of Tl toxicity in the liver of rainbow trout.

9. General Conclusion

9.1. Significant findings

The main objective of this thesis was to develop a greater understanding of the interactions between waterborne Tl and aquatic animals, with respect to bioavailability, bioaccumulation and mechanisms of toxicity. The goal was to provide data that could support future risk assessment for Tl in freshwater environments. Below, the key research outcomes are identified and briefly described.

In Chapter 2, AF4 analysis was used to provide experimental evidence that the major species of Tl in natural waters is likely to be the free ion (Tl^+), and that Tl(I) does not readily form complexes with dissolved ligands such as DOM. This confirmed the outcomes of biogeochemical modelling. As ionic metal species are those considered most bioavailable (Bury et al. 2003), this also provided an explanation for the high bioaccumulation of Tl noted later in Chapter 6 of the thesis. Importantly, this finding will greatly simplify site-specific risk assessments of Tl in natural waters in that DOC can largely be ignored as a measured variable.

The other major finding of the thesis with respect to the effect of water chemistry on Tl toxicity, is that water K^+ is clearly protective against Tl-induced mortality in daphnids (Chapters 2, 5). Mechanistically, evidence supporting a role for Tl in disruption of K^+ homeostasis was equivocal. In particular, effects on whole-body K^+ depended on the length of the exposure to Tl. This suggests that daphnids have the capacity to compensate for Tl-induced impairment at a whole-body level, and that may mask tissue level effects of Tl in the nervous system that may drive toxicity. Evidence for a neurological effect of Tl on *D. magna* was provided in Chapter 4, which showed that Tl affects the sensory component of the phototactic response. Ultimately, a K^+:Tl ratio of 6:1 was shown to be effective in protecting against Tl mortality (Chapter 5). Given

the concentrations of K^+ in natural waters, only in highly impacted waters would Tl be likely to reach concentrations where K^+ would not protect against toxicity.

A significant finding from this thesis was that, overall, *D. magna* and rainbow trout are not highly sensitivity to Tl toxicity. This conclusion is based on comparison of Tl toxicity to the toxicity of other trace metals to daphnids, the relative lack of sub-lethal Tl toxicity to rainbow trout, and the high toxicity of Tl to humans. First, Figure 9.1 shows that Tl is less toxic to *Daphnia* than trace metals such as Hg, Ag, Cd, and Cu, with a species mean acute value calculated at 1480 μg L^{-1}. Second, Chapter 7 and 8 show that even at very high acute Tl exposures, or 28-d sub-chronic exposures to Tl at elevated environmental concentrations, relatively minor changes in activity of ionoregulatory enzymes and no effects on oxidative stress were measured in rainbow trout. Third, in humans Tl is considered among the most toxic of all trace metals, with significantly higher toxicity for Tl than other trace elements such as Cd and Hg (Cheam 2001; Virarghavan and Srinivasan 2001; Peter and Viraghavan 2004). This is the opposite of the relative toxicities observed for daphnids. Together, these three lines of evidence support the concept that Tl toxicity to aquatic biota is relatively low. However, there is still risk associated with waters elevated in Tl, such as those contaminated by base metal mine tailing leachates, where Tl can accumulate to concentrations in the high μg L^{-1} to mg L^{-1} range (Table 1.2).

Although this study focused on Tl toxicity in the context of regulations for the protection of aquatic animal health, a key finding was the high bioaccumulation of Tl in fish muscle tissue. In fact, accounting for fish consumption rates, and ADI values proposed by the USEPA, the muscle Tl concentration in fish could reach levels that may cause harm to human populations. Further work would be required to identify the threshold water Tl concentration at which fish

muscle reaches a critical concentration, and therefore to identify waters that may represent a human health risk.

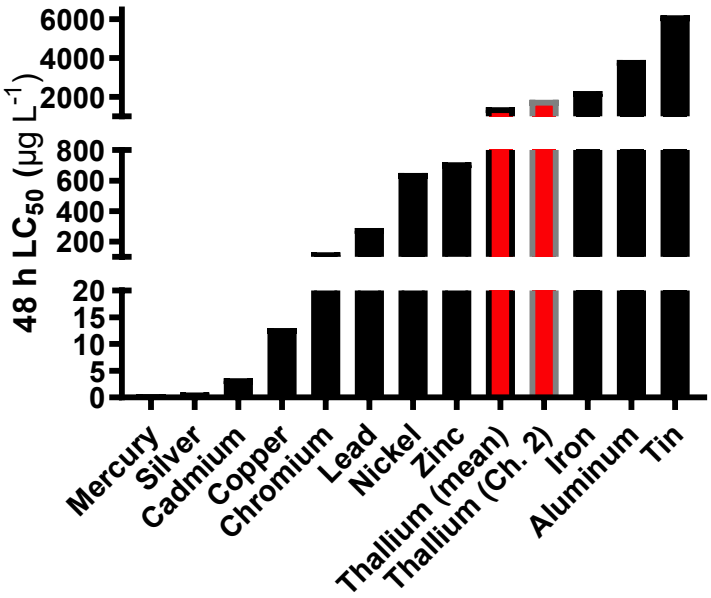

Figure 9.1. Acute toxicity of metals to *Daphnia magna.* Median lethal toxicity values for metals with black bars were compiled from Okamoto et al. (2015). Thallium (Ch. 2; red bar, grey border) depicts data from Chapter 2 of this thesis. Thallium (mean; red bar, black border) shows the mean Tl LC_{50} based published values (Pickard et al. 2001; Lin et al. 2005; Okamoto et al. 2015; Chapter 2).

9.2. Environmental and regulatory considerations

A key finding of this thesis is that the K^+ concentrations of most natural waters are likely to protect aquatic animals against any toxic effects of Tl. This is largely a consequence of the fact that the dominant form of Tl in most waters is Tl(I), which shares pathways of uptake with K^+, and this the presence of K^+ reduces Tl bioaccumulation and/or toxicity (see Chapters 2, 5). The exception to this scenario is waters that are highly elevated in Tl, where the capacity of water K^+

to ameliorate Tl uptake and toxicity is likely reduced. The highest risks are represented by low-flow waters receiving base metal mine effluents. However, it should be highlighted that such effluents will contain other toxic components such as the trace elements As, Cu, Zn, Pb and other toxicants such as ammonia, and perhaps, cyanide (Environment Canada 2012). These constituents may prove to be more toxic than the Tl associated with such effluents.

This thesis exclusively focused on waterborne Tl. However, in natural settings animals will also be exposed to Tl through the diet. In general, dietary metals are less bioavailable than waterborne metals, due to factors such as metal chelation by dietary constituents, mucus production, and sloughing of gut epithelial cells (DeForest and Meyer 2015). Consequently, dietary Tl is likely to have less toxicological impact than waterborne Tl. The few studies to date that have examined the relative contributions of diet and water to Tl handling indicate that waterborne route is more important than the dietborne route. For example, in a marine snail 20 times as much Tl was taken up from the water than from a Tl-contaminated diet (Turner and Pilsbury 2013). Studies in fish early life-stages note a similar effect, but of a lesser magnitude (Lapointe and Couture 2010), possibly a consequence of a relatively poor dietary assimilation efficiency for Tl (~35%; Lapointe and Couture 2009). Despite this, sublethal effects of dietary Tl have been observed in fish, with decreased glutathione-S-transferase and nucleoside diphosphate kinase activities observed in fathead minnows feeding on Tl-contaminated *D. magna* (Lapointe et al. 2009). These findings do indicate that although dietary Tl may be less bioavailable, it has the potential to exert toxic effects, and this may ultimately affect sensitivity to Tl in natural settings.

This thesis highlights a number of important considerations from a regulatory perspective. For example, it is likely that the current CCME guideline value of 0.8 $\mu g\ L^{-1}$, which is largely

derived from data in the aquatic plant *L. minor* is likely to also be protective of aquatic animals. Additionally, in terms of site-specific field assessment of toxicity, there is limited need or value in developing a BLM for Tl. Certainly, measurements of DOC which can be cost- and time-intensive are of limited importance given its poor affinity for Tl binding. Instead, toxicity assessment could be based solely on measures of dissolved Tl and K^+, noting the caveat above regarding the possible influence of dietary Tl.

9.3. Future studies

In this thesis the main focus was on Tl(I), largely because this is the form of Tl that dominates most freshwaters. However, under some environmental conditions Tl(III) may be present. This form of Tl is more reactive with environmental ligands (Wade and Banister 1973), and studies indicate that it has a markedly greater toxicity to aquatic biota (e.g., Rickwood et al. 2015; Molina et al. 2017). Some researchers have studied Tl(III) toxicity by oxidizing Tl(I) through ultraviolet light, and coupling this reaction to an electron acceptor to maintain oxidation state (Campanella et al. 2018). As such studies such as those in Chapters 2 and 3 could be repeated with Tl(III) to obtain a more complete perspective of Tl toxicity by accounting for those environments in which Tl(III) may occur.

One of the key assumptions in this thesis is that intracellular Tl remains unliganded and as such behaves similarly to, and interferes with, K^+. In Chapter 2 only a small number of organic ligands were examined for their effect on Tl speciation, but from that study it was theorized that Tl is generally resistant to complexation. However, it is possible that within the cell there are ligands that might bind Tl, and effectively diminish its bioreactivity. Future work could test this hypothesis. Specifically, techniques such as X-ray differential absorption-edge computed microtomography, micro-X-ray absorption near edge (mu-XANES) and micro-X-ray

fluorescence (mu-XRF) could be used to assess the speciation of Tl inside tissues of rainbow trout and *D. magna*, providing insight into subcellular speciation, compartmentalization, and the interactions between Tl and mitochondria. Such techniques have been successfully used to assess Tl speciation and distribution in plant tissues (Scheckel et al., 2004; 2007).

One common theme in the current thesis was the potential for Tl toxicity to be mediated by its effects on mitochondria. For example, the inhibition of NKA activity was proposed to be mediated by the cellular depletion of ATP, a consequence of Tl accumulation and toxicity in mitochondria (Chapter 7). However, in the current work effects of Tl on mitochondrial function were not specifically examined. This would, therefore, be an interesting focus of future studies. Of particular interest would be the effects of Tl on chloride cells in the gills of fish. These cells perform much of the active ion transport associated with salt and water homeostasis, and because of the large energetic demand of these processes, are packed with mitochondria (Evans et al. 1999). Future studies could take advantage of techniques that facilitate isolation, and subsequent enrichment of chloride cells (e.g., Goss et al. 2011), allowing examination of cellular energy equivalents (Morciano et al. 2020) in the presence of Tl. Future work could also look to isolate mitochondria themselves (e.g., Liao et al. 2020), and examine functional changes in response to Tl. This is an approach that has been used successfully to measure the effects of temperature acclimation and hypoxia on mitochondrial function in fish (e.g., Iftikar et al. 2015; Devaux et al. 2019). Organelle and cellular isolation may also facilitate a more nuanced examination of the Tl/K^+ interaction in cells, removing the complications associated with processes such as cross-epithelial feedback that may have obscured identification of Tl/K^+ interactions in the current study, which relied on whole-animal techniques. These approaches could be combined with flow cytometry to allow detection of oxidative stress markers, such as the production of H_2O_2 (De

Biasi et al. 2016). This would facilitate further interrogation of the conclusions of Chapter 8, which suggested oxidative stress is not a mechanism of waterborne Tl toxicity in rainbow trout.

Alternatively, techniques such as the scanning ion-selective electrode technique (SIET) may have significant application for the understanding of Tl transport across intact epithelia of *D. magna*. This is an approach that allows ion fluxes to be measured in intact animals/tissues, and recently has been successfully used to characterize ion transport across the nuchal organ in daphnids (Morris and O'Donnell 2019). This technique could facilitate direct measurement of K^+ exchanges in the presence of Tl, and provide evidence to support the efficacy of pharmacological agents used in Chapter 5 to help characterize pathways of K^+/Tl^+ uptake. This would provide significant clarity in a study system where the current data is sometimes contradictory and difficult to interpret.

Finally, this study provided some support for the development of advanced regulatory tools for the assessment of Tl risk in freshwater settings. For example, laboratory manipulation of water chemistry showed that water K^+ is a factor that strongly influences Tl toxicity (Chapter 2, 5). This is a factor that could be incorporated into risk assessment tools such as the BLM. However, evidence was also provided that showed some of the toxic endpoints altered by Tl exposure were not correlated to tissue Tl burden (e.g., NKA activity; Chapter 7). Consequently, further studies that relate short-term Tl accumulation to Tl toxicity would be required to determine whether this important principle of the BLM (Niyogi and Wood 2004) is applicable to Tl risk in fresh waters.

Bibliography

Abdollahi M, Dehpour A, Baharnouri G. 1998. Effects of rubidium on the secretory function of the rat submandibular gland. Toxic Substance Mechanisms 17: 121-131.

Adam C, Garnier-Laplace J, Baudin JP. 2001. Bioaccumulation of ^{110M}Ag, ^{60}Co, ^{137}Cs and ^{54}Mn by the freshwater crustacean *Daphnia magna* from dietary sources (*Scenedesmus obliquus* and *Cyclotella meneghiana*). Water, Air and Soil Pollution 136: 125-146.

Adams SM, Crumby WD, Greeley Jr MS, Ryon MG, Schilling EM. 1992. Relationships between physiological and fish population responses in a contaminated stream. Environmental Toxicology and Chemistry 11: 1549-1557.

Aebi H. 1984. Catalase in vitro. Methods in Enzymology 105: 121-126.

Agency for Toxic Substances and Disease Registry (ATSDR). 1992. Toxicological Profile for Thallium. U.S. Department of Health and Services, Public Health Service, Atlanta, GA, USA, pp 1-90.

Aladin NV, Potts WTW. 1995. Osmoregulatory capacity of the Cladocera. Journal of Comparative Physiology B- Biochemical, Systemic and Environmental Physiology 164: 671-683.

Alfonso-Prieto M, Biarnés X, Vidossich P, Rovira C. 2009. The molecular mechanism of the catalase reaction. Journal of the American Chemical Society 131: 11751-11761.

Ali H, Khan E. 2019. Trophic transfer, bioaccumulation, and biomagnification of non-essential hazardous heavy metals and metalloids in food chains/webs: Concepts and implications for wildlife and human health. Human and Ecological Risk Assessment 25: 1353-1376.

Alkaladi A. 2019. Vitamins E and C ameliorate the oxidative stress induced by zinc oxide nanoparticles on liver and gill of *Oreochromis niloticus*. Saudi Journal of Biological Sciences 26: 357-362.

Anaya-Ramos L, Díaz-Ruíz A, Ríos C, Mendez-Armenta M, Montes S, Aguirre-Vidal Y, García-Jiménez S, Baron-Flores V, Monroy-Noyola A. 2021. The acute systemic toxicity of thallium in rats produces oxidative stress: Attenuation by metallothionein and Prussian blue. Biometals 34: 1295-1311.

Anderson BG. 1950. The apparent thresholds of toxicity to *Daphnia magna* for chlorides of various metals when added to Lake Erie water. Transactions of the American Fisheries Society 78: 96-113.

Ankley GT, Bennett RS, Erickson RJ, Hoff DJ, Hornung MW, Johnson RD, Mount DR, Nichols JW, Russom CL, Schmieder PK, Serrano JA, Tietge JE, Villeneuve DL. 2010. Adverse outcome pathways: A conceptual framework to support ecotoxicology research and risk assessment. Environmental Toxicology and Chemistry 29: 730-741.

Antunes CD, Lucena MN, Garçon DP, Leone FA, McNamara JC. 2017. Low salinity-induced alterations in epithelial ultrastructure, Na^+/K^+-ATPase immunolocalization and enzyme kinetic characteristics in the gills of the thinstripe hermit crab, *Clibanarius vittatus* (Anomura, Diogenidae). Journal of Experimental Zoology- Part A: Ecological and Integrative Physiology 327: 380-397.

Appenroth D, Gambaryan S, Winnefeld K, Leiterer M, Fleck C, Bräunlich H. 1995. Functional and morphological aspects of thallium-induced nephrotoxicity in rats. Toxicology 96: 203-215.

Appenroth D, Winnefeld K. 1998. Vitamin E and C in the prevention of metal nephrotoxicity in developing rats. Experimental and Toxicologic Pathology 50: 391-396.

Appenroth D, Winnefeld K. 1999. Is thallium-induced nephrotoxicity in rats connected with riboflavin and/or GSH? Reconsideration of hypotheses on the mechanism of thallium toxicity. Journal of Applied Toxicology 19: 61-66.

Aquilano K, Baldelli S, Ciriolo MR. 2014. Glutathione: new roles in redox signaling for an old antioxidant. Frontiers in Pharmacology 26: 196.

Arabi M, Alaeddini MA. 2005. Metal-ion-mediated oxidative stress in gill homogenate of rainbow trout (*Oncorhynchus mykiss)*: Antioxidant potential of manganese, selenium, and albumin. Biological Trace Element Research 108: 155-168.

Arai T, Ohji M, Hirata T. 2007. Trace metal deposition in teleost fish otolith as an environmental indicator. Water, Air, and Soil Pollution 179: 255-263.

Atli G, Canli M. 2007. Enzymatic responses to metal exposures in a freshwater fish *Oreochromis niloticus*. Comparative Biochemistry and Physiology- Part C: Toxicology & Pharmacology 145: 282-287.

Avci A, Kaçmaz M, Durak I. 2005. Peroxidation in muscle and liver tissues from fish in a contaminated river due to petroleum refinery industry. Ecotoxicology and Environmental Safety 60: 101-105.

Babić M, Radić S, Cvjetko P, Roje V, Pevalek-Kozlina B, Pavlica M. 2009. Antioxidative response of *Lemna minor* plants exposed to thallium(I) acetate. Aquatic Botany 97: 166-172.

Bačeva K, Stafilov T, Šajn R, Tănăselia C, Makreski P. 2014. Distribution of chemical elements in soil and stream sediments in the area of abandoned Sb-As-Tl Allchar mine, Republic of Macedonia. Environmental Research 133: 77-89.

Baes CF, Mesmer RS. 1976. The Hydrolysis of Cations. John Wiley and Sons, New York, NY, USA, pp 328-335.

Baillieul M, Smolders R, Blust R. 2005. The effect of environmental stress on absolute and mass-specific scope for growth in *Daphnia magna* Straus. Comparative Biochemistry and Physiology- Part C: Toxicology & Pharmacology 140: 364-373.

Banci L, Bertini I, Ciofi-Baffoni S, Kozyreva T, Zovo K, Palumaa P. 2010. Affinity gradients drive copper to cellular destinations. Nature 465: 645-648.

Barata C, Alañon P, Gutierrez-Alonso S, Riva MC, Fernández C, Tarazona JV. 2008. A *Daphnia magna* feeding bioassay as a cost effective and ecological relevant sublethal toxicity test for environmental risk assessment of toxic effluents. Science of the Total Environment 405: 78-86.

Barón-Jaimez J, Joya MR, Barba-Ortega J. 2013. Anodic stripping voltammetry- ASV for determination of heavy metals. Journal of Physics: Conference Series 466: 012023.

Barrera H, Gómez-Puyou A. 1975. Characteristics of the movement of K^+ across the mitochondrial membrane and the inhibitory action of Tl^+. Journal of Biological Chemistry 250: 5370-5374.

Barron MG, Anderson MJ, Lipton J, Dixon DG. 1997. Evaluation of critical body residue QSARs for prediction of organic chemical toxicity to aquatic organisms. SAR and QSAR in Environmental Research 6: 47-62.

Barroso-Moguel R, Villeda-Hernández J, Méndez-Armenta M, Ríos C, Monroy-Noyola A. 1994. Combined D-penicillamine and Prussian blue as antidotal treatment against thallotoxicosis in rats: evaluation of cerebellar lesions. Toxicology 89: 15-24.

Barrozo ER, Fowler DA, Beckman ML. 2015. Exposure to D2-like dopamine receptor agonists inhibits swimming in *Daphnia magna*. Pharmacology, Biochemistry and Behavior 137: 101-109.

Baudo R. 1987. Ecotoxicological testing with *Daphnia*. Memorie dell'Istituto Italiano di Idrobiologia 45: 461-482.

Baylor ER. 1942. Cardiac pharmacology of the Cladoceran, *Daphnia*. Biological Bulletin 82: 165-172.

Bedrossiantz J, Fuertes I, Raldua D, Barata C. 2021. Pharmacological modulation of fish-induced depth selection in *D. magna*: The role of cholinergic and GABAergic signalling. Scientific Reports 11: 19407.

Belowitz R, O'Donnell MJ. 2013. Ion-selective microelectrode measurements of Tl^+ and K^+ transport by the gut and associated epithelia in *Chironomus riparius*. Aquatic Toxicology 138-139: 70-80.

Belzile N, Chen YW. 2017. Thallium in the environment: A critical review focused on natural waters, soils, sediments and airborne particles. Applied Geochemistry 84: 218-243.

Berenbrink M, Volkel S, Koldkjaer P, Heisler N, Nikinmaa M. 2006. Two different oxygen sensors regulate oxygen-sensitive K^+ transport in crucian carp red blood cells. Journal of Physiology 575: 37-48.

Besser JM, Dorman R, Ivey CD, Cleveland D, Steevens JA. 2020. Sensitivity of warm-water fishes and rainbow trout to selected contaminants. Bulletin of Environmental Contamination and Toxicology 104: 321-326.

Beyers DW, Rice JA, Clements WH, Henry CJ. 1999. Estimating physiological cost of chemical exposure: Integrating energetics and stress to quantify toxic effects in fish. Canadian Journal of Fisheries and Aquatic Sciences 56: 814-822.

Bianchini A, Wood CM. 2003. Mechanism of acute silver toxicity in *Daphnia magna.* Environmental Toxicology and Chemistry 22: 1361-1367.

Biesinger KE, Christensen GM. 1972. Effects of various metals on survival, growth, reproduction, and metabolism of *Daphnia magna.* Journal of the Fisheries Research Board of Canada 29: 1691-1700.

Biesinger K, Williams L, Schalie W. 1987. Procedures for Conducting '*Daphnia magna'* Toxicity Bioassays. User's Guide. U.S. Environmental Protection Agency, Washington, DC, EPA/600/8-87/011.

Birge WJ. 1978. Aquatic toxicology of trace elements of coal and fly ash. In: Thorp JH, Gibbons JW, eds., Energy and Environmental Stress in Aquatic Systems, DOE Symposium Series (CONF-771114), Washington, DC. USA, pp 219-240.

Borgatti AR, Pagliarani A, Ventrella V. 1992. Gill ($Na^+ + K^+$)-ATPase involvement and regulation during salmonid adaptation to salt water. Comparative Biochemistry and Physiology- Part A: Physiology 102: 637-643.

Borgmann U, Cheam V, Norwood WP, Lechner J. 1998. Toxicity and bioaccumulation of thallium in *Hyalella azteca*, with comparison to other metals and prediction of environmental impact. Environmental Pollution 99: 105-114.

Bradford MM. 1976. A rapid and sensitive method for the quantitation of microgram quantities of protein utilizing the principle of protein-dye binding. Analytical Biochemistry 72: 248-254.

Bramanti E, Onor M, Colombaioni L. 2019. Neurotoxicity induced by low thallium doses in living hippocampal neurons: Evidence of early onset mitochondrial dysfunction and correlation with ethanol production. ACS Chemical Neuroscience 10: 451-459.

Brismar T. 1998. Thallium transport in cellular membranes. In: Nriagu JO, ed., Thallium in the Environment, Vol 29- Advances in Environmental Science and Technology. Wiley, New York, NY, USA, pp 241–262.

Brismar T, Collins VP, Kesselberg M. 1989. Thallium-201 uptake relates to membrane potential and potassium permeability in human glioma cells. Brain Research 500: 30-36.

Britten JS, Blank M. 1968. Thallium activation of the (Na^+-K^+)-activated ATPase of rabbit kidney. Biochimica et Biophysica Acta 159: 160-166.

Brown BT, Rattigan BM. 1979. Toxicity of soluble copper and other metal ions to *Elodea canadensis.* Environmental Pollution 20: 303-314.

Buckingham SD, Kidd JF, Law RJ, Franks CJ, Sattelle DB. 2005. Structure and function of two-pore-domain K^+ channels: Contributions from genetic model organisms. Trends in Pharmacological Sciences 26: P361-P367.

Buffle J, Leppard GG. 1995. Characterization of aquatic colloids and macromolecules. 1. Structure and behavior of colloidal material. Environmental Science & Technology 29: 2169- 2175.

Bury NR, Wood CM. 1999. Mechanism of branchial apical silver uptake by rainbow trout is via the proton-coupled Na^+ channel. American Journal of Physiology, Regulatory, Integrative and Comparative Physiology 277: R1385-R1391.

Bury NR, Walker PA, Glover CN. 2003. Nutritive metal uptake in teleost fish. Journal of Experimental Biology 206: 11-23.

Cain DJ, Buchwalter DB, Luoma SN. 2006. Influence of metal exposure history on the bioaccumulation and subcellular distribution of aqueous cadmium in the insect *Hydropsyche californica.* Environmental Toxicology and Chemistry 25: 1042-1049.

Calamari D, Gaggino GS, Pacchetti G. 1982. Toxicokinetics of low levels of Cd, Cr, Ni and their mixture in long-term treatment on *Salmo gairdneri* Rich. Chemosphere 11: 59-70.

Campanella B, D'Ulivo A, Ghezzi L, Onor M, Petrini R, Bramanti E. 2018. Influence of environmental and anthropogenic parameters on thallium oxidation state in natural waters. Chemosphere 196: 1-8.

Canadian Council of Ministers of the Environment (CCME). 1991. A protocol for the derivation of water quality guidelines for the protection of aquatic life. In: Canadian Water Quality Guidelines: Appendix IX. Prepared by the Task Force on Water Quality Guidelines of the Canadian Council of Ministers of the Environment. Water Quality Branch. Environment Canada. Ottawa, Canada. 24 pp.

Canadian Council of Ministries of the Environment (CCME). 1999. Canadian Water Quality Guidelines for the Protection of Aquatic Life: Thallium. Winnipeg, MB: Canadian Council of Ministers of the Environment.

Canadian Council of Ministers of the Environment (CCME). 2007. A Protocol for the Derivation of Water Quality Guidelines for the Protection of Aquatic Life 2007. Winnipeg, MB: Canadian Council of Ministers of the Environment.

Carmosino M, Rizzo F, Torretta S, Procino G, Svelto M. 2013. High-throughput fluorescent-based NKCC functional assay in adherent epithelial cells. BMC Cell Biology 14: 16.

Caron A, Rosabal M, Drevet O, Couture P, Campbell PGC. 2017. Binding of trace elements (Ag, Cd, Co, Cu, Ni, and Tl) to cytosolic biomolecules in livers of juvenile yellow perch (*Perca flavescens)* collected from lakes representing metal contamination gradients. Environmental Toxicology and Chemistry 37: 576-586.

Casiot C, Egal M, Elbaz-Poulichet F, Bruneel O, Bancon-Montigny C, Cordier MA, Gomez E, Aliaume C. 2009. Hydrological and geochemical control of metals and arsenic in a Mediterranean river contaminated by acid mine drainage (the Amous River, France); preliminary assessment of impacts on fish (*Leuciscus cephalus)*. Applied Geochemistry 24: 787-799.

Casiot C, Egal M, Bruneel O, Verma N, Parmentier M, Elbaz-Poulichet F. 2011. Predominance of aqueous Tl(I) species in the river system downstream from the abandoned Carnoulès mine (Southern France). Environmental Science & Technology 45: 2056-2064.

Castaldo G, Pillet M, Ameryckx L, Bervoets L, Town RM, Blust R, De Boeck G. 2021. Temperature effects during a sublethal chronic metal mixture exposure on common carp (*Cyprinus carpio*). Frontiers in Physiology 12: 651584.

Cavieres JD, Ellory JC. 1974. Thallium and the sodium pump in human red cells. Journal of Physiology 243: 243-266.

Chan WS, Routh J, Lou CL, Dario M, Miao Y, Lou D, Wei L. 2021. Metal accumulations in aquatic organisms and health risk in an acid mine-affected site in South China. Environmental Geochemistry and Health 43: 4415-4440.

Cheam V. 2001. Thallium contamination of water in Canada. Water Quality Research Journal 36: 851-877.

Cheam V, Lechner J, Desrosiers R, Sekerka I, 1996. Direct determination of dissolved and total thallium in lake waters by laser-excited atomic fluorescence spectrometry. International Journal of Environmental Analytical Chemistry 63: 153-165.

Chen L, Sampson KJ, Kass RS. 2016. Cardiac delayed rectifier potassium channels in health and disease. Cardiac Electrophysiology Clinics 8: 307-322.

Chen DY, Zhou ZX. 2000. Studying situation about Lanmuchang type Tl (mercury) ore deposits in Southwestern Guizhou. Guizhou Geology 17: 236-241.

Chiaverini N, De Ley M. 2010. Protective effect of metallothionein on oxidative stress-induced DNA damage. Free Radical Research 44: 605-613.

Chinese Ministry of Environmental Protection (CMEP). 2002. Environmental Quality Standards for Surface Water. CMEP, GB3838-2002.

Civitello DJ, Hite JL, Hall SR. 2014. Potassium enrichment stimulates the growth and reproduction of a clone of *Daphnia dentifera*. Oecologia 175: 773-780.

Clarke GL. 1932. Quantitative aspects of the change of phototropic sign in *Daphnia*. Journal of Experimental Biology 9: 180-211.

Clay JR, Shlesinger MC. 1984. Analysis of the effects of cesium ions on potassium channel currents in biological membranes. Journal of Theoretical Biology 107: 189-201.

Cleven R, Fokkert L. 1994. Potentiometric stripping analysis of thallium in natural waters. Analytica Chimica Acta 289: 215-221.

Cohen G, Hochstein P. 1963. Glutathione peroxidase: The primary agent for the elimination of hydrogen peroxide in erythrocytes. Biochemistry 2: 1420-1428.

Colatsky TJ, Follmer CH, Starmer CF. 1990. Channel specificity in antiarrhythmic drug action. Mechanism of potassium channel block and its role in suppressing and aggravating cardiac arrhythmias. Circulation 82: 2235-2242.

Cotton FA, Wilkinson G. 1988. Advanced Inorganic Chemistry. 5th ed. John Wiley and Sons, New York, NY, USA. .

Couto N, Wood J, Barber J. 2016. The role of glutathione reductase and related enzymes on cellular redox homeostasis network. Free Radical Biology and Medicine 95: 27-42.

Couture P, Fortin C, Hare L, Lapointe D, Pitre D. 2011. Critical Review of Thallium in Aquatic Ecosystems. Environment Canada, Research Reports No R-1272. Gatineau, QC.

Craven AM, Aiken GM, Ryan JN. 2012. Copper(II) binding by dissolved organic matter: Importance of the copper-to-dissolved organic matter ratio and implications of the biotic ligand model. Environmental Science & Technology 46: 9946-9955.

Cuss CW, Guéguen C. 2012. Determination of relative molecular weights of fluorescent components in dissolved organic matter using asymmetrical flow field-flow fractionation and parallel factor analysis. Analytica Chimica Acta 733: 98–102.

Cuss CW, Grant-Weaver I, Shotyk W. 2017. AF4-ICPMS with the 300 Da membrane to resolve metal-bearing "colloids" <1 kDa: Optimization, fractogram deconvolution, and advanced quality control. Analytical Chemistry 89: 8027-8035.

Cuss CW, Donner MW, Grant-Weaver I, Noernberg T, Pelletier R, Sinnatamby RN, Shotyk W. 2018. Measuring the distribution of trace elements amongst dissolved colloidal species as a fingerprint for the contribution of tributaries to large boreal rivers. Science of the Total Environment 642: 1242-1251.

Cuss CW, Glover CN, Javed MB, Nagel A, Shotyk W. 2020. Geochemical and biological controls on the ecological relevance of total, dissolved, and colloidal forms of trace elements in large boreal rivers: review and case studies. Environmental Reviews 28: 138-163.

Cvjetko P, Cvjetko I, Pavlica M. 2010. Thallium toxicity in humans. Arhiv Za Higijenu Rada I Toksikologiju 61: 111-119.

D'Orazio M, Campanella B, Bramanti E, Ghezzi L, Onor M, Vianello G, Vittoria-Antisari L, Petrini R. 2020. Thallium pollution in water, soils and plants from past-mining site of Tuscany: Sources, transfer processes and toxicity. Journal of Geochemical Exploration 209: 106434.

Dawson GW, Jennings AL, Drozodowski D, Rider E. 1977. The acute toxicity of 47 industrial chemicals to fresh and saltwater fishes. Journal of Hazardous Materials 1: 303-318.

De Biasi S, Gibellini L, Bianchini E, Nasi M, Pinti M, Salvioli S, Cossarizza A. 2016. Quantification of mitochondrial reactive oxygen species in living cells by using multi-laser polychromatic flow cytometry. Cytometry- Part A 89: 1106-1110.

De Boeck G, Ngo TTH, Van Campenhout K, Blust R. 2003. Differential metallothionein induction patterns in three freshwater fish during sublethal copper exposure. Aquatic Toxicology 65: 413-424.

De Coen W, Janssen CR. 2003. The missing biomarker link: Relationships between effects on the cellular energy allocation biomarker of toxicant-stressed *Daphnia magna* and corresponding population characteristics. Environmental Toxicology and Chemistry 22: 1632-1641.

De Meester L. 1989. An estimation of the heritability of phototaxis in *Daphnia magna* Straus. Oecologia 78: 142-144.

De Meester L. 1991. An analysis of the phototactic behaviour of *Daphnia magna* clones and their sexual descendants. Hydrobiologia 225: 217-227.

De Meester L. 1992. The phototactic behavior of male and female *Daphnia magna*. Animal Behaviour 43: 696-698.

De Meester L. 1993. Genotype, fish-mediated chemical, and phototactic behavior in *Daphnia magna*. Ecology 74: 1467-1474.

De Meester L, Dumont HJ. 1989. Phototaxis in *Daphnia*: Interaction of hunger and genotype. Limnology and Oceanography 34: 1322-1325.

De Schamphelaere KAC, Janssen CR. 2002. A biotic ligand model predicting acute copper toxicity for *Daphnia magna*: The effects of calcium, magnesium, sodium, potassium, and pH. Environmental Science & Technology 36: 48-54.

De Schamphelaere KAC, Vasconcelos FM, Tack FMG, Allen HE, Janssen CR. 2009. Effect of dissolved organic matter source on acute copper toxicity to *Daphnia magna*. Environmental Toxicology and Chemistry 23: 1248-1255.

Deb MK, Agnihortri PK, Thakur M, Mishra RK. 1998. Fractionation and spectrophotometric determination of thallium with N,N'-diphenylbenzamidine, brilliant green and cetylpyridinium chloride. Chemical Speciation and Bioavailability 10: 53-60.

DeForest DK, Brix KV, Adams WJ. 2007. Assessing metal bioaccumulation in aquatic environments: The inverse relationship between bioaccumulation factors, trophic transfer factors and exposure concentration. Aquatic Toxicology 84: 236-246.

DeForest DK, Meyer JS. 2015. Toxicity of dietborne metals to aquatic organisms. Critical Reviews in Environmental Science and Technology 45: 1176- 1241.

Deigweiher K, Koschnick N, Pörtner HO, Lucassen M. 2008. Acclimation of ion regulatory capacities in gills of marine fish under environmental hypercapnia. American Journal of Physiology: Regulatory, Integrative and Comparative Physiology 295: R1660-R1670.

Delompré PLM, Blewett TA, Goss GG, Glover CN. 2019a. Shedding light on the effects of hydraulic fracturing flowback and produced water on phototactic behavior in *Daphnia magna*. Ecotoxicology and Environmental Safety 174: 315-323.

Delompré PLM, Blewett TA, Snihur KN, Flynn SL, Alessi DS, Glover CN, Goss GG. 2019b. The osmotic effect of hyper-saline hydraulic fracturing fluid on rainbow trout, *Oncorhynchus mykiss*. Aquatic Toxicology 211: 1-10.

Desenclos JC, Wilder MH, Coppenger GW, Sherin K, Tiller R, VanHook RM. 1992. Thallium poisoning: An outbreak in Florida, 1988. Southern Medical Journal 85: 1203-1206.

Dethloff GM, Naddy RB, Gorsuch JW. 2007. Effects of sodium chloride on chronic silver toxicity to early life stages of rainbow trout (*Oncorhynchus mykiss)*. Environmental Toxicology and Chemistry 26: 1717-1725.

Devaux JBL, Hedges CP, Birch N, Herbert N, Renshaw GMC, Hickey AJR. 2019. Acidosis maintains the function of brain mitochondria in hypoxia-tolerant triplefin fish: A strategy to survive acute hypoxic exposure? Frontiers in Physiology 9: 1941.

Di Toro DM, Allen HE, Bergman HL, Meyer JS, Paquin PR, Santore RC. 2001. Biotic ligand model of the acute toxicity of metals. 1. Technical basis. Environmental Toxicology and Chemistry 20: 2383-2396.

Dodson SI, Ramcharan CW. 1991 Size-specific swimming behavior of *Daphnia pulex*. Journal of Plankton Research 13: 1367-1379.

Doig LE, Liber K. 2007. Nickel speciation in the presence of different sources and fractions of dissolved organic matter. Ecotoxicology and Environmental Safety 66: 169-177.

Dumas J, Hare L. 2008. The internal distribution of nickel and thallium in two freshwater invertebrates and its relevance to trophic transfer. Environmental Science & Technology 42: 5144-5149.

Dwyer FJ, Sappington LC, Buckler DR, Jones SB. 1995. Use of Surrogate Species in Assessing Contaminant Risk to Endangered and Threatened Fishes. U.S. Environmental Protection Agency, Washington, DC, EPA/600/R-96/029.

Dyomin V, Davydova A, Morgalev V, Olshukov A, Polovtsev I, Morgaleva T, Morgalev S. 2020. Planktonic response to light as a pollution indicator. Journal of Great Lakes Research 46: 41-47.

Eddy FB. 1985. Uptake and loss of potassium by rainbow trout (*Salmo gairdneri*) in fresh water and dilute sea water. Journal of Experimental Biology 118: 277-286.

Ellman GL, Courtney KD, Andres Jr V, Featherstone RM. 1961. A new and rapid colorimetric determination of acetylcholinesterase activity. Biochemical Pharmacology 7: 88-95.

Environment Canada. 2000a. Persistence and bioaccumulation regulations. Canada Gazette 133: 3645-3649.

Environment Canada. 2000b. Biological Test Method: Reference Method for Determining Acute Lethality of Effluents to *Daphnia magna*. Method Development and Application Section, Ottawa, ON: EPS 1/RM/14 Second Edition.

Environment Canada. 2000c. Biological Test Method: Acute Lethality of Effluents to Rainbow Trout. Environmental Protection Series, Method Development and Application Section, Environmental Technology Centre, Environment Canada. Ottawa, ON: EPS 1/RM/13.

Environment Canada. 2012. Metal Mining Technical Guidance for Environmental Effects Monitoring. National Environmental Effects Monitoring Office, Ottawa, ON.

Erickson RJ, Benoit DA, Mattson VR, Nelson Jr HP, Leonard EN. 1996. The effects of water chemistry on the toxicity of copper to fathead minnows. Environmental Toxicology and Chemistry 15: 181-193.

Etsuo N, Jyunichi T, Ritsuko T, Yoshio K. 1982. Regeneration of vitamin E from α -chromanoxyl radical by glutathione and vitamin C. Chemistry Letters 11: 789-792.

Evans DH, Piermarini PM, Potts WTW. 1999. Ionic transport in the fish gill epithelium. Journal of Experimental Biology 283: 641-652.

Farag MR, Alagawany M, Khalil SR, Moustafa AA, Mahmoud HK, Abdel-Latif HMR. 2021. *Astragalus membranaceus* polysaccharides modulate growth, hemato-biochemical indices,

hepatic antioxidants, and expression of HSP70- and apoptosis-related genes in *Oreochromis niloticus* exposed to sub-lethal thallium toxicity. Fish and Shellfish Immunology 118: 251-260.

Fehsenfeld S, Wood CM. 2020. A potential role for hyperpolarization-activated cyclic nucleotide-gated sodium/potassium channels (HCNs) in teleost acid-base and ammonia regulation. Comparative Biochemistry and Physiology- Part B: Biochemistry and Molecular Biology 248-249: 110469.

Fong PP, Ford AT. 2014. The biological effects of antidepressants on the molluscs and crustaceans: A review. Aquatic Toxicology 151: 4-13.

Forbes VE, Calow P. 2002. Species sensitivity distributions revisited: A critical appraisal. Human and Ecological Risk Assessment 8: 473-492.

Foster DB, Ho AS, Rucker J, Garlid AO, Chen L, Sidor A, Garlid KD, O'Rourke B. 2012. Mitochondrial ROMK channel is a molecular component of MitoK_{ATP}. Circulation Research 111: 446-454.

Franklin NM, Glover CN, Nicol JA, Wood CM. 2005. Calcium/cadmium interactions at uptake surfaces in rainbow trout: Waterborne versus dietary routes of exposure. Environmental Toxicology and Chemistry 24: 2954-2964.

Fuentes J, Eddy FB. 1997. Drinking in marine, euryhaline and freshwater teleost fish. In: Hazon N, Eddy FB, Flik G, eds., Ionic Regulation in Animals: A Tribute to Professor W.T.W. Potts. Springer, Berlin, pp 135- 149.

Fuentes J, Eddy FB. 1998. Cardiovascular responses *in vivo* to angiotensin II and the peptide antagonist saralasin in rainbow trout *Oncorhynchus mykiss.* Journal of Experimental Biology 201: 267-272.

Fukumoto M, Yoshida D, Yoshida S. 1997. Subcellular distribution of thallium: Morphological and quantitative study in rat myocardium. Annals of Nuclear Medicine 11: 291-297.

Furukawa F, Watanabe S, Kimura S, Kaneko T. 2011. Potassium excretion through ROMK potassium channel expressed in gill mitochondrion-rich cells of Mozambique tilapia. American Journal of Physiology: Regulatory, Integrative and Comparative Physiology 302: R568-R576.

Gaillardet J, Viers J, Dupré B. 2003. Trace elements in river water. In: Holland HD, Turekian KK, eds., Treatise on Geochemistry, Vol 5. Pergamon, Oxford, UK, pp 225-272.

Galván-Arzate S, Martínez A, Medina E, Santamaría A, Ríos C. 2000. Subchronic administration of sublethal doses of thallium to rats: Effects on distribution and lipid peroxidation in brain regions. Toxicology Letters 116: 37-43.

Galván-Arzate S, Santamaria A. 1998. Thallium toxicity. Toxicology Letters 99: 1-13.

Gantner N, Power M, Babaluk JA, Reist JD, Köck G, Lockhart LW, Solomon KR, Muir DCG. 2009. Temporal trends of mercury, cesium, potassium, selenium, and thallium in Arctic char (*Salvelinus alpinus*) from Lake Hazen, Nunavut, Canada: Effects of trophic position, size, and age. Environmental Toxicology and Chemistry 28: 254-263.

Garbarino JR. 1999. Methods of Analysis by the U.S. Geological Survey National Water Quality Laboratory- Determination of Dissolved Arsenic, Boron, Lithium, Selenium, Strontium, Thallium, and Vanadium using Inductively Coupled Plasma Mass Spectrometry. U.S. Geological Survey: Branch of Information Services, Denver, CO, USA: 99-093.

Garbutt JS, Little TJ. 2017. Bigger is better: Changes in body size explain a maternal effect of food on offspring disease resistance. Ecology and Evolution 5: 1403-1409.

Gardaire E, Isaia J, Bornancin M. 1991. Kinetics of potassium transport across trout gills. Comparative Biochemistry and Physiology- Part A: Comparative Physiology 99: 615-620.

Garlid KD, Paucek P. 2003. Mitochondrial potassium transport: The K^+ cycle. Biochimica et Biophysica Acta 1606: 23-41.

Gehring PJ, Hammond PB. 1967. The interrelationship between thallium and potassium in animals. Journal of Pharmacology and Experimental Therapeutics 155: 187-201.

Genchi G, Carocci A, Lauria G, Sinicropi MS, Catalano. 2021. Thallium use, toxicity, and detoxification therapy: An overview. Applied Sciences 11: 8322.

Gerhardt A, de Bisthoven LJ, Schmidt S. 2006. Automated recording of vertical negative phototactic behaviour in *Daphnia magna* Straus (Crustacea). Hydrobiologia 559: 433-441.

Ghotbizadeh M, Cuss CW, Grant-Weaver I, Markov A, Noernberg T, Ulrich A, Shotyk W. 2022. Spatiotemporal variations of total and dissolved trace elements and their distributions amongst major colloidal forms along and across the lower Athabasca River. Journal of Hydrology: Regional Studies 40: 101029.

Gillis PL, Chow-Fraser P, Ranville JF, Ross PE, Wood CM. 2005. *Daphnia* need to be gut-cleared too: The effect of exposure to and ingestion of metal-contaminated sediment on the gut-clearance patterns of *D. magna*. Aquatic Toxicology 71: 143-154.

Gleich M. 1931. Thallium acetate poisoning in the treatment of ringworm of the scalp: Report of two cases. Journal of the American Medical Association 97: 851.

Glover CN. 2018. Defence mechanisms: The role of physiology in current and future environmental protection paradigms. Conservation Physiology 6: coy012.

Glover CN, Goss GG. 2020. In vitro characterisation of calcium influx across skin and gut epithelia of the Pacific hagfish, *Eptatretus stoutii*. Journal of Comparative Physiology B, 190: 149-160.

Glover CN, Playle RC, Wood CM. 2005. Heterogeneity of natural organic matter amelioration of silver toxicity to *Daphnia magna*: Effect of source and equilibration time. Environmental Toxicology and Chemistry 24: 2934-2940.

Glover CN, Wood CM. 2005a. Accumulation and elimination of silver in *Daphnia magna* and the effect of natural organic matter. Aquatic Toxicology 73: 406- 417.

Glover CN, Wood CM. 2005b. Physiological characterisation of a pH- and calcium-dependent sodium uptake mechanism in the freshwater crustacean, *Daphnia magna*. Journal of Experimental Biology 208: 951-959.

Gobas FAPC, Morrison HA. 2000. Bioconcentration and biomagnification in the aquatic environment. In: Boethling RS, Mackay D, eds., Handbook of Property Estimation Methods for Chemicals, Lewis Publishers, Boca Raton, FL, USA, pp 189–231.

Gondek JC, Gensemer RW, Claytor CA, Canton SP, Gorsuch JW. 2017. Framework for derivation of water quality criteria using the biotic ligand model: Copper as a case study. Integrated Environmental Assessment and Management 14: 736-749.

González C, Baez-Nieto D, Valencia I, Oyazún I, Rojas P, Naranjo D, Latorre R. 2012. K^+ channels: Function- structural overview. Comprehensive Physiology 2: 2087-2149.

Goss G, Gilmour K, Hawkings G, Brumbach JH, Huynh M, Galvez F. 2011. Mechanism of sodium uptake in PNA negative MR cells from rainbow trout, *Oncorhynchus mykiss* as revealed by silver and copper inhibition. Comparative Biochemistry and Physiology-Part A: Molecular and Integrative Physiology 159: 234-241.

Griffith MB. 2016. Toxicological perspective on the osmoregulation and ionoregulation physiology of major ions by freshwater animals: Teleost fish, crustacea, aquatic insects, and Mollusca. Environmental Toxicology and Chemistry 36: 576-600.

Grosell M, Nielsen C, Bianchini A. 2002. Sodium turnover rate determines sensitivity to acute copper and silver exposure in freshwater animals. Comparative Biochemistry and Physiology-Part C: Toxicology and Pharmacology 133: 287-303.

Grosell M, Wood CM. 2002. Copper uptake across rainbow trout gills: Mechanism of apical entry. Journal of Experimental Biology 205: 1179-1188.

Guilhermino L, Lopes MC, Carvalho AP, Soares AMVM. 1996. Inhibition of acetylcholinesterase activity as effect criterion in acute tests with juvenile *Daphnia magna*. Chemosphere 32: 727-738.

Gustafsson JP. 2015. Visual MINTEQ. Ver. 3.1. KTH, Division of Land and Water Resource Engineering, Stockholm, Sweden.

Haas M, Forbush III B. 1998. The Na-K-Cl cotransporters. Journal of Bioenergetics and Biomembranes 30: 161-172.

Hamilton SJ, Mehrle PM. 1986. Metallothionein in fish: Review of its importance in assessing stress from metal contaminants. Transactions of the American Fisheries Society 115: 596-609.

Hamza W, Bonacina C, Canale C. 1998. Side effects of water liming on body size and eggs development of *Daphnia* species in Lake Orta (N. Italy). Hydrobiologia 368: 129–136.

Hansson SV, Desforges JP, van Beest FM, Bach L, Halden NM, Sonne C, Mosbech A, Sondergaard J. 2020. Bioaccumulation of mining derived metals in blood, liver, muscle and otoliths of two Arctic predatory fish species (*Gadus ogac* and *Myoxocephalus scorpius)*. Environmental Research 183: 109194.

Harada M. 1995. Minamata disease: Methylmercury poisoning in Japan caused by environmental pollution. Critical Reviews in Toxicology 25: 1-24.

Hasan M, Ali SF, Tariq M. 1978. Levels of dopamine, norepinephrine and 5-hydroxytryptamine in different regions of the rat brain in thallium toxicosis. Acta Pharmacologica et Toxicologica 43: 169-173.

Hassler CS, Chafin RD, Klinger MB, Twiss MR. 2007. Application of the biotic ligand model to explain potassium interaction with thallium uptake and toxicity to plankton. Environmental Toxicology and Chemistry 26: 1139-1145.

Hauser-Davis RA, Bastos FF, Dantas RF, Tobar SAL, Neto JDB, Bastos VLFD, Ziolli RL, Arruda MAZ. 2014. Behaviour of the oxidant scavenger metallothionein in hypoxia-induced neotropical fish. Ecotoxicology and Environmental Safety 103: 24-28.

He E, Qiu H, Qiu R, Rentenaar C, Devresse Q, Van Gestel CAM. 2017. Time-dependent uptake and toxicity of nickel to *Enchytraeus crypticus* in the presence of humic acid and fulvic acid. Environmental Toxicology and Chemistry 36: 3019-3027.

Henning CH, Forth W. 1982. The excretion of thallium(I) ions into the gastrointestinal tract in situ of rats. Archives of Toxicology 49: 149-158.

Herman MM, Bensch KG. 1967. Light and electron microscopic studies of acute and chronic thallium intoxication in rats. Toxicology and Applied Pharmacology 10: 199-222.

Hibino H, Inanobe A, Furutani K, Murakami S, Findlay I, Kurachi Y. 2010. Inward rectifying potassium channels: Their structure, function, and physiological roles. Physiological Reviews 90: 291-366.

Hill AP, Perrin MJ, Heide J, Campbell TJ, Mann SA, Vandenberg JI. 2014. Kinetics of drug interaction with the $K_v11.1$ potassium channel. Molecular Pharmacology 85: 769-776.

Hogstrand C, Wilson RW, Polgar D, Wood CM. 1994. Effects of zinc on the kinetics of branchial calcium uptake in freshwater rainbow trout during adaptation to waterborne zinc. Journal of Experimental Biology 186: 55-73.

Horng JL, Yu LL, Liu ST, Chen PY, Li LY. 2017. Potassium regulation in medaka (*Oryzias latipes)* larvae acclimated to freshwater: Passive uptake and active secretion by skin cells. Scientific Reports 7: 16215.

Hou LP, Yang Y, Shu H, Ying GG, Zhao JL, Chen YB, Chen YH, Fang GZ, Li X, Liu JS. 2017. Changes in histopathology, enzyme activities, and the expression of relevant genes in zebrafish (*Danio rerio*) following long-term exposure to environmental levels of thallium. Bulletin of Environmental Contamination and Toxicology 99: 574-581.

Hsu YC, Thia E, Chen PJ. 2022. Monitoring of ion release, bioavailability and ecotoxicity of thallium in contaminated paddy soils under rice cultivation conditions. Journal of Hazardous Materials 424: 126513.

Hu XF, Chan HM. 2021. Seafood consumption and its contribution to nutrients intake among Canadians in 2004 and 2015. Nutrients 13: 77.

Hunter DR, Haworth RA, Goknur AB, Hegge JO, Berkoff HA. 1986. Control of thallium and sodium fluxes in isolated adult rat heart cells by anthopleurin-A, verapamil and magnesium. Journal of Molecular and Cellular Cardiology 18: 1125-1132.

Hüssy K, Limburg KE, Pontual HD, Thomas ORB, Cook PK, Heimbrand Y, Blass M, Sturrock AM. 2020. Trace element patterns in otoliths: The role of biomineralization. Reviews in Fisheries Science & Aquaculture 29: 445-477.

Hwang PP, Lee TH, Lin LY. 2011. Ion regulation in fish gills: Recent progress in cellular and molecular mechanisms. American Journal of Physiology: Regulatory, Integrative and Comparative Physiology 301: R28-R47.

Iftikar FI, Morash AJ, Cook DG, Herbert NA, Hickey AJR. 2015. Temperature acclimation of mitochondria function from the hearts of a temperature wrasse (*Notolabrus celidotus*). Comparative Biochemistry and Physiology- Part A: Molecular and Integrative Physiology 184: 46-55.

International Programme on Chemical Safety (IPCS). 1996. Environmental Health Criteria 182: Thallium. World Health Organization, Geneva, Switzerland. https://inchem.org/documents/ehc/ehc/ehc182.htm

Israelsen WJ, Vander Heiden MG. 2015. Pyruvate kinase: Function, regulation and role in cancer. Seminars in Cell and Developmental Biology 43: 43-51.

Jardine TD, Doig LE, Jones PD, Bharadwaj L, Carr M, Tendler B, Lindenschmidt KE. 2019. Vanadium and thallium exhibit biodilution in a northern river food web. Chemosphere 233: 381-386.

Johnsen GH, Jakobsen PJ. 1987. The effect of food limitation on vertical migration in *Daphnia longispina*. Limnology and Oceanography 32: 873-880.

Jonckheere AI, Smeitink JAM, Rodenburg RJT. 2012. Mitochondrial ATP synthase: Architecture, function and pathology. Journal of Inherited Metabolic Disease 35: 211-225.

Jorgensen PL, Pedersen PA. 2001. Structure-function relationships of Na^+, K^+, ATP, or Mg^{2+} binding and energy transduction in Na,K-ATPase. Biochimica et Biophysica Acta 1505: 57-74.

Jurković S, Osredkar J, Marc J. 2008. Molecular impact of glutathione peroxidases in antioxidant processes. Biochemia Medica 18: 162-174.

Kanye FJ. 1971. Thallium(I) activation of pyruvate kinase. Archives of Biochemistry and Biophysics 143: 232-239.

Kaplan DI, Mattigold SV. 1998. Aqueous Geochemistry of Thallium. In: Nriagu JO, ed., Thallium in the Environment, Vol 29- Advances in Environmental Science and Technology. Wiley, New York, NY, USA, pp 15-29.

Karbowska B. 2016. Presence of thallium in the environment: Sources of contaminations, distribution and monitoring methods. Environmental Monitoring and Assessment 188: 640.

Karlsson U, Düker A, Karlsson S. 2006a. Separation and quantification of Tl(I) and Tl(III) in freshwater samples. Journal of Environmental Science and Health- Part A: Toxic/Hazardous Substances and Environmental Engineering 41: 1155-1167.

Karlsson U, Karlsson S, Duker A. 2006b. The effect of light and iron(II)/iron(III) on the distribution of Tl(I)/Tl(III) in fresh water systems. Journal of Environmental Monitoring 8: 634-640.

Katoh F, Cozzi RRF, Marshall WS, Goss GG. 2008. Distinct $Na^+/K^+/2Cl^-$ cotransporter localization in kidneys and gills of two euryhaline species, rainbow trout and killifish. Cell and Tissue Research 334: 265-281.

Kernan RP. 1969. Accumulation of caesium and rubidium in vivo by red and white muscles of the rat. Journal of Physiology 204: 195-205.

Kerstetter TH, Kirschner LB. 1972. Active chloride transport by gills of rainbow trout (*Salmo gairdneri*). Journal of Experimental Biology 56: 263-272.

Kiliç V, Altunsov F, Kiliç G. 2011. Effect of thallium on the survival and morphology of *Tubifex tubifex* (Oligochaeta, Tubificidae). Fresenius Environmental Bulletin 20: 2442-2445.

Kiliç GA, Kiliç V. 2017. Antioxidative responses in *Tubifex* against thallium-induced oxidative stress. Anadolu University Journal of Science and Technology C: Life Sciences and Biotechnology 6: 84-94.

Kiliç GA, Kutlu M. 2010. Effects of exogenous metallothionein against thallium-induced oxidative stress in rat liver. Food and Chemical Toxicology 48: 980-987.

Kimball G. 1978. The Effects of Lesser Known Metals and One Organic to Fathead Minnows (*Pimephales promelas)* and *Daphnia magna.* Department of Entomology, Fisheries and Wildlife, University of Minnesota. Minneapolis, Mn, USA.

Klassen DC, Liu J, Diwan BA. 2009. Metallothionein protection of cadmium toxicity. Toxicology and Applied Pharmacology 238: 215-220.

Knops M, Altenburger R, Segner H. 2001. Alterations of physiological energetics, growth and reproduction of *Daphnia magna* under toxicant stress. Aquatic Toxicology 53: 79-90.

Kolkmeier MA, Brooks BW. 2013. Sublethal silver and NaCl toxicity in *Daphnia magna*: A comparative study of standardized chronic endpoints and progeny phototaxis. Ecotoxicology 22: 693-706.

Komada I, Kamiya K, Toyama J. 1999. Amiodarone: Ionic and cellular mechanisms of action of the most promising class III agent. American Journal of Cardiology 84: R20- R28.

Korkisch J, Steffan I. 1979. Determination of thallium in natural waters. International Journal of Environmental Analytical Chemistry 6: 111-118.

Kou HC, Huang CC, Tsai YT. 2005. Acute painful neuropathy in thallium poisoning. Neurology 65: 302-304.

Kramer HJ, Gonick C, Lu E. 1986. In vitro inhibition of Na-K-ATPase by trace metals: Relation to renal and cardiovascular damage. Nephron 44: 329-336.

Kravenska Y, Checchetto V, Szabò I. 2021. Routes for potassium ions across mitochondrial membranes: A biophysical point of view with special focus on the ATP-sensitive K^+ channel. Biomolecules 11: 1172.

Krezel A, Maret W. 2007. Dual nanomolar and picomolar Zn(II) binding properties of metallothionein. Journal of American Chemical Society 129: 10911-10921.

Kwan KHM, Smith S. 1988. The effect of thallium on the growth of *Lemna minor* and plant tissue concentration in relation to both exposure and toxicity. Environmental Pollution 52: 203-219.

Kwan KHM, Smith S. 1991. Some aspects of the kinetics of cadmium and thallium uptake by fronds of *Lemna minor* L. New Phytologist 117: 91-102.

Lamy CA. 1862. De l'existence d'un nouveau metal, le thallium. Comptes Rendus 54: 1255-1258.

Lan CH, Lin TS. 2005. Acute toxicity of trivalent thallium compounds to *Daphnia magna*. Ecotoxicology and Environmental Safety 61: 432-435.

Land Institute of Protection against Emissions (LIS). 1980. Environmental burden by thallium. Investigations in the neighbourhood of the Dyckerhoff cement plant in Lengerich and other thallium-emitting plants in the country NW. Bonn, Bonn University Press (in German). [As cited in Couture et al., 2011]

Lang VY, Fatehi M, Light PE. 2012. Pharmacogenomic analysis of ATP-sensitive potassium channels coexpressing the common type 2 diabetes risk variants E23K and S1369A. Pharmacogenetics and Genomics 22: 206-214.

Lapointe D, Couture P. 2009. Influence of the route of exposure on the accumulation and subcellular distribution of nickel and thallium in juvenile fathead minnows (*Pimephales promelas*). Archives of Environmental Contamination and Toxicology 57: 571-580.

Lapointe D, Couture P. 2010. Accumulation and effects of nickel and thallium in early-life stages of fathead minnows (*Pimephales promelas*). Ecotoxicology and Environmental Safety 73: 572-578.

Lapointe D, Gentes S, Ponton DE, Hare L, Couture P. 2009. Influence of prey type on nickel and thallium assimilation, subcellular distribution and effects in juvenile fathead minnows (*Pimephales promelas*). Environmental Science & Technology 43: 8665-8670.

Laskowski M, Augustynek B, Kulawiak B, Koprowski P, Bednarczyk P, Jarmuszkiewicz W, Szewczyk A. 2016. What do we not know about mitochondrial potassium channels? Biochimica et Biophysica Acta- Bioenergetics 1857: 1247-1257.

Latini R, Tognoni G, Kates RE. 1984. Clinical pharmacokinetics of amiodarone. Clinical Pharmacokinetics 9: 136-156.

Law S, Turner A. 2011. Thallium in the hydrosphere of southwest England. Environmental Pollution 159: 3484-3489.

Lazorchak JM, Smith ME. 2007. Rainbow trout (*Oncorhynchus mykiss)* and brook trout (*Salvelinus fontinalis)* 7-day survival and growth test method. Archives of Environmental Contamination and Toxicology 53: 397-405.

LeBlanc GA, Dean JW. 1984. Antimony and thallium toxicity to embryos and larvae of fathead minnows (*Pimephales promelas).* Bulletin of Environmental Contamination and Toxicology 32: 565-569.

Lechelt M, Blohm W, Kirschneit B, Pfeiffer M, Gresens E, Liley J, Holz R, Luring C, Moldaenke C. 2000. Monitoring of surface water by ultrasensitive *Daphnia* toximeter. Environmental Toxicology 15: 390-400.

Lee JW, Choi H, Hwang UK, Kang JC, Kang YJ, Kim KI, Kim JH. 2019. Toxic effects of lead exposure on bioaccumulation, oxidative stress, neurotoxicity, and immune responses in fish: A review. Environmental Toxicology and Pharmacology 68: 101-108.

Leguay S, Campbell PGC, Fortin C. 2016. Determination of the free-ion concentration of rare earth elements by an ion-exchange technique: Implementation, evaluation and limits. Environmental Chemistry 13: 478-488.

Leonard A, Gerber GB. 1997. Mutagenicity, carcinogenicity and teratogenicity of thallium compounds. Mutation Research/Reviews in Mutation Research 387: 47-53.

Leonard EM, Marentette JR, Balshine S, Wood CM. 2014. Critical body residues, Michaelis-Menten analysis of bioaccumulation, lethality and behaviour as endpoints of waterborne Ni toxicity in two teleosts. Ecotoxicology 23: 147-162.

Lewis P, Horning W. 1987. Short-term Chronic Toxicity Test Using *Daphnia magna*. U.S. Environmental Protection Agency, Washington, DC, EPA/600/D-87/080 (NTIS PB87167078).

Li B, Zhang JX, Ma JC, Qiao LL, Ren BX, Chen M, Ren ZM. 2020. The continuous physiological changes of zebrafish (*Danio rerio*) based on metabolism under controlled thallium stress. Chemosphere 240: 124974.

Li P, Feng X, Liang P, Chan HM, Yan H, Chen L. 2013. Mercury in the seafood and human exposure in coastal area of Guangdong province, South China. Environmental Toxicology and Chemistry 32: 541-547.

Liao PC, Bergamini C, Fato R, Pon LA, Pallotti F. 2020. Isolation of mitochondria from cells and tissues. Methods in Cell Biology 155: 3-31.

Lin CH, Lee TH. 2005. Sodium or potassium ions activate different kinetics of gill Na,K-ATPase in three seawater- and freshwater-acclimated euryhaline teleosts. Journal of Experimental Zoology-Part A: Comparative Experimental Biology 303: 57-65.

Lin CH, Tsai RS, Lee TH. 2004. Expression and distribution of Na, K-ATPase in gill and kidney of the spotted green pufferfish, *Tetraodon nigroviridis,* in response to salinity challenge. Comparative Biochemistry and Physiology- Part A: Molecular & Integrative Physiology 138: 287-295.

Lin H, Randall DJ. 1993. H^+-ATPase activity in crude homogenates of fish gill tissue: Inhibitor sensitivity and environmental and hormonal regulation. Journal of Experimental Biology 180: 163-174.

Lin TS, Meier P, Nriagu J. 2005. Acute toxicity of thallium to *Daphnia magna* and *Ceriodaphnia dubia.* Bulletin of Environmental Contamination and Toxicology 75: 350-355.

Lin TS, Nriagu JO. 1998. Speciation of thallium in natural waters. In: Nriagu JO, ed., Thallium in the Environment, Vol 29- Advances in Environmental Science and Technology. Wiley, New York, NY, USA, pp 31-43.

Lin TS, Nriagu J. 1999. Thallium speciation in the Great Lakes. Environmental Science & Technology 33: 3394- 3397.

Lin TS, Nriagu J, Wang XQ. 2001. Thallium concentration in lake trout from Lake Michigan. Bulletin of Environmental Contamination and Toxicology 67: 921-925.

Liu J, Jin W, Chen YH, Qi JY, Lippold H, Wang CL. 2010. Thallium distribution in sediment from the Pearl River Basin, China. Clean Soil Air Water 38: 909-915.

Liu J, Lou X, Sun Y, Tsang DCW, Qi J, Zhang W, Li N, Yin M, Wang J, Lippold H, Chen Y, Sheng G. 2019. Thallium pollution in China and removal technologies for waters: A review. Environment International 126: 771-790.

Liu J, Wang J, Chen YH, Xie X, Qi J, Lippold H, Wang CL, Su LX, He LC, Wu QW. 2016. Thallium transformation and partitioning during Pb-Zn smelting and environmental implications. Environmental Pollution 212: 77-89.

Livak KJ, Schmittgen TD. 2001. Analysis of relative gene expression data using real-time quantitative PCR and the $2^{-\Delta\Delta CT}$ method. Methods 25: 402-408.

Livingstone DR. 2003. Oxidative stress in aquatic organisms in relation to pollution and agriculture. Revue de Médecine Vétérinaire 154: 427-430.

Lloyd DR, Phillips DH. 1999. Oxidative DNA damage mediated by copper(II), iron(II) and nickel(II) Fenton reactions: Evidence for site-specific mechanisms in the formation of double-strand breaks, 8-hydroxydeoxyguanosine and putative intrastrand cross links. Mutation Research 424: 23-36.

Loncoman CA, Gutiérrez L, Strobel P, Alarcón P, Contreras C, Conejeros I, Morera FJ. 2015. Application of a real-time PCR assay to detect BK potassium channel expression in samples from Atlantic salmon (*Salmo salar*) and rainbow trout (*Oncorhynchus mykiss)* acclimated to freshwater. Archivos de Medicina Veterinaria 47: 215-220.

Loro VL, Jorge MB, da Silva KR, Wood CM. 2012. Oxidative stress parameters and antioxidant response to sublethal waterborne zinc in a euryhaline teleost *Fundulus heteroclitus*: Protective effects of salinity. Aquatic Toxicology 110-111: 187-193.

Lu CI, Huang CC, Chang YC, Tsai YT, Kou HC, Chuang YH, Shih TS. 2007. Short-term thallium intoxication. Archives of Dermatology 143: 93-98.

Lu T, Wu L, Xiao J, Yang J. 2001. Permeant ion-dependent changes in gating of Kir2.1 inward rectifier potassium channel. Journal of General Physiology 118: 509-522.

Lukaszewski Z, Zembrzuski W, Piela A. 1996. Direct determination of ultratraces of thallium in water by flow-injection-differential-pulse anodic stripping voltammetry. Analytica Chimica Acta 318: 159-165.

Lushchak VI. 2011. Environmentally induced oxidative stress in aquatic animals. Aquatic Toxicology 101: 13-30.

Ma J, Qiao L, Ji L, Ren B, Hu Y, Zhao R, Ren Z. 2019. The online monitoring and assessment of thallium stress using oxygen consumption rate and carbon dioxide excretion rate in zebrafish (*Danio rerio*). Chemosphere 216: 103-109.

Mahoney MC, Connolly BF, Smith CM. 1999. A clozapine overdose with markedly elevated serum levels. Journal of Clinical Pharmacology 39: 97-100.

Maier T, Güell M, Serrano L. 2009. Correlation of mRNA and protein in complex biological samples. FEBS Letters 583: 3966-3973.

Maki AW. 1979. Correlations between *Daphnia magna* and fathead minnow (*Pimephales promelas*) chronic toxicity values for several classes of test substances. Journal of the Fisheries Research Board of Canada 36: 411-421.

Martin LA, Simonucci C, Rad S, Benedetti MF. 2020. Effect of natural organic matter on thallium and silver speciation. Journal of Environmental Sciences 93: 185-192.

Mathys W. 1981. Thallium in river sediments of North-West Germany: Its sources of input and its relation to other heavy metals. In: Proceedings of the International Conference on Heavy Metals in the Environment, Amsterdam, pp 347-350.

Matteson DR., Swenson Jr RP. 1986. External monovalent cations that impede the closing of K channels. Journal of General Physiology 87: 795-816.

Maya-López M, Mireles-García MV, Ramírez-Toledo M, Colín-González AL, Galván-Arzate S, Túnez I, Santamaría A. 2018. Thallium-induced toxicity in rat brain crude synaptosomal/mitochondrial fractions in sensitive to anti-excitatory and antioxidant agents. Neurotoxicity Research 33: 634-640.

McCoole MD, Baer KN, Christie AE. 2011. Histaminergic signaling in the central nervous system of *Daphnia* and a role for it in the control of phototactic behavior. Journal of Experimental Biology 214: 1773-1782.

McCormick SD. 1993. Methods for nonlethal gill biopsy and measurement of Na^+, K^+-ATPase activity. Canadian Journal of Fisheries and Aquatic Sciences 50: 656-658.

McGeer JC, Brix KV, Skeaff JM, DeForest DK, Brigham SI, Adams WJ, Green A. 2003. Inverse relationship between bioconcentration factor and exposure concentrations for metals: Implications for hazard assessment of metals in the aquatic environment. Environmental Toxicology and Chemistry 22: 1017-1037.

McMahon JW. 1965. Some physical factors influencing the feeding behavior of *Daphnia magna* Straus. Canadian Journal of Zoology 43: 603-611.

McRae NK, Gaw S, Glover CN. 2016. Mechanisms of zinc toxicity in the galaxiid fish, *Galaxias maculatus.* Comparative Biochemistry and Physiology- Part C: Toxicology and Pharmacology 179: 184-190

McRae NK, Gaw S, Glover CN. 2018. Effects of waterborne cadmium on metabolic rate, oxidative stress, and ion regulation in the freshwater fish, inanga (*Galaxias maculatus).* Aquatic Toxicology 194: 1-9.

Meador JP, McCarty LS, Escher BI, Adams WJ. 2008. The tissue-residue approach for toxicity assessment: Concepts, issues, application, and recommendations. Journal of Environmental Monitoring 10: 1486-1498.

Meena RAA, Sathishkumar P, Ameen F, Yusoff ARM, Gu FL. 2018. Heavy metal pollution in immobile and mobile components of lentic ecosystems- a review. Environmental Science and Pollution Research 25: 4134-4148.

Melnick RL, Monti LG, Motzkin SM. 1976. Uncoupling of mitochondrial oxidative phosphorylation by thallium. Biochemical and Biophysical Research Communications 69: 68-73.

Michels E, De Meester L. 1998. The influence of food quality on the phototactic behaviour of *Daphnia magna* Straus. Hydrobiologia 379: 199-206.

Michels E, Leynen M, Cousyn C, De Meester L, Ollevier F. 1999 Phototactic behavior of *Daphnia* as a tool in the continuous monitoring of water quality: Experiments with a positively phototactic *Daphnia magna* clone. Water Research 233: 401-408.

Migaszewski ZM, Galuszka A. 2021. Abundance and fate of thallium and its stable isotopes in the environment. Reviews in Environmental Science and Bio/Technology 20: 5-30.

Mijošek T, Marijić VF, Dragun Z, Ivanković, Krasnići N, Redžović Z, Veseli M, Gottstein S, Lajtner J, Perić MS, Kepčija RM, Erk M. 2020. Thallium accumulation in different organisms from karst and lowland rivers of Croatia under wastewater impact. Environmental Chemistry 17: 201-212.

Miner BE, De Meester L, Pfrender ME, Lampert W, Hairston NG. 2012. Linking genes to communities of ecosystems: *Daphnia* as an ecogenomic model. Proceedings of the Royal Society B 279: 1873-1882.

Ministry of Health of China (MHC). 2006. Standards for drinking water quality. Ministry of Health of China, Beijing, China.

Moeschlin S. 1980. Thallium poisoning. Clinical Toxicology 17: 133-146.

Molina LCP, Fréchou DMS, Verstraeten SV. 2017. Early response of glutathione- and thioredoxin-dependent antioxidant defense systems to Tl(I) and Tl(III) mediated oxidative stress in adherent pheochromocytoma (PC12adh) cells. Archives of Toxicology 92: 195-211.

Moller JV, Juul B, le Maire M. 1996. Structural organization, ion transport, and energy transduction of P-type ATPases. Biochimica et Biophysica Acta- Reviews on Biomembranes 1286: 1-51.

Morciano G, Imamura H, Petergnani S, Pedriali G, Giorgi C, Pinton P. 2020. Measurements of ATP concentrations in mitochondria of living cells using luminescence and fluorescence approaches. Methods in Cell Biology 155: 199-219.

Morgan IJ, McDonald DG, Wood CM. 2001. The cost of living for freshwater fish in a warmer, more polluted world. Global Change Biology 7: 345-355.

Morgan TP, Wood CM. 2004. A relationship between gill silver accumulation and acute silver toxicity in the freshwater rainbow trout: Support for the acute silver biotic ligand model. Environmental Toxicology and Chemistry 23: 1261-1267.

Morris C, O'Donnell M. 2019. Multiple functions of ion transport by the nuchal organ in embryos and neonates of the freshwater branchiopod crustacean *Daphnia magna.* Journal of Experimental Biology 222: jeb211128.

Morris Jr RC, Schmidlin O, Frassetto LA, Sebastian A. 2006. Relationship and interaction between sodium and potassium. Journal of the American College of Nutrition 25: S262-S270.

Morrison JF, Guynn SR, Scofield MA, Dowd FJ, Petzel DH. 2006. Warm acclimation changes the expression of the Na^+, K^+-ATPase α subunit isoforms in Antarctic fish gills. Journal of Experimental Marine Biology and Ecology 333: 129-139.

Mount DR, Erickson RJ, Highland TL, Hockett JR, Hoff DJ, Jenson CT, Norberg-King TJ, Peterson KN, Polaske ZM, Wisniewski S. 2016. The acute toxicity of major ion salts to *Ceriodaphnia dubia*: I. Influence of background water chemistry. Environmental Toxicology and Chemistry 35: 3039-3057.

Moyson S, Liew HJ, Fazio A, Van Dooren N, Delcroix A, Faggio C, Blust R, DeBoeck G. 2016. Kidney activity increases in copper exposed goldfish (*Carassius auratus auratus*). Comparative Biochemistry and Physiology- Part C: Toxicology and Pharmacology 190: 32-37.

Munch JC. 1934. Human thallotoxicosis. Journal of the American Medical Association 102: 1929–1934.

Munch JC, Ginsburg HM, Nixon CE. 1933. The 1932 thallotoxicosis outbreak in California. Journal of the American Medical Association 100: 1315–1319.

Munch JC, Silver J. 1931. The Pharmacology of Thallium and its use in Rodent Control. Technical Bulletins 163063, United States Department of Agriculture, Economic Research Service. Washington D.C., USA.

Nakano M, Imumura H, Toei M, Tamakoshi M, Yoshida M, Yokoyama K. 2008. ATP hydrolysis and synthesis of rotary motor V-ATPase from *Thermus thermophilus.* Journal of Biological Chemistry 283: 20789-20796.

Nehring D. 1962. Untersuchungen über die toxikologische Wirkung von Thallium-Ionen auf Fische und Fischnährtiere. Zeitschrift für Fischerei 11: 557-561.

Niyogi S, Wood CM. 2004. Biotic ligand model, a flexible tool for developing site-specific water quality guidelines for metals. Environmental Science & Technology 38: 6177- 6192.

Nriagu JO. 1998. History, production and uses of thallium. In: Nriagu JO, ed., Thallium in the Environment, Vol 29- Advances in Environmental Science and Technology. Wiley, New York, NY, USA, pp 1-14.

Nriagu JO, Lawson G, Wong HKT, Azcue JM. 1993. A protocol for minimizing contamination in the analysis of trace metals in Great Lake waters. Journal of Great Lakes Research 19: 175-182.

Nunes B, Caldeira C, Pereira JL, Gonçalves F, Correia AT. 2015. Perturbations in ROS-related processes of fish *Gambusia holbrooki* after acute and chronic exposure to the metals copper and cadmium. Environmental Science and Pollution Research 22: 3756-3765.

Okamoto A, Yamamuro M, Tatarazoko N. 2015. Acute toxicity of 50 metals to *Daphnia magna.* Journal of Applied Toxicology 35: 824-830.

Olkova AS, Kantor GY, Kutyavina TI, Ashikhmina TY. 2018. The importance of maintenance conditions of *Daphnia magna* Straus as a test organism for ecotoxicological analysis. Environmental Toxicology and Chemistry 37: 376–384.

Olsson PE, Hogstrand C. 1987. Subcellular distribution and binding of cadmium to metallothionein in tissues of rainbow trout after exposure to ^{109}Cd in water. Environmental Toxicology and Chemistry 6: 867-874.

Olsson PE, Kling P, Hogstrand C. 1998. Mechanisms of heavy metal accumulation and toxicity in fish. In: Langston WJ, Bebianno MJ, eds., Metal Metabolism in Aquatic Environments. Springer, Boston, MA, USA, pp 321-350.

Omay HS, Schwarz W. 1992. Voltage-dependent stimulation of Na/K-pump current by external cations: Selectivity of different K congeners. Biochimica et Biophysica Acta 17: 167-173.

Organisation for Economic Co-operation and Development (OECD). 2004. Test No. 202: *Daphnia* sp., Acute Immobilisation Test. OECD Guidelines for the Testing of Chemicals. Paris, France.

Organisation for Economic Co-operation and Development (OECD). 2012. Test No. 211: *Daphnia magna* Reproductive Test. OECD Guidelines for the Testing of Chemicals. Paris, France.

Oria-Hernández J, Cabrera N, Pérez-Montfort R, Ramírez-Silva L. 2005. Pyruvate kinase revisited: The activating effect of K^+. Journal of Biological Chemistry 280: 37924-37929.

Osorio-Rico L, Santamaria A, Galván-Arzate S. 2017. Thallium toxicity: General issues, neurological symptoms, and neurotoxic mechanism. Advances in Neurobiology 18: 345-353.

Osorio-Rico L, Villeda-Hernández J, Santamaría A, Königsberg M, Galván-Arzate S. 2015. The N-methyl-D-aspartate receptor antagonist MK-801 prevents thallium-induced behavioral and biochemical alterations in the rat brain. International Journal of Toxicology 34: 505-513.

Ospina-Alvarez N, Burakiewicz P, Sadowska M, Krasnodebska-Ostrega B. 2015. Tl^{I} and Tl^{III} presence in suspended particulate matter: Speciation analysis of thallium in wastewater. Environmental Chemistry 12: 374-379.

Overturf MD, Overturf CL, Baxter D, Hala DN, Constantine L, Venables B, Huggett DB. 2012. Early life-stage toxicity of eight pharmaceuticals to fathead minnow, *Pimephales promelas.* Archives of Environmental Contamination and Toxicology 62: 455-464.

Palmer BF. 2015. Regulation of potassium homeostasis. Clinical Journal of the American Society of Nephrology 10: 1050-1060.

Park YM, Choi JY, Nho EY, Lee CM, Hwang IM, Khan N, Jamila N, Kim KS. 2018. Determination of macro and trace elements in canned marine products by inductively coupled plasma-optical emission spectrometry (ICP-OES) and ICP-mass spectrometry (ICP-MS). Analytical Letters 52: 1018-1030.

Pearre S. 2003. Eat and run? The hunger/satiation hypothesis in vertical migration: History, evidence and consequences. Biological Reviews 78: 1-79.

Perotti M, Petrini R, D'Orazio M, Ghezzi L, Giannecchini R, Vezzoni S. 2017. Thallium and other potentially toxic elements in the Baccatoio stream catchment (Northern Tuscany, Italy) receiving drainages from abandoned mines. Mine Water and the Environment 37: 431-441.

Perry SF, Beyers ML, Johnson DA. 2000. Cloning and molecular characterisation of the trout (*Oncorhynchus mykiss)* vacuolar H^+-ATPase B subunit. Journal of Experimental Biology 203: 459-470.

Perry SF, Shahsavarani A, Georgalis T, Bayaa M, Furimsky M, Thomas SLY. 2003. Channels, pumps and exchangers in gill and kidney of freshwater fishes: Their role in ionic and acid-base regulation. Journal of Experimental Zoology- Part A: Ecological and Integrative Physiology 300: 53-62.

Peter ALJ, Viraraghavan T. 2005. Thallium: A review of public health and environmental concerns. Environment International 31: 493-501.

Pichon Y, Abbott NJ, Lieberman EM, Larmet Y. 1987. Potassium homeostasis in the nervous system of cephalopods and crustacea. Journal de Physiologie 82: 346-356.

Pickard J, Yang R, Duncan B, McDevitt CA, Eickhoff C. 2001. Acute and sublethal toxicity of thallium to aquatic organisms. Bulletin of Environmental Contamination and Toxicology 66: 94-101.

Pickering AM, Davies KJA. 2013. Degradation of damaged proteins- the main function of the 20S proteasome. Progress in Molecular Biology and Translational Science 109: 227-248.

Pisam M, Rambourg A. 1991. Mitochondria-rich cell in the gill epithelium of teleost fishes: An ultrastructural approach. International Review of Cytology 130: 191-232.

Pizzino G, Irrera N, Cucinotta M, Pallio G, Mannino F, Arcoraci V, Squadrito F, Altavilla D, Bitto A. 2017. Oxidative stress: Harms and benefits for human health. Oxidative Medicine and Cellular Longevity 2017: 8416763.

Playle RC. 1998. Modelling metal interactions at fish gills. Science of the Total Environment 219:147-163.

Pleßow A, Heinrichs H. 2000. Speciation of trace elements in acidic pore waters from waste rock dumps by ultrafiltration and ion exchange combined with ICPMS and ICPOES. Aquatic Geochemistry 6: 347–366.

Pourahmad J, Eskandari MR, Daraei B. 2010. A comparison of hepatocyte cytotoxic mechanisms for thallium(I) and thallium(III). Environmental Toxicology 25: 456-467.

Pourahmad J, O'Brien PJ. 2000. Contrasting role of Na^{+} ions in modulating Cu^{+2} or Cd^{+2} induced hepatocyte toxicity. Chemico-Biological Interactions 126: 159-169.

Printes LB, Callaghan A. 2004. A comparative study on the relationship between acetylcholinesterase activity and acute toxicity in *Daphnia magna* exposed to anticholinesterase insecticides. Environmental Toxicology and Chemistry 5:1241-1247.

Qu R, Feng M, Wang X, Qin L, Wang C, Wang Z, Wang L. 2014. Metal accumulation and oxidative stress biomarkers in liver of freshwater fish *Carassius auratus* following in vivo exposure to waterborne zinc under different pH values. Aquatic Toxicology 150: 9-16.

Rabon EC, Sachs G. 1981. Thallium interactions with the gastric (K,H)-ATPase. Journal of Membrane Biology 62: 19-27.

Radić S, Cvjetko P, Glavas K, Roje V, Pevalek-Kozlina B, Pavlica M. 2009. Oxidative stress and DNA damage in broad bean (*Vicia faba* L.) seedlings induced by thallium. Environmental Toxicology and Chemistry 28: 189-196.

Rainbow PS. 2002. Trace metal concentrations in aquatic invertebrates: Why and so what? Environmental Pollution 120: 497-507.

Randall DJ, Lin H. 1993. Effects of water pH on gas and ion transfer across fish gills. In: Rankin JC, Jensen FB, eds., Vol 9-Fish Ecophysiology. Chapman & Hall Fish and Fisheries Series, Springer, Dordrecht, pp 265-275.

Rauws AG, Canton JH. 1976. Adsorption of thallium ions by Prussian Blue. Bulletin of Environmental Contamination and Toxicology 15: 335.

Ren Q, Zhao RB, Wang C, Li SG, Zhang TT, Ren ZM, Yang MY, Pan HW, Xu SG, Zhu JP, Wang X. 2017. The role of AChE in swimming behavior of *Daphnia magna*: Correlation analysis of both parameters affected by deltamethrin and methomyl exposure. Journal of Toxicology 2017: 3265727.

Repetto G, Sanz P, Repetto M. 1994. In vitro effects of thallium on mouse neuroblastoma cells. Toxicology In Vitro 8: 609-611.

Rickwood CJ, King M, Huntsman-Mapila P. 2015. Assessing the fate and toxicity of thallium I and thallium III to three aquatic organisms. Ecotoxicology and Environmental Safety 115: 300-308.

Ringelberg J. 1999. The photobehaviour of *Daphnia* spp. as a model to explain diel vertical migration in zooplankton. Biological Reviews 74: 397-423.

Risso-de Faverney C, Devaux A, Lafaurie M, Girard JP, Bailly B, Rahmani R. 2001. Cadmium induces apoptosis and genotoxicity in rainbow trout hepatocytes through generation of reactive oxygen species. Aquatic Toxicology 53: 65-76.

Robinson JD. 1970. Interactions between monovalent cations and the ($Na^+ + K^+$)- dependent adenosine triphosphatase. Archives of Biochemistry and Biophysics 139: 17-27.

Robinson JD. 1975. Functionally distinct classes of K^+ sites on the (Na^+ + K^+)- dependent ATPase. Biochimica et Biophysica Acta- Enzymology 384: 250-264.

Ronov AB, Yaroshevsky AA. 1969. Earth's crust geochemistry. In: Fairbridge RW, ed., Encyclopedia of Geochemistry and Environmental Sciences. Van Nostrand, New York.

Rosabal M, Mounicou S, Hare L, Campbell PGC. 2016. Metal (Ag, Cd, Cu, Ni, Tl, and Zn) binding to cytosolic biomolecules in field-collected larvae of the insect *Chaoborus.* Environmental Science & Technology 50: 3247-3255.

Rossi RC, Norby JG. 1993. Kinetics of K^+-stimulated dephosphorylation and simultaneous K^+ occlusion by Na, K-ATPase, studied with the K^+ congener Tl^+. The possibility of differences between the first turnover and steady state. Journal of Biological Chemistry 268: 12579–12590.

Rowan DJ, Rasmussen JB. 1994. Bioaccumulation of radiocesium by fish: The influence of physicochemical factors and trophic structure. Canadian Journal of Fisheries and Aquatic Sciences 51: 2388-2410.

Rubino JG, Wilson JM, Wood CM. 2019. An in vitro analysis of intestinal ammonia transport in fasted and fed freshwater rainbow trout: Roles of NKCC, K^+ channels, and Na^+, K^+ ATPase. Journal of Comparative Physiology B: Biochemical, Systemic, and Environmental Physiology 189: 549-566.

Rüdel H, Muñiz CD, Garelick H, Kandile NG, Miller BW, Munoz LP, Peijnenburg WJGM, Purchase D, Shevah Y, van Sprang P, Vijver M, Vink JPM. 2015. Consideration of the bioavailability of metal/metalloid species in freshwaters: Experiences regarding the implementation of biotic ligand model-based approaches in risk assessment frameworks. Environmental Science and Pollution Research 22: 7405-7421.

Sadeq SA, Beckerman AP. 2019. The chronic effects of copper and cadmium on life history traits across Cladocera species: A meta-analysis. Archives of Environmental Contamination and Toxicology 76: 1-16.

Sager M. 1992. Speciation of thallium in river sediments by consecutive leaching techniques. Microchimica Acta 106: 241-251.

Sahl K, Albuquerque CAR, Shaw DM. 1978. Thallium. In: Wedepohl KH, ed., Handbook of Geochemistry. Berlin Springer-Verlag.

Sanders MJ, Kirschner LB. 1983. Potassium metabolism in seawater teleosts. I. The use of ^{86}Rb as a tracer for potassium. Journal of Experimental Biology 104: 15-28.

Sappington KG, Bridges TS, Bradbury SP, Erickson RJ, Hendriks AJ, Lanno RP, Meador JP, Mount DR, Salazar MH, Spry DJ. 2011. Application of the tissue residue approach in ecological risk assessment. Integrated Environmental Assessment and Management 7: 116-140.

Sartor G, Melander A, Sherstén B, Wåhlin-Boll E. 1980. Comparative single-dose kinetics and effects of four sulfonylureas in healthy volunteers. Acta Medica Scandinavica 208: 301-307.

Sato R, Koumi SI, Singer DH, Hisatome I, Jia H, Eager S, Wasserstrom A. 1994. Amiodarone blocks the inward rectifier potassium channel in isolated guinea pig ventricular cells. Journal of Pharmacology and Experimental Therapeutics 269: 1213-1219.

Scheckel KG, Hamon R, Jassogne L, Rivers M, Lombi, E. 2007. Synchrotron X-ray absorption-edge computed microtomography imaging of thallium compartmentalization in *Iberis intermedia*. Plant and Soil 290: 51-60.

Scheckel KG, Lombi E, Rock SA, McLaughlin MJ. 2004. In vivo synchrotron study of thallium speciation and compartmentation in *lberis intermedia*. Environmental Science & Technology 38: 5095-5100.

Schoer J. 1984. Thallium. In: Hutzinger O, ed., Handbook of Environmental Chemistry, Vol 3, Springer-Verlag, New York, NY, USA, pp 143-214.

Sessler MJ, Geck P, Maul FD, Hör G, Munz DL. 1986. New aspects of cellular thallium uptake: Tl^{+}-Na^{+}-$2Cl^{-}$ cotransport is the central mechanism of ion uptake. Journal of Nuclear Medicine 25: 24-27.

Shannon R.D. 1976. Revised effective ionic radii and systematic studies of interatomic distances in halides and chalogenides. Acta Crystallographica Section A 32: 751-767.

Shekh K, Alcaraz AJ, Niyogi S, Hecker M. 2020. Comparative analysis of oxidative stress response and metallothionein induction in white sturgeon and rainbow trout during acute waterborne copper exposure. Comparative Biochemistry and Physiology- Part C: Toxicology and Pharmacology 231: 108723.

Sherstobitov AO, Lapin AA, Glazunov VV, Nikiforov AA. 2010. Transport of monovalent thallium across the membrane of oocyte of the lamprey *Lampetra fluviatilis.* Journal of Evolutionary Biochemistry and Physiology 46: 235-240.

Shotyk W, Bicalho B, Cuss CW, Donner MW, Grant-Weaver I, Haas-Neill S, Javed MB, Krachler M, Noernberg T, Pelletier R, Zaccone C. 2017. Trace metals in the dissolved fraction (<0.45 μm) of the lower Athabasca River: Analytical challenges and environmental implications. Science of the Total Environment 580: 660-669.

Shotyk W, Bicalho B, Cuss CW, Grant-Weaver I, Nagel A, Noernberg T, Poesch M, Sinnatamby NR. 2019. Bioaccumulation of Tl in otoliths of trout perch (*Percopsis omiscomaycus)* from the Athabasca River, upstream and downstream of bitumen mining and upgrading. Science of the Total Environment 650: 2559-2566.

Shui C, Shi Y, Hua X, Zhang Z, Zhang H, Lu G, Xie Y. 2018. Serum osmolality and ions, and gill Na^+/K^+-ATPase of spottedtail goby *Synechogobius ommaturus* (R.) in response to acute salinity changes. Aquaculture and Fisheries 3: 79-83.

Siegel BZ, Siegel SM. 1976. Effect of potassium on thallium toxicity in cucumber seedlings: Further evidence for potassium-thallium ion antagonism. Bioinorganic Chemistry 6: 341-345.

Sillen LG, Martell AE, Bjerrum J. 1964. Stability Constants of Metal-Ion Complexes: Vol. 2. London: Chemical Society, London, UK, pp 754.

Sitte N. 2003. Oxidative damage to proteins. In: Von Zglinicki T, ed., Aging at the Molecular Level. Springer, Netherlands, pp-27-45.

Skulskii IA, Manninen V, Järnefelt J. 1975. Thallium inhibition of ouabain-sensitive sodium transport and of the $(Na^+ + K^+)$-ATPase in human erythrocytes. Biochimica et Biophysica Acta 394: 569-576.

Smith IC, Carson BL. 1977. Trace Metals in the Environment: Vol. 1- Thallium. Ann Arbor Scientific, Ann Arbor, MI, USA, pp 138-139.

Souid G, Souayed N, Yaktiti F, Maaroufi K. 2013. Effect of acute cadmium exposure on metal accumulation and oxidative stress biomarkers of *Sparus aurata.* Ecotoxicology and Environmental Safety 89: 1-7.

Suhail M. 2010. Na^+, K^+-ATPase: Ubiquitous multifunctional transmembrane protein and its relevance to various pathophysiological conditions. Journal of Clinical Medicine Research 2: 1-17.

Szabò I, Leanza L, Gulbins E, Zoratti M. 2012. Physiology of potassium channels in the inner membrane of mitochondria. Pflügers Archiv- European Journal of Physiology 463: 231-246.

Tabassum R, Jeong NY. 2019. Potential for therapeutic use of hydrogen sulfide in oxidative stress-induced neurodegenerative diseases. International Journal of Medical Sciences 16: 1386-1396.

Takvam M, Wood CM, Kryvi H, Nilsen TO. 2021. Ion transporters and osmoregulation in the kidney of teleost fishes as a function of salinity. Frontiers in Physiology 12: 664588.

Talas A, Pretschner DP, Wellhöner HH. 1983. Pharmacokinetic parameters for thallium(I) ions in man. Archives of Toxicology 53: 1-7.

Tao Z, Gameiro A, Grewer C. 2008. Thallium ion can replace both sodium and potassium ions in the glutamate transporter EAAC1. Biochemistry 48: 12923-12930.

Tarfeño-Saldivia E, Aguilar A, Contreras D, Mercado L, Morales-Lange B, Márquez K, Henríquez A, Riquelme-Vidal C, Boltana S. 2018. Iron overload is associated with oxidative stress and nutritional immunity during viral infection in fish. Frontiers in Immunology 9: 1296.

Tatsi K, Turner A. 2014. Distributions and concentrations of thallium in surface waters of a region impacted by historical metal mining (Cornwall, UK). Science of the Total Environment 473-474: 139-146.

Tatsi K, Turner A, Handy RD, Shaw BJ. 2015. The acute toxicity of thallium to freshwater organisms: Implications for risk assessment. Science of the Total Environment 536: 382-390.

Testai L, Martelli A, Marino A, D'Antongiovanni V, Ciregia F, Giusti L, Lucacchini A, Chericoni S, Breschi MC, Calderone V. 2013. The activation of mitochondrial BK potassium channels contributes to the protective effects of naringenin against myocardial ischemia/reperfusion injury. Biochemical Pharmacology 85: 1634-1643.

Thompson DF. 1981. Management of thallium poisoning. Clinical Toxicology 18: 979-990.

Thorgaard GH, Bailey GS, Williams D, Buhler DR, Kaattari SL, Ristow SS, Hansen JD, Winton JR, Bartholomew JL, Nagler JJ, Walsh PJ, Vijayan MM, Devlin RH, Hardy RW, Overturf KE,

Young WP, Robison BD, Rexroad C, Palti Y. 2002. Status and opportunities for genomics with rainbow trout. Comparative Biochemistry and Physiology- Part B: Biochemistry and Molecular Biology 133: 609-646.

Thurman EM. 1985. Organic Geochemistry of Natural Waters. Martinus Nijhof/Dr. W. Junk Publishers, Boston, USA.

Tipping E, Lofts S, Sonke JE. 2011 Humic Ion-Binding Model VII: A revised parameterisation of cation-binding by humic substances. Environmental Chemistry 8: 225-235.

Tirtom NE, Okuno D, Nakano M, Yokoyama K, Noji H. 2013. Mechanical modulation of ATP-binding affinity of V_1-ATPase. Journal of Biological Chemistry 288: 619-623.

Tomasik P, Warren DM. 1996. The use of *Daphnia* in studies of metal pollution of aquatic systems. Environmental Reviews 4: 25-64.

Traber MG, Stevens JF. 2011. Vitamins C and E: Beneficial effects from a mechanistic perspective. Free Radical Biology and Medicine 51: 1000-1013.

Tse WKF, Au DWT, Wong CKC. 2006. Characterization of ion channel and transporter mRNA expressions in isolated gill chloride and pavement cells of seawater acclimating eels. Biochemical and Biophysical Research Communications 346: 1181-1190.

Turner A, Furniss O. 2012. An evaluation of the toxicity and bioaccumulation of thallium in the coastal marine environment using microalga, *Ulva lactuca.* Marine Pollution Bulletin 62: 2720-2724.

Turner A, Pilsbury A. 2013. Accumulation of aqueous and dietary thallium by the marine snail, *Littorina littorea*. Estuarine, Coastal and Shelf Science 129: 73-76.

Twining BS, Twiss MR, Fisher NS. 2003. Oxidation of thallium by freshwater plankton communities. Environmental Science & Technology 37: 2720-2726.

Twiss MR, Twining BS, Fisher NS. 2004. Bioconcentration of inorganic and organic thallium by freshwater phytoplankton. Environmental Toxicology and Chemistry 23: 968-973.

United States Environmental Protection Agency (USEPA). 1980. Ambient Water Quality Criteria for Thallium. Office of Water, Washington, D.C., USA, 71 p.

United States Environmental Protection Agency (USEPA). 1983. Methods for Chemical Analysis of Water and Wastes (Method 207.3). Monitoring and Support Laboratory, Cincinnati, OH, USA, EPA-600/4-79-020.

United States Environmental Protection Agency (USEPA). 1992. Interim Guidance on Interpretation and Implementation of Aquatic Life Criteria for Metals. Washington, D.C., USA, EPA-821/R-92-009.

United States Environmental Protection Agency (USEPA). 2002a. National Recommended Water Quality Criteria. Office of Water, Washington, D.C., USA, EPA-822-R-02-047.

United States Environmental Protection Agency (USEPA). 2002b. Methods for Measuring the Acute Toxicity of Effluents and Receiving Waters to Freshwater and Marine Organisms. Office of Water, Washington, D.C., USA, EPA-821-R-02-012.

United States Environmental Protection Agency (USEPA). 2007. Aquatic Life Ambient Freshwater Quality Criteria - Copper. Office of Water, Washington, D.C., USA, 204 p.

United States Environmental Protection Agency (USEPA). 2009a. National Primary Drinking Water Regulations. Office of Ground Water and Drinking Water, Washington D.C., USA, EPA-816-F-09-004.

United States Environmental Protection Agency (USEPA). 2009b. Selected Issues Associated with the Risk Assessment Process for Pesticides with Persistent, Bioaccumulative and Toxic Characteristics. FIFRA Scientific Advisory Panel. Arlington, VA, USA, 363 p.

United States Environmental Protection Agency (USEPA). 2014. Appendix A to Part 423- 126 Priority Pollutants. In: USEPA., Title 40- Protection of Environment 40 CFR Part 423.

United States Environmental Protection Agency (USEPA). 2016. Ecological Effects Test Guidelines- OCSPP 850.1730: Fish Bioconcentration Factor (BCF). Office of Chemical Safety and Pollution Prevention. Washington D.C., USA, 35 p.

United States Geological Survey (USGS). 1998. Revised Methods for Characterizing Stream Habitat in the National Water Quality Assessment Program. Water-Resources Investigations Report. Raleigh, NC, USA, 98-4052.

United States Geological Survey (USGS). 2018. Mineral Commodity Summary: Thallium, Reston, VA.

Urien N, Farfarana A, Uher E, Fechner LC, Chaumot A, Geffard O, Lebrun JD. 2017. Comparison in waterborne Cu, Ni and Pb bioaccumulation kinetics between different gammarid species and population: Natural variability and influence of metal exposure history. Aquatic Toxicology 193: 245-255.

Van der Oost R, Beyer J, Vermeulen NP. 2003. Fish bioaccumulation and biomarkers in environmental risk assessment: A review. Environmental Toxicology and Pharmacology 13: 57-149.

Van Gool E, Ringelberg J. 1995. Swimming of *Daphnia galeata x hyalina* in response to changing light intensities: Influence of food availability and predator kairomone. Marine and Freshwater Behaviour and Physiology 26: 259-265.

Van Gool E, Ringelberg J. 1998. Light-induced migration behaviour of *Daphnia* modified by food and predator kairomones. Animal Behaviour 56: 741-747.

Van Gool E, Ringelberg J. 2003. What goes down must come up: Symmetry in light-induced migration behaviour of *Daphnia*. Hydrobiologia 491: 301-307.

Van Loon AJ. 2012. Analytical Atomic Absorption Spectroscopy: Selected methods. Academic Press, New York, NY, USA, pp 348.

Vandenberg JI, Perry MD, Perrin MJ, Mann SA, Ke Y, Hill AP. 2012. hERG K^+ channels: Structure, function, and clinical significance. Physiological Reviews 92: 1393-1478.

Varão AM, Silva JDS, Amaral LO, Aleixo LLP, Onduras A, Santos CS, Silva LPD, Ribeiro DE, Filho JLL, Bornhorst J, Stilboller M, Schwerdtle T, Alves LC, Soares FAA, Gubert P. 2021. Toxic effects of thallium acetate by acute exposure to the nematode *C. elegans.* Journal of Trace Elements in Medicine and Biology 68: 126848.

Veith GD, DeFoe DL, Bergstedt BV. 1979. Measuring and estimating the bioconcentration factor of chemicals in fish. Journal of the Fisheries Research Board of Canada 36: 1040-1048.

Veltman K, Huijbregts MAJ, Van Kolck M, Wang WX, Hendriks AJ. 2008. Metal bioaccumulation in aquatic species: Quantification of uptake and elimination rate constants using physiochemical properties of metals and physiological characteristics of species. Environmental Science & Technology 42: 852-858.

Vesela S, Vijverberg J. 2007. Effect of body size on toxicity of zinc in neonates of four differently sized *Daphnia* species. Aquatic Ecology 41: 67-73.

Villaverde MS, Hanzel CE, Verstraeten SV. 2004. In vitro interactions of thallium with components of the glutathione-dependent antioxidant defense system. Free Radical Research 9: 977-984.

Wade K, Banister AJ. 1973. The chemistry of aluminum, gallium, indium, and thallium. In: Bailar JC, Emeléus HJ, Nyholm R, eds., Pergamon Texts in Inorganic Chemistry, Vol 12. Pergamon Press, New York, NY, USA, pp 214.

Wahlund KG, Giddings JC. 1987. Properties of an asymmetrical flow field-flow fractionation channel having one permeable wall. Analytical Chemistry 59: 1332-1339.

Wang Y, Zhou Y, Wei X, Chen Y, Beiyuan J, She J, Wang L, Liu J, Liu Y, Wang J, Cao J, Jiang Y, Zheng S, Zhong Q, Liu W. 2021. Effects of thallium exposure on intestinal microbial community and organ functions in zebrafish (*Danio rerio*). Elementa: Science of the Anthropocene 9: 00092.

Weeks ME. 1932. The discovery of the elements. XIII. Some spectroscopic discoveries. Journal of Chemical Education 9: 1413-1434.

West KR, Pitman MG. 1967. Rubidium as a tracer for potassium in marine algae *Ulva lactuca* L. and *Chaetomorpha darwinii* (Hooker) Kuetzing. Nature 214: 1262-1263.

Whitman LJ, Miller RJ. 1982. The phototactic behavior of *Daphnia magna* as an indicator of chronic toxicity. Proceedings of the Oklahoma Academy of Sciences 62: 22-23.

Wiegand H, Csicsaky M, Krämer U. 1984. The action of thallium acetate on neuromuscular transmission in the rat phrenic nerve-diaphragm preparation. Archives of Toxicology 55: 55-58.

Williams-Beam C, Twidwell LG. 2003. Removal of thallium from wastewater. In: Young C, Alfantazi A, Anderson C, James A, Dreisinger D, Harris B, eds., Electrometallurgy and Environmental Hydrometallurgy, Vol 2. John Wiley & Sons, Hoboken, NJ, USA, pp 1717–1727.

Wilschefski S, Baxter M. 2019. Inductively coupled plasma mass spectrometry: Introduction to analytical aspects. Clinical Biochemist Reviews 40: 115-133.

Wood CM, LeMoigne J. 1991. Intracellular acid-base responses to environmental hyperoxia and normoxic recovery in rainbow trout. Respiration Physiology 86: 91-113.

Wright DA. 1995. Trace metal and major ion interactions in aquatic animals. Marine Pollution Bulletin 31: 8-18.

Wright SH. 2004. Generation of resting membrane potential. Advances in Physiology Education 28: 139-142.

Wu Y, Lin C, Yuan L. 2008. Phototaxis index of *Daphnia carinata* as an indicator of joint toxicity of copper, cadmium, zinc, nitrogen and phosphorus in aqueous solutions. Ecological Indicators 8: 69-74.

Wydeven N, Fernandez de Velasco EM, Du Y, Benneyworth MA, Hearing MC, Fischer RA, Thomas MJ, Weaver CD, Wickman K. 2014. Mechanisms underlying the activation of G-protein-gated inwardly rectifying K^+ (GIRK) channels by the novel anxiolytic drug, ML297. Proceedings of the National Academy of Sciences USA 111: 10755-10760.

Xiao T, Yang F, Li S, Zheng B, Ning Z. 2012. Thallium pollution in China: A geoenvironmental perspective. Science of the Total Environment 421-422: 51-58.

Xu H, Luo Y, Wang P, Zhu J, Yang Z, Liu Z. 2019. Removal of thallium in water/wastewater: A review. Water Research 165: 114981.

Xuereb B, Lefèvre E, Garric J, Geffard O. 2009 Acetylcholinesterase activity in *Gammarus fossarum* (Crustacea Amphipoda): Linking AChE inhibition and behavioral alteration. Aquatic Toxicology 94: 114-122.

Yu RQ, Wang WX. 2002. Trace metal assimilation and release budget in *Daphnia magna*. Limnology and Oceanography 47: 495-504.

Zhang H, 2017. Guangyuan: The first time to deal with the pollution incident in Jialingjiang River, China. Environmental Super Ministry Reform 6: 53-54.

Zhang Z, Zhang B, Long J, Zhang X, Chen G. 1998. Thallium pollution associated with mining of thallium deposits. Science in China Series D 41: 75-81.

Zhao RZ, Jiang S, Zhang L, Yu ZB. 2019. Mitochondrial electron transport chain, ROS generation and uncoupling (Review). International Journal of Molecular Medicine 44: 3-15.

Zia S, McDonald DG. 1994. Role of the gills and gill chloride cells in metal uptake in the freshwater-adapted rainbow trout, *Oncorhynchus mykiss*. Canadian Journal of Fisheries and Aquatic Sciences 51: 2482-2492.

Zini S, Ben-Ari Y, Ashford ML. 1991. Characterization of sulfonylurea receptors and the action of potassium channel openers on cholinergic neurotransmission in guinea pig isolated small intestine. Journal of Pharmacology and Experimental Therapeutics 256: 566-573.

Zitko V. 1975. Toxicity and pollution potential of thallium. Science of the Total Environment 4: 185-192.

Zitko V, Carson WV. 1975. Accumulation of thallium in clams and mussels. Bulletin of Environmental Contamination and Toxicology 14: 530-533.

Zitko V, Carson WV, Carson WG. 1975. Thallium: Occurrence in the environment and toxicity to fish. Bulletin of Environmental Contamination and Toxicology 13: 23-30.